
Real-time evolution of quenched quantum systems

Michael Möckel



München 2009

© Michael Möckel 2009
Selbstverlag
Berger Straße 19, 95119 Naila, Germany

All rights reserved

This publication is in copyright. Subject to statutory exceptions no reproduction of any part may take place without the written permission of Michael Möckel. In particular, this applies to any hardcopy, printout, storage, or distribution of any electronic version of this publication.

ISBN 978-3-00-028464-9

First published 2009
Printed in Germany

Real-time evolution of quenched quantum systems

Michael Möckel

Doktorarbeit
an der Fakultät für Physik
der Ludwig-Maximilians-Universität
München

vorgelegt von
Michael Möckel
aus Naila

München, den 30. April 2009

Erstgutachter: Prof. Dr. Stefan Kehrein
Zweitgutachter: Prof. em. Dr. Herbert Wagner
Tag der mündlichen Prüfung: 24. Juni 2009

Meinen Eltern
Siegfried und Brigitte

Percy Bysshe Shelley

(1792 – 1822)

Invocation

Rarely, rarely comest thou,
Spirit of Delight!
Wherefore hast thou left me now
Many a day and night?
Many a weary night and day
'Tis since thou art fled away.

How shall ever one like me
Win thee back again?
With the joyous and the free
Thou wilt scoff at pain.
Spirit false! thou hast forgot
All but those who need thee not.

As a lizard with the shade
Of a trembling leaf,
Thou with sorrow art dismay'd;
Even the sighs of grief
Reproach thee, that thou art not near,
And reproach thou wilt not hear.

Let me set my mournful ditty
To a merry measure; –
Thou wilt never come for pity,
Thou wilt come for pleasure: –
Pity thou wilt cut away
Those cruel wings, and thou wilt stay.

I love all that thou lovest,
Spirit of Delight!
The fresh Earth in new leaves drest
And the starry night;
Autumn evening, and the morn
When the golden mists are born.

I love snow and all the forms
Of the radiant frost;
I love waves, and winds, and storms,
Everything almost
Which is Nature's, and may be
Untainted by man's misery.

I love tranquil solitude,
And such society
As is quiet, wise, and good;
Between thee and me
What difference? but thou dost possess
The things I seek, nor love them less.

I love Love - though he has wings,
And like light can flee,
But above all other things,
Spirit, I love thee -
Thou art love and life! O come!
Make once more my heart thy home!

Contents

I	Introduction	3
1	The world beyond equilibrium	5
1.1	Fundamental concepts of nonequilibrium physics	6
1.1.1	Transport	6
1.1.2	Metastable states of glasses and spin glasses: avoided relaxation . . .	7
1.1.3	Time dependent nonequilibrium phenomena	8
1.2	Definition of a quantum quench	9
1.2.1	Nonequilibrium initial conditions	9
1.2.2	Nonequilibrium initialization of a system by a quantum quench	9
1.2.3	Treatment of quench problems by Hamiltonian diagonalization	9
1.2.4	Energetic implications of a quench	10
1.3	Nonequilibrium phenomena in correlated many-body quantum systems	11
1.3.1	The X-ray edge problem	11
1.3.2	Nonequilibrium dynamics of spin systems	11
1.3.3	Kibble-Zurek mechanism	12
1.3.4	Landau-Zener problem	13
1.3.5	Nonequilibrium dynamics of BCS systems	14
1.3.6	Nonequilibrium dynamics of lattice systems	14
1.4	Questions and concepts in time-dependent nonequilibrium many-particle systems	15
1.4.1	Time scales	15
1.4.2	Time evolution and integrability	16
1.4.3	Ergodicity and thermalization in classical systems	17
1.4.4	Thermalization debate in quantum systems	20
1.4.5	(Quantum) Boltzmann equation	25
2	Landau's theory of a Fermi liquid	29
2.1	Concept and prerequisite: Adiabatic connection between interacting and non-interacting degrees of freedom	29
2.2	Macroscopic approach to Fermi liquid theory	30
2.2.1	The momentum distribution for interacting and noninteracting cases .	30
2.2.2	Expansion of the free energy functional	31
2.2.3	Quasiparticle picture	32
2.2.4	Boltzmann dynamics of the momentum distribution	32
2.2.5	Range of validity of the quasiparticle picture	33
2.2.6	Thermodynamic properties of a Fermi liquid	34
2.3	Microscopic foundation of Fermi liquid theory	34

3	Hubbard model	39
3.1	Definition of the Hubbard model	39
3.2	Properties of the Hubbard model	41
4	Experimental motivation	45
4.1	Ultrafast spectroscopy of condensed matter systems	45
4.1.1	Ultrafast spectroscopy for semiconductors	45
4.1.2	Ultrafast spectroscopy for metals	47
4.1.3	Discussion of the observed time scales	47
4.2	Ultracold atoms on optical lattices	47
5	Time evolution in quantum mechanics	53
5.1	Schrödinger dynamics and Heisenberg picture	53
5.2	Greens function formalism	54
5.3	Time dependent perturbation theory	56
5.3.1	Fermi's golden rule	56
5.3.2	Coherent perturbation theory with respect to the ground state	57
5.3.3	Keldysh nonequilibrium perturbation theory and secular terms	58
5.3.4	Canonical perturbation theory	60
5.3.5	Unitary perturbation theory	62
6	Unitary perturbation theory for the squeezed oscillator	65
6.1	Squeezed one-particle oscillator	65
6.2	Perturbative study of squeezing	66
6.3	Exact (Bogoliubov) treatment of squeezing	69
7	Generic mismatch of equilibrium and nonequilibrium expectation values	73
7.1	Prerequisites	73
7.2	Theorem	74
7.3	Proof of the Theorem	74
7.3.1	First proof of the theorem by analyzing overlap matrix elements	75
7.3.2	Second proof of the theorem by applying unitary perturbation theory	76
7.4	Corollary to the Theorem regarding the kinetic energy of quenched systems	78
8	Flow equations	79
8.1	General introduction	79
8.1.1	Renormalization group ideas.	80
8.1.2	Philosophy of the flow equations.	80
8.1.3	Limited diagonalization of the flow equation method.	81
8.2	Definition of the infinitesimal transformations	81
8.2.1	Setup of a differential flow equation for observables	81
8.2.2	Canonical generator.	82
8.2.3	Intrinsic flexibility and fine-tuning of the method.	82
8.3	Representations of observables and normal ordering.	82
8.3.1	Representations of flowing observables	83
8.3.2	Normal ordering and truncations	83
8.4	Continuous sequence of infinitesimal transformations	85

II	Quench of a Fermi liquid	87
9	The flow equation transformation for the Hubbard Hamiltonian	89
9.1	Construction of the canonical generator	89
9.1.1	Implicit definition of the canonical generator	89
9.1.2	Leading order renormalization flow of the Hamiltonian	90
9.1.3	Leading order parametrization of the canonical generator	90
9.2	Transformation of the creation operator	90
9.2.1	Constructing an ansatz for the creation operator	91
9.2.2	Flow equations for the creation operator	91
9.2.3	Equilibrium momentum distribution	96
10	Unitary perturbation theory for the quenched Fermi liquid	97
10.1	Time dependent fermion operator $C_{k\uparrow}^\dagger(B=0, t)$	97
10.1.1	Time evolution	98
10.1.2	Inverse transformation	98
10.1.3	Composite transformation	99
10.2	Nonequilibrium momentum distribution	100
10.2.1	Comparison with a golden rule argument and long-time limit	100
10.2.2	Plot of the time dependent momentum distribution function	100
10.2.3	Findings for the 2 nd order nonequilibrium momentum distribution	101
10.3	Vanishing influence of leading secular terms	102
10.3.1	Factorization of two parts of the diagonal dynamics	102
10.3.2	Discussion of individual secular terms	103
10.4	Nonequilibrium energy relaxation	106
10.4.1	Equilibrium energies	106
10.4.2	Nonequilibrium energies	107
11	Discussion of the dynamics of a quenched Fermi liquid	109
11.1	Short-time quasiparticle buildup and nonequilibrium transient state	109
11.1.1	Buildup of a correlated many-particle state	109
11.1.2	Nonequilibrium transient state	110
11.2	Long-time behavior – Thermalization	112
11.2.1	Self-consistent treatment of the momentum distribution	112
11.2.2	Quantum Boltzmann equation	113
11.3	Physical origin of the observed dynamics	115
11.3.1	Delayed relaxation caused by Pauli principle and translation invariance	115
11.3.2	Generalization to large class of interactions	115
11.4	Comparison of the Hubbard dynamics	115
11.4.1	Hubbard model in one dimension	115
11.4.2	Bose-Hubbard model in one dimension	117
11.5	Numerical confirmation of the results	118

12 Conjectures on the generic nature of the findings for a quenched Fermi liquid	121
12.1 Similar observations in other many-particle systems	121
12.1.1 Spin relaxation in the ferromagnetic Kondo model	121
12.1.2 Interaction quench in the sine-Gordon model	122
12.2 Synopsis of the discussed findings	122
12.2.1 Conclusion on the behavior of integrable model systems	123
12.2.2 Conclusions on the behavior of nonintegrable model systems	123
12.3 Formulation of conjectures	124
12.4 Call for debate	124
III Outlook	125
13 Nonequilibrium physics of a system with a Fermi-liquid instability	127
14 Keldysh approach to time dependent switching processes	129
14.1 Different requirements in the case of slow switching	129
14.2 Second order nonequilibrium perturbation theory for the Hubbard model . .	130
14.2.1 Momentum distribution from Keldysh component Greens function . .	130
14.2.2 Nonequilibrium Feynman rules for Hubbard interaction	130
14.2.3 Discussion of vanishing diagrams	131
14.2.4 The 'setting sun' diagram	132
14.3 Explicit calculation of the second order correction to the Keldysh component	133
14.3.1 Noninteracting Greens functions and polarization operator	133
14.3.2 Keldysh component Greens function	133
14.3.3 Linear ramp up of a time dependent interaction	135
14.4 Evaluation of the momentum distribution	135
14.4.1 Result for a linear ramping of the interaction	135
14.4.2 No secular terms	136
14.4.3 Limiting cases for the linear ramping	136
14.4.4 Comparison of the Keldysh and the flow equation approach to the nonequilibrium momentum distribution function	137
14.4.5 Kinetic energy	138
14.4.6 Addressing nonequilibrium BCS behavior	139
15 Further prospects	141
15.1 Further analysis of the quenched Fermi liquid	141
15.1.1 Higher correlation functions and other observables	141
15.1.2 Calculation to higher orders for the momentum distribution	141
15.2 Further quenches in the Hubbard model	142
15.3 Nonadiabatic switching processes and fully time dependent Hamiltonian . . .	142
15.4 Measuring non-adiabaticity in systems with a continuous energy spectrum . .	143
15.5 Extension to the nonequilibrium Bose-Hubbard model	143
16 Conclusions	145

IV Appendix	149
A Brief dictionary of definitions, formulae and commutators	151
List of Figures	153
List of Tables	155
Summary in German language	157
Acknowledgements	159
Bibliography	161
List of Previous Publications	177

Abstract

The study of the interplay between interaction-induced correlations and nonequilibrium initial conditions in many-body systems has recently attracted a lot of attention. New experimental techniques provide high control over many-body systems and systematic access to their nonequilibrium regime: Detailed geometries in heterostructures allow for nonequilibrium transport measurements in correlated systems, pump-probe experiments for time-resolved study of many-body relaxation in molecules and solids and ultracold atom gases loaded onto optical lattices for high control of system parameters in real time. In all of these fields of research the nonequilibrium properties of a Fermi liquid can be relevant. A first approach to their understanding is the main content of this thesis.

At the beginning I will first collect a variety of nonequilibrium phenomena and introduce to basic questions and concepts for their study (cf. chapter 1). Then Landau's theory of a Fermi liquid (2), the Hubbard model (3), time evolution in quantum mechanics (5), related experiments (4), and the flow equation method (8) are reviewed.

The key observation of this thesis, namely a characteristic mismatch of expectation values in equilibrium and nonequilibrium, is first illustrated for the squeezed oscillator (6). For this one-particle model Hamiltonian the perturbative approach can be compared with the exact solution and it is seen that the mismatch holds even beyond perturbation theory. Afterwards, these observations are generalized to a larger class of one-particle models (7).

Then the nonequilibrium behavior of a Fermi liquid is examined by analyzing the Fermi liquid phase of the Hubbard model in more than one dimension. After a sudden switch-on of a weak two-particle interaction to the noninteracting Fermi gas the relaxation of the many-body system is observed. For this purpose, the flow equation transformation is implemented for the Hubbard Hamiltonian (9). This technique applies a continuous sequence of infinitesimal transformations which are defined to make the Hamiltonian approximately diagonal in energy. Its unitary character implies the transformation of all observables which turns out to be a major merit of this approach (10). Then the discussion of the momentum distribution function and of the kinetic energy displays a three-step relaxation behavior of the Fermi liquid from the initial perturbation until thermalization is reached (11). Firstly, the sudden switch inserts excitation energy into the system which drives the following dynamics. Then a rapid initial build-up of correlations is caused by initial dephasing and leads to the establishment of a quasiparticle picture. By that the system enters into a quasi-stationary state which can be long-lasting for weak interaction. This state shows prethermalization of the kinetic energy which already has relaxed to its final values. However, the momentum distribution still resembles a zero temperature Fermi liquid. Its later relaxation on a second time scale is caused by a residual two-particle interaction which allows for scattering processes and can be described by a quantum Boltzmann equation. The physical origin of this delayed relaxation can be traced back to an interplay of translational invariance of the Hubbard model and the Pauli principle for fermions; together they restrict the phase space for scattering events. Comparing with similar work I conjecture on the generic nature of the findings made for the quenched Fermi liquid in other many-body systems (12).

Finally I point out to the potential relevance of the delayed relaxation for the observation of further nonequilibrium phenomena, for instance in BCS systems (13). In order to extend the study of sudden switching to arbitrary switching processes the calculation is repeated using the Keldysh perturbation theory (14). First evaluations for a linear increase of the interaction strength are given. Extensions of this work are suggested (15) and motivate further research.

Part I

Introduction

Chapter 1

The world beyond equilibrium

Nonequilibrium phenomena are ubiquitous in virtually all aspects of all-day life as well as of scientific research, and they can boast themselves with a great reputation: While nonequilibrium processes, starting with nuclear reactions deep inside the sun, radiative energy transport towards earth, the induced convective transport by atmospheric winds or oceanic currents, the build-up of complex organic structures in living cells or the collective and reactive behavior of human societies (including all functions of their technologies) are essential to sustain all life, their missing has to be imagined as a completely equilibrated world, free of any dynamics beyond that of quantum or thermal fluctuations and aptly described as heat death. Therefore it should not surprise that scientific research reaches out to study nonequilibrium phenomena. Up to now, their behavior has been and is continuously addressed in a multitude of publications stemming from many branches in the physical, chemical, biological, economical, and social sciences as well as engineering, reaching from the structures of the universe down to the behavior of elementary particles.

Similarly omnipresent are many-particle systems, even when restricting to the domain of the physical sciences. From the constituents of nuclear matter, via large molecules to macroscopic systems of liquids or crystals — all of them combine a large number of elementary degrees of freedom. The resulting collective properties of the condensed particles can be fundamentally different from their individual behavior: While valence electrons are fairly well bound to individual atoms of a metal, they delocalize in a metallic crystal. There they form a quasi-free gas of crystal electrons which is responsible for characteristic properties like the electric resistance, heat conductance or optical reflectivity. Moreover, in a many-particle system correlations between particles can exist. For noninteracting particles strong correlations already originate from quantum statistics. For instance, particles which obey the Fermi-Dirac statistics (fermions) are severely constrained by the Pauli exclusion principle which forbids the multiple occupation of a quantum state and leads to the description of a Fermi surface in momentum space. Moreover, interacting particles are additionally correlated because of interaction effects. Depending on the kind and strength of the interactions this implies that the elementary degrees of freedom are different from those of a system of noninteracting particles. Generically, this difference may be large. For zero temperature fermions, however, one has to relate the newly generated correlations to those induced by the Pauli principle. Since the latter implies a huge degeneracy of the Fermi system, in many cases interaction effects due to various interactions create generic correlations which can be described in the rather universal language of Landau's Fermi liquid theory.

Therefore it is a natural question to combine these two aspects and address the nonequilibrium behavior of a generic weakly interacting fermionic many-particle system, namely the nonequilibrium Fermi liquid.

1.1 Fundamental concepts of nonequilibrium physics

The first challenge when addressing nonequilibrium physics is the ample field of very different phenomena carrying this label. Limiting oneself, for the first, to current research in classical physics, one finds as versatile examples as nonlinear dynamics of complex systems in classical mechanics [1], turbulences in hydrodynamical systems and pattern formation [2], diffusive heat transport [3–5], the amorphous ground state of materials like glasses [6], and many more.

They share the common feature that they are not explained by the sole reference to the (equilibrium) ground state properties of a suitable theory. Instead, excited states become important. While a system in (one of) its ground state(s) is, typically, dynamically invariant, excited states may introduce a nontrivial time dependence. Hence I ground a first classification of nonequilibrium phenomena on the rôle which time plays in three different scenarios. Each of them originated from its own branch of research and will serve to illustrate one aspect of nonequilibrium systems which will become influential – in a more or less direct way – in the understanding of a nonequilibrium Fermi liquid.

1.1.1 Transport

Thermodynamic understanding of transport

Transport is an effective thermodynamic concept on the level of macroscopic quantities. While equilibrium thermodynamics can be grounded on extremal principles for thermodynamic potentials, transport theory discusses open systems which are subjected to both the proliferation of a transportable extensive quantity like energy, matter, charge, etc. and a sustained gradient of an intensive parameter like temperature, a chemical or electrical potential, etc. The emerging transport is described by a transport equation which links the flux of the extensive quantity (a temporal derivative) to a spatial derivative of the intensive parameter. An electric current, for instance, is linked to its causal origin, an electric voltage. The conventional thermodynamic description of transport assumes that the transport equation is a linear relation with a constant coefficient. Historically important examples are Fourier’s law, Fick’s law and Ohm’s law for dissipative heat, particle and electric transport, respectively. For convenience, I illustrate only the commonly discussed regime of steady state transport for which fluxes do not depend on time.

Statistical understanding of transport

In 1896 Ludwig Boltzmann presented in his *Lectures on Gas Theory* [7] a statistical interpretation of thermodynamics based on a probabilistic theory of microscopic motion. The underlying statistical concept of equipartition in phase space, subject only to a weighting measure given by the Boltzmann factor and otherwise justified by the principle of maximal ignorance of presumably equal states, was seen as the driving motor of all equilibration processes, including transport. This was first studied for dilute gases which became the paradigmatic

model for describing the tendency of dynamical but globally imbalanced systems to achieve equipartition in many fields of physics. In condensed matter systems, transport is typically discussed for gas-like quasiparticle systems like (crystal) electrons (to describe electric currents) or the bosonic gas of phonons (heat transport) [8]. Recent research has widened the view on further transport mechanisms like active transport, e.g. in biological systems or to simulate traffic flows. A paradigmatic model for such active transport processes, the 'totally asymmetric simple exclusion process (TASEP)' counts among the most studied models of nonequilibrium phenomena [9].

Linear response and the fluctuation-dissipation theorem

Discussing transport in terms of microscopic models, however, does not always allow to derive linear transport equations. Simple models like the harmonic crystal exhibit ballistic instead of diffusive heat transport; there an internal temperature cannot be defined and, consequently, a description based on temperature gradients and transport coefficients is not adequate [10]. The relation between microscopic dynamics and macroscopic transport laws, particularly in the case of low dimensions, remains a current field of research [3–5]. It mirrors the fundamental question of thermalization of excited closed systems which I discuss in section (1.4.4).

The microscopic discussion of transport often starts with the approximation that, to first order, external forces cause the same dynamics of a system as elongations by internal fluctuations. Whenever the effect of external forces can be expressed in terms of a perturbative interaction¹, the linear response of the system (described by a response function) can be related to the equilibrium thermal fluctuations. This important result of linear response theory, now known as the famous fluctuation-dissipation theorem [13, 14], has reduced linear approximations to nonequilibrium problems to equilibrium properties [15]. This has shifted the notion of 'nonequilibrium' in the case of transport to the study of nonlinear response to external forces.

A second approach to steady state transport is by the Boltzmann equation. I will give a thorough introduction to it in section 1.4.5.

I finally briefly note that macroscopic transport in the steady state regime cannot be observed on ideal periodic lattices where electrons, when subjected to a constant external force, undergo Bloch oscillations such that no net transport occurs in the absence of any relaxation process [16, 17].

1.1.2 Metastable states of glasses and spin glasses: avoided relaxation

A second scenario is devoted to many phenomena which are characterized by metastable configurations of excited states. Examples can be as diverse as particular points in phase space of a mechanical motion, metastable chemical substances, energetically disadvantaged structures of large molecules or crystal phases, or radioactive isotopes. As the metastable state corresponds to a local but not global minimum in the free energy landscape, relaxation is hindered by an energy barrier. An analogous idea of inhibitors to nonequilibrium relaxation will be a central element of my interpretation of the nonequilibrium behavior of the Fermi liquid in chapter (11).

¹As M. Michel points out in his very inspiring thesis [11], Luttinger [12] raises doubts whether this is justified for heat transport since there is no Hamiltonian which describes a temperature gradient.

From a nonequilibrium point of view, glasses [6] and spin glasses [18] are particularly interesting although meanwhile some equilibrium approaches to glassy materials have appeared (see, for instance, [19]). Produced by a temperature quench, i.e. a sudden supercooling of a liquid, these systems are, macroscopically, comparable to solids but, microscopically, isotropic and without long-range order, like a liquid. Since the microscopic structure does not correspond to the macroscopic ground state of a crystallized system at the lower temperature, it is regarded as a nonequilibrium configuration. Two time scales appear and can be linked to a separable motional behavior of the particles in a glass: Fast vibrational motions resemble the thermal fluctuations of a particle in a solid, while there is a slow structural relaxation caused by a dispersive particle wandering like in a liquid [20]. The second (slow) time scale relates to aging phenomena which can occur on extremely long time intervals; again this is considered as being caused by a trapping in local minima of a free energy potential landscape and constitutes a metastable state. Moreover, one can relate the two-fold particle motion to the spectrum of fluctuation modes which, at high frequency, already resemble closely an equilibrated thermal distribution. At low frequencies, however, characteristic nonequilibrium becomes most relevant. In chapter (11) I will develop a similar picture for a Fermi liquid and observe nonequilibrium signatures of its momentum distribution particularly within the low-frequency momentum modes around the Fermi surface.

1.1.3 Time dependent nonequilibrium phenomena

Yet most generic are time dependent nonequilibrium phenomena. Those who believe in recent big-bang cosmology may credit them with the existence of all the material world we know and claim that their history is just a tiny bit younger than the history of the universe itself. While the initial state of the universe is assumed as an equilibrium state, characterized by extremely high densities and temperatures (and consequently high reaction rates) which would immediately cancel out any imbalances, nonequilibrium conditions were born by the successive rapid expansion of the universe: energy and particle density became more diluted, particle interactions got weaker, equilibration processes less efficient and thus the growing universe lost its ability to respond immediately to its own dynamics. A new time scale related to its internal equilibration emerged, fell behind the time scale of its dynamical expansion and so a first nonequilibrium episode was entered.

As its most prominent effect, the nucleosynthesis can be explained as a consequence of the competition between the expansion rate of the universe, equilibration processes and temperature dependent production rates [21]. A rapid cooling of the universe was decisive for creating a nonequilibrium distribution of nucleons with an excess of neutrons. Since their equilibration with respect to the weak interaction occurred on a much longer time scale, neutrons did not decay but could be captured by protons and light nuclei to form heavier and stable compounds.

Although this example can be counted among scientific folklore, it illustrates the dramatic influence nonequilibrium initial conditions may have on the later dynamics. Hence for a time dependent nonequilibrium system both the transient behavior and the long-time limit of its evolution are relevant questions. In section (1.4.4) I will discuss recent approaches for quantum systems to answer the second question without answering the first one, referring only to the initial nonequilibrium conditions. While for a deterministic theory which includes all aspects of the evolution the initial conditions already do determinate the final state, both for the universe and for the nonequilibrium Fermi liquid the interesting behavior lies in between.

This motivates my study of the time evolution of some of its observables.

1.2 Definition of a quantum quench

1.2.1 Nonequilibrium initial conditions

In general a system in nonequilibrium is described by two pieces of information: Firstly, the Hamiltonian contains the full dynamics of an arbitrary state at an arbitrary time. In equilibrium, the Hamiltonian is often already sufficient to discuss the main properties of the system. In nonequilibrium, however, initial conditions have to be specified which describe the deviation of the system from its equilibrium ground state.

In transport problems, where typically stationary nonequilibrium situations are discussed, nonequilibrium initial conditions are given by externally enforced and maintained gradients, e.g. a gradient of temperature, of the electrical potential or of the chemical potential.

However, if time dependent nonequilibrium problems are studied, the initial conditions are set by an initial state which is defined at a certain point in time (say $t_0 = 0$). In order to make for a nonequilibrium problem these states must represent (highly) excited states of the system. Unfortunately, it is difficult to make highly excited many-body states explicit, in particular when correlated systems are discussed. A quench is a simple procedure to bypass this difficulty.

1.2.2 Nonequilibrium initialization of a system by a quantum quench

The simplest way to find an excited state of a system is to use the ground state of a different system (which, certainly, must not agree with the ground state of the earlier system). Then the initial condition can be linked to another Hamiltonian. This motivates the concept of quantum quench: There an initial Hamiltonian $H(t = 0_-)$ is suddenly promoted to the new Hamiltonian $H(t = 0_+)$ by external influence while the state of the system remains, for the first, unchanged. This situation is particularly simple if the initial Hamiltonian represents a noninteracting model and under the quench a perturbation is suddenly 'switched on'. Then the quench initializes an interacting system in the ground state of the noninteracting system. Since the noninteracting ground state can be, in many cases, written down rather straightforwardly this is a convenient setup for dynamical calculations. After the quench the former ground state (which is unchanged) represents an excited state with respect to the later Hamiltonian. Hence, a quench is a convenient way to initialize a many-body system in a nonequilibrium initial condition. For instance, the ionization process in the X-ray edge problem (cf. the next section) constitutes a sudden local perturbation of a many-particle system. In the following, however, the technical term "quench" may be reserved for the sudden change in a *global* (and not local) parameter of the system².

1.2.3 Treatment of quench problems by Hamiltonian diagonalization

In the main part of this thesis I only consider a quench of a static interaction. The sudden switch-on is modeled by the Heaviside step function $\Theta(t)$.

$$H(t) = H_0 + \Theta(t)H_{\text{int}} \tag{1.1}$$

²Nonetheless, local quantum quenches have been examined in some cases, see e.g. [22].

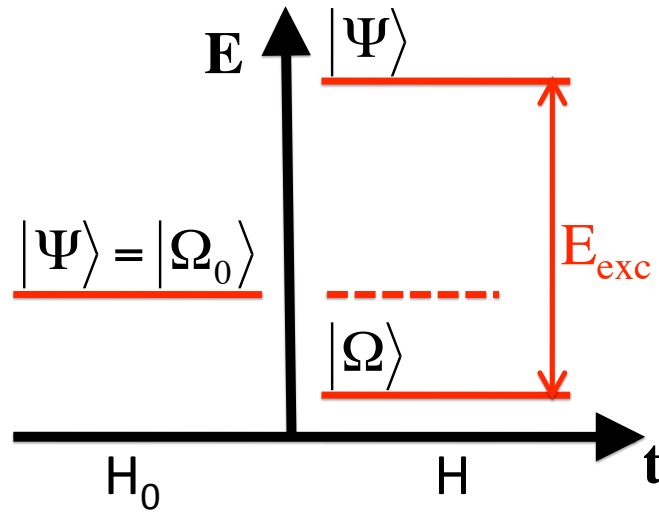


Figure 1.1: Typical energy level relations during a quantum quench. The initial state $|\Psi\rangle$ equals the ground state of the Hamiltonian H_0 , denoted by $|\Omega_0\rangle$ (left hand side). The state $|\Psi\rangle$ remains unchanged under the quench; however, its energy is now given with respect to the changed Hamiltonian H by $E_{\Psi,H} = \langle\Psi|H|\Psi\rangle$. For comparison, the ground state of the quenched Hamiltonian $|\Omega\rangle$ is sketched; in general its energy differs from that of $|\Omega_0\rangle$. The excitation energy E_{EXC} after the quench is indicated.

This implies that the quench problem is not a truly time dependent problem but can be represented as a time independent Hamiltonian with a particular initial condition. In this sense quench scenarios resemble the exact one-particle solution of the X-ray absorption and emission problem in metals by P. Nozières and C. T. de Dominicis [23] (see the discussion of the X-ray problem in section 1.3.1 at the beginning of the following page).

The observation that any time dependence can be attributed to initial conditions is important since it sets the technical frame for the main part of this thesis: For a time independent Hamiltonian, the eigenbasis representation is privileged as there the time evolution of the eigenstates decouples. Therefore diagonalization, i.e. transforming into an (approximate) eigenbasis representation, is advantageous; in this thesis it even is the decisive step of studying the time evolution of the system that follows the quantum quench. This diagonalization is performed for one-particle systems in chapter 6 and 7 as well as for the quenched Fermi liquid in chapter 9.

1.2.4 Energetic implications of a quench

At the time of the quench, the system is open for the exchange of energy with an unspecified environment that enforces the quench. Moreover, the state of the system $|\Psi\rangle$, once the ground state of the initial Hamiltonian $|\Omega_0\rangle$, has to be re-interpreted as an excited state with respect to the ground state of the quenched Hamiltonian $|\Omega\rangle$. Both aspects together allow to draw the generic energy level diagram of a quantum quench (see Fig. 1.1).

1.3 Nonequilibrium phenomena in correlated many-body quantum systems

1.3.1 The X-ray edge problem

One of the earliest examples for sudden time-dependent manipulations of many-body systems is known as the X-ray edge problem which has been extensively studied in the late 1960ies [23–26] and reviewed, for example, in [27]. By X-ray scattering an electron is excited from a deep level and a localized deep hole is created. It serves as a suddenly switched on but transient scattering center for conduction electrons which react according to two competing many-body effects: the Anderson orthogonality catastrophe [28] reduces the overlap of the ionized and non-ionized ground state and suppresses the absorption process; on the other hand the additional charge transferred into the conduction band gives rise to a many-body enhancement [29]. Together, they account for a characteristic resonance in the X-ray absorption or emission spectra near the Fermi level threshold. Long readjustment times of the electrons at the Fermi surface to the changed environment are its physical origin [25]. Recombination finally switches off the scattering potential.

Since it turned out to be tractable by many different approaches, the description of the X-ray absorption and emission problem stimulated the development of new techniques to analyze the many-body response of an electron gas to a temporary defect, i.e. to a time dependent scattering potential. Firstly, this potential was understood as a many-body interaction and treated diagrammatically by means of Abrikosov’s many-body perturbation theory. A summation of parquet diagrams allowed to reproduce the X-ray resonance [25]. An extended self-consistent formulation followed [26], as well as an explanation based on an early bosonization approach [30]. The already mentioned interpretation of the problem as a one-particle scattering potential [23] which is switched on by the radiative creation of the hole and remains constant until its recombination can be read as an early exhibition of a quantum quench scenario. There the time dependence of the potential can be fully included into initial (and final) conditions of the evolution. Pointing out and comparing to the later discussion of an interaction quench in a Fermi liquid, which constitutes the key part of this thesis, a difference has to be mentioned: In the X-ray edge problem a quantum quench is performed only locally (i.e. at the position of the static hole a local potential is switched on and off), while in the case of a Fermi liquid, which is modeled on a lattice, the two-particle interaction is changed on every lattice site.

I briefly mention that later a special nonequilibrium version of the X-ray problem was investigated. It is characterized by the presence of two Fermi seas with different chemical potentials. Such research was stimulated by the observation that the different approaches mentioned above, which all lead to equivalent predictions in the equilibrium case (i.e. in the presence of only a single Fermi sea), provide different answers when applied to the nonequilibrium X-ray edge problem [31–33]. The study of the nonequilibrium X-ray problem in mesoscopic systems has been a recent interest in this field of research [34–36].

1.3.2 Nonequilibrium dynamics of spin systems

Motivated by the idea to test approaches and approximations applied in nonequilibrium statistical mechanics in a nontrivial but exactly solvable model system Barouch et al. discussed the nonequilibrium behavior of the quantum mechanical XY-model in 1970 [37]. Then it took several decades until new interest in the examination of interacting model systems in nonequi-

librium came up. In the 1990ies, the discussion of spin glasses fostered a revival of studies about the real-time dynamics of nonequilibrium quantum spin systems for understanding their aging phenomena [38, 39]; for the Ising spin chain long-range correlations were found following the front of a coherent spin signal [40]. Interest in the nonequilibrium properties of paradigmatic spin models [41] focussed on their response to driven quantum phase transitions at quantum critical points by either a sudden switch of model parameters, i.e. by a quantum quench [42–45] or by a dynamical approach towards a phase transition [46–49]. While in quantum phase transitions quantum fluctuations become important and may vitiate the validity of approximative approaches (like mean-field theory or perturbative expansions, c.f. [41]), quantum critical points often exhibit symmetries which allow for a mapping to exactly solvable models. Those serve as theoretical laboratories to study in many-body systems two nonequilibrium effects which I will briefly discuss here.

1.3.3 Kibble-Zurek mechanism

For many second-order and continuous phase transitions driven non-adiabatically through a critical point the production of topological defects can be observed or has been predicted. Examples are phase transitions in ^4He and ^3He [50–52], nematic liquid crystals [53–55], superconductors [56, 57] and ultracold atoms in optical lattices [58, 59]. The underlying mechanism was formulated by Kibble and Zurek [60, 61] and is grounded on the paradigmatic Landau-Ginzburg theory for equilibrium phase transitions. There the free energy (a thermodynamic quantity) is expanded in (even) powers of the order parameter and the phase transition is signaled by a symmetry breaking [62]. Nonequilibrium conditions, i.e. driving, enter by making the control parameter of the transition time dependent; typically this is the relative value of, e.g. temperature or pressure, with respect to their values at the critical point. In the Kibble-Zurek framework the control parameter is linearly approaching the phase transition in time [63]; hence the timescale of the driving is controlled by the (fixed) rate at which the control parameter is changed. Simultaneously, the correlation length of the system increases (it diverges at the critical point) and its response to the parameter change slows down until a second time-scale, the relaxation time, diverges at the critical point, too. As soon as the time scale of the driving becomes comparable to the relaxation time, the order parameter loses its ability to adjust to the imposed changes, the correlation length is frozen in, and a nonequilibrium regime is entered. In the Kibble-Zurek picture, this sets the initial configuration for the following nonequilibrium dynamics. The freezing of the correlation length implies that the order parameter cannot completely relax but stable topological defects remain, distributed on a scale set by the frozen correlation length³. This result has motivated the suggestion to explain the mass distribution of the universe or the inhomogeneities of the cosmic microwave background as originating from topological defects caused by nonequilibrium phase transitions in an early era of its existence [63].

The Kibble-Zurek mechanism illustrates that nonequilibrium driving of a system can lead to a permanent locking of features which are present in the initial configuration (that one

³I repeat this for a recent example [59]: If the temperature of a bosonic gas is lowered towards the transition temperature of the Bose-Einstein condensation, regions with an extension set by the scale of a finite correlation length exhibit *independently of each other* phase coherence. Thus the phase of the wavefunction – an order parameter of the transformation – is constant only within these regions. Finally, these regions merge to form a single condensate with a continuously varying order parameter. The continuity requirement, however, can lead to topological defects.

when the nonequilibrium region is entered) and appear as defects in a later regime. Hence relaxation of such a system to its new equilibrium ground state (or thermal ground state, if conservation of excitation energy is expected) is generically prohibited by a memory of initial conditions. Seen in the light of the discussion of chapter (1.4.4) it would be interesting to discuss, for instance, the importance of integrability on the defect production.

1.3.4 Landau-Zener problem

While the Kibble-Zurek formalism addresses the non-adiabatic approach to a thermodynamic phase transition, the non-adiabatic transition between the levels of a quantum mechanical, coupled two-level system is known as the Landau-Zener problem [64–66]. One assumes that the difference between the (bare) energy levels $\epsilon_i(B(t))$ depends on a continuous parameter $B(t)$, which can be tuned in time. The coupling between the leads may be nonvanishing and, for convenience, in all cases time independent. The Landau-Zener problem became a paradigmatic example for the description of dynamical nuclear or atomic collisions, the dynamics of chemical reactions, and the behavior of quantum systems in time dependent external magnetic or electric fields [67–71].

In the adiabatic case, i.e. for arbitrary slow parameter variation, and due to the nonvanishing coupling, the energy levels exhibit an avoided crossing with an energy gap Δ of two times the coupling strength. This means that the eigenvalues of the two-level system approach each other up to this minimal distance in energy and then recede while the corresponding eigenfunctions exchange their character. An initial ground state occupation always remains in the lowest energy state (which, however, changes at the avoided crossing).

In the non-adiabatic case, the parameter variation is such that difference between the (bare) energy levels depends linearly on time, i.e. there is a constant parameter velocity $v = |\frac{d}{dt}(\epsilon_1 - \epsilon_2)|$. For simplicity, time varies from $-\infty$ to ∞ . Now transitions into the energetically excited state become possible. More precisely, there is a nonvanishing probability that an initial ground state occupation remains in the former ground state even if its energy is raised beyond that of a later ground state. Thus the Landau-Zener problem, again, is an example that nonequilibrium conditions (here: driving) may prevent optimal relaxation of a system. The differential transition probability into the new ground state is largest at the (avoided) crossing of the energy levels since it depends on the energy difference between the interacting states. Therefore, the parameter velocity enters exponentially into the exact solution of the integrated transition probability P

$$P \sim e^{-\frac{\pi^2 \Delta^2}{\hbar v}} \quad (1.2)$$

Note that the exponential dependence results from a nontrivial quantum interference of contributions arising from the approach to and the recession from the avoided crossing.

The Landau-Zener formula (1.2) holds analogously for non-adiabatic transitions in multiple level crossings [72, 73] and the Landau-Zener problem has recently found a revival in the discussion of driven many-particle systems [74–76]. Other works presented a close link between Landau-Zener physics and the Kibble-Zurek mechanism: the transition from the initial ground state to the final ground state can be compared with a phase transition such that the Landau-Zener problem can be restated as a quantum analogue for the Kibble-Zurek mechanism. Then the inverse of the energy gap between the states of the two-level system at a particular point of time in a Landau-Zener transition represents the relaxation time in the Kibble-Zurek

mechanism and the occupation of the excited state is a measure for the created topological defects. In such a simple model, the dependence of their density on the parameter velocity (quench rate) agrees with Kibble-Zurek predictions [77]. Regarded from the opposite point of view, driving the exactly solvable quantum Ising model through its critical point can be described as a sequence of Landau-Zener transitions for suitably defined quasiparticles [47]. For the sweep through the critical point of an anisotropic XY chain a multi-particle Landau-Zener approach has been developed [48]. A Jordan-Wigner fermionization of the spin model allows to reduce to a Landau-Zener problem in each fermionic momentum mode separately. Then the crossover scale from adiabatic to non-adiabatic behavior, i.e. the minimal velocity for non-adiabaticity, becomes momentum dependent. Similarly, a characteristic crossover momentum can be defined which corresponds to the correlation length (i.e. domain size) at that momentum value. The exactly calculated correlation functions decrease exponentially and monotonically for fast sweep speed, crossing over to oscillatory behavior at slower speed.

1.3.5 Nonequilibrium dynamics of BCS systems

While the nonequilibrium examination of spin systems pioneered in the field of nontrivial time-dependent phase transitions, the discussion of the nonequilibrium behavior of BCS systems subjected to a quantum quench focussed on the time behavior of the order parameter [78–82].

BCS theory [83] has been introduced in 1957 as an effective model for superconductivity in many-particle systems; an attractive pairwise interaction between constituent fermions gives rise to a Fermi liquid instability towards the formation of bound *Cooper pairs*. Their anomalous expectation value acts as the order parameter of the superconductivity phase transition; by a mean field calculation, it can be identified with an energy gap Δ in the one-particle spectrum. In nonequilibrium, the dynamics of the order parameter following a quantum quench either exhibits persistent oscillations or a decay towards a constant steady state value, depending on the initial state before the quench [81]. This is because the BCS mean-field dynamics is integrable, thus the initial conditions are memorized by the state of the system and the properties of the order parameter are frozen for all later times. Therefore, a classification scheme allows to predict the long time behavior directly from the initial state without solving the equations of motion.

Similar observations have been made studying the BCS to BEC crossover in fermionic condensates. A quantum quench is implemented by a sudden shift in the position of a Feshbach resonance. Depending on the initial state, the quench triggers coherent oscillations in the order parameter and oscillatory 'hole burning' in the momentum distribution [84], or it does not [85].

1.3.6 Nonequilibrium dynamics of lattice systems

It is convenient to study many-particle systems on the restricted geometry of a particular lattice. For a variety of models, the nonequilibrium properties of interacting lattice particles have been examined using quantum quenches. Examples in one dimension include a generalization of BCS theory, the Richardson model [86], 1D hard-core bosons [87–89], the Bose-Hubbard model [90], the quantum sine-Gordon model [91, 92], the Luttinger liquid [93, 94], and strongly correlated spinless fermions [95].

In more than one dimensions, only few results are available, e.g. for the Falicov-Kimball model [96] or in optical (super-)lattices [97].

1.4 Questions and concepts in time-dependent nonequilibrium many-particle systems

From the abundance of example systems for which quantum quenches have been studied some general questions and approaches can be distilled. They form a conceptual framework which underlies my further discussions.

1.4.1 Time scales

In a time dependent many-particle problem various time scales may be present. Since the sudden parameter change in a quantum quench does not introduce an independent time scale related to the switching procedure itself (no 'ramp-up' time), all time regimes originate from the intrinsic energy scales of the discussed model, e.g. interactions and couplings, a bandwidth, etc. Naturally, scales related to the quenched parameter, to a possible energy or momentum intake, etc. should be most important. Nonetheless, the nonequilibrium dynamics of a model system following a quantum quench may be interesting on further time scales and a separation of different time regimes may occur. Then, for instance, transient behavior can be distinguished from the long-time limit.

Questions addressed to transient behavior

Typically, transient behavior of a time dependent system refers to its early evolution after a perturbation has been applied but before a periodic state or a (meta-)stable steady state is reached. It often depicts the dynamics of (highly) excited states which, whenever no restrictions are in place, relaxes. Consequently, questions may address the kind and the time scale of this relaxation process, the characterization of possible intermediate states, the underlying physical processes which generate the early dynamics, possible restrictions to their dynamics, a dependence on the details of the quench and, in particular, a memory of the initial conditions.

Questions addressed to the long-time limit

Due to accumulating errors, approximate calculations of time dependent quantities often become less reliable with increasing time. This may complicate the evaluation of the long-term behavior of quenched systems. In particular, many established numerical techniques suffer from this constraint. If, however, an approach to long time scales is possible, one may ask if the limiting state exhibits periodic variations (e.g. 'collapse and revival'), or if it is a steady state. For a steady state, the question of quantum thermalization (see below) becomes relevant, including the issues of a potential memory of initial conditions, a suitable classification of the initial states (e.g. in terms of a nonequilibrium 'phase diagram' [90]), the applicability of generalized statistical ensembles [88], etc.

1.4.2 Time evolution and integrability

The time evolution of any classical or quantum mechanical system can be described by a set of coupled equations of motion. For given initial conditions, they represent a deterministic and complete description of the state of the system at any point in time.

Classical systems

Integrability, however, implies more than the practicality of having found an analytical, closed solution for these equations of motions. Let us consider a classical Hamiltonian system $H(p_i, q_i)$ which does not explicitly depend on time. Then integrability can be defined as *canonical integrability*, arising when a canonical transformation exists which allows to represent the Hamiltonian in action-angle variables $H(\mathcal{A}_i, \phi_i)$ [98]. Then the action variables represent invariant frequencies of the motion and a set of as many smooth, functionally independent conserved integrals of motion exists as there are degrees of freedom. These conserved quantities incorporate a precise and lasting memory of the initial conditions which is, for instance, robust against time averaging over the trajectory of the motion. They constrain the dynamics of an integrable system: its phase space is foliated into invariant submanifolds (so-called 'tori') and the motions on them is quasi-periodic. Hence, integrable systems are not ergodic (see below).

Quantum mechanical systems

In quantum mechanics, time evolution is always a linear operation generated by the Hamiltonian and acting on the Hilbert space of quantum mechanical states. Unfortunately, quantum integrability is less well-defined than classical integrability⁴. This can be motivated by noting that all physically allowed Hamiltonians can be –in principle– diagonalized. Again, let me restrict to time independent Hamiltonians for which diagonalization is a meaningful approach. The diagonal representation of the Hamiltonian in terms of dynamically decoupled eigenmodes shows that there always exists a set of conserved quantities. This is obvious for the occupation numbers of all eigenmodes. Corresponding good quantum numbers, i.e. the expectation values of the eigenmodes with respect to a complete set of commuting observables, are time invariants. In consequence, quantum time evolution can always be described as a pure dephasing of eigenmodes with constant mode occupation. Hence, generic differences (which hold for arbitrary initial states) between integrable and nonintegrable models can be expected to show up in the spectral distribution of eigenvalues. Studies on quantum chaos have suggested universal characteristics in the statistical distribution of eigenenergies as a criterion to differ between integrable and chaotic (nonintegrable) systems. The Bohigas, Giannoni and Schmidt conjecture [101], which is based on numerical calculations, postulates that whenever the nearest-neighbor spacing distribution of the quantum eigenenergies obeys a Wigner-Dyson distribution for the Gaussian orthogonal or unitary ensemble, chaotic behavior is observed. On the other hand, Poissonian statistics indicates integrability. Under the assumptions of this conjecture, generic integrability in quantum systems appears to be a spectral property of the model. In 2004 the 'semiclassical core' of a proof based on linking

⁴Although formal correspondence between classical and related quantum models has been engaged and action-angle operators have been suggested, a fully satisfying link between classical integrability and quantum integrability has not been reached (c.f., for instance, [99, 100]).

classical chaos to universal level statistics of corresponding quantum systems was given [102] and the Bohigas, Giannoni and Schmidt conjecture put onto solid grounds [103].

Particular situations like the time evolution of different initial states of a fixed model system can be analyzed by looking at the overlap matrix elements of the initial state and Hamiltonian eigenstates [86] or elements of the density matrix containing equivalent information [104]. Such approaches may also be suited for Hamiltonians which are integrable only within some limited parameter regimes but are nonintegrable otherwise.

Examples for integrable condensed matter model systems solved by Bethe ansatz techniques include the spin-1/2 quantum spin chain [105], the fermionic Hubbard model in one dimension [106], the Kondo model [107], the single impurity Anderson model [108], or the Richardson model [109].

The Bose-Hubbard model in one dimension, for which a Wigner-Dyson distribution of eigenenergies has been observed in some parameter regime [110], or the fermionic Hubbard model in more than one dimension, however, are examples for nonintegrable quantum many-body model systems.

1.4.3 Ergodicity and thermalization in classical systems

Although the analysis of classical systems is not part of this thesis, it is instructive to discuss the background of the thermalization debate as it developed historically. While some conceptual ideas outreach into a similar debate for quantum systems, the reader may be reminded that a close and direct correspondence does not always hold.

Deterministic vs. probabilistic theories

The great scenery of physical descriptions can be divided into two hemispheres: On the one hand, deterministic dynamical theories like Newton's mechanics or quantum mechanics aim at the derivation of precise evolution equations which allow to develop the state of a system at any time from some initial conditions. Knowing the later already determines the behavior of the system completely. On the other hand, probabilistic theories like classical or quantum statistical mechanics establish results by applying statistical methods to ensembles of systems which are in microscopically different configurations but show the same behavior of macroscopic observables. Both approaches are fundamentally different. While deterministic dynamics is time reversible, statistical descriptions do not keep memory on particular microscopic configurations. This apparent conflict is one of the main roots of many difficulties whenever relations between probabilistic and deterministic theories are discussed.

Classical ergodicity, Boltzmann hypothesis and thermalization

For classical physics, it was Boltzmann and Maxwell who tried to bridge this gap and to set up a dynamical foundation of statistical mechanics almost 150 years ago. A cornerstone of this approach is Boltzmann's ergodic hypothesis [111] which assumes the coincidence of a statistical and a dynamical description of a system by the equivalence of two averages taken for an arbitrary observable $\mathcal{O}(\{q_i(t), p_i(t)\})$:

$$\left(\prod_{i=1}^N \int dq_i dp_i \right) \mu(\{q_i, p_i\}) \mathcal{O}(\{q_i(t), p_i(t)\}) \stackrel{!}{=} \lim_{T \rightarrow \infty} \frac{1}{T} \int_{t_0}^{t_0+T} dt \mathcal{O}(\{q_i(t), p_i(t)\}) \quad (1.3)$$

Firstly, the statistical (thermal) average of this observable with respect to an ensemble of phase space configurations taken at a fixed point in time. Only those configurations which are in consistence with trivial constants of the motion (those which correspond to thermodynamic parameters, e.g. energy) contribute. This constrains the statistical average effectively to an energy hypersurface in phase space where the normalized probability measure μ is nonzero. Secondly, the time-averaged value of the observable as it is obtained from the solution of its equations of motion, is restricted by the same constants of the motion. It is assumed that it coincides for almost all macroscopically equivalent initial conditions. If Boltzmann's hypothesis holds a system is called ergodic.

The question of thermalization of a system is closely related to ergodicity but stronger motivated from a dynamical point of view. It asks whether the dynamical evolution of a system from a particular initial point in phase space onwards finally approaches a state which resembles a statistical thermal state. For all practical purposes, this can be expected since unavoidable couplings of a system to a thermal environment finally cause equilibration at an external temperature. Discussed for the theoretical concept of a closed system with many degrees of freedom, however, it focusses on the necessary loss of time reversibility. Time averaging the deterministic dynamics like in (1.3) is a possible way but only meaningful if the related averaging time T is not too large with respect to the intrinsic time scales of the dynamics. (Obviously, a slowly varying sequence of various microscopic states does not appear as a thermal state.)

Obviously, integrable systems are neither ergodic nor do they thermalize since their motion is restricted to submanifolds of the phase space only. While Boltzmann assumed that small perturbations would always render an integrable system ergodic, later observations exposed that this may not always be the case. Thus contrary to Boltzmann's intuition nonergodic behavior is the stable behavior of a certain class of physical systems.

Fermi-Pasta-Ulam problem

While the non-ergodicity of integrable systems was a matter of debate already in the 19th century, studies of nonintegrable models had to wait for the availability of sufficiently powerful computing facilities in the early 1950s. Then Fermi, Pasta and Ulam together with Mary Tsingou numerically integrated the equations of motions for a one-dimensional chain of classical oscillators subject to a weak ($\alpha = 1/4$) anharmonic perturbation defined by the Hamiltonian

$$H = \frac{1}{2} \sum_{k=1}^{N-1} P_k^2 + \frac{1}{2} \sum_{k=0}^{N-1} (Q_{k+1} - Q_k)^2 + \frac{\alpha}{3} \sum_{k=0}^{N-1} (Q_{k+1} - Q_k)^3 + \frac{\beta}{4} \sum_{k=0}^{N-1} (Q_{k+1} - Q_k)^4 \quad (1.4)$$

and initialized in the unperturbed ground state mode only. Surprisingly, they could not find the expected approach to thermal equilibrium with equipartition of energy onto all degrees of freedom. Instead, an almost complete revival of the initial state was reached after a time much shorter than the Poincare recurrence time of the system. This observation entered the scientific literature as the Fermi-Pasta-Ulam problem (FPU) and from their seminal preprint [112] an ample field of research into the long-time dynamical behavior of nonlinear systems developed [113]. Nonetheless the FPU remained the benchmark problem for the discussion of ergodicity and thermalization in classical and in quantum systems and continues to fuel ample consecutive research [114].

Dynamics of the Fermi-Pasta-Ulam problem. Since the dynamics of the classical Fermi-Pasta-Ulam problem is in great analogy with the main results of this thesis for a quantum many-body system its key features are briefly presented. In the beginning, the energy of the ground state is partially transferred to a small number of modes with shorter wavelengths. They are excited one after another as, for weak interaction strength $\alpha \ll 1$ and a linear dispersion relation $\omega_i \approx \pi i/N = i\omega_1$, acoustic resonance conditions hold approximately between the oscillator modes. Since these excitations happen on a short time scale they are referred to as 'secular avalanche' [115]. However, if the energy content of the initial state is not too large this cascade of energy transfers stops at a critical mode when the resonance condition is not matched any more. Therefore, instead of instant equipartition of energy (i.e. thermalization) a quasi-steady state is reached. Its energy spectrum is exponentially localized in the long wavelength modes, the time for its buildup sets the first time scale of the FPU dynamics. Following the lines of a similar analysis for the nonlinear Klein-Gordon equation [116], the metastable character of this state has been first proposed in analogy with the behavior of glasses [117]. Later a further phase of the FPU dynamics which leads to equipartition of energy has been numerically confirmed. This gives rise to a second relaxation time scale in the FPU problem. While it is commonly assumed that both time scales are well-separated for small excitation energies but merge for energies larger than a critical value, the scaling of the second time scale with the excitation energy or the strength of the nonlinearity in (1.4) is still subject to an intensive debate [118]. Therefore it is only noted that already an early work observed numerically that the equilibration time scale – however in a somewhat special case – could be described by a power law dependence on the strength of the nonlinearity with an exponent close to -4 [119]. This would directly relate to the observations made for the Hubbard model, a many-body quantum model, which are discussed in this thesis.

Stabilization of a transient state by closeness to an integrable model. The observation of a transient state which exists on a long time scale has been related to the closeness of the FPU Hamiltonian (1.4) to other Hamiltonians \underline{H} which are integrable. Early and influential studies by Kruskal and Zabuski applied such integrable approximations and linked the FPU problem, for instance, to the completely integrable Korteweg-deVries (KdV) equation [113]. Its solution space contains solitons which are, in one dimension, localized excitations⁵. Since they are stable solutions they already represent the long-time limit of a KdV-based dynamics and are approximations to the quasi-steady state of the FPU problem.

Recently, another integrable model, the Toda chain model, has been used by Antonio Ponno and collaborators to motivate a three-step dynamics of the FPU problem [115, 120]. The rapid initial resonant energy transfer and the buildup of a quasi-steady state form the first two steps are well-described by the Toda chain model. Since the latter is integrable, its long-time dynamics corresponds to the transient state of the FPU. The thermalization of the FPU dynamics on a third scale has been only observed in numerical simulations and can never be deduced from the integrable model.

However, the idea that the dynamics of closely related integrable models relates to the initial phase(s) of the dynamics of the nonintegrable model forms a general concept for a real-time analysis of almost integrable quantum systems. Then the difference between the integrable

⁵In dimensions two and three there can be plain wave solitons, i.e. wave packets which do not disperse. Similar wave phenomena have been observed already in the 17th century as non-dispersive water waves in the straight channels of the Netherlands.

Hamiltonian \underline{H} and the nonintegrable Hamiltonian H appears as a residual interaction between the "action variables" or "quasiparticles", i.e. between the diagonalized degrees of freedom of the integrable model, and causes a further dynamics. The integrable and the nonintegrable model are closely related to each other if this residual interaction is weak and, therefore, the residual dynamics becomes important only on long time scales.

Mathematical approach to ergodic theory

This approach is backed by substantial mathematical research and ergodic theory became an established field of mathematical physics. Discussion of nonanalytic structures in phase space led to important observations, starting with the **K**olmogorov-**A**rnol'd-**M**oser (KAM)-theorem on the influence of nonintegrable perturbations to integrable Hamiltonians. It revealed the particularities of perturbative expansions which approximate dynamics on a nowhere dense subset of phase space carrying almost the full measure of phase space [113]. For a wide range of initial conditions (the *Kolmogorov set*) this implies dynamical stability and motivates the notion of a 'nearly integrable' system. Outside of this set the action variables are subjected to a drift caused by the perturbation of the integrable model. It is of order one on a very long but finite time scale. This behavior, known as *Arnol'd diffusion* [121], leads to delocalization of an orbit in phase space on a long diffusion time scale. Therefore, thermalization of almost integrable models is possible.

The question of ergodicity of a model, however, remains an unsolved problem. A related result by Markus and Meyer [122] claims that a certain class of infinitely differentiable, but generic Hamiltonian systems is neither ergodic nor completely integrable. This encourages to think of Hamiltonian systems as being integrable for some initial conditions but nonintegrable for others, both with nonvanishing measure in phase space.

1.4.4 Thermalization debate in quantum systems

While in classical physics thermalization is regarded as a consequence of nonlinearities in the equations of motion, time evolution of a quantum system is governed by the linear Schrödinger equation. The state space of classical mechanics and the Hilbert space of quantum mechanical states are disparate and further differences will be pointed out later on. Therefore it is plausible to conjecture that different mechanisms may lead to thermalization in the classical and in the quantum case. Here I will illustrate recent work for open quantum systems [123–127] which supports this conjecture. For closed quantum systems, however, a similar analysis has not been performed so far and less general descriptions applicable to the thermalization of (particular) observables will be used.

Ergodicity and quantum mechanics

In equation (1.3) ergodicity was defined for classical systems as the coincidence of a statistical and a time-averaged mean value of a physical quantity (an observable). A direct translation of this definition to the quantum case, however, would not be meaningful.

An almost trivial objection is that considering only the dynamics of single quantum mechanical states or single observables is meaningless since only the behavior of expectation values corresponds to reality. Hence, ergodicity cannot be directly discussed in the quantum mechanical state space, the Hilbert space. Although in a Schrödinger picture quantum mechanical time evolution maps, analogous to the classical equations of motion, an initial state onto a

time-parametrized orbit of states, any directly applied long-time average would project this orbit onto the ground state(s) of the system⁶.

A more adequate approach towards the time evolution of arbitrary expectation values of a quantum system is by reference to its statistical operator $\hat{\rho}$. It contains the complete information on an arbitrary state of a quantum system and allows to calculate expectation values of arbitrary observables \mathcal{A} as $\langle \mathcal{A} \rangle = \text{Tr}(\hat{\rho}\mathcal{A})$. A density operator description allows to discriminate coherent from incoherent superposition of states: The earlier ones, *pure* quantum states, are elements of the Hilbert space and are characterized by $\text{Tr}[\hat{\rho}_P^2] \equiv 1$. On the other hand, quantum statistically defined thermal states are constructed as an incoherent *mixture* of weighted pure states such that $\text{Tr}[\hat{\rho}_M^2] < 1$.

This discrimination pinpoints the fundamental disagreement between deterministic Schrödinger evolution and a quantum statistical description: A system, once initialized in a pure quantum state, remains pure at any later point in time⁷. Hence thermalization cannot be described as a simple evolution from a pure state into a mixed state. Nonetheless, the expectation is that – at least under some conditions – the unitary evolution of an interacting but nonintegrable quantum many-body system may transfer the 'information' on constraints which are imposed by an initial state into complicated and practically not accessible many-particle correlations such that the commonly discussed one- or few-particle correlations appear as thermal quantities. In the following scenarios which concretize this expectation will be discussed.

Thermalization of subsystems

Different approaches have been chosen to discuss thermalization in closed and in open quantum systems. The later are typically modeled by studying local subsystems of larger, closed systems (up to the entire universe) or bipartite systems. There one part of the closed system is singled out and called the 'system' which is of physical interest. This system is coupled to the complementary degrees of freedom which act effectively as a decohering environment and are labeled the *bath*. Hence the Hamiltonian H of the total system is split into three parts: the Hamiltonian of the considered (sub-) system H_S , that one of the bath H_B and of the interaction H_{int} . For the subsystem a reduced density operator can be obtained by tracing out all states related to the bath in the density matrix of the total system $\hat{\rho}_S = \text{Tr}_B \hat{\rho}$. The coupling to the bath allows for local thermalization of the reduced density matrix of the subsystem or of local observables [123, 128–131]. Some authors report that the actually observed or avoided relaxation still depends on the spectral properties of the full quantum system [132, 133]. This backs a relation between the aspect of local thermalization and the

⁶The projection of a time dependent state onto the zero energy (ground) state(s) of the Hamiltonian by time averaging can be easily seen by applying the time evolution operator $\mathcal{U}(t_0+T, t_0)$ in an eigenstate representation of the time-evolved state where $|M\rangle$ are eigenstates of the Hamiltonian and ϵ_M the corresponding eigenenergies:

$$\begin{aligned} \lim_{T \rightarrow \infty} \frac{1}{T} \int_{t_0}^{t_0+T} \mathcal{U}(t_0+T, t_0) |\Psi(t_0)\rangle &= \lim_{T \rightarrow \infty} \frac{1}{T} \int_{t_0}^{t_0+T} \sum_M \mathcal{U}(t_0+T, t_0) |M\rangle \langle M| \Psi(t_0)\rangle \\ &= \lim_{T \rightarrow \infty} \frac{1}{T} \int_{t_0}^{t_0+T} \sum_M e^{i\epsilon_M T} |M\rangle \langle M| \Psi(t_0)\rangle = |0\rangle \langle 0| \Psi(t_0)\rangle \end{aligned}$$

Certainly, this does not lead to any relevant observation.

⁷This is a straightforward consequence of the cyclic property of the trace: $1 \equiv \text{Tr}[\hat{\rho}_P^2] = \text{Tr}[\mathcal{U}^\dagger(t, t_0) \hat{\rho}_P^2 \mathcal{U}(t, t_0)]$. Note that this argument is not applicable for expectation values of arbitrary observables $\langle \mathcal{O} \rangle = \text{tr}[\mathcal{U}^\dagger(t, t_0) \hat{\rho}_P \mathcal{U}(t, t_0) \mathcal{O}]$.

integrability of quantum systems as discussed in (1.4.2).

Canonical typicality

Another recent line of research examines the *typical* behavior of individual wavefunctions Ψ of the total system H . It is grounded on the prerequisite that the dimension of the subspace of the Hilbert space which represents the bath degrees of freedom exceeds that one which represents the considered system significantly. Then the reduced density matrix of the considered system ρ_S^Ψ is for almost all wave functions arbitrary close to the canonical density matrix $\rho_\beta = \frac{1}{Z} \exp(-\beta H_S)$ of a thermal state with inverse temperature $\beta = 1/k_B T$ and partition function $Z = \text{Tr} \exp(-\beta H_S)$. This statement follows as an application of the law of large numbers to the many dimensions of a many-particle Hilbert space. It opens the way to understand thermalization in quantum systems independently of any explicit randomness in the initial conditions, particularities of time evolution or averaging procedures [125–127, 134]. Contrary to classical systems, the prediction of canonical behavior of the considered system follows from the structure of the Hilbert space alone. This implies the generic nature of the result. A statistical treatment of initial conditions (or quantum states in general) is only needed to define the notion of a typical wave function: Each normalized wave function which is compatible with global constraints of the total system (e.g. energy) represents a microstate of its statistical micro-canonical description; *a priori*, all microstates are assumed to be equally probable, following an earlier suggestion by Schrödinger [135].

Similar observations have been made by Gemmer et al. who calculated different phase space volumes of the Hilbert space directly [124]. Firstly, they restricted the full Hilbert space to appropriate hypersurfaces which account for external constraints like a fixed total energy. Then they found typicality in a large dominant region of (typical) wavefunctions. They assumed exponentially large degeneracy for energy eigenstates and the divisibility of the bath into substructures with an approximately equal density of state. The later assumption allowed to conclude on the main (generic) features of the spectral density of the full system by applying a large number argument which led, finally, to the derivation of the Boltzmann distribution for the energies of the considered system. Hence they proposed that thermodynamics can be understood as an emergent behavior of composite quantum systems.

Time evolution of individual observables

A different approach dispenses from a full analysis of a quantum system or subsystem as it is expressed in the (reduced) density operator. Instead, only the *evolution of particular observables* is discussed. Thermalization, then, is regarded as a particular property of thermodynamically relevant observables for which it is expected. Choosing such an observable \mathcal{O} allows to describe its time evolution from an initial state $|\Psi(t_0)\rangle$ as a consequence of a mismatch of two systems of eigenvectors⁸: The one of the Hamiltonian $\{|M, \alpha\rangle\}_{M, \alpha}$ (the index notation separates energy (M) from other (α) quantum numbers explicitly) and the one of the observable under consideration $\{|j\rangle\}_j$. The corresponding eigenvalues of the Hamiltonian

⁸I remark that an understanding of thermalization as a mismatch of eigenmodes is implicitly already present in the early Fermi-Pasta-Ulam problem [112]: Based on a perturbative approach the unperturbed system of noninteracting harmonic oscillators defines the energy eigenmodes of the system; while their modal energies remain unchanged, the effect of a weak interaction is seen only in a redistribution of the occupation between different modes.

and the observable may be denoted by ϵ_M and O_j , respectively. Then time evolution of its initial state expectation value can be written as

$$\begin{aligned}
 O(t) &= \langle \Psi(t_0) | \mathcal{U}^\dagger(t, t_0) \mathcal{O} \mathcal{U}(t, t_0) | \Psi(t_0) \rangle \\
 &= \sum_{M, M', \alpha, \alpha', j} \langle \Psi(t_0) | \mathcal{U}^\dagger(t, t_0) | M, \alpha \rangle \langle M, \alpha | \mathcal{O} | j \rangle \langle j | \mathcal{U}(t, t_0) | M', \alpha' \rangle \langle M', \alpha' | \Psi(t_0) \rangle \\
 &= \sum_{M, M', \alpha, \alpha', j} O_j e^{i(\epsilon_M - \epsilon_{M'})(t - t_0)} \langle \Psi(t_0) | M, \alpha \rangle \langle M, \alpha | j \rangle \langle j | M', \alpha' \rangle \langle M', \alpha' | \Psi(t_0) \rangle
 \end{aligned}$$

From the matrix elements, one easily reads off the ingredients of any later evolution: The time invariant eigenmode occupation numbers of the initial state $\langle \Psi(t_0) | M \rangle$, the eigenvalues of the observable O_j , the constant overlap matrix elements between the eigenbasis representations of the Hamiltonian and the observable, $\langle M | j \rangle$, and a dephasing of the Hamiltonian eigenmodes with time. For short times, a perturbative analysis of the overlap matrix elements encapsulates the most relevant physics, as will be shown in chapter (7). Moreover, whenever a long-time limit is meaningful,

$$\bar{O} = \lim_{t \rightarrow \infty} O(t, t_0) = \sum_{M, \alpha, \alpha', j} O_j \langle \Psi(t_0) | M, \alpha \rangle \langle M, \alpha | j \rangle \langle j | M, \alpha' \rangle \langle M, \alpha' | \Psi(t_0) \rangle \quad (1.5)$$

$$\stackrel{\text{ND}}{=} \sum_{M, j} O_j |\langle \Psi(t_0) | M \rangle|^2 |\langle M | j \rangle|^2 \quad (\text{nondegenerate case}) \quad (1.6)$$

one observes that the features of a possible later steady state must have been present already from the very beginning in the constant matrix elements or eigenvalues.

Thermalization. Let us first discuss observables which thermalize in a given model system. As thermalization should hold generically for a large class of initial conditions, it can either be found in a statistical distribution of the eigenvalues O_j or of the overlap matrix elements. In the first case, it would be a characteristic feature of the particular observable, independent of the model system under consideration; typical observables, however, do not represent a statistical distribution of eigenvalues. For example, the momentum mode number operator $\mathcal{N} = \sum_k c_k^\dagger c_k$, which is already in its diagonal representation, has constant eigenvalues $N_j = 1$. In the second case, one traces back the reason for thermalization to a mismatch between the eigenmodes of the model Hamiltonian and the eigenvectors of the considered observable. While thermal behavior arises from the incoherent summation of statistically distributed overlap matrix elements, an initial quantum coherent state appears as their delicate coherent superposition which dephases with time.

Discussed for the momentum mode number operator \mathcal{N} this respells the eigenstate thermalization hypothesis proposed by Deutsch [136] and Srednicki [137] which found new attention recently [49, 138].

Eigenstate thermalization hypothesis. The eigenstate thermalization hypothesis is motivated by semiclassical understanding of quantum chaos, linking it to the chaotic behavior of a formally corresponding classical system. Built on Berry's conjecture [139] and its prerequisites, its fundamental assumption is that individual energy eigenstates of nonintegrable systems with sufficiently high eigenenergies can be represented as Gaussian waves. Then the corresponding ensemble of all individual energy eigenstates is Gaussian such that multi-point

correlation functions decompose into products of two-point correlators. Similar factorization properties have been repeatedly used as a definition of quantum chaos and a prerequisite of thermalization [140].

The hypothesis then states that each of these energy eigenstates already contains the thermal behavior of the momentum distribution function. Then the long-time average of $\mathcal{O} = \mathcal{N}(1.5)$ with respect to an initial energy eigenstate $|\Psi(t_0)\rangle = |M_0\rangle$ equals the microcanonical average at a mean energy given by the corresponding eigenenergy ϵ_{M_0} .

$$\sum_j N_j |\langle M_0 | j \rangle|^2 = \langle N \rangle(\epsilon_{M_0}) \quad (1.7)$$

In [138] it was conjectured that the eigenstate thermalization hypothesis should hold for any few-body observable in an energy eigenstate of the Hamiltonian of a large interacting many-body system. Obviously, the idea of eigenstate mismatch requires a significant difference in the structural complexity of the Hamiltonian and the observable and the eigenstate thermalization hypothesis will not hold for observables similar to the Hamiltonian itself. Further research into the necessary structural relation between observables and Hamiltonians would be interesting. It is another open question how the relaxation of observables relates in detail to the spectral criterion of quantum integrability. A plausible argument may read that for (nonintegrable) Hamiltonians which exhibit level repulsion, i.e. are characterized by a Wigner-Dyson distribution of nearest neighbor energy level spacings, energy degeneracies are less important. Then the loss of initial quantum coherence under time evolution is more effective (1.5). Moreover, insights into the generic differences between the eigenfunctions of integrable and nonintegrable Hamiltonians beyond the Gaussian wave criterion of Berry's conjecture could shed more light on the actual prerequisites for thermalization.

Outlook: Relaxation to non-thermal steady states. To conclude this rough overview over the current state of the thermalization debate for quantum systems a short outlook – not relevant for the main statements of this thesis – to the relaxation of integrable systems is given. Assumed that such a system approaches a long time steady state, it is commonly stated, in regression to classical analogues, that the relaxation of expectation values in an integrable system were restricted because of additional conserved integrals of motion. Arising from an exact integration of the equations of motion they would prevent a wipe-out of initial conditions. Hence, thermalization with respect to a conventional Gibbs ensemble can no longer be expected.

Instead, it was suggested that the long-term steady state can be reproduced by a statistical description based on a generalization [141] of the conventional Gibbs ensemble [89]. Additional constraints of the motion are included as constraints for the maximization of entropy, leading to additional Lagrangian multipliers. Results on explicit model systems [89, 93, 96] agree with this approach and its prerequisites and limitations have been discussed [87, 129].

Similar ideas based on a operational implementation of additional constraints by a complete set of commuting observables has led to the formulation of a generic ergodic theorem for arbitrary finite-dimensional quantum systems [142]. There it is claimed that the equilibrium state arising from time averaging unitary evolution always equals the statistical average with respect to a particularly defined grand canonical density operator.

1.4.5 (Quantum) Boltzmann equation

In 1872, Ludwig Boltzmann introduced heuristically, following his splendid intuition, an effective description for the relaxation of the distribution function for particles in a dilute gas from an initial nonequilibrium condition to a thermal state [143]. It distills the time irreversible dynamics of the macroscopic momentum distribution function from a time-reversible microscopic scattering theory by linking the macroscopic drift $\mathcal{D}[n(\mathbf{r}, \mathbf{p}, t)]$ (a differential operator) of the distribution $n(\mathbf{r}, \mathbf{p}, t)$ to a microscopic collision integral $\mathcal{I}[n(\mathbf{r}, \mathbf{p}, t)]$. The resulting integro-partial differential equation⁹ is now known as the *Boltzmann equation* and serves until today as the basis of the kinetic theory of gases.

$$\mathcal{D}[n(\mathbf{r}, \mathbf{p}, t)] = \mathcal{I}[n(\mathbf{r}, \mathbf{p}, t)] \quad (1.8)$$

Naturally, this link includes all conceptual difficulties which have been already discussed above for thermalization. On the one hand, they pose great challenges to a mathematical rigorous derivation of the Boltzmann equation in physically meaningful regimes [140, 145–147]. On the other hand, the Boltzmann equation can be regarded as a prototype of reduced descriptions taking into account only partial information about the underlying microscopic theory [144]. Despite its complicated structure, the Boltzmann equation represents the simplest commonly accepted description of equilibration and its predictions are backed by ample numerical and experimental evidence. For both reasons, it received remarkable attention by physicists as well as by mathematicians.

Here a first introduction to its classical derivation will be followed by motivating an analogue approach for quantum systems.

Motivation of the Boltzmann equation for a dilute classical gas

Drift of distribution function. Motivating the Boltzmann equation, one starts with writing down the evolution of a distribution in phase space when a system is driven by (velocity-independent) external forces, ignoring processes caused by internal damping. Assuming ballistic, Newtonian evolution of all hard-core particles one compares two equal representations of a very general particle distribution

$$n(\mathbf{r}, \mathbf{p}, t) = n\left(\mathbf{r} - \frac{\mathbf{p}}{m}dt, \mathbf{p} - \mathbf{F}dt, t - dt\right) \quad (1.9)$$

Taylor expanding with respect to dt defines the differential drift operator

$$\mathcal{D} n(\mathbf{r}, \mathbf{p}, t) := \left(\frac{\partial}{\partial t} + \frac{\mathbf{p}}{m} \cdot \nabla_r + \mathbf{F} \cdot \nabla_p \right) n(\mathbf{r}, \mathbf{p}, t) = 0 \quad (1.10)$$

Note that this is an evolution equation for a momentum distribution, depending on a single macroscopic position and momentum variable only. Here it is for the limiting case of a vanishing collision integral. It should not be mistaken as Liouville's theorem which states a vanishing divergence for the microscopic many-particle phase space probability $P(\langle \mathbf{r}_i, \mathbf{p}_i \rangle_{i=1\dots N}, t)$, a much more detailed object.

⁹Strictly speaking, the Boltzmann equation is even an integro-partial differential *functional* equation since the momentum distribution enters the collision integral as a functional of the transformation mapping, under the scattering process, initial coordinates onto final coordinates [144].

Microscopic theory. However, a typical approach to a microscopic derivation of the Boltzmann equation starts with Liouville's theorem, subjecting the probability distribution to coarse-graining procedures and decomposing it into a hierarchy of higher order correlation functions. This allows to compute corrections to the macroscopic drift which depend on the microscopic model considered. Under the assumptions made in Boltzmann's Stoßzahlansatz the leading one can be denoted as an intuitive collision integral. An instructive presentation for a gas of hard-core particles can be found in [144].

Stoßzahlansatz. The main requirement for the applicability of Boltzmann's equation is the vanishing of strong particle correlations both locally and in time. This is known as Boltzmann's Stoßzahlansatz and can be expressed by a factorization property of higher order correlation functions into products of the one-particle correlation function, e.g.

$$P^{(2)}(\mathbf{r}_1, \mathbf{p}_1, \mathbf{r}_2, \mathbf{p}_2, t) = n(\mathbf{r}_1, \mathbf{p}_1, t)n(\mathbf{r}_2, \mathbf{p}_2, t) \quad (1.11)$$

Alternative but similar ansätze have been used, e.g. demanding restricted quasi-freeness of the scattering particles [140]. They are assumed to hold in the thermodynamic limit of large particle numbers¹⁰ and in nonequilibrium. So scattering events do not correlate particles which each other. Moreover, subsequent scattering events are considered as independent. This demand wipes out all temporal memory effects and renders the Boltzmann equation a Markovian approximation to the full Schrödinger dynamics of the momentum distribution. This implies that a Boltzmann description can only be justified when nonlocalities in time are not influential. In particular, this means that for rapid transient relaxation phenomena, e.g. those responding to a sudden perturbation, a more refined approach is required.

Collision integral. The collision integral contains all details of the microscopic dynamics and depends in its details on the discussed microscopic model. Each scattering process is defined by a transition between different momentum states caused by particle interactions and characterized by a scattering amplitude (probability) and a phase space factor. Because of the particle accounting conducted by a distribution function scattering-in (gain) and inverted scattering-out (loss) processes appear in pairs. Typically, only lowest order scattering processes are considered. This approximation is justified by assuming low densities; nonetheless, the collision integral cannot be understood as a strict first order correction in a density expansion [148]. In most cases, the lowest order processes are two-particle scattering. If these, however, are suppressed for some dynamical reason, multi-particle scattering has to be included¹¹. A comprehensible presentation of Boltzmann's two-particle scattering model can be found in [150]. There the functional dependence on the scattering coordinates is included in the angle between ingoing and outgoing momenta ω and the scattering cross section $\sigma(\omega)$; with the relative velocity of the ingoing particles $|\mathbf{p} - \mathbf{p}_2|/m$, the classical Boltzmann collision integral reads

$$\mathcal{I}[n(\mathbf{r}, \mathbf{p}, t)] = \int d\omega d\mathbf{p}_2 \frac{|\mathbf{p} - \mathbf{p}_2|}{m} \sigma(\omega) [n(\mathbf{r}, \mathbf{p}', t)n(\mathbf{r}, \mathbf{p}'', t) - n(\mathbf{r}, \mathbf{p}, t)n(\mathbf{r}, \mathbf{p}_2, t)] \quad (1.12)$$

¹⁰The thermodynamic limit for a model of gas particles is taken as $N \rightarrow \infty$ and $R \rightarrow \infty$ such that the total surface of all particles NR^2 with radius R remains constant.

¹¹A prominent example is Peierls' kinetic theory for lattice vibrations [149] which reverts to third order phonon scattering.

Application of the (quantum) Boltzmann equation to condensed matter systems

H. A. Lorentz is credited with the first application of the Boltzmann equation to study the kinetics of classical condensed matter systems in 1905 [151]. Based on the incorrect Drude model of a classical free electron gas, his work led to various wrong predictions [152]. Nonetheless, it marked the road for further improvements.

From a modern point of view, the subsequent development of a quantum theory of solids can be understood as a continuous progression to extract those degrees of freedom which are least correlated among each other. Nonetheless, on every step of this scientific journey a residual interaction between those degrees of freedom remained, giving rise to further particle scattering. Consequently, a Boltzmann equation approach always suggested itself. Hence, tracing the history of the application of the Boltzmann equation to solids is a suitable way to coequally sketch the theoretical grounds on which this thesis rests.

Arnold Sommerfeld and Fermi degeneracy in metals. The first venturer of this endeavor was Arnold Sommerfeld. In his famous theory of metals [153], published in 1927, he discussed consequences of the Pauli principle for crystal electrons. First of all this is their high degeneracy caused by the Fermi quantum statistics which imposes strong (statistical) correlations between the electrons¹². A noninteracting Fermi gas described by the Fermi-Dirac distribution where ϵ_k is the energy related to the k -momentum mode, T the temperature and k_B the Boltzmann constant,

$$n(\epsilon_k) = \frac{1}{1 + e^{(\epsilon_k - \mu)/k_B T}} \quad (1.13)$$

is said to be fully degenerate at zero temperature; there the distribution equals the Heaviside step function with a discontinuity of size one at the chemical potential μ , forming a sharp Fermi surface in momentum space. It separates occupied from unoccupied states of a one-particle many-electron model. Its radius, the Fermi momentum k_F , only depends on the particle density ρ . In three dimensions, it reads $k_F = (3\pi^2\rho)^{1/3}$. A crossover from a degenerate Fermi gas to a classical gas occurs with increasing temperature. It is characterized by a smearing-out of the sharp Fermi surface and is relevant on a temperature scale set by the Fermi degeneracy temperature, $T_F = \mu_0/k_B$. For a metal, Sommerfeld estimated it to roughly 36,000 degrees, which means that at room temperature (300K) the electronic system is almost fully degenerate. In semimetals ($T_F \approx 100K$), semiconductors ($T_F \approx 3K$) or in optical lattices ($T_F \approx 330nK$ [154]) much lower degeneracies appear.

Sommerfeld's application of the Boltzmann equation to the degenerate Fermi gas followed, as he quotes, explicitly the lines of Lorentz, only replacing the Maxwell-Boltzmann distribution of a classical gas by the Fermi-Dirac distribution. This constituted the first use of the Boltzmann equation to describe the evolution of quantum systems.

Felix Bloch and the fortunes of periodicity. The next important step was taken by Felix Bloch [152, 155], showing that in a perfectly regular lattice potential there is no scattering between Bloch states of electrons. These many-particle states of delocalized electrons reflect the underlying periodicity of the lattice and can be understood as solutions of a self-consistent

¹²Arnold Sommerfeld's (published!) shrewd illustration of the Pauli principle as the 'Wohnungsamt für Elektronen' (housing office for electrons) may allow to conclude on his wit and sense of humor. Unfortunately, due to a original misprint in the table of contents [stating incorrectly page 825 instead of 855] of the journal's annual volume 1927 and unchecked copying for many decades, a wrong quotation of his work [153] is widespread.

response of the electron gas. Hence Bloch states already include partly correlations imposed by electron-electron (Coulomb) interaction. They form bands with limited band width. However, there is a residual interaction between Bloch states due to scattering at lattice defects. For these scattering processes, Bloch wrote down a quantum Boltzmann equation, including the collision integral for electron-phonon scattering.

Lew Davidowitsch Landau and the way towards Fermi liquid theory. Yet Bloch's picture is not sufficient to describe all electron-electron interactions in a many-body system and strong electron-electron interactions are remaining. Again, they are responsible for large particle correlations in systems which, therefore, should be understood as fermionic quantum liquids. A way to treat these interactions is Landau's theory of a Fermi liquid [156–158] which will be reviewed in greater detail in (2); here only key points are mentioned. I.M. Khalatnikov, a colleague of Landau at the academy of sciences of the USSR, reports: [159] "It is interesting to note, that the Boltzmann kinetic equation happened to be the starting point for the construction of the Fermi liquid theory." As he explains, difficulties with the conservation of momentum when applying the quantum Boltzmann equation to elementary excitations could only be solved assuming that the energy of the system is only a functional of the distribution function [156]. This observation became the first cornerstone of Fermi liquid theory. Now Landau developed a picture of quasiparticles; while most of the correlations between the original electrons could be absorbed into their definition, a weak residual interaction remained. Consequently, Landau was able to describe their dynamics by means of a Boltzmann equation [157]. The collision integral for the degenerate Fermi gas of these weakly interacting quasiparticles is constructed following Fermi's golden rule, assuming a two-particle symmetric scattering potential \mathcal{W}

$$\begin{aligned} \mathcal{I}[n(\mathbf{r}, \mathbf{p}, t)] = & - \sum_{\mathbf{p}', \mathbf{p}_1, \mathbf{p}'_1} \omega(\mathbf{p}, \mathbf{p}_1, \mathbf{p}', \mathbf{p}'_1) \{ n(\mathbf{r}, \mathbf{p}, t) n(\mathbf{r}, \mathbf{p}_1, t) [1 - n(\mathbf{r}, \mathbf{p}', t)] [1 - n(\mathbf{r}, \mathbf{p}'_1, t)] \\ & - [1 - n(\mathbf{r}, \mathbf{p}, t)] [1 - n(\mathbf{r}, \mathbf{p}_1, t)] n(\mathbf{r}, \mathbf{p}', t) n(\mathbf{r}, \mathbf{p}'_1, t) \} \quad (1.14) \end{aligned}$$

where the scattering probability ω can be calculated using Feynman rules: In lowest order, the H-shaped Feynman diagram has to be evaluated for anti-symmetrized two-particle electronic states. Expressed in a one-particle picture, they read $|\mathbf{p}, \mathbf{p}_1\rangle = [|\mathbf{p}\rangle |\mathbf{p}_1\rangle - |\mathbf{p}_1\rangle |\mathbf{p}\rangle]/\sqrt{2}$ and give rise to a phase coherent superposition of one-particle scattering matrix elements even in a golden rule argument

$$\begin{aligned} \omega(\mathbf{p}, \mathbf{p}_1, \mathbf{p}', \mathbf{p}'_1) &= |\langle \mathbf{p}, \mathbf{p}_1 | \mathcal{W} | \mathbf{p}', \mathbf{p}'_1 \rangle|^2 \frac{2\pi}{\hbar} \delta(\epsilon_{\mathbf{p}} + \epsilon_{\mathbf{p}_1} - \epsilon_{\mathbf{p}'} - \epsilon_{\mathbf{p}'_1}) \delta_{\mathbf{p}+\mathbf{p}_1, \mathbf{p}'+\mathbf{p}'_1} \\ &= \frac{2\pi}{\hbar} \left\{ |[\langle \mathbf{p} | \langle \mathbf{p}_1 | \mathcal{W} | [\mathbf{p}' \rangle | \mathbf{p}'_1 \rangle] - [\langle \mathbf{p} | \langle \mathbf{p}_1 | \mathcal{W} | [\mathbf{p}'_1 \rangle | \mathbf{p}' \rangle]]|^2 \right\} \delta_{\epsilon_{\mathbf{p}'} - \epsilon_{\mathbf{p}'_1}}^{\epsilon_{\mathbf{p}} + \epsilon_{\mathbf{p}_1}} \delta_{\mathbf{p}+\mathbf{p}_1, \mathbf{p}'+\mathbf{p}'_1} \end{aligned}$$

Energy and momentum conservation apply. The phase space factor reflects out- and in-scattering events (with respect to the external momentum mode \mathbf{p}). They correspond to a loss and gain of occupation in the external (\mathbf{p}) momentum mode, respectively, and define the global sign of the scattering integral.

Chapter 2

Landau's theory of a Fermi liquid

In the last section, Landau's theory of a Fermi liquid [156–158] has been frankly motivated as a frame developed for a generalization of the original Boltzmann description to strongly interacting fermionic liquids. This may be historically justified but, of course, does not merely meet the great success of this theory which became a benchmarking effective description for the study of many equilibrium properties of (normal) interacting Fermi systems. Its almost universal character is owed to the fact that many interactions modify but do not completely lift Fermi degeneracy¹. The exceptional rôle of the Fermi surface remains unbroken and these modifications can be, in good approximation, generically discussed in terms of elementary excitations; in particular, reference to other details of the quantum mechanical ground state of a particular interacting model is not required. This allowed Landau to establish a most intuitive and simple picture of quasiparticles. While on the one hand it provides a fundamentally new understanding of many-body systems, on the other it smoothly relates to and explains the astonishing success of the (incorrect) free electron model of early condensed matter theory. Furthermore, since prior views could easily be adapted to the new theory, Fermi liquid theory became a widespread and popular explanation of interacting Fermi systems and deeply influenced the thinking of physicists in many fields of research. While its description of liquid ³He is paradigmatic and its application to the electron gas in solids original, it has also been successfully applied, for instance, to nuclear matter.

Following the reviews by Baym and Pines [160, 161], Fermi liquid theory can be discussed on two levels: Originally it has been designed as an effective macroscopic theory, discussing the expansion of an energy functional in terms of a distribution function. This gives access to some thermodynamic observables, describing them in terms of Landau (input) parameters. Later, its microscopic origins have been explored and Landau parameters have been derived from microscopic models.

2.1 Concept and prerequisite: Adiabatic connection between interacting and noninteracting degrees of freedom

The main requirement of Landau's phenomenological theory of a Fermi liquid is an implicit constraint on the nature of the interaction. It assumes that the interacting theory can be

¹For example, in real metals the Fermi surface is distorted with respect to that one of a free electron gas, but its continuing existence ensures Fermi degeneracy. However, for interactions which lead to the emergence of bound states, pair formation or other so-called Fermi liquid instabilities, Landau's theory is not applicable.

developed in a Gedankenexperiment from a noninteracting model of free particles by switching on the interaction adiabatically, i.e. continuously and arbitrary slow in time. Tracing the eigenstates of the noninteracting system under this procedure it is, furthermore, assumed that the ground state of the interacting model evolves from the noninteracting ground state and no level crossings appear for the low energy excited states. Then a one-to-one correspondence between the eigenstates of the noninteracting system and the adiabatically evolved states of the interacting system holds. Except for the ground state, the later states are in general *not* the eigenstates of the interacting system. However, they form a distinguished set of states since they can be labeled by the same quantum numbers used to describe the noninteracting system; this allows for a meaningful comparison between states of the interacting and of the noninteracting system. Their occupations are called quasiparticles, and due to their generation they inherit many properties of noninteracting particles which I label the *physical* or elementary particles, i.e. the naïve constituents of many-body system.

The modern reader may be reminded that the concept of adiabatic connectivity is older than all explicitly formulated renormalization group ideas and provides its own conceptual frame for analyzing interacting many-body systems. Moreover, it is not based on perturbative arguments. Originally introduced to establish Fermi liquid theory, its key point of linking complicated interacting to simple noninteracting Hamiltonians has been elevated to a "basic notion of condensed matter physics" by Anderson [162]. It became relevant for other fields of research, for instance in density functional theory [163] or, recently, for linking spin systems and band insulators [164, 165].

For this thesis it is important to notice that the concept of adiabatic connection compares two Hamilton operators. If it is proven in equilibrium by studying an adiabatic link between *all* eigenenergies, it holds as an operator property both in equilibrium and for any nonequilibrium dynamics. If, however, adiabatic connectivity has only been assumed or observed for low energy eigenstates (as it is often the case in physical models), the nonequilibrium dynamics may include highly excited states for which this reduced notion of adiabatic connection does not hold; then the equilibrium and the nonequilibrium behavior of the model may show significantly different physics.

However, such an adiabatic connection is not possible for all interactions conceivable; whenever the interacting ground state is topologically different from the noninteracting one because of, for instance, a phase transition, the opening of a gap in the energy spectrum or similar reasons it cannot be taken for granted (but may hold accidentally). The most prominent example of a Fermi liquid instability is the BCS theory of superconductivity.

2.2 Macroscopic approach to Fermi liquid theory

2.2.1 The momentum distribution for interacting and noninteracting cases

Before entering a presentation of Landau's approach and to foster intuition the momentum distribution $n_{\mathbf{p}}$ in the case of noninteracting and interacting Fermions may be compared. In both cases, it provides a one-particle picture of the many-body system.

For the noninteracting case, the features of the Fermi-Dirac distribution have already been mentioned. It describes the occupation of one-particle momentum modes. Hence in a microscopic fermionic theory the distribution can only take the discrete values 0 and 1 and is indexed by the (identifying) quantum number of the momentum mode. In a macroscopic approach, however, a suitable averaging over (energetically) close momentum modes allows to

write it as a continuous function. Then momentum labels lose their original rôle of quantum numbers and, if a separation of different momentum orientations is not relevant, it is sufficient to consider the momentum distribution as a function of energy $n(\epsilon_{\mathbf{p}}) =: n(\epsilon_p)$.

At zero temperature and no interactions, it is given by a Heaviside step function with a discontinuity of size one at the Fermi energy. Interaction effects modify this momentum distribution in the same way as one-particle excitations would do: occupation from states inside is shuffled to states outside of the Fermi surface of the noninteracting gas, leaving excited electrons ($|\mathbf{p}| > k_F$) and holes ($|\mathbf{p}| < k_F$). Since this process is most effective around the Fermi energy, it leads to the emergence of tapered tails of the distribution which cause a reduction of the discontinuity at the Fermi energy. Its remaining size is called the quasiparticle residue Z and serves as a measure for the strength of interaction effects.

In a microscopic picture, considering interaction effects as a shift of occupation often comes along with an implicit perturbative view: While the noninteracting Hamiltonian is thought to define invariant momentum modes ("physical particles") which remain unchanged by the interaction, the redistribution of occupation appears as a leading perturbation effect due to a weak interaction (since a strong perturbation would change the elementary modes and with it the character of the assumed "particles"). This, for example, is the point of view taken in the Fermi-Pasta-Ulam problem. The macroscopic approach of Landau's theory, understanding the momentum distribution as a continuous function, avoids this perturbative notion.

Instead, it uses the departure of the interacting momentum distribution function $n_{\mathbf{p}}$ from the noninteracting one $n_{\mathbf{p}}^{(0)}$, the continuous function

$$\delta n_{\mathbf{p}} = n_{\mathbf{p}} - n_{\mathbf{p}}^{(0)} \quad (2.1)$$

as an expansion parameter.

2.2.2 Expansion of the free energy functional

The expansion of the free energy functional $F[n_{\mathbf{p}}] = E[n_{\mathbf{p}}] - \mu N[n_{\mathbf{p}}]$ in powers of this deviation lies the foundation of Landau's phenomenological theory of a Fermi liquid. Discussing this form of the free energy, which is the thermodynamic potential of a variant of the grand canonical ensemble, includes fluctuations of the particle number at a chemical potential $\mu = \epsilon_F$ ² which I fix at the Fermi energy $\mu = \epsilon_F$. The total difference in the number of particles follows trivially from counting $N - N_0 = \sum_{\mathbf{p}} \delta n_{\mathbf{p}}$. Moreover I define the first order and second order functional derivatives

$$\epsilon_{\mathbf{p}} = \frac{\delta E[n_{\mathbf{p}}]}{\delta(\delta n_{\mathbf{p}})} \quad \text{and} \quad f_{\mathbf{p}\mathbf{p}'} = \frac{\delta^2 F[n_{\mathbf{p}}]}{\delta(\delta n_{\mathbf{p}})\delta(\delta n_{\mathbf{p}'})} \quad (2.2)$$

By definition, f is symmetric in \vec{p} and \vec{p}' and known as a (potentially large) set of Landau parameters. Then the expansion reads

$$F[n_{\mathbf{p}}] - F_0 = \sum_{\mathbf{p}} (\epsilon_{\mathbf{p}} - \mu) \delta n_{\mathbf{p}} + \frac{1}{2} \sum_{\mathbf{p}\mathbf{p}'} f_{\mathbf{p}\mathbf{p}'} \delta n_{\mathbf{p}} \delta n_{\mathbf{p}'} + \mathcal{O}(\delta n^3) \quad (2.3)$$

It is assumed that Fermi degeneracy largely persists in the case of interactions, i.e. $\sum_{\mathbf{p}} \delta n_{\mathbf{p}}/N \ll 1$. Then the one-particle energy difference $\epsilon_{\mathbf{p}} - \mu \sim \delta n_{\mathbf{p}}$ is also small of order $\delta n_{\mathbf{p}}$ wherever

²Working at zero temperature, the thermodynamic definition $\mu = \partial E/\partial N|_T - T\partial S/\partial N|_T$ obviously simplifies. Pressure and volume variations are not considered.

$\delta n_{\mathbf{p}'}$ is significantly different from zero. Hence, both terms in (2.3) are, effectively, second order in $\delta n_{\mathbf{p}}$ and of equal importance! Rewriting them jointly as

$$F[n_{\mathbf{p}}] - F_0 = \sum_{\mathbf{p}} \left(\epsilon_{\mathbf{p}} - \mu + \frac{1}{2} \sum_{\mathbf{p}'} f_{\mathbf{p}\mathbf{p}'} \delta n_{\mathbf{p}'} \right) \delta n_{\mathbf{p}} + \mathcal{O}(\delta n^3) \quad (2.4)$$

This looks like a leading order expansion in the excitations $\delta n_{\mathbf{p}}$ with a renormalized one-particle energy

$$\tilde{\epsilon}_{\mathbf{p}} = \epsilon_{\mathbf{p}} - \mu + \frac{1}{2} \sum_{\mathbf{p}'} f_{\mathbf{p}\mathbf{p}'} \delta n_{\mathbf{p}'} \quad (2.5)$$

2.2.3 Quasiparticle picture

Landau recognized that a quasiparticle description provides a consistent interpretation of these relations. The free energy (2.3) to second order in $\delta n_{\mathbf{p}}$ appears as the sum over free excitations with a renormalized energy which allows to understand these excitations as excited quasiparticles. Their energy (2.5) includes interactions with other excited quasiparticles; the interaction strength is described by the Landau parameters $f_{\mathbf{p}\mathbf{p}'}$. These can be either calculated from microscopic models or represent experimental input parameters.

Landau quasiparticles are ambivalent objects. In terms of physical fermions they are composite many-particle objects, but they are neither true eigenstates of the interacting system. Nonetheless they represent, to second order in $\delta n_{\mathbf{p}}$, approximately noninteracting degrees of freedom. Therefore they inherit many properties of the free Fermi gas: Firstly, this is the fermionic statistics. Quasiparticles are noninteracting fermions, the volume of their Fermi sea does not differ from that of the physical particles [166], around the Fermi surface the density of states is linear and their momentum distribution function equals that of free fermions $\bar{n}_{\mathbf{p}}^{(0)} = n^{(0)}(\tilde{\epsilon}_{\mathbf{p}})$. Consequently, since quantum numbers correspond, they carry the same momentum, spin, and, in charged systems, also the same charge as physical fermions. On the other hand, they have different quasiparticle energies given by (2.5) and a different effective mass (which can be related to the Landau parameters). Moreover, since the expansion of the free energy functional has been truncated, a residual interaction between quasiparticles remains; the later leads to a quasiparticle dynamics described by a Boltzmann equation.

2.2.4 Boltzmann dynamics of the momentum distribution

As already mentioned, the kinetic equation of the quasiparticles is given by a Boltzmann equation. This is a plausible approach since the main part of the particle-particle interaction has been absorbed into their definition, and the residual one can be assumed to be weak. Hence the macroscopic drift of the quasiparticle momentum distribution is linked to the microscopic scattering integral for free fermions (1.14) with appropriately modified scattering amplitudes. However, the true quasiparticle interactions are unknown. For some limiting cases, their scattering amplitudes can be linked to Landau parameters, i.e. to equilibrium properties like the compressibility (sound velocity) and the spin susceptibility (see below). Conceptually, this is close to the motivation of the fluctuation-dissipation theorem. These approximations for the quasiparticle scattering amplitudes, which are valid for some particular scattering momenta, are usually used as parametrizations for the unknown true momentum dependent scattering amplitudes.

Since the momentum dependence of the scattering amplitudes is ignored anyway, the main focus in Fermi liquid theory lies on generic phase space arguments in quasiparticle scattering. These arguments do not require to specify detailed features of the quasiparticles but only refer to Fermi degeneracy. Although a golden rule approach to scattering is perturbative, correlations imposed by the Pauli principle easily outweigh other interaction effects. Since its phase space factor vanishes for the equilibrium Maxwell-Boltzmann distribution at any temperature, there is no contribution based on scattering to the evolution of the distribution function in equilibrium. Boltzmann dynamics only becomes relevant for nonequilibrium quasiparticle distributions.

2.2.5 Range of validity of the quasiparticle picture

Moreover, the residual interaction between the quasiparticles implies their finite lifetime. This leads to a final breakdown of the quasiparticle picture. Since quasiparticles are not eigenstates of the interacting system such a decay is obvious. Let quasiparticles be described by their creation operators q_k^\dagger acting on a ground state $|\Psi_0\rangle$ and eigenstates analogously by a_k^\dagger . Expanding a time evolving quasiparticle state $q_k^\dagger(t) = \sum_{k'} M_{kk'} a_{k'}^\dagger e^{i\epsilon_{k'}t}$ in terms of true eigenstates of the system and restricting to the leading order time evolution shows a dephasing of its various components. However, eigenstate dephasing does not affect the evolution of the ground state momentum distribution:

$$\langle \Psi_0 | q_k^\dagger(t) q_k(t) | \Psi_0 \rangle = \sum_{k'k''} M_{kk'} M_{k''k} e^{i(\epsilon_{k'} - \epsilon_{k''})t} \langle \Psi_0 | a_{k'}^\dagger a_{k''} | \Psi_0 \rangle = \sum_{k'} |M_{kk'}|^2 = \text{const}(t) \quad (2.6)$$

This observation is mirrored in the effective treatment provided by Fermi liquid theory: Describing the evolution of the momentum distribution by a Boltzmann equation including the full scattering integral, 'gain' and 'loss' terms of a scattering picture perfectly match in equilibrium. This depicts a kind of dynamical balance of equal in- and out-scattering into a particular momentum mode; its net occupation remains unchanged, and so does the number of quasiparticles. This defines thermal equilibrium of stable net occupations. Concluding, what is seen as coherence from a quantum point of view translates into a balance argument in the effective Boltzmann treatment.

For calculating the lifetime of individual particles, the conventional way is to reduce the drift term in the Boltzmann equation according to the relaxation time (τ) approximation. The relaxation time is no longer thought of as the relaxation of the momentum distribution but as the lifetime of a single particle. Furthermore, the scattering integral is re-interpreted and no balancing of in- and out-scattering is considered. The loss process is discussed independent of any gains, depicting the decay of an individual quasiparticle into two quasiparticles and one quasihole.

$$\frac{1}{\tau_p} = - \left. \frac{\mathcal{I}[n(\mathbf{r}, \mathbf{p}, t)]}{n(\mathbf{r}, \mathbf{p}, t)} \right|_{\text{loss}} = \sum_{\mathbf{p}', \mathbf{p}_1, \mathbf{p}'_1} \omega(\mathbf{p}, \mathbf{p}_1, \mathbf{p}', \mathbf{p}'_1) n(\mathbf{r}, \mathbf{p}_1, t) [1 - n(\mathbf{r}, \mathbf{p}', t)] [1 - n(\mathbf{r}, \mathbf{p}'_1, t)] \quad (2.7)$$

The scattering matrix element is assumed constant; then the phase space summation can be evaluated [167] and results in

$$\tau_p \sim 1/(\epsilon_p - \epsilon_F)^2.$$

The diverging lifetime indicates that around the Fermi energy quasiparticles are stable. The lifetime of quasiparticles is inversely related to their spectral width which vanishes at the

Fermi surface. There quasiparticles are arbitrary close to the real eigenstates of the interacting Fermi system (the only truly time independent states). Since quasiparticle stability follows from a phase space argument it is obvious that the Pauli principle and Fermi degeneracy are responsible for the suppression of decay processes. This is the origin of the generic nature of Landau's description.

Away from the Fermi surface, however, Landau's theory is ill-defined. An adiabatic switching-on of the interaction in time is required as a prerequisite to ensure the quasiparticle picture but quasiparticles themselves decay on a finite time scale. Thus the range of applicability of Landau's theory depends on intrinsic details of the model. First, a limiting time scale for adiabaticity has to be estimated on which a more rapid switching-on procedure does not lead to excitations from the ground state. Then it can be compared with τ_p which defines a 'window of applicability' around the Fermi surface. For systems with a discrete energy spectrum the energy difference between the ground and the excited state sets such a scale. Yet for systems with a continuous energy spectrum around the Fermi surface, such a scale does not exist. It is an interesting question to define adiabaticity for continuous systems. In this work I will suggest a route on which a possible criterion could be examined.

2.2.6 Thermodynamic properties of a Fermi liquid

Before ending the discussion of Fermi liquid theory as a macroscopic framework a short outlook to its main successes is justified. Contrary to many other approaches discussing interacting systems this is not an analysis of the interacting ground state. Since in the quasiparticle picture the ground state is represented approximately by a featureless ground state of free quasiparticles and since the details of the adiabatic procedure remain unspecified, a precise mapping between both ground states is not possible. While this should be seen as a virtue of Landau's approach, allowing for very generic conclusions, Fermi liquid theory is not suited for exploring details of interacting ground states.

Its main merit, however, lies in the calculation of thermodynamic properties like the specific heat, the compressibility or the spin susceptibility at low temperature. Each of these quantities is governed by the physics of low-energy excitations, i.e. departures from the unknown interacting ground state. These departures are most adequately described as a free gas of excited quasiparticles. Hence the thermodynamic properties of the Fermi liquid at low temperatures resemble those of a noninteracting Fermi gas which are only modified by a limited set of effective parameters. These results explain why simple models assuming free electrons described reasonably well real metals.

For simple reference some thermodynamic properties of a Fermi liquid are quoted and compared here [160, 161]. Only the specific heat, which is linear in the temperature T , will be relevant for this thesis. Since the chemical potential of a Fermi liquid $\mu = -(\partial F/\partial n)_T$ only varies with T^2 the specific heat at constant volume and under constant pressure coincide to first order in T .

Typically, these relations are used to fix the Landau parameters by measurable quantities.

2.3 Microscopic foundation of Fermi liquid theory

Fermi liquid theory has been introduced as a framework based on a rather unspecific functional expansion of the free energy. It provides a description of interacting fermions depending on unspecified Landau parameters; their calculation depends on details of the underlying

Quantity	Definitions	Fermi liquid	w.r.t free Fermi gas
Specific heat	$c_V = \left(\frac{\partial E}{\partial T}\right)_N$ $= \frac{T}{N} \left(\frac{\partial S}{\partial T}\right)_V$	$= \frac{m^*}{3\hbar^3} k_F k_B^2 T$ $= \frac{\pi^2}{2} n k_B \frac{T}{T_F}$	larger by m^*/m
Compressibility	$\kappa = \frac{1}{V} \left(\frac{\partial V}{\partial P}\right)$ $= \frac{1}{n^2} \frac{\partial n}{\partial \mu}$	$= \frac{1}{n^2} \frac{N}{1+F_0^s}$	stiffer ($F_0^s > 0$)
Spin susceptibility	$\chi = \frac{1}{V} \frac{dM}{dH}$	$= \frac{\hbar^2}{4} \frac{\gamma^2 N}{1+F_0^a}$	enhanced ($F_0^a < 0$)

Table 2.1: Some paradigmatic properties of a Fermi liquid for later reference. Here V denotes the volume, S the entropy, P the pressure, T_F the Fermi temperature, k_F the Fermi momentum, k_B the Boltzmann constant, μ the chemical potential, M the magnetization, H the magnetic field, $F_0^{(s/a)}$ the (anti-)symmetrized Landau parameter (cf [160]), and γ the gyromagnetic ratio.

quantum theory and is usually performed in a perturbational way based on a Greens functions approach [168]. This restricts to the regime of small expansion parameters, i.e. usually to small interaction strength. From the exact spectral (Lehmann) representation of the Fourier transformed zero-temperature one-particle Greens function ($\eta \gtrsim 0$)

$$G(\mathbf{k}, \omega) \stackrel{\text{L}}{=} \sum_n \left[\frac{|\langle \Psi_n^{N+1} | c_{\mathbf{k}}^\dagger | \Psi_0 \rangle|^2}{\omega - (E_n^{N+1} - E_0) + i\eta} + \frac{|\langle \Psi_n^{N-1} | c_{\mathbf{k}} | \Psi_0 \rangle|^2}{\omega + (E_n^{N-1} - E_0) - i\eta} \right] \quad (2.8)$$

with E_n and $|\Psi_n\rangle$ being the exact eigenenergies and eigenstates of the $N \pm 1$ particle system, one reads off that poles in the Greens function correspond to the excitation spectrum of the interacting many-particle problem and the related residues to the overlap of interacting eigenstates with a one-particle (one-hole) excitation from the initial state $|\Psi_0\rangle$. Both features can be extracted from the self-energy $\Sigma(k, \omega)$ which contains all interaction effects and can be read off from the Dyson representation of the Greens function [169]

$$G(\mathbf{k}, \omega) \stackrel{\text{D}}{=} \frac{1}{\omega - \epsilon_k - \Sigma(k, \omega) + i\eta \operatorname{sgn}(\omega)} \quad (2.9)$$

Comparing with the Greens function for noninteracting fermions ($\Sigma \equiv 0$) it provides an implicit definition of the quasiparticle dispersion relation

$$\tilde{\epsilon}_k := \epsilon_k + \Sigma(k, \tilde{\epsilon}_k) = \epsilon_k + \Re(\Sigma(k, \tilde{\epsilon}_k)) + i\Im(\Sigma(k, \tilde{\epsilon}_k)) \quad (2.10)$$

The real part of the self-energy describes the renormalization of the quasiparticle energies, the imaginary part their spectral width. From the quasiparticle dispersion relation one determines the Fermi surface of the interacting system as the set of momenta $\text{FS} = \{\mathbf{k} | \mu = \tilde{\epsilon}_{\mathbf{k}} + \Re(\Sigma(\mathbf{k}, \mu))\}$ [166]. A Taylor expansion of the self-energy around the pole $\omega = \tilde{\epsilon}_k$ exposes the related quasiparticle residue Z_k

$$Z_k = \operatorname{Res}(\tilde{\epsilon}_k) = \frac{1}{1 - \frac{\partial}{\partial \omega} \Sigma(k, \omega)|_{\omega=\tilde{\epsilon}_k}} \quad (2.11)$$

Special rôle of the quasiparticle residue. This quasiparticle residue is the microscopic observable which is most relevant for this work. Taken at the Fermi surface, it is simply referred to as the Z -factor; it corresponds to the renormalization factor for the wave function in a RG approach to interacting models. But first of all, it serves as an indicator for quasiparticle behavior in an interacting theory as it measures the overlap between the 'bare' particle states and the exact low-energy eigenstate excitations of the interacting system. A nonvanishing value implies that the one-to-one correspondence of free fermions and quasiparticles persists. A vanishing Z -factor, however, would indicate that the exact excitations of the interacting system do not show any similarities with the noninteracting degrees of freedom. Such a behavior can be observed in other theories, like the composition of bare quarks to –fundamentally different– nucleons, or for one-dimensional interacting fermions. In the later case, the geometric constraint to one dimension makes individual fermion motion impossible. Instead, only collective excitations can occur. Hence, a fermionic quasiparticle picture fails and instead of a Fermi liquid a Luttinger liquid is observed, characterized by the vanishing of a sharp Fermi surface and a bosonic statistics of the low-energy collective excitations.

Signatures of the quasiparticle residue. As a renormalization factor, the quasiparticle residue enters many parameters. For instance, the *effective mass* can be extracted from $k/m_k^* = d\tilde{\epsilon}_k/dk$ which is motivated by the dispersion relation for free fermions $\epsilon_k = k^2/2m$.

$$\frac{d\tilde{\epsilon}_k}{dk} = \frac{d\epsilon_k}{dk} + \frac{\partial\Sigma(k, \tilde{\epsilon}_k)}{\partial k} + \frac{\partial\Sigma(k, \tilde{\epsilon}_k)}{\partial\tilde{\epsilon}_k} \frac{d\tilde{\epsilon}_k}{dk} \quad \Longrightarrow \quad \frac{k}{m^*} \approx Z \left(\frac{d\epsilon_k}{dk} + \frac{\partial\Sigma(k, \epsilon_k)}{\partial k} \right) \quad (2.12)$$

More insight into the rôle of the quasiparticle residue is provided by the one-particle *spectral function* $A(\epsilon_k, \omega) = -\frac{1}{\pi} \Im(G^R(\mathbf{k}, \omega))$ and in particular by the *momentum distribution function* which can be obtained from it by integration: $n(\epsilon_k) = \int_{-\infty}^{\mu} d\omega A(\epsilon_k, \omega)$. The later is a conveniently accessible observable and exhibits the quasiparticle residue as the size of its discontinuity at the chemical potential, i.e. $n(\mu - 0) - n(\mu + 0) = Z$.

The quasiparticle residue as a signature of a Fermi liquid While the above relations provide an exact framework for a microscopic study of Fermi liquid theory, the calculation of the self-energy for explicit models requires typically its perturbative expansion.

For a Fermi liquid, however, characteristic frequency dependencies at small positive frequencies hold for its real and imaginary part [170]:

$$\Re(\Sigma(k, \omega)) \xrightarrow{\omega \rightarrow 0^+} \left(1 - \frac{1}{Z_k}\right) \omega < 0, \quad \Im(\Sigma(k, \omega)) \xrightarrow{\omega \rightarrow 0^+} -\gamma\omega^2 < 0 \quad (2.13)$$

Moreover it is known that both real and imaginary part are smooth functions in ω [171] and that $\omega \rightarrow 0$ describes the only zero point of $\Im(\Sigma(k, \omega))$. This is why discontinuous behavior is expected only at the Fermi surface. This becomes more clear when one studies the spectral shape of a quasiparticle: Around the Fermi energy the spectral function A can be decomposed into a coherent quasiparticle contribution of weight Z_k and an incoherent background [171]

$$A(\epsilon_k, \omega \rightarrow 0) = Z_k \delta(\omega - Z_k \epsilon_k) + A^{\text{inc}}(\epsilon_k, \omega \rightarrow 0) \quad (2.14)$$

At the Fermi energy, the spectral weight of quasiparticles amounts to the quasiparticle residue and is sharply peaked around the quasiparticle energy. Further away the quasiparticles acquire a nonvanishing spectral width, corresponding to a finite lifetime.

The sharp spectral distribution of quasiparticles at the Fermi energy translates directly into the discontinuity of the momentum distribution which is the most characteristic feature of the momentum distribution function of a zero temperature Fermi liquid. Its size is given by the quasiparticle residue and its deviation from the noninteracting value ($Z = 1$) is a rough measure for the interaction strength between the fermions of the liquid.

Chapter 3

Hubbard model

Modeling real interacting many-body systems poses a great challenge to physicists. While the nature of the elementary constituent particles and their interactions are well-known, emergent phenomena originating from their interplay are difficult to predict. To keep the complexity of these problems manageable and to gain insight into the fundamental principles and consequences of collective behavior often bold approximations and a far-going reductionism are required. Doing so for the problem of electrons in real crystalized materials leads to the Hubbard model for interacting fermions [172]. It is an exemplary minimal model which nonetheless captures surprisingly rich physical behavior.

3.1 Definition of the Hubbard model

Starting from the picture of a crystal as a regular lattice of equal atoms, one assumes that each atom contributes exactly one electron into a delocalized electron gas. The remaining positive ions form a periodic electrostatic potential for these itinerant electrons. The electrons occupy Bloch states of momentum k and energy ϵ_k , which inherit the same periodicity as the underlying lattice structure [155]. While this implies their delocalization across the whole crystal, their spatial probability distribution remains peaked around the lattice sites. This motivates restricting the occupation of electrons to discrete points on an arbitrary mathematical point lattice Γ with $|\Gamma|$ lattice sites. This is the first fundamental abstraction of the Hubbard model.

Local point of view on delocalized electrons. The abstraction to a point lattice strengthens a local view on itinerant electrons and suggests to develop their properties from those of an individual lattice site; hybridization of local one-particle states of isolated single sites lead to the many-particle states of the entire lattice. In the Hubbard model, each lattice site can be occupied by up to two spin – 1/2 – fermions. Due to the Pauli principle this implies a local state space of dimension four¹. Without fermion interaction, all local states are degenerate in energy; hence their hybridization leads to a single band of energies, constituting the Hubbard model as a one-band model with bandwidth D and total occupation N . Appropriate local fermionic creation and annihilation operators $c_{\mathbf{j}\sigma}^{(\dagger)}$ carrying a site (\mathbf{j}) and a

¹Note the following configurations of the four-dimensional local state space: zero occupation, the spin up or spin-down configuration of single occupancy and the antisymmetric combination of two antiparallel spins (double occupation).

spin ($\sigma = \uparrow, \downarrow$) index are defined. Vector notation for the indices is only used for special illustration but generally suppressed. Delocalization of electrons is ensured by quantum mechanical coherence across the lattice, captured by the overlap matrix elements t_{ij} of the electronic wavefunction at two lattice sites i and j . In the handy, most popular but sometimes misleading local picture this coherence shows up as quantum coherent hopping processes of 'localized particles' between lattice sites with an amplitude given by the hopping matrix element t_{ij} ; in the conventional Hubbard model, t is assumed real, constant for nearest neighbor hopping $t_{ij} = t$ and zero otherwise. Hopping to more distant sites is by a coherent sequence of nearest neighbor hopping processes involving intermediate sites and of higher order in t . Working in a grand canonical ensemble defined by the chemical potential μ includes fluctuations of the particle number; it corresponds to the average filling factor of the lattice $N/|\Gamma|$ (between zero and two electrons per lattice site) and couples to the local spin dependent occupation numbers $n_{j,\sigma} = c_{j\sigma}^{(\dagger)} c_{j\sigma}$. Most relevant is the case of half filling where, on average, every site is occupied with one fermion and half the Hubbard band is occupied. Throughout this thesis I restrict to the case of half filling only. The kinetic term of the Hubbard model on a real-space lattice then reads

$$H_{\text{kin}}^{\text{HM}} = -t \sum_{\langle i,j \rangle \sigma} c_{i\sigma}^\dagger c_{j\sigma} - \mu \sum_j (n_{j\uparrow} + n_{j\downarrow}) \stackrel{\text{FT}}{=} \sum_{k \in \mathcal{K}, \sigma \in \{\uparrow, \downarrow\}} (\epsilon_k - \mu) c_{k\sigma}^\dagger c_{k\sigma} \quad (3.1)$$

Applying a Fourier transformation $c_{k\sigma}^\dagger = \frac{1}{\sqrt{N}} \sum_j e^{i\mathbf{k}\cdot\mathbf{j}} c_{j\sigma}^\dagger$ it can be easily rewritten in momentum space. The dispersion relation ϵ_k depends on the details of the lattice. For instance, for a square lattice in d dimensions it reads

$$\epsilon_{\mathbf{k}} = -2t \sum_{i=1..d} \cos(k_i) \quad (3.2)$$

where k_i is the i^{th} component of the vector \mathbf{k} . For this work, however, the specification of a particular lattice is not necessary. The allowed momenta are restricted to agree with a limited bandwidth $\mathcal{K} = \{\mathbf{k} \in \mathbf{R}^d : \epsilon(k) \in [-D, D]\}$.

Local on-site Coulomb interaction. The second fundamental abstraction of the Hubbard model concerns the interaction of electrons. Although the bare Coulomb interaction is long-ranged, in many-particle systems of itinerant electrons metallic screening effects shield it to a much more localized effective potential. The Hubbard model simplifies this physics and assumes a strictly local two-particle on-site repulsion U of electrons dwelling on the same lattice site². There is no interaction between electrons on different sites. Regarding the local state space discussed above, it can be effective only between electrons of different spin; this motivates the choice of the interaction as proportional to the local spin dependent occupations $\tilde{H}_{\text{int}}^{\text{HM}} \sim n_{j\uparrow} n_{j\downarrow}$. To make the energy gain and loss in the case of half filling (i.e. on average half an electron of each spin species dwells on every lattice site) more explicit³ it is defined

²For the discussion of Fermi liquid behavior (and hence for this work) this is a sufficient approximation. For other phases of the Hubbard model (v. i.) which exhibit strong fermionic localization there is no good justification for it beyond achieving simplicity.

³Adding particles or reducing particles (i.e. adding holes) increases the interaction energy, but imbalancing spin occupation reduces it. This is the reason why in the regime of strong interactions the Hubbard model shows correlation induced magnetism which, however, is not relevant in the Fermi liquid phase.

in a slightly modified way.

$$H_{\text{int}}^{\text{HM}} = U \sum_j \left(n_{j\uparrow} - \frac{1}{2} \right) \left(n_{j\downarrow} - \frac{1}{2} \right) \quad (3.3)$$

This local variant of the Coulomb repulsion lifts the energy degeneracy of the local state, increasing the energy of the doubly occupied site $[\uparrow\downarrow]_i$ by U . Consequently, the mobility of the lattice fermions is reduced as, in an imaginative saying, 'hopping onto singly occupied sites becomes energetically less favorable'. Its Fourier transform of the two-particle interaction is constant on all matrix elements in momentum space, obviously nondiagonal and momentum conserving.

$$H_{\text{int}}^{\text{HM}} \stackrel{\text{FT}}{=} \frac{U}{N} \sum_{k_1, k_1', k_2, k_2'} c_{k_1', \uparrow}^\dagger c_{k_1, \uparrow} c_{k_2, \downarrow}^\dagger c_{k_2', \downarrow} \delta(k_1' + k_2' - k_1 - k_2) - \frac{U(N_\uparrow + N_\downarrow)}{2} + \frac{U}{4} \quad (3.4)$$

Hubbard Hamiltonian. Summing the kinetic and the interaction term, the Hubbard model $H = H_{\text{kin}}^{\text{HM}} + H_{\text{int}}^{\text{HM}}$ [172] depicts in a simple way the competition between delocalizing effects of the kinetic energy and localizing effects of two-particle interactions in many-body systems for different filling factors of the lattice. Depending on the strength of the interaction, this gives rise to a large variety of phenomena characterizing different phases of the Hubbard model. Therefore it became the paradigmatic minimal model of the physics of correlations and its rôle has been compared to that of the Ising model for spin systems. In the case when particle-hole symmetry applies, i.e. on a bipartite lattice and for half filling, only even orders appear in a perturbative expansion with respect to the interaction strength. This implies that the attractive and repulsive Hubbard model coincide.

3.2 Properties of the Hubbard model

In equilibrium and depending on the dimensionality as well as the underlying lattice structure many properties of the Hubbard model have been extensively studied and a great variety of different methods has been used. Introducing lecture notes [173], reviews focussing on particular aspects like mathematically rigorous analysis [174], its ferromagnetism [175], the Mott-Hubbard transition [176, 177], its treatment in the limit of infinite dimensions [178, 179] or edited volumes of reprinted papers [180, 181] are available and may serve for further reference.

Mott-Hubbard transition. The complicated phase diagram of the Hubbard model is not addressed in this work. However, its most characteristic transition, the Mott-Hubbard phase transition, has been studied extensively. Since it reflects ideally the competition between localizing and delocalizing effects of a repulsive interaction and because it has become a paradigmatic example in modern experiments, a short detour seems appropriate. At low temperatures and for small repulsive interactions the Hubbard model exhibits a Fermi liquid phase; there fermions are delocalized such that conductivity is finite. Fluctuations of the fermions between different lattice sites are strong such that their number on a particular lattice site is stochastically distributed following Poissonian statistics with the mean value equalling the filling factor. If the latter is an integer number (for fermions: one), increasing

the interaction beyond a critical value U_c leads to an electronic phase transition towards a Mott insulator state. Fluctuations are frozen out and the mobility of electrons is strongly restricted – they become largely localized. In the limit of infinite U a simplified picture holds, stating that each site is equally occupied with exactly as many fermions as is demanded for by the filling factor. A gap opens in the energy spectrum. While the conductivity vanishes, the compressibility shows an increased stiffness. For fermions, this transition only happens at half filling, i.e. for a filling factor one [182]. The same transition, however, can be observed in the bosonic version of the Hubbard model, replacing fermions by bosons. Then higher filling factors become possible and, for sufficiently strong interaction, the transition occurs repeatedly with increasing chemical potential.

Hubbard model in various dimensions. For the Hubbard model in one dimension, Lieb and Wu have presented an exact solution in 1968 based on Bethe ansatz methods [106, 183]. This dimension shows untypical behavior: As in one dimension no Fermi liquid exists, the regime of low interaction is a Luttinger liquid. Moreover, there is no Mott transition in the one dimensional Hubbard model.

In higher dimensions than one, no exact solutions are known and the model is believed to be nonintegrable. Particular interest exists in the phase diagram of the Hubbard model in two dimensions since this has been linked to high- T_c superconductivity in cuprates [184]. Again, this is beyond the interest of this thesis.

Simplifications arise in the limit of infinite dimensions when a local approximation of the self energy becomes exact [171, 185–187]. This is the scenario of dynamical mean field theory (DMFT) [178, 179] where the momentum dependence of the self-energy is neglected while the frequency dependence is retained; this allows for the inclusion of dynamical aspects into a mean-field theory.

Symmetries of the Hubbard model. For the interaction (3.3) the Hubbard Hamiltonian on a bipartite lattice⁴ is particle-hole symmetric in the following sense [188]: Under the transformation \mathcal{P} which is defined by its action on the operators and implements particle-hole symmetry within a single spin species.

$$\left. \begin{array}{l} c_{x\downarrow} \\ c_{x\downarrow}^\dagger \\ c_{x\downarrow} \\ c_{x\uparrow} \\ c_{x\uparrow}^\dagger \\ c_{x\uparrow} \end{array} \right\} \xrightarrow{\mathcal{P}} \left\{ \begin{array}{l} (-1)^x c_{x\downarrow}^\dagger \\ (-1)^x c_{x\downarrow} \\ c_{x\uparrow} \\ c_{x\uparrow}^\dagger \end{array} \right. \implies \left. \begin{array}{l} U \\ t_{ij} \\ \bar{N}_\downarrow \end{array} \right\} \xrightarrow{\mathcal{P}} \left\{ \begin{array}{l} -U \\ t_{ji}^* \\ |\Gamma| - \bar{N}_\downarrow \end{array} \right. \quad (3.5)$$

For real and symmetric hopping matrix elements, which are commonly assumed, the kinetic energy remains invariant. The total number of down spins N_\downarrow changes into its complement. In the case of half filling $N = N_\uparrow + N_\downarrow = |\Gamma|$ this is another invariant. However, an attractive interaction is mapped onto a repulsive one and vice versa.

Hence, if one *assumes* particle-hole symmetry for physical reasons, the Hubbard dynamics must be the same for repulsive and attractive interactions. This implies that under the assumptions of a bipartite lattice and at half filling perturbative expansions of dynamical quantities, e.g. of the Greens function, contain only even powers of the interaction.

⁴A lattice is called *bipartite* if its graph $\Gamma = \Gamma_A \cup \Gamma_B$ consists of two disjoint subgraphs Γ_A and Γ_B such that there is no bond connecting two points $x, y \in \Gamma_A$ or $x, y \in \Gamma_B$.

Studying Fermi liquid properties on the Hubbard model. In this work the Hubbard model solely serves as a quantum implementation of a Fermi liquid. Naturally, this restricts to *dimensions larger than one*. There a Fermi liquid regime exists for weak on-site interaction strength.

No particular lattice structure will be chosen here. However, the thermodynamic limit is taken, promoting the number of lattice sites to infinity. *Translation invariance* is assumed on the lattice. Nesting of the Fermi surface can occur on some lattice geometries. Then parallel segments of the Fermi surface lead to an enhancement of scattering for certain momentum vectors, giving rise to nesting instabilities. In order to discuss generic properties of a Fermi liquid, these lattices are excluded from the observations here.

For convenience, explicit calculations (e.g. of the momentum distribution) are performed on a hypercubic lattice in the limit of infinite dimensions. Then the components k_i of a generic momentum vector \mathbf{k} can be assumed random numbers. So are their contributions $\cos(k_i)$ to the dispersion (3.2). Then the central limit theorem is applicable and a Gaussian density of states is obtained [173].

$$\rho(\epsilon) = \exp(-(\epsilon/t^*)^2/2) / \sqrt{2\pi t^*} \quad (3.6)$$

t^* is linked to the hopping matrix element by dimensional scaling $t \rightarrow \frac{t^*}{\sqrt{2d}}$ to retain a non-trivial relation between the kinetic and the interaction energy in all dimensions [173]. Using this Gaussian density of states allows to reduce d-dimensional summations in momentum space to one-dimensional energy integrations which, certainly, implies a dramatic reduction of the required numerical resources.

Chapter 4

Experimental motivation

Many parameters in condensed matter systems like lattice constants of particular crystals, values of effective interaction potentials or the large particle number have long been considered as input parameters fixed by nature and beyond the control of experimentalists. Hence, nonequilibrium physics stimulated by their variation seemed to be a highly academic idea. The advent of new technology during the last two decades has changed this dramatically. Two lines of research which both emerged from advances in quantum optics are presented here. For both of them, the fascination of a technological breakthrough beyond former technical barriers was engraved into their naming: ultra-fast and ultra-cold.

4.1 Ultrafast spectroscopy of condensed matter systems

One of them is ultrafast spectroscopy of solids [189, 190]. In pump-probe experiments a first laser pulse excites the electron gas of a solid and photogenerates an electron-hole plasma. After some delay time t_D a second pulse is used to detect the time evolved state of the system. Pulse durations of less than 10 fs have been reached in experiments and are much shorter than the dephasing or energy relaxation times. Hence a sequence of probings at different delay times allows to follow its transient quantum dynamics directly in the time domain.

4.1.1 Ultrafast spectroscopy for semiconductors

Experiments have been conducted, for example, in *semiconductors* like GaAs [191, 192]. There the complex dielectric function $\epsilon_q(\omega, t_D)$ was studied in an extremely early stage of the dynamics and its frequency dependence extracted by a third pulse measurement. A retarded buildup of Coulomb screening in the plasma and the formation of dressed quasiparticles has been observed. Before screening becomes effective the plasma consists of independent particles interacting via the bare Coulomb interaction. The onset of Coulomb screening corresponds to the time scale of the plasma frequency (in GaAs this is $2\pi/\omega_{pl} = 70$ fs). This should not surprise since the later is the period of the collective electronic oscillation and, consequently, the characteristic frequency related to collective behavior. Then, with increasing time higher-order correlations develop [195].

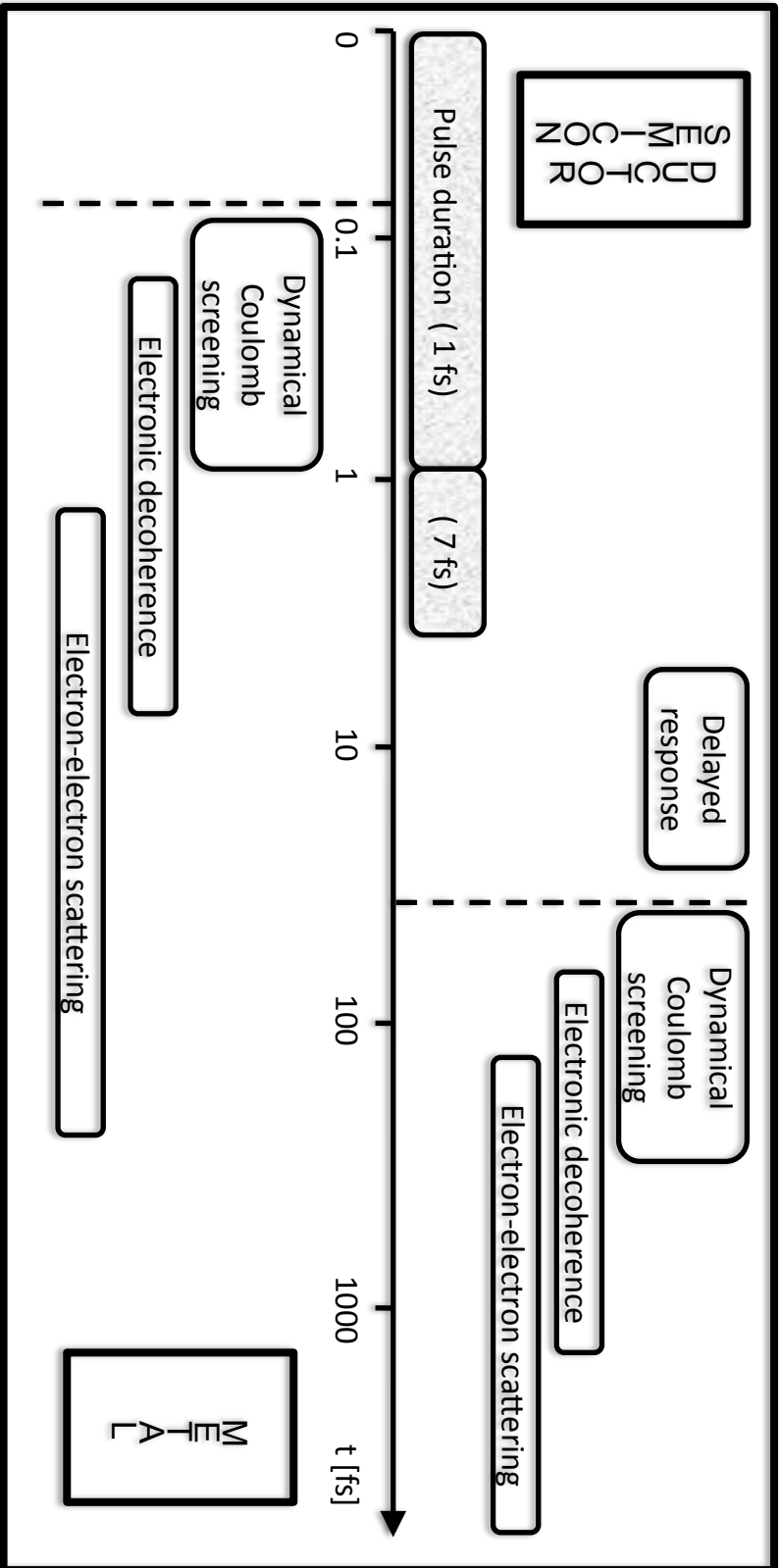


Figure 4.1: The experimentally observed relaxation time scales in semiconductors (e.g. GaAs, [191, 192]) are compared with the analogous scales in metals [193]. The plasma frequencies $2\pi/\omega_{pl} = 70$ fs for the semiconductor and $2\pi/\omega_{pl} = 0.1$ fs for the metal are indicated by the dashed line. Pulses with a duration of 1 fs are feasible today. In the experimental study of GaAs a pulse length of approximately 7 fs has been used. A lower bound on pulse durations is set by the delay time of photon emission in condensed matter which has been found to be around 100 as [194].

4.1.2 Ultrafast spectroscopy for metals

These works complement and exceed earlier examinations for *metals* which were obtained from an indirect linewidth analysis of resonances in photoemission or, later, with time-resolved two-photon photoemission spectroscopy. They aimed at the determination of the frequency and temperature dependence of the electronic scattering length (or scattering time) which enter fundamental properties like electric or thermal conductivity. These methods have been largely applied, for instance to study properties of surfaces [196]. Like in semiconductors, unscreened Coulomb interactions have been predicted for metals at very short times after an initial excitation [197] and transient excitonic states in metals have been expected in an early time regime [198]. However, since the plasma frequency in metals is very high and corresponds to an "attosecond" time scale $2\pi/\omega_{pl} = 0.1$ fs, the direct observation of retardation effects in metals and the onset of Coulomb screening is still beyond the reach of experimental technology [193, 199, 200]. Nonetheless, a 'proof of principle' suggests that relaxation properties in metals can be studied by attosecond spectroscopy [194].

4.1.3 Discussion of the observed time scales

In Fig. 4.1 the time scales observed in the relaxation of an optically excited semiconductor are compared with analogous scales of a metal. In both cases one expects a delay before collective Coulomb screening effects become effective on the scale of the plasma frequency. Afterwards, dephasing effects of electrons and, on a larger time scale, electron-electron interactions are the origin of further relaxation behavior. For any experimental system one expects thermalization due to two- or many-particle scattering processes.

This picture of a delayed build-up of correlations indicates that Markovian kinetic equations like the Boltzmann equation are not appropriate to describe short-time processes [201, 202]. Instead, a full solution of quantum mechanical time evolution, e.g. in terms of nonequilibrium Keldysh Greens functions [201], is needed on an early stage of the dynamics. Only after an initial relaxation regime has been accomplished and many-particle effects have become effective, an approximate treatment of time evolution based on a Markovian kinetic equation becomes justified.

The discussion of a nonequilibrium Fermi liquid in this thesis will proceed in a closely related way. This is because an interaction quench and an exciting laser pulse lead to comparable excited initial configurations: For the first, solving the Schrödinger dynamics on a short time scale will allow to establish a quasiparticle picture even under nonequilibrium conditions. In a second step, the dynamics of the nonequilibrium quasiparticle distribution function will be described by a quantum Boltzmann equation. Since the Boltzmann equation conserves the kinetic quasiparticle energy, a prior energy relaxation by conversion of potential Coulomb energy into kinetic energy of quasiparticles must be accomplished before a kinetic description can be applied.

4.2 Ultracold atoms on optical lattices

A second and much more prominent line of experimental and theoretical research was opened by fast technological progress in the field of ultracold atoms. New cooling methods opened the way to observe the behavior of bosonic and fermionic atoms at very low temperature. Their characteristic features originating from the quantum coherence of the particles and

their quantum statistics are dominant: Bosons undergo a phase transition towards a Bose-Einstein condensate (BEC) which has first been observed in 1995 [203, 204]. For fermions, the Pauli exclusion principle leads to Fermi degeneracy which has been, to a lesser degree, experimentally reached from 1999 onwards. Unfortunately, cooling of Fermions is very difficult, partly because of small system sizes. Since only a small numbers of atoms can be confined into an experimental trap, the resulting many-fermion system is characterized by a very low Fermi degeneracy temperature T_F which sets the reference scale for temperature measurements. Ambitious world leading experimentalists expect for 2009 to reach temperatures around $T \approx 0.05T_F$ [205]. For ordinary metals with $T_K \approx 36,000K$ this still would correspond to temperatures of –merely ultracold– 1800 K.

Obviously, it is not just low temperature which motivates such experiments. It is high control, optical precision and long coherence times which makes these many-body systems exceptional. Quantum coherence of 10^6 atoms allowed to study quantum effects for almost macroscopic system sizes. Due to Feshbach resonances, the effective scattering length of individual atoms can be tuned by a magnetic field in a large parameter regime; even transitions from attractive to repulsive interaction is possible. In 1998, ultracold atoms confined by a harmonic trapping potential have first been loaded [206] onto arrays of standing light waves known as optical lattices [207]. There optical dipol forces localize the atoms in the minima or maxima of the stationary and monochromatic electromagnetic potential. Then the easily tunable properties of the light field determine the features of the many-body arrangement: The half wavelength equals the lattice spacing, its strength both defines the separation between the different lattice sites and influences the two-particle interaction. In particular, these parameters can be easily made time dependent. The resulting pattern is strongly reminiscent of condensed matter systems, modeling an artificial crystal. It can be approximately described by a one-band Hubbard model. Its tunnel coupling t and the onsite interaction U directly relate to the strength of the light field. Inspired by an old proposal of Feynman to model quantum systems by other quantum systems [208] this motivated many experiments and proposals. This research aims at the implementation of paradigmatic condensed matter models, which were originally designed – like the Hubbard model – to describe electronic properties of solids, in systems of ultracold atoms loaded on optical lattices. There the slow dynamics of ultracold atoms facilitates, for instance, to follow the dynamics of excited states and to study the nonequilibrium behavior of the modeled system. Details can be found in many reviews, e.g. in [209, 210]. Here I will point out to some experiments which provide insight into the nonequilibrium behavior and thermalization properties of many-body coherent quantum systems.

Quench through the Mott transition of the Bose-Hubbard Hamiltonian

A series of seminal experiments was performed by M. Greiner in the group of I. Bloch and T. Hänsch in 2002 [211, 212]: By a sudden quench in the strength of the optical potential the Hubbard Hamiltonian is changed from the weakly interacting superfluid regime to the strongly interacting Mott insulator regime. The first regime is characterized by phase coherence across a large number of lattice sites. However, in the second regime the particle number is fixed locally such that phase coherence is lost. Time-of flight measurements of the momentum distribution function reflect this difference in phase coherence. Only in the superfluid regime coherent peak structures, similar to Bragg reflections, appear. Hence time-of-flight measurements of the momentum distribution allow to compare the time evolved state

of this many-body quantum system to its ground states in the superfluid or the Mott insulator regime. 'Snapshots' of the time evolution following the quench have been obtained and are reprinted in Fig. 4.2. Initially, the characteristic coherent peak signatures of the superfluid regime are clearly visible and reflect the superfluid initial conditions. Although the switch in the Hamiltonian is nonadiabatically fast, the initial decay of superfluid correlations only occur on a slower time scale which characterizes the response of the system. Then the Mott state is reached where signatures of superfluid phase coherence are wiped out. The surprising observation, however, is the later revival of the superfluid phase coherence. Its observation parallels the approximate reappearing of initial configurations in the classical Fermi-Pasta-Ulam problem or Rabi oscillation of occupations [213] for a fully coherent many-body quantum system.

In this experiment, a quench across a phase transition highlights a suppressed dephasing of an excited many-body quantum system. A detailed explanation has been published [215] but also a simple argument in real space following a Gutzwiller ansatz already illustrates the origin of the revivals. There the initial superfluid state can be approximated by a product of coherent local states. Represented in a Fock basis, their weights are distributed according to a Poissonian distribution. Quenched into the Mott phase, however, the Hubbard Hamiltonian can be well-approximated by its interaction term only; it factorizes in real space and on each lattice site it is diagonal with respect to number states and a discrete set of eigenenergies $\omega \sim Un(n-1)$. It generates the periodic time evolution of the initial state

$$|\alpha\rangle(t) = e^{-|\alpha|^2/2} \sum_n \frac{\alpha^n}{\sqrt{n!}} e^{-iUn(n-1)t/\hbar} \quad (4.1)$$

First it leads to a dephasing of the number states with respect to each other. However, from the lowest frequency one reads off a revival period $T_r \sim h/U$ after which the initial configuration is restored. Note that this time is independent of the lattice site such that it equally holds for the many-particle system. Since the state itself is time periodic, so are all expectation values like the momentum distribution. This description, however, approximates both the initial state and the Hamiltonian. Corrections due to the nonvanishing kinetic part of the Hamiltonian break the periodicity on a longer time scale which is, in first order perturbation theory, given by t/U .

Here, collapse and revival are solely due to eigenmode dephasing caused by an (approximately) integrable Hamiltonian with a discrete and bounded set of frequencies. This is a leading order result, representing the free evolution of an excited (nonequilibrium) many-body quantum state¹. Collapse and revival occur on the same time scale and before thermalization processes may become effective.

Nonrelaxation of hard-core bosons in one dimension

Another experiment by Kinoshita, Wenger and Weiss [216] has shown that the time scale on which a many-particle system evolves freely can be made extremely large. A BEC of ⁸⁷Rb atoms was constrained by a strong optical lattice into an array of one dimensional isolated tubes. By a phase grating pulse applied to the tube the condensate was split into a coherent superposition of a left- and a rightmoving wavepacket, i.e. a nonequilibrium

¹Quenching through the Mott-Hubbard phase transition only serves to easily create a locally factorizing initial state with a nontrivial particle distribution function on every site. Details of a phase transition are not relevant.

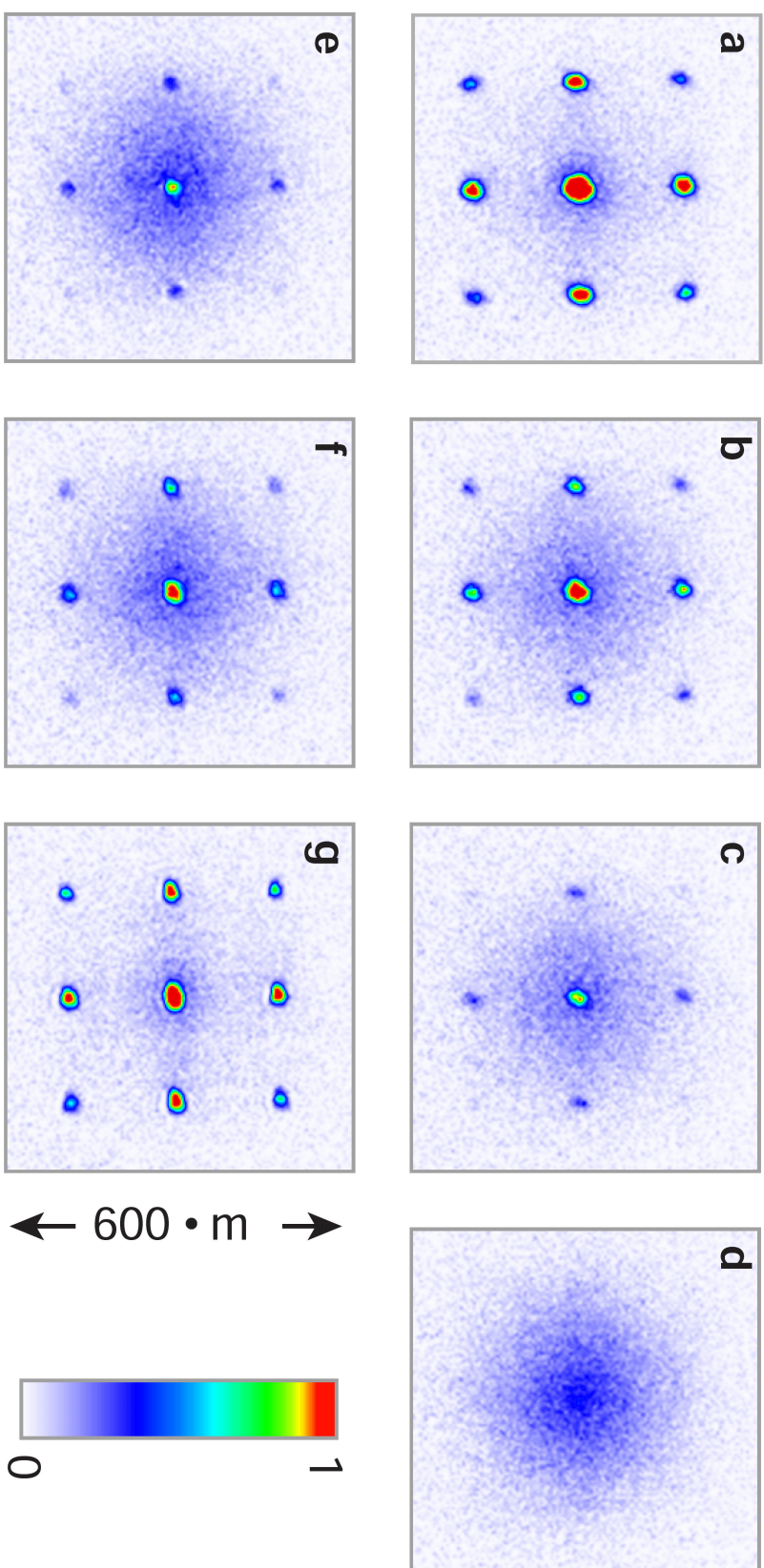


Figure 4.2: Time of flight measurements of the momentum distribution are taken at different times after a quantum quench. They show the collapse and revival of the initial macroscopic superfluid state following a quantum quench at times (a), 0 μs ; (b), 100 μs ; (c), 150 μs ; (d), 250 μs ; (e), 350 μs ; (f), 400 μs ; (g), 550 μs ; (h), 650 μs ; (i), 750 μs . $m = 1 \mu\text{m}$ sets the length scale of the expanding cloud of atoms. The images are taken from [214] and are reprinted with kind permission by M. Greiner.

momentum distribution was created. Then the oscillation of the wavepackets in the harmonic trap potential was studied which did not cease even after hundreds of oscillation cycles; although dephasing, i.e. the loss of coherence among the condensed bosons occurred, the initial momentum distribution did not relax. This has been explained by referring to the integrability of one dimensional hard-core bosons [89, 217].

Superlattices

A very recent development of this branch of research lies in the modification of the optical lattice by superimposing two lattice structure with different periodicities. The resulting patterns, named superlattices, allow to study more detailed model systems. If the two wavelengths are incommensurate or quasi-periodic, random potentials are mimicked [218]. For two commensurate frequencies regular superlattices with two periods are feasible, representing local double-well potentials [219]. Controlling the relative phase and intensity regular density patterns can be created on the lattice. For instance, this allows to model magnetically ordered states and their dynamics [220–222]. These systems open the possibility, among many others, to study the local relaxation of subsystems [223]. In this direction they complement the global view on thermalization taken in this thesis.

Ultracold fermions

While many proposals highlight the relevance of experiments with ultracold fermions, for instance to experimentally answer the questions related to the origin of high T_c -superconductivity [224], the manipulation of ultracold fermions in optical lattices is technically more demanding. The observation of a Fermi surface in ultracold atoms [225] was followed by measurements of fermionic correlations [226] and the observation of superfluidity [227]. A study of interaction-controlled transport by a quench in the trapping potential [228] prepared the recent observation of the Mott-Hubbard transition in the repulsive fermionic Hubbard model [229]. This rapid progress of experimental sophistication may give hope that the predictions formulated in this thesis, although they are characteristic zero temperature effects, may be experimentally traceable in the near future.

Metastable state of doubly occupied sites. Finishing this brief review, I point out to a proposal by A. Rosch et al. suggesting the creation of a metastable state in the strongly repulsive fermionic Hubbard model by a quench in the trapping potential [97]. Initialized in a densely packed doubly occupied Mott phase, the sudden widening of the trapping potential leads to a dilute gas of metastable doubly occupied sites diffusively spreading out into the extended trap. This gas forms a Bose-Einstein condensate of superfluid doubly occupied sites. Similar to the behavior of a Fermi liquid presented in this thesis (cf. 11.3), metastability occurs because of a bottleneck in the relaxation dynamics of an excited state. However, the conditions are somewhat inverted. In the proposal, the decay of excited doubly occupied sites of the Hubbard model is prevented. As the on-site Coulomb interaction is assumed large, their energy level lies far above of the limited bandwidth. Hence energy relaxation into continuum band states is only possible by multi-particle scattering processes. These are, however, exponentially suppressed. Consequentially, *energy* conservation restricts the relaxation of the excited state.

Chapter 5

Time evolution in quantum mechanics

5.1 Schrödinger dynamics and Heisenberg picture

Following Schrödinger, the dynamics of a quantum system follows from a differential evolution equation for its wave function $\Psi(t)$ which describes the state of the system completely. This evolution is driven by the energy conditions of the system which can be expressed as the interplay between its generic energetic structure (formulated in terms of its Hamiltonian H) and the current state of the system. The resulting evolution is described by the Schrödinger equation

$$i\hbar \frac{d}{dt} \Psi(t) = H \Psi(t) \quad (5.1)$$

Integrating this differential equation formally allows to represent time evolution by an evolution operator

$$\mathcal{U}(t, t_0) = e^{-i \int_{t_0}^t dt' H(t')/\hbar} \quad (5.2)$$

which maps initial states $|\Psi(t_0)\rangle$ onto time evolved states $|\Psi(t)\rangle = \mathcal{U}(t, t_0) |\Psi(t_0)\rangle$. From (5.2) one reads easily off that for the evolution operator always holds $\mathcal{U}^\dagger(t, t_0) = \mathcal{U}(t_0, t)$; moreover, for not explicitly time dependent Hamiltonians the composition property $\mathcal{U}(t, t_0)\mathcal{U}(t_0, t') = \mathcal{U}(t, t')$ is valid. Note that even time-evolved states and operators themselves do not correspond to measurements in the empirical physical reality directly; only expectation values of particular observables \mathcal{O} , which are meaningfully chosen self-adjoint operators acting on the state space, with respect to the quantum mechanical state of a system do.

For this reason, one has to demand for the invariance of an expectation value under a formal redistribution of time dependence between observables and states $\langle \Psi_S(t) | \mathcal{O}_S | \Psi_S(t) \rangle = \langle \Psi_H | \mathcal{O}_H(t) | \Psi_H \rangle$. This isometry allows to establish isomorphic representations usually referred to different *pictures* of time evolution:

- In the *Schrödinger picture* solely the states carry the time dependence of expectation values; observables are time invariant and the time evolution operator acts on states only.
- In the *Heisenberg picture* it is solely the operators. Due to the isometry the time evolution operator in the Schrödinger picture (5.2) induces a superoperator $\tilde{\mathcal{U}}(t, t_0)$ acting on operators \mathcal{O} such that $\mathcal{O}(t) = \tilde{\mathcal{U}}(t, t_0)\mathcal{O}(t_0) := \mathcal{U}^\dagger(t, t_0)\mathcal{O}\mathcal{U}(t, t_0)$.

- Splitting the time evolution carried by a 'free' part of the Hamiltonian H_0 and an interacting part H_{int} and attributing the first to the operators and the second to the states defines, as a mixed variant, the *interaction picture* representation [230].

Although all of these pictures are completely equivalent they allow for different technical approaches to features of a quantum theory.

Heisenberg picture. For the aim of this thesis, the Heisenberg picture turns out to be advantaged since there time evolution can be expressed as an algebraic (super-)operation in operator space, namely as the commutation with the Hamilton operator. This allows to rewrite (5.1) as an operator relation which holds independently of any basis representation

$$\frac{d\mathcal{O}_H(t)}{dt} = \frac{1}{i\hbar}[\mathcal{O}_H(t), H] + \left(\frac{\partial\mathcal{O}(t)}{\partial t}\right)_{\text{expl}} \quad (5.3)$$

The index H denoting that operators are taken in a Heisenberg picture will be suppressed furtheron; the partial time derivative is only relevant for explicitly time dependent operators. Throughout the rest of this thesis all operators are understood as Heisenberg operators and explicit time dependence is not considered.

For later reference the free time evolution of a creation operator with respect to the time independent and noninteracting (kinetic) Hamiltonian $H_0 = \sum_k \epsilon_k c_k^\dagger c_k$ is given:

$$c_k^\dagger(t) = e^{i\epsilon_k t/\hbar} c_k^\dagger(t=0) \quad (5.4)$$

While in general time evolution with respect to a generic Hamiltonian implies the mapping of an operator onto an arbitrarily different one, the particular time evolution of a time independent quadratic Hamiltonian (in terms of creation and annihilation operators) is particular simple. For an interacting Hamiltonian, this motivates diagonalization strategies to represent it as a quadratic Hamiltonian in appropriate degrees of freedom; then an exact computation of time evolution is straightforward. For non-integrable interacting many-particle Hamiltonians this is, however, not possible and approximate methods are needed.

5.2 Greens function formalism

A nonperturbative way to formulate and to analyze the dynamics of a many-body quantum system is provided by the framework of Greens functions. As Greens function methods became an indispensable tool in condensed matter theory, extensive introductions can be found in any modern textbook [167–169, 231]. Their main merit is to decompose the dynamics of a quantum theory in a hierarchy of correlation functions. The later are given as (thermal) averages (denoted by $\langle \dots \rangle$) of strings of Heisenberg operators Ψ_H . These operators incorporate the dynamics generated by the Hamiltonian. In a many-body problem which is modeled by a continuous quantum field theory, these are the field operators of the field theory. Commonly discussed physical quantities like occupations or response functions can be obtained from the Greens functions by taking appropriate limits.

Definitions

Here I only state definitions for later reference. For fermions the *lesser* and the *greater* Greens function are defined as

$$G^<(x, t, \sigma_z, x', t', \sigma'_z) = +i \langle \Psi_H^\dagger(x', t', \sigma'_z) \Psi_H(x, t, \sigma_z) \rangle \quad (5.5)$$

$$G^>(x, t, \sigma_z, x', t', \sigma'_z) = -i \langle \Psi_H(x, t, \sigma_z) \Psi_H^\dagger(x', t', \sigma'_z) \rangle \quad (5.6)$$

Then the *time ordered* Greens function G and the *anti-time ordered* Greens function \bar{G} are written as

$$G(x, t, \sigma_z, x', t', \sigma'_z) = -i \langle \mathcal{T} \Psi_H(x, t, \sigma_z) \Psi_H^\dagger(x', t', \sigma'_z) \rangle = \begin{cases} G^<(x, t, \sigma_z, x', t', \sigma'_z) & t' > t \\ G^>(x, t, \sigma_z, x', t', \sigma'_z) & t' < t \end{cases} \quad (5.7)$$

$$\bar{G}(x, t, \sigma_z, x', t', \sigma'_z) = -i \langle \bar{\mathcal{T}} \Psi_H(x, t, \sigma_z) \Psi_H^\dagger(x', t', \sigma'_z) \rangle = \begin{cases} G^>(x, t, \sigma_z, x', t', \sigma'_z) & t' > t \\ G^<(x, t, \sigma_z, x', t', \sigma'_z) & t' < t \end{cases} \quad (5.8)$$

where \mathcal{T} and $\bar{\mathcal{T}}$ denote time ordering and anti-time ordering of the subsequent operators. If time evolution is made explicit by introducing the time evolution operator \mathcal{U} the time ordered Greens function reads

$$\begin{aligned} G(x, t, \sigma_z, x', t', \sigma'_z) &= -i \langle \Omega | \mathcal{T} \Psi_H(x, t, \sigma_z) \Psi_H^\dagger(x', t', \sigma'_z) | \Omega \rangle \\ &= -i \langle \Omega | \mathcal{T} \mathcal{U}^\dagger(t, t_0) \Psi(x, t, \sigma_z) \mathcal{U}(t, t_0) \mathcal{U}^\dagger(t', t_0) \Psi^\dagger(x', t', \sigma'_z) \mathcal{U}(t', t_0) | \Omega \rangle \\ &= -i \langle \Omega | \mathcal{T} \mathcal{U}(t_0, t) \Psi(x, t, \sigma_z) \mathcal{U}(t, t') \Psi^\dagger(x', t', \sigma'_z) \mathcal{U}(t', t_0) | \Omega \rangle \end{aligned} \quad (5.9)$$

This notation shows that in any picture different from the Heisenberg picture the Greens function represents a (thermal) expectation value of a string of mixed field and evolution operators taken at different times. In section (5.3.2) this will be the starting point both for the introduction of a (contour) ordering relation of these operators and for a perturbative expansion of the evolution operator.

Another alternative representation of Greens functions is commonly used for the discussion of nonequilibrium problems, consisting of the *retarded*, *advanced* and *Keldysh* Greens function

$$G^R(x, t, \sigma_z, x', t', \sigma'_z) = +\Theta(t - t')(G^>(x, t, \sigma_z, x', t', \sigma'_z) - G^<(x, t, \sigma_z, x', t', \sigma'_z)) \quad (5.10)$$

$$G^A(x, t, \sigma_z, x', t', \sigma'_z) = -\Theta(t' - t)(G^>(x, t, \sigma_z, x', t', \sigma'_z) - G^<(x, t, \sigma_z, x', t', \sigma'_z)) \quad (5.11)$$

$$G^K(x, t, \sigma_z, x', t', \sigma'_z) = G^>(x, t, \sigma_z, x', t', \sigma'_z) + G^<(x, t, \sigma_z, x', t', \sigma'_z) \quad (5.12)$$

While in equilibrium these three Greens functions are dependent functions, they are independent objects in a nonequilibrium theory.

Equilibrium Fourier transformed Greens functions

In equilibrium, the Greens functions only depend on the relative time $\tau = t - t'$ and a Fourier transform in time displays their energy dependence. Moreover, for translation invariant systems a momentum representation can be obtained by a spatial Fourier transform.

$$G_{\sigma_z \sigma'_z}^K(q, \epsilon_q) = \int_{-\infty}^{\infty} d(t - t') \int_{-\infty}^{\infty} d^d(x - x') e^{-\frac{i}{\hbar}(q(x-x') - \epsilon_q(t-t'))} G^K(x, t, \sigma_z, x', t', \sigma'_z) \quad (5.13)$$

5.3 Time dependent perturbation theory

The most common analytic method to approach a time dependent interacting system is time dependent perturbation theory. It can be applied in a variety of different ways. Each of them represents a particular way to expand and to resum the time evolution operator in terms of an infinite perturbation series. As the perturbation series is truncated, results from different approaches may differ even at the same formal order of the expansion. Therefore the challenge is to find the most appropriate but still technically manageable method.

5.3.1 Fermi's golden rule

The simplest, most commonly applied and straightforward approach to time-dependent perturbation theory is given by Fermi's golden rule. Its derivation is based on a Taylor-like series expansion of the time evolution operator in the interaction picture,

$$\mathcal{U}_I(t, t_0) = \mathcal{T} \exp \left(-\frac{i}{\hbar} \int_0^t dt' H_{\text{int}}(t') \right)$$

where \mathcal{T} denotes the time ordering operator [230]. In perturbation theory, the eigenstates of the noninteracting Hamiltonian H_0 form the frame of reference to study the evolution of the occupation of quantum states. Initially, only a single eigenstate $|i\rangle$ with eigenenergy E_i may be occupied. First order interaction effects are responsible for the possibility of transitions from this single occupied initial state into an non-occupied eigenstate $|n\rangle$; with increasing time, these transition probabilities cause a redistribution of the occupation into different eigenmodes of H_0 . For formerly unoccupied eigenmodes $|n\rangle$ with eigenenergy E_n the time dependent amplitudes read in first order non-degenerate perturbation theory $c_n^{(1)}(t) = -i \int_0^t dt' \exp(i(E_n - E_i)t'/\hbar) \langle n | H_{\text{int}} | i \rangle / \hbar$. For a constant interaction which is switched on at zero time this can be easily integrated; then the time dependent occupations indicate the total (integrated) transition probability and depend on the energy distance of the initial and the final state

$$|c_n^{(1)}(t)|^2 = 4 |\langle n | H_{\text{int}} | i \rangle|^2 \frac{\sin^2[(E_n - E_i)t/2\hbar]}{|E_n - E_i|^2} \quad (5.14)$$

Transitions are only possible if both a kinematic and a dynamic requirement are fulfilled: Firstly, the interaction part of the Hamiltonian must couple the initial and final state. In general, this leads to selection rules for allowed transitions. Secondly, the energy kernel implements quantum uncertainty. For short times, transitions may violate energy conservation. In a long-time limit, however, it approaches a delta function in energy

$$|c_n^{(1)}(t \rightarrow \infty)|^2 = \frac{2\pi}{\hbar} |\langle n | H_{\text{int}} | i \rangle|^2 \delta(E_n - E_i) t \quad (5.15)$$

Obviously, the validity of this expression is limited since the occupation would continuously grow in time. Such an artificial behavior is characteristic for a *secular term* and indicates a breakdown of first-order perturbation theory on a certain time scale.

In a golden rule argument, however, this vice is turned into a virtue and a *transition rate* is defined as

$$\Gamma_{|i\rangle \rightarrow |n\rangle} = \lim_{t \rightarrow \infty} \frac{|c_n^{(1)}(t)|^2}{t} = \frac{2\pi}{\hbar} |\langle n | H_{\text{int}} | i \rangle|^2 \delta(E_n - E_i)$$

Moreover, if a transition into a continuum of states is considered, the individual contributions are *incoherently* summed up, weighted by the density of states $\rho(E)$ at the particular energy [230]. This is a bold description of coherent quantum evolution but can be justified *a posteriori*.

$$\Gamma_{|i\rangle \rightarrow \{|n\rangle\}_n} = \frac{2\pi}{\hbar} |\langle n | H_{\text{int}} | i \rangle|^2 \rho(E_n) |_{E_n \approx E_i}$$

Discussing microscopic scattering processes, instead of a density of states the phase space factor related to the particular scattering process enters. For a nonequilibrium Fermi liquid this phase space factor dramatically changes the time behavior.

5.3.2 Coherent perturbation theory with respect to the ground state

The effective treatment of time evolution by an incoherent summation of transition rates neglects possible interference effects between different degrees of freedom. Therefore a correct perturbative approximation of the quantum dynamics caused by an interacting many-body Hamiltonian requires a more advanced field theoretical approach.

A proper way to set up time dependent perturbation theory with respect to the ground state of an interacting quantum system is to construct the interacting quantum theory from a corresponding noninteracting one. This is done by switching on the interaction $H_{H_0}^{\text{int}}(t) = e^{-\alpha|t|} \tilde{H}_{H_0}^{\text{int}}(t)$ *adiabatically* in time, i.e. in the limit $\alpha \rightarrow 0$. This procedure ensures that there is a continuous evolution from the noninteracting ground state $|\Omega_0\rangle$ in the far past to the interacting ground state $|\Omega\rangle$ in the present. Then the time evolution operator $\mathcal{U}(t, t_0)$ links both ground states $|\Omega\rangle = \mathcal{U}(t, -\infty) |\Omega_0\rangle$. In the far future, the interaction is adiabatically switched off again, leading to $|\Omega\rangle = \mathcal{U}(t, \infty) |\Omega_0\rangle$ which is applied in the form $\langle \Omega | = \langle \Omega_0 | \mathcal{U}^\dagger(t, \infty)$. Hence the string of operators in (5.9) can be extended such that the expectation value is with respect to the noninteracting ground state only. For convenience, the different segments of time evolution in (5.9) are denoted by a single evolution operator under time ordering. This defines the action of the time ordering operator \mathcal{T} onto the time-nonlocal operator $\mathcal{U}(\infty, -\infty)$.

This arrangement is advantageous since, according to the Gell-Mann and Low theorem [232], the evolution of the ground state under the adiabatic switching-on and switching off procedure only accounts for a phase $e^{i\Phi} = \langle \Omega_0 | \mathcal{U}(\infty, -\infty) | \Omega_0 \rangle$; it can be easily divided out and hence allows for a novel representation of the time-ordered Greens function (5.7) with respect to the noninteracting ground state.

$$G(x, t, \sigma_z, x', t', \sigma'_z) = -i \frac{\langle \Omega_0 | \mathcal{T} \Psi(x, t, \sigma_z) \Psi^\dagger(x', t', \sigma'_z) \mathcal{U}(\infty, -\infty) | \Omega_0 \rangle}{\langle \Omega_0 | \mathcal{U}(\infty, -\infty) | \Omega_0 \rangle} \quad (5.16)$$

The time-ordered operator product in the denominator motivates a pictorial representation of lining up the field operators and time evolution on a linear and open time contour. Then the expansion of the time evolution operator in an interaction picture leads to a perturbation series in powers of the interaction.

This approach is explicitly designed to describe ground state properties of a system in equilibrium. In most cases the time dependent setup is considered as a mere ancillary technique to establish a controlled and practically time independent perturbation expansion of quantum field theory¹. Since the Gell-Mann and Low theorem does not extend to excited states a different and less simple route has to be taken in nonequilibrium situations.

¹It is worth to point out that this is the origin of the dynamical character of Feynman's perturbation theory

5.3.3 Keldysh nonequilibrium perturbation theory and the problem of secular terms

The breakdown of the Gell-Mann and Low theorem for excited states implies that there is no straightforward and simple procedure to connect an excited state in the far past to a corresponding excited state in the far future (as there is for the ground state). This implies that the linear ordering of operators on a timeline is not possible any more.

Contour ordering of operators

Instead, one has to go back to analyze (5.9) directly, now assuming that $|\Omega\rangle$ is an arbitrary initial state given at an initial time t_0 . Time evolution must be considered on a *closed* contour which starts and ends at this initial state or initial time. The contour ordering operator \mathcal{T}_c represents an ordering procedure of its own kind which is unrelated to the linear time ordering by \mathcal{T} . Therefore, real times t are promoted to 'contour times' τ which parametrize the contour. While at some point of the string of operators in (5.9) time evolution is reversed, the contour times continue monotonously². This defines the contour ordered Greens function

$$\begin{aligned} G^C(x, \tau, \sigma_z, x', \tau', \sigma'_z) &= -i \langle \Omega_0 | \mathcal{T}_c \mathcal{U}(\tau_0, \tau) \Psi(x, \tau, \sigma_z) \mathcal{U}(\tau, \tau') \Psi^\dagger(x', \tau', \sigma'_z) \mathcal{U}(\tau', \tau_0) | \Omega_0 \rangle \\ &= -i \langle \Omega_0 | \mathcal{T}_c \mathcal{U}_c(t_0, t_0) \Psi(x, \tau, \sigma_z) \Psi^\dagger(x', \tau', \sigma'_z) | \Omega_0 \rangle \end{aligned} \quad (5.17)$$

Again, the different sections of contour evolution can be formally rewritten as one evolution operator with respect to a (non-vanishing!) contour integration $\mathcal{U}_c(t_0, t_0) = e^{-i \int_c d\tau H(\tau)}$ under the contour ordering operation.

Perturbative expansion

On this contour, a perturbative expansion of the time evolution operator in an interaction picture representation is possible, leading to Keldysh perturbation theory [231]. Then the perturbative expansion for the contour-ordered Greens function in powers of the interaction H_{int} reads

$$\begin{aligned} G^C(x, \tau, \sigma_z, x', \tau', \sigma'_z) &= -i \langle \Omega_0 | \mathcal{T}_c e^{-i \int_c d\tau H_{H_0}^{\text{int}}} \Psi(x, \tau, \sigma_z) \Psi^\dagger(x', \tau', \sigma'_z) | \Omega_0 \rangle \\ &= -i \sum_n \frac{1}{n} \int_c d\tau_1 \dots d\tau_n \langle \Omega_0 | \mathcal{T}_c H_{H_0}^{\text{int}}(\tau_1) \dots H_{H_0}^{\text{int}}(\tau_n) \Psi(x, \tau, \sigma_z) \Psi^\dagger(x', \tau', \sigma'_z) | \Omega_0 \rangle \end{aligned} \quad (5.18)$$

In analogy to ground state quantum field theory in real space Feynman rules can be formulated for contour-ordered Greens functions and a diagrammatic language exists. The 'contour time' replaces physical time and internal integration at the vertices is performed as a contour integration. Details depend on the particular interacting theory and can be found in [231].

which depicts static properties of a quantum field theory by their underlying quantum dynamical behavior. Therefore, for example, the 'propagation of particles between interaction vertices' has to be considered even in perturbative treatments of equilibrium problems. This dynamical picture of quantum field theory became a paradigm for the understanding of many of its properties, e.g. the quantum state of the vacuum.

²Note that a sequence of time ordered operators can be contour ordered (if all operators lie on the forward path), anti-contour ordered (if all operators lie in the backward path) or not ordered at all (intermingled distribution onto forward and backward path)

Real-time formalism

However, as the contour ordering is a formal construct and its parameters, the 'contour times', are no intuitive physical quantities a real-time formalism for contour ordering has been developed. There the 'contour times' are split up into physical time t and a contour index κ labeling the forward ($\kappa = 1$) and backward ($\kappa = 2$) path. Since the Greens function (5.17) depends on two contour times it is mapped onto a 2×2 -matrix *Keldysh matrix Greens function* $\hat{\mathbf{G}}_{\kappa, \kappa'}$ in *Keldysh space*.

$$G^C(x, \tau, \sigma_z, x', \tau', \sigma'_z) \rightarrow \hat{\mathbf{G}}(x, t, \sigma_z, x', t', \sigma'_z) = \begin{pmatrix} \hat{G}_{11} & \hat{G}_{12} \\ \hat{G}_{21} & \hat{G}_{22} \end{pmatrix} (x, t, \sigma_z, x', t', \sigma'_z) \quad (5.19)$$

Representations in Keldysh space

Referring to the definitions in section (5.2) the components of the Keldysh matrix Greens function can be directly related to ordinary Greens functions.

$$\hat{\mathbf{G}}(x, t, \sigma_z, x', t', \sigma'_z) = \begin{pmatrix} G & G^< \\ G^> & \bar{G} \end{pmatrix} (x, t, \sigma_z, x', t', \sigma'_z) \quad (5.20)$$

Larkin - Ovchinnikov - representation

However, since this representation does not allow for a simple inversion of the matrix, Larkin and Ovchinnikov introduced a rotation in Keldysh space which transform it into an upper triangular matrix. Its components, again, refer to well-known ordinary Greens functions.

$$\mathbf{G}(x, t, \sigma_z, x', t', \sigma'_z) = \mathbf{L}\tau^{(3)}\hat{\mathbf{G}}(x, t, \sigma_z, x', t', \sigma'_z)\mathbf{L}^\dagger = \begin{pmatrix} G^R & G^K \\ 0 & G^A \end{pmatrix} (x, t, \sigma_z, x', t', \sigma'_z) \quad (5.21)$$

where $\mathbf{L} = (\mathbb{1} - i\tau^{(2)})/\sqrt{2}$ is an orthogonal transformation and $\{\tau^{(i)}\}_{i=1,2,3}$ are the Pauli spin matrices.

The Feynman rules found for the contour-ordered Greens function can be mapped directly onto Keldysh space where propagators and vertices are 2×2 - dimensional objects. Internal integration over contour times τ is mapped onto a contraction of internal Keldysh indices and integration over physical time t . I will establish Keldysh perturbation theory for the Hubbard model in chapter (14).

Problem of secular terms

Here I briefly conclude with remarking that this technique, although it allows for the treatment of excited states, only provides a perturbative treatment of the interaction-induced time evolution. This leads naturally to the emergence of *secular terms* which are proportional both to the interaction strength and to time in (5.18); they render a perturbative result unreliable already on short time scales. Hence, while a Keldysh approach provides a faithful microscopic and perturbative formulation of the dynamics of an interacting many-body quantum system it does not improve on the problem of long-time reliability of low order results. Since the aim of this thesis is to give a conclusive description of the short- and longtime evolution of the quenched Hubbard model the question of avoiding secular terms is most relevant. An excursion to perturbation theory in classical mechanics will illustrate answers.

5.3.4 Canonical perturbation theory

Canonical perturbation theory in classical mechanic is a more ingenious variant of doing classical perturbation theory. Instead of its direct brute-force application, first a canonical transformation is applied to change to new coordinates which are closer to the eigenmodes of the Hamilton function. A perturbation expansion of the remaining interaction term is then performed in these new degrees of freedom. This leads to a rearrangement of the perturbation expansion which appears as a renormalization of model parameters. By this way, secular terms can be avoided.

A simple illustration of this approach has been published recently in [233] for a single harmonic oscillator with frequency $\omega_0 = 1$, mass $m = 1$ and a weak anharmonic quartic perturbation of strength g . Here, the key points are quoted.

$$H(q, p) = H_0(q, p) + H_{\text{int}}(q), \quad H_0(q, p) = \frac{p^2}{2m} + \frac{m\omega_0^2}{2}q^2, \quad H_{\text{int}}(q) = \frac{g}{4}q^4 \quad (5.22)$$

Direct application of perturbation theory. In a direct application of perturbation theory and for the initial conditions $q(0) = 0$ and $p(0) = v + 3gv^3/8$ the well-known solution of the harmonic oscillator $q_0(t) = v \sin(\omega_0 t)$ serves as a zeroth order approximation for the full, perturbatively expanded solution $q(t) = q_0(t) + g q_1(t) + \mathcal{O}(g^2)$. This allows for a first order parametrization of the Hamilton equations of motion

$$\dot{q}(t) = \frac{\partial H}{\partial p} = p(t) \quad (5.23)$$

$$\dot{p}(t) = -\frac{\partial H}{\partial q} = -\omega^2 q(t) + gq^3(t) \stackrel{\text{PT}}{=} -\omega^2 q(t) + gq_0^3(t) \quad (5.24)$$

Solving these differential equations for the leads to the explicit solution

$$q(t) = \frac{3}{8}v^3 \sin(t) - \frac{v^3}{8} (\sin(t) \cos^2(t) + 2 \sin(t) - 3t \cos(t)) \quad (5.25)$$

A shift of the unperturbed frequency is indicated by the generation of a higher harmonics. However, the calculation is reliable only on a short time scale as a secular term proportional to time leads to the artefact of an continuously increasing amplitude of the oscillation.

Canonical perturbation theory. A less naïve way to a perturbative solution of the anharmonic oscillator starts with applying a canonical transformation $(p, q) \rightarrow (P, Q)$ [234]. It is defined by a time independent generating functional $F_2(q, P)$ which can be motivated from (5.24). Since the interaction leads to a term gq^3 in the equation of motion (5.24), a term $\sim Pq^3$ in F_2 is plausible because of the transformation law (5.28). Symmetry in q and P suggests another term $\sim P^3q$ and suitable coefficients can be determined *a posteriori*.

$$F_2(q, P) = qP + g \left(\frac{3}{32}Pq^3 + \frac{5}{32}P^3q \right) \quad (5.26)$$

The transformation is then generated such that

$$p(t) = \frac{\partial F_2(q, P)}{\partial q} = P(t) + g \frac{9}{32}P(t)q^2(t) + g \frac{5}{32}P^3(t) \quad (5.27)$$

$$Q(t) = \frac{\partial F_2(q, P)}{\partial P} = q(t) + g \frac{3}{32}q^3(t) + g \frac{15}{32}P^2(t)q(t) \quad (5.28)$$

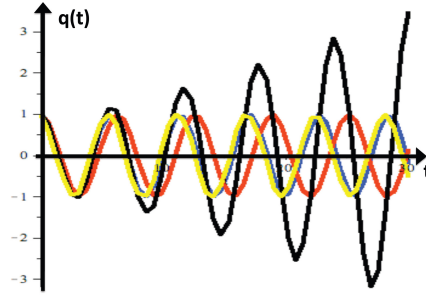


Figure 5.1: This plot shows the dynamics of the coordinate $q(t)$ of a harmonic oscillator ($\omega = 1$) which is perturbed by a weak anharmonicity ($g = 1$). The practically exact numerical solution (blue) is well-approximated by canonical perturbation theory (yellow). Only slight derivations from the exact frequency can be observed at large times. A direct application of perturbation theory in leading order (black) is unconvincing. Secular terms lead to a linear increase of the amplitude and the renormalization of the frequency is insufficient. For comparison, the solution for the unperturbed harmonic oscillator is given (red).

Expressing the Hamiltonian (invariant as F_2 is not explicitly time dependent) in terms of the transformed coordinates and deriving the equations of motions

$$\dot{Q}(t) = \frac{\partial H(P, Q)}{\partial P} = \left(1 - 2g\frac{3}{8}H_0(P, Q)\right)P \quad (5.29)$$

$$\dot{P}(t) = -\frac{\partial H(P, Q)}{\partial Q} = -\left(1 - 2g\frac{3}{8}H_0(P, Q)\right)Q \quad (5.30)$$

Now perturbation theory is applied by linearizing the equations of motion such that $H_0(P, Q)$ is replaced by ω_0 . Then the equations of motion for P and Q are those of a harmonic oscillator with a renormalized frequency $\tilde{\omega} = (1 - 2g\frac{3}{8}\omega_0)$. Transforming back into the original coordinates produces a second order result without secular terms

$$q(t) = \sin(\tilde{\omega}t) \left[v - \frac{3}{32}gv^3 \left(3\cos^2(\tilde{\omega}t) + \frac{5}{3}\sin^2(\tilde{\omega}t) \right) \right] + \mathcal{O}(g^2) \quad (5.31)$$

$$p(t) = \cos(\tilde{\omega}t) \left[v + \frac{3}{32}gv^3 (\cos^2(\tilde{\omega}t) + 5\sin^2(\tilde{\omega}t)) \right] + \mathcal{O}(g^2) \quad (5.32)$$

Now the effect of the anharmonicity is included in the renormalization of the frequency and a fluctuation of the amplitude which, since periodic in time, remains small. Expanding the leading oscillation in powers of g leads back to the secular term observed in (5.25). This great improvement by canonical perturbation theory is visualized in figure (5.1).

5.3.5 Unitary perturbation theory

An equivalent idea of applying advanced perturbation theory to follow the time evolution of an interacting quantum many-body system has been named unitary perturbation theory [235]. In the way it is presented here it applies to Hamiltonians which are not explicitly dependent on time. Similar to the application of canonical transformations in the classical case, a unitary *forward transformation* maps the Hamiltonian into an alternative basis representation in which time evolution can be treated in a simpler way than in the original one. Typically, this is the eigenbasis of the full Hamiltonian and the forward transformation implements its diagonalization. Then the time dependent solution is mapped back into the original basis by the inverse or *backward transformation*; this constitutes the solution for the variables of physical interest.

Both the diagonalizing transformations and the time evolution can now be subjected to a perturbative treatment. The main success of this method roots in the partial separation of time dependence and interaction effects: A perturbative treatment of the diagonalizing transformation leads to a renormalization of model parameters, including some part of the interaction effects. Their absorption into more adequate degrees of freedom is independent of time; any success achieved here reduces the relevance of secular terms. However, in the generic case the perturbative implementation of a diagonalizing transformation does not lead to an exact eigenbasis representations. Errors in the description of the eigenstates and their occupations unavoidably grow in time. Moreover, an approximate treatment of the diagonalization corresponds to an only approximately diagonal Hamiltonian. Its remaining non-diagonal contributions typically destroy the simplicity of time evolution, call for the application of time-dependent perturbation theory and, by that, lead to the reappearance of secular terms. Nonetheless it can be shown in many cases that a perturbative treatment of the diagonalization is sufficient to shift these secular terms to higher orders of the perturbation series. This drastically improves the time reliability of lower orders.

Diagonalizing transformations are unitary and act both on the Hamiltonian and on all observables. Contrary to most other renormalization schemes which construct an effective Hamiltonian describing the appropriate low energy physics of the problem but leave the form of the observables invariant, unitary perturbation theory takes the opposite route: Since a transformation towards a diagonal Hamiltonian is intended, the form of the transformed Hamiltonian is –at least in a perturbative meaning– constrained by this intention. Hence there is no particular interest in the renormalization of the Hamiltonian itself. It is present only indirectly by defining the appropriate transformation. The transformation of the observables, however, becomes the cornerstone of unitary perturbation theory. In the same way as the change towards eigenstates of the full (interacting) Hamiltonian frees the Hamiltonian from explicit interactions, a formerly simple one-particle observable (like the number operator) acquires a nontrivial composite many-particle structure which makes interaction effects explicit. Next to the original one-particle term many-particle contributions add up to form the representation of the transformed observable. This will be seen in great clarity later. Straightforward time evolution with respect to an (approximately) energy diagonal Hamiltonian allows for an independent evolution of these many-particle components; this is the origin of nontrivial dynamics which becomes visible when the backward transformation recombines the differently evolved parts to a time dependent multi-particle observable in the original basis representation of the problem. See figure 5.2 for a sketch. In conclusion, unitary perturbation theory is intended to describe correlation effects with respect to observables. Since all is done in

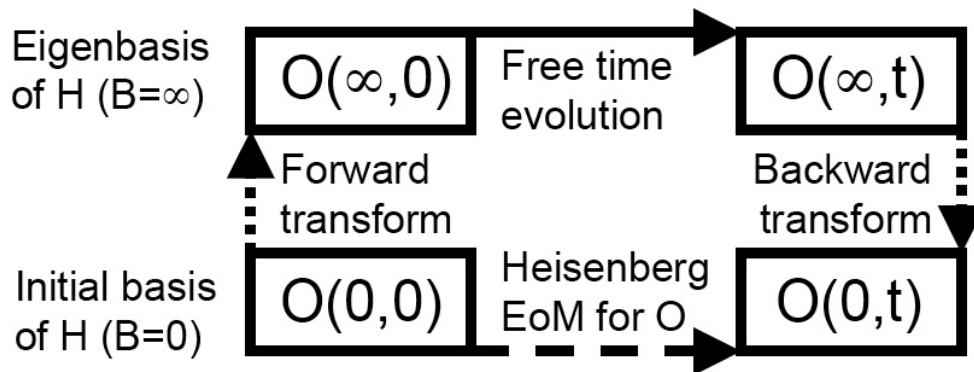


Figure 5.2: The Heisenberg equation of motion for an observable O is solved by transforming to the $B = \infty$ eigenbasis of the interacting Hamiltonian H (forward transformation), where the time evolution can be computed easily. Time evolution introduces phase shifts, and therefore the form of the observable in the initial basis $B = 0$ (after a backward transformation) changes as a function of time.

a Heisenberg picture, observables become the explicit carriers both of time evolution and of correlation effects and change from the usually considered one-particle observables to non-trivial time-dependent many-particle observables which represent a part of the interparticle correlations. In a many-particle problem, this can improve perturbative approaches whenever the transformation of a suitably chosen observables turns out to be tractable. Moreover, there is a natural restriction to those interparticle correlations which are relevant for the dynamics of the considered observable. This reduces the larger complexity of a interacting many-body state which depends in general nontrivially on *all* many-particle correlations.

Chapter 6

Unitary perturbation theory for the squeezed oscillator

In the following chapter the application of unitary perturbation theory is illustrated for the straightforward example of the squeezed oscillator. Since squeezing corresponds to a sudden quench in the oscillator potential this provides a first opportunity to study the full quantum dynamics of a model system. The simplicity of this one-particle problem allows to explicitly compare different implementations of the diagonalizing transformation and their consequences on the observed properties of the model.

6.1 Squeezed one-particle oscillator

The squeezed oscillator is a well-studied one-particle model system which found appreciation in many branches of physics. For two decades researchers have discussed squeezed states of the electromagnetic field which found interest because of their characteristic reduced fluctuations in one field quadrature as compared to coherent states. This suppression of quantum fluctuations in one variable out of a set of non-commuting variables below the threshold obtained for a state of symmetrically distributed minimal uncertainty, i.e. a coherent state, has motivated the naming: In this parameter the phase space portrait of the squeezed state shows sharp details and appears 'squeezed' when compared to that one of a coherent state while fluctuations are inevitably increased in the others. The physical relevance of squeezed states in optics is grounded on the fact that some interesting phenomena [236] are characterized by oscillations with amplitudes below the width of the ground state wave function of a quantum mechanical oscillator due to Heisenberg uncertainty. Exemplary applications may be improved signal-to-noise ratios beyond the quantum limit of coherent light or the interferometric detection of the weak signatures of gravitational waves are still present in the scientific debate.

It has been shown early by [237] that squeezed states cannot be generated adiabatically from the ground state of a quantum mechanical oscillator but sudden changes have to be applied to its parameters, e.g. its frequency or spring constant. Therefore, squeezed states represent a first example of what is now, in the context of a many-body system, called a quench of a quantum system.

In many-body theory, the squeezing operation comes under the name of a Bogoliubov transformation. Recently, it was applied to study the behavior of a quenched Luttinger liquid

in terms of bosonic degrees of freedom by Cazalilla [93]. The implementation of a Bogoliubov transformation in (6.3) follows tightly his work. However, my focus is shifted towards a comparison of perturbative and exact diagonalization methods which serves to illustrate the structure of an analogous flow equation transformation. This is intended to foster the understanding of later results for the Fermi liquid.

Hamiltonian. On the level of the Hamiltonian, squeezing is inferred by an instantly applied change of the prefactor of the quadratic potential, namely the spring constant. Neglecting a linear shift of the potential minimum and squeezing is reduced to a sudden switch in the coupling constant $g(t) = g\Theta(t)$ of the quadratic particle non-conserving operators. With $\hbar = \omega_0 = 1$

$$H = H_0 + H_{\text{int}}, \quad H_0 = a^\dagger a + \frac{1}{2}, \quad H_{\text{int}} = g(t) \left((a^\dagger)^2 + a^2 \right) \quad (6.1)$$

In the following a perturbative analysis of this quench is compared with an exact solution based on the exact diagonalization of H . In both cases the occupation is calculated, i.e. the expectation value of the number operator $\hat{N} = c^\dagger c$ both in the equilibrium ground state of the interacting Hamiltonian H and as a long-time limit of the dynamics of an initial state. The interest is in a remarkable relation between the equilibrium result and the nonequilibrium result which are described by the same functional dependence but variant prefactors. These nontrivial prefactors will later play a key rôle and can already be appreciated in this simple system.

6.2 Perturbative study of squeezing

It may be assumed that the coupling g is a small parameter and nondegenerate perturbation theory can be applied to the interacting Hamiltonian. The perturbative approach is set up in an operator language such that an obvious analogy to the flow equation method for the Hubbard model (cf. chapter 9) holds. Firstly, the diagonalizing transformation is constructed in a perturbative way, then the forward/backward scheme of unitary perturbation theory (following Fig. 5.2) is applied.

Perturbative definition of the diagonalizing transformation

The first step is to implement a *discrete* unitary transformation which diagonalizes the Hamiltonian to leading order in g . The unitary transformation $U(\varphi) = e^{-\eta\varphi}$ is represented by its generator η , i.e. by an anti-hermitian operator, and by a scalar angle variable φ . Then the action of the transformation onto the Hamiltonian can be expanded according to the Baker-Hausdorff-Cambell relation as

$$\begin{aligned} \tilde{H} \equiv U^\dagger H U &= e^{\eta\varphi} H e^{-\eta\varphi} \approx \\ &H_0 + H_{\text{int}} + ([\eta, H_0] + [\eta, H_{\text{int}}])\varphi + \frac{1}{2}[\eta, [\eta, H_0]]\varphi^2 + \dots \end{aligned} \quad (6.2)$$

Demanding that to leading order the interaction term should vanish leads to an implicit definition of the generator

$$\varphi[\eta, H_0] = -H_{\text{int}}. \quad (6.3)$$

Note that it implies $\eta \sim \mathcal{O}(g)$. It can be easily checked that the *canonical generator* defined as the commutator of the noninteracting and the interacting part of the Hamiltonian fulfils this implicit definition (6.3) if an angle $\varphi = 1/4$ is chosen:

$$\eta = [H_0, H_{\text{int}}] = 2g \left((a^\dagger)^2 - a^2 \right) \quad (6.4)$$

Transformed Hamiltonian

In a second step I consider the corrections beyond leading order in the (approximately) diagonalized Hamiltonian which are, in general, second order in g .

$$\begin{aligned} \tilde{H} &= H_0 + [\eta, H_{\text{int}}]\varphi + \frac{1}{2}[\eta, [\eta, H_0]]\varphi^2 \\ &= H_0 - 16\varphi g^2 H_0 + 32\varphi^2 g^2 H_0 + \mathcal{O}(g^3) \\ &\stackrel{\varphi=1/4}{=} (1 - 2g^2)H_0 + \mathcal{O}(g^3) \end{aligned}$$

Thus the transformed Hamiltonian is described by a renormalized frequency $\omega = (1 - 2g^2)\omega_0$. This equation constitutes the discrete analogue of a flow equation for the Hamiltonian which will be discussed later (cf. 9.3). Due to the particular simplicity of squeezing a harmonic oscillator the second order correction can be fully absorbed in a renormalization of parameters.

Transformation of quantum mechanical observables

Similarly to its action onto the Hamiltonian the unitary transformation implies a transformation of all quantum mechanical observables which constitutes the third step of a unitary diagonalization approach.

$$\tilde{\mathcal{O}} = \mathcal{O} + [\eta, \mathcal{O}]\varphi + \frac{1}{2}[\eta, [\eta, \mathcal{O}]]\varphi^2 + \dots \quad (6.5)$$

Making the transformation of creation and annihilation operators explicit up to second order in g allows to represent the action of the diagonalization as a matrix T acting on two-dimensional vector operators.

$$\begin{pmatrix} \tilde{a}^\dagger \\ \tilde{a} \end{pmatrix} = \begin{pmatrix} 1 + g^2/2 & -g \\ -g & 1 + g^2/2 \end{pmatrix} \begin{pmatrix} a^\dagger \\ a \end{pmatrix} =: T^{(2)}(g) \begin{pmatrix} a^\dagger \\ a \end{pmatrix} \quad (6.6)$$

The three steps (6.2 - 6.2) establish a diagonal representation and are, altogether, referred to as the forward transformation. This transformation of the observables can be easily inverted. Up to second order in g the inverse of T , called the *backward transformation*, is given by $T^{-1}(g) = T(-g)$.

Spin-off: The equilibrium occupation

I interrupt the calculation of the nonequilibrium occupation for a short detour in order to evaluate the equilibrium one. To be more specific, the interest is in the occupation of the interacting ground state with 'physical' particles (i.e. particles which are defined by the eigenmodes of the interaction-free Hamiltonian H_0). Denoting the interacting ground state by $|\Omega\rangle$ the equilibrium occupation reads $N^{EQU} = \langle \Omega | a^\dagger a | \Omega \rangle = \langle \Omega | \mathcal{U}^\dagger \mathcal{U} a^\dagger a \mathcal{U}^\dagger \mathcal{U} | \Omega \rangle = \langle \Omega_0 | \mathcal{U}^\dagger a^\dagger a \mathcal{U} | \Omega_0 \rangle$.

This is unitarily equivalent to the evaluation of a transformed number operator with respect to the noninteracting ground state $|\Omega_0\rangle$. Fortunately, the transformation U which links both representations is the inverse of the forward transformation. With the shorthand notation $n_a \equiv \langle \Omega_0 | a^\dagger a | \Omega_0 \rangle$ up to second order in g N^{EQU} reads

$$\begin{aligned} N^{EQU} &= \langle \Omega_0 | \tilde{a}^\dagger \tilde{a} | \Omega_0 \rangle \approx \left(1 + \frac{g^2}{2}\right)^2 \langle \Omega_0 | a^\dagger a | \Omega_0 \rangle + g^2 \langle \Omega_0 | a a^\dagger | \Omega_0 \rangle \\ &\approx (1 + 2g^2)n_a + g^2 \end{aligned} \quad (6.7)$$

Note that even in equilibrium, i.e. by an *adiabatic* switching-on of an interaction, the occupation of the oscillator measured in terms of the original 'particles' is increased. In the following this result will be compared with the nonequilibrium occupation obtained after sudden squeezing.

Time evolution of transformed observables

I resume the calculation for the nonequilibrium case. The forward transformation has already been completed in (6.2 - 6.2). In a fourth step the transformed observables are time evolved for all positive times with respect to the transformed Hamiltonian. This, effectively, accounts for the insertion of time dependent phase factors.

$$\begin{aligned} \begin{pmatrix} \tilde{a}^\dagger(t) \\ \tilde{a}(t) \end{pmatrix} &= \begin{pmatrix} e^{iHt} \tilde{a}^\dagger e^{-iHt} \\ e^{iHt} \tilde{a} e^{-iHt} \end{pmatrix} = \begin{pmatrix} e^{i\omega t} \tilde{a}^\dagger \\ e^{-i\omega t} \tilde{a} \end{pmatrix} \\ &\stackrel{(6.6)}{=} \begin{pmatrix} e^{i\omega t}(1 + g^2/2) & -e^{i\omega t}g \\ -e^{-i\omega t}g & e^{-i\omega t}(1 + g^2/2) \end{pmatrix} \begin{pmatrix} a^\dagger \\ a \end{pmatrix} \end{aligned}$$

Backward transformation

Finally, the time-evolved observables are mapped back to the eigenbasis of the noninteracting Hamiltonian, completing the scheme of Fig. 5.2. Up to second order in g I obtain

$$\begin{aligned} \begin{pmatrix} a^\dagger(t) \\ a(t) \end{pmatrix} &= T^{-1}(g) \begin{pmatrix} \tilde{a}^\dagger(t) \\ \tilde{a}(t) \end{pmatrix} = \\ &\begin{pmatrix} e^{i\omega t} + 2ig^2 \sin(\omega t) & -2ig(1 + g^2/2) \sin(\omega t) \\ 2ig(1 + g^2/2) \sin(\omega t) & e^{-i\omega t} - 2ig^2 \sin(\omega t) \end{pmatrix} \begin{pmatrix} a^\dagger \\ a \end{pmatrix} \end{aligned}$$

This constitutes a consistent perturbative solution of the Heisenberg equations of motion for the operators a^\dagger and a .

Nonequilibrium occupation

In a final step the time dependent number operator is constructed from the time dependent creation and annihilation operator in an obvious way. Since time evolution is unitary, the time evolution of a product of operators is always the product of the time evolved operators which can be easily checked by inserting unity $\mathbb{1} = U(t, t_0)U^\dagger(t, t_0)$. Evaluating the expectation value of the number operator for the initial state $|\Omega_0\rangle$ leads to the nonequilibrium occupation

$$\begin{aligned} N^{\text{NEQ}}(t) &= \langle \Omega_0 | a^\dagger(t)a(t) | \Omega_0 \rangle \\ &= 1 + 4g^2(2 \sin^2(\omega t))(\langle \Omega_0 | a^\dagger a | \Omega_0 \rangle + \frac{1}{2}) \end{aligned} \quad (6.8)$$

The large time limit is obtained by time averaging which is defined for a time dependent variable $A(t)$ as $\overline{A} := \lim_{T \rightarrow \infty} \frac{1}{T} \int_0^T dt A(t)$. Then $\overline{N}^{\text{NEQ}} = n_a + 4g^2 n_a + 2g^2$. Comparing with (6.7), one finds with $\Delta N(t) := N(t) - n_a$

$$\overline{\Delta N^{\text{NEQ}}} = 2 \Delta N^{\text{EQU}} + \mathcal{O}(g^3) \quad \Rightarrow \quad m \stackrel{\text{def}}{=} \frac{\overline{\Delta N^{\text{NEQ}}}}{\Delta N^{\text{EQU}}} \stackrel{\mathcal{O}(g^2)}{=} 2 \quad (6.9)$$

The ratio of the nonequilibrium and the equilibrium occupation, i.e. the **mismatch** $m = 2$, constitutes the main result of this calculation. It states that even in a long-time limit the nonequilibrium occupation does not approach the equilibrium one. The numerical value of two can be considered as a consequence of applying two transformations, the forward and the backward one, such that changes to the occupation due to interaction effects double. In the following I will show that, although the numerical value gets corrections in order g^3 , the mismatch of both occupations is retained for all orders of perturbation theory.

6.3 Exact (Bogoliubov) treatment of squeezing

In a second approach, I follow Cazalilla and implement the diagonalizing transformation by means of a Bogoliubov transformation; the later can be found in many textbooks, e.g. [213]. In condensed matter theory it is commonly used to treat interactions quadratic in creation or annihilation operators. As already mentioned, my aim is to illustrate that the prior perturbative approach exhibits, up to numerical details, the correct nonequilibrium behavior of the system.

The exact diagonalization of the squeezing Hamiltonian (6.1) can be constructed from the action of the (inverse) unitary squeezing operator

$$S(\xi) = e^{1/2\xi^* a^2 - 1/2\xi(a^\dagger)^2} \quad (6.10)$$

where $\xi = r e^{i\theta}$ is an arbitrary complex number which will be specified later. Applying the squeezing operator to the ground state generates squeezed states in analogy with the displacement operator which maps the ground state onto coherent states. On the other hand, applying its inverse is suitable to diagonalize the squeezing Hamiltonian.

Exact transformation of observables

I directly start with writing down the action of $S(\xi)$ onto the creation operator and the annihilation operator.

$$\begin{aligned} \begin{pmatrix} \tilde{a}^\dagger \\ \tilde{a} \end{pmatrix} &= S^\dagger(\xi) \begin{pmatrix} a^\dagger \\ a \end{pmatrix} S(\xi) = \\ &= \begin{pmatrix} \cosh(r) & -e^{-i\theta} \sinh(r) \\ -e^{i\theta} \sinh(r) & \cosh(r) \end{pmatrix} \begin{pmatrix} a^\dagger \\ a \end{pmatrix} =: T^F(\xi) \begin{pmatrix} a^\dagger \\ a \end{pmatrix} \end{aligned} \quad (6.11)$$

Note that $T^F(\xi)$ is not a unitary matrix despite the fact that $\det(T^F(\xi)) = 1$.

Exact Hamiltonian diagonalization

Inserting this transformation into the interacting Hamiltonian (6.1) results in a sum of four terms:

$$\begin{aligned} \tilde{H} = & (\tilde{a}^\dagger)^2 \times \left[e^{i\theta} \cosh(r) \sinh(r) + g \cosh^2(r) + g e^{2i\theta} \sinh^2(r) \right] + h.c. + \\ & \tilde{a}^\dagger \tilde{a} \times \left[\cosh^2(r) + \sinh^2(r) + 4g \cos(\theta) \cosh(r) \sinh(r) \right] + \\ & \mathbb{1} \times \left[2 \cos(\theta) \cosh(r) \sinh(r) \right] \end{aligned}$$

To achieve a diagonal Hamiltonian we demand that the terms quadratic in \tilde{a}^\dagger and \tilde{a} should vanish. This fixes the free parameter $\xi := r e^{i\theta} = r$. For small interactions $|g| \leq 1/2$ real solutions with $\theta = 0$ can be found. With $\sinh(2r) = 2 \sinh(r) \cosh(r)$, $\cosh(2r) = \sinh^2(r) + \cosh^2(r)$ the real parameter r can be linked to the interaction

$$\tanh(2r) = -2g$$

For small values of $g \ll 1/2$ the expansion $\operatorname{arctanh}(x) \sim x$ for $x \ll 1$ implies that $r \approx -g$. Then the nonperturbative Bogoliubov transformation coincides with the perturbative approach in (6.2), with $S(\xi(g) \approx -g) = e^{\eta(g)\varphi}|_{\varphi=1/4}$. The diagonal Hamiltonian shows a renormalized frequency $\omega = \cosh(2r) + 2g \sinh(2r)$ compared to the original frequency $\omega_0 = 1$ in (6.1). For all values of $g < 1/2$ the renormalized frequency is positive and the Hamiltonian is bounded from below. Its dependence on g is plotted in Fig. 6.1. In the limit of small g we find for the renormalized frequency its perturbative value $\omega = (1 - 2g^2)$.

Exact equilibrium occupation

Again, I first calculate the expectation value of the equilibrium number operator, using $\cosh^2(r) - \sinh^2(r) = 1$

$$\begin{aligned} N^{\text{EQU}} &= \langle \Omega | a^\dagger a | \Omega \rangle = \langle \Omega_0 | \tilde{a}^\dagger \tilde{a} | \Omega_0 \rangle \\ &= \cosh^2(r) \langle \Omega_0 | a^\dagger a | \Omega_0 \rangle + \sinh^2(r) \langle \Omega_0 | a a^\dagger | \Omega_0 \rangle \\ &= n_a + 2 \sinh^2(r) \left(n_a + \frac{1}{2} \right) \end{aligned} \tag{6.12}$$

Again, the perturbative limit for small g agrees with (6.7).

Exact nonequilibrium occupation

For the nonequilibrium occupation I solve the Heisenberg equations of motions for the creation and annihilation operators in the (now exact) eigenbasis of the Hamiltonian. The forward transformation of these operators is given by (6.11). Again, I complete the scheme in Fig. 5.2 and compute the time evolution of the transformed operators with respect to the diagonalized Hamiltonian, i.e. with respect to the renormalized frequency ω . The final backward transformation is given by $T^B(r) = T^F(-r)$. These three steps can be easily denoted as subsequent matrix multiplications:

$$\begin{aligned}
\begin{pmatrix} a^\dagger(t) \\ a(t) \end{pmatrix} &= \begin{pmatrix} \cosh(r) & e^{-i\theta} \sinh(r) \\ e^{i\theta} \sinh(r) & \cosh(r) \end{pmatrix} \begin{pmatrix} e^{-i\omega t} & 0 \\ 0 & e^{i\omega t} \end{pmatrix} \begin{pmatrix} \cosh(r) & -e^{-i\theta} \sinh(r) \\ -e^{i\theta} \sinh(r) & \cosh(r) \end{pmatrix} \begin{pmatrix} a^\dagger \\ a \end{pmatrix} \\
&= \begin{pmatrix} e^{-i\omega t} \cosh^2(r) - e^{i\omega t} \sinh^2(r) & i \sin(\omega t) e^{-i\theta} \sinh(2r) \\ -i \sin(\omega t) e^{i\theta} \sinh(2r) & -(e^{i\omega t} \cosh^2(r) - e^{-i\omega t} \sinh^2(r)) \end{pmatrix} \begin{pmatrix} a^\dagger \\ a \end{pmatrix} \quad (6.13)
\end{aligned}$$

$$= \left[\cos(\omega t) \begin{pmatrix} 1 & 0 \\ 0 & -1 \end{pmatrix} - i \sin(\omega t) \begin{pmatrix} \cosh(2r) & -e^{-i\theta} \sinh(2r) \\ e^{i\theta} \sinh(2r) & \cosh(2r) \end{pmatrix} \right] \begin{pmatrix} a^\dagger \\ a \end{pmatrix} \quad (6.14)$$

Composing the number operator reads

$$\begin{aligned}
N^{\text{NEQ}}(t) &= \langle \Omega_0 | a^\dagger(t) a(t) | \Omega_0 \rangle \\
&= \langle \Omega_0 | \left[(e^{-i\omega t} \cosh^2(r) - e^{i\omega t} \sinh^2(r)) a^\dagger + i \sin(\omega t) e^{-i\theta} \sinh(2r) a \right] \times \\
&\quad \left[-i \sin(\omega t) e^{i\theta} \sinh(2r) a^\dagger - (e^{i\omega t} \cosh^2(r) - e^{-i\omega t} \sinh^2(r)) a \right] | \Omega_0 \rangle
\end{aligned}$$

Only the particle number conserving terms $\sim a^\dagger a, aa^\dagger$ contribute and such that the nonequilibrium occupation reads

$$N^{\text{NEQ}}(t) = n_a + (2 \sin^2(\omega t)) \sinh^2(2r) \left(n_a + \frac{1}{2} \right) \quad (6.15)$$

Again, the long time limit is taken as a time average. This implies that the renormalization of the frequency does not affect the occupation at late times and may be neglected.

$$\overline{N^{\text{NEQ}}} = n_a + \sinh^2(2r) \left(n_a + \frac{1}{2} \right) \quad (6.16)$$

Nonperturbative relation between the equilibrium occupation and the nonequilibrium occupation

Comparing (6.16) with (6.12) one observes that for the squeezing Hamiltonian the relation between the equilibrium and nonequilibrium occupation is given by

$$m(r(g)) = \frac{\overline{\Delta N^{\text{NEQ}}}}{\Delta N^{\text{EQU}}} = \frac{\sinh^2(2r)}{2 \sinh^2(r)} \quad (6.17)$$

The precise numerical value of the ratio depends via r on the coupling strength g and is plotted in Fig. 6.1. Note that it is increasing with growing interaction strength. A similar growing behavior of m can be found from a numerical analysis of quenches within the Fermi liquid phase of the Hubbard model. There it shows up as an excessive reduction of the quasiparticle residue below the values predicted in a perturbative calculation (cf. Fig. 11.2). Expanding $\sinh(r) \approx r + r^3/3! + \mathcal{O}(r^5)$ confirms that in the perturbative limit this relation approaches a factor of two. The precise numeric value of the ratio, however, depends on the coupling strength g .

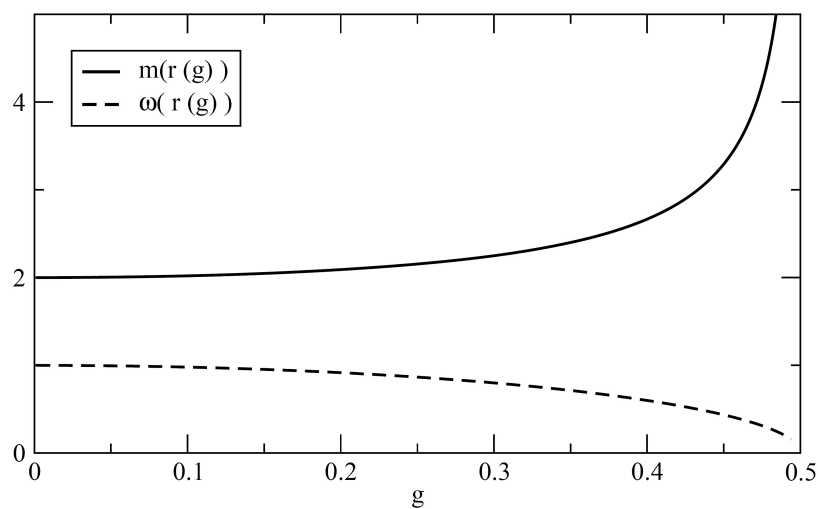


Figure 6.1: This plot illustrates the nonperturbative ratio $m(r(g)) = \frac{\sinh^2(2r(g))}{2\sinh^2(r(g))}$ in (6.17) of the nonequilibrium and the equilibrium correction to the noninteracting occupation due to interaction effects. The real solution for the diagonalization transformation $\xi(g) = r(g)$ is valid only for $g < 1/2$. In the limit of small interaction the factor $m = 2$ is exact. Additionally the renormalized frequency $\omega(g)$ of the diagonal Hamiltonian is shown (dashed line).

Chapter 7

Generic mismatch of equilibrium and nonequilibrium expectation values for one-particle systems

As the discussion of the squeezed oscillator has shown a perturbative approach to quenched one-particle systems captures important features of their nonequilibrium occupation. First of all this is the mismatch between an equilibrium and a nonequilibrium expectation value, namely that of the occupation. In leading order perturbation theory the corresponding ratio acquires a value of $m = 2$.

The following chapter intends to generalize this observation to a large class of weakly interacting one-particle model systems and to more general observables. The statement is formulated as a theorem proven in two ways to illustrate the origin of the mismatch and its relation to unitary perturbation theory. The central point of the proof is a dephasing argument which cannot naïvely be extended to the case of generic many-body systems. Therefore the following statements are rigorously shown for one-particle systems only.

7.1 Prerequisites

Firstly the prerequisites for the following theorem are listed. Reference to them will also be in the discussion of many-body systems in chapter 12.

Demands on the Hamiltonian

Let me consider nondegenerate quantum system with a discrete energy spectrum only and let the Hamiltonian model a weak quantum quench. This implies that it can be split up into a time-independent part H_0 and a time dependent part which is coupled to the earlier by a weak interaction strength g . The time dependence of a quantum quench is modeled by the Heaviside function $\Theta(t)$, and the additionally switched on operator by H_{int} .

$$H = H_0 + g \Theta(t)H_{\text{int}} \tag{7.1}$$

The ground state of H may be denoted by $|\Omega\rangle$, that one of H_0 by $|\Omega_0\rangle$. To avoid trivial cases I assume that H_0 and H_{int} do not commute. Moreover, it is assumed that nondegenerate perturbation theory with respect to the noninteracting ground state is applicable.

Demands on the observables

Furtheron, let \mathcal{O} be a quantum mechanical observable which does not depend explicitly on time and obeys the following relations:

$$\langle \Omega_0 | \mathcal{O} = \mathcal{O} | \Omega_0 \rangle = 0 \quad (7.2)$$

$$[\mathcal{O}, H_0] = 0 \quad (7.3)$$

Then its time evolution in a Heisenberg picture $\mathcal{O}(t)$ is generated solely by the Hamiltonian (7.1). Time evolution is studied from an arbitrary small negative time onwards.

Definitions and notation

- (i) I define as the *nonequilibrium expectation value* of the observable \mathcal{O} in the quenching scenario the long-time limit of the time-averaged quantum mechanical expectation value of the time evolved observable in the initial state (the noninteracting ground state). It is denoted by the overlined observable.

$$\overline{\mathcal{O}} := \lim_{T \rightarrow \infty} \frac{1}{T} \int_0^T dt \langle \Omega_0 | \mathcal{O}(t) | \Omega_0 \rangle \quad (7.4)$$

- (ii) The *equilibrium expectation value* of the observable \mathcal{O} is defined by its quantum mechanical expectation value in the interacting ground state $\langle \Omega | \mathcal{O} | \Omega \rangle$.
- (iii) The *mismatch* of the nonequilibrium and the equilibrium expectation value of the observable \mathcal{O} in the quenching scenario is defined as their ratio

$$m := \frac{\overline{\mathcal{O}}}{\langle \Omega | \mathcal{O} | \Omega \rangle} \quad (7.5)$$

7.2 Theorem

Then in perturbation theory up to second order the nonequilibrium expectation value equals two times the equilibrium expectation value of the observable.

$$\overline{\mathcal{O}} \stackrel{\mathcal{O}(g^2)}{=} 2 \langle \Omega | \mathcal{O} | \Omega \rangle \quad (7.6)$$

This is obviously equivalent to the statement $m = 2$ in second order perturbation theory.

7.3 Proof of the Theorem

I will give two proofs to this theorem. The first one is intended to motivate the physical origins of the prerequisites by relating it to the more conventional picture of overlapping eigenstates. This allows to conclude on its general relevance. The second proof of the theorem is constructed in analogy to unitary perturbation theory and aims at a clearer understanding of how this method displays the finding of a mismatch of nonequilibrium and equilibrium expectation values.

7.3.1 First proof of the theorem by analyzing overlap matrix elements

Eigenstate representation: Firstly, I introduce eigenbasis representations for the noninteracting Hamiltonian H_0 $\{|m\rangle | m \in N_0\}$, the interacting Hamiltonian $\{|M\rangle | M \in N_0\}$ and the observable $\{|j\rangle | j \in N_0\}$ with the eigenvalues $\epsilon_m^0 \stackrel{\text{PT}}{\approx} \epsilon_M$ (for $m = M$) and O_j , respectively. The requirement (7.3) implies the existence of a common eigenbasis of the observable \mathcal{O} and the noninteracting Hamiltonian H_0 such that I can assume pairwise coinciding eigenvectors $|m\rangle = |j\rangle$. For clarity, however, I will keep a separate notation. The equilibrium ground state expectation value is rewritten by inserting unity.

$$\langle \Omega | \mathcal{O} | \Omega \rangle = \sum_j O_j |\langle j | \Omega \rangle|^2 \quad (7.7)$$

An analogous evaluation of the time dependent expectation value by inserting unities, extracting time dependent phase factors and taking their time average leads to

$$\begin{aligned} \overline{\langle \Omega_0 | e^{-iHt} \mathcal{O} e^{iHt} | \Omega_0 \rangle} &= \\ &= \lim_{T \rightarrow \infty} \frac{1}{T} \int_0^T dt \sum_{MM'jj'} \langle \Omega_0 | e^{-iHt} | M \rangle \langle M | j \rangle \langle j | \mathcal{O} | j' \rangle \langle j' | M' \rangle \langle M' | e^{iHt} | \Omega_0 \rangle \\ &= \lim_{T \rightarrow \infty} \frac{1}{T} \int_0^T dt \sum_{MM'jj'} O_{j'} e^{i(\epsilon_{M'} - \epsilon_M)t} \langle \Omega_0 | M \rangle \langle M | j \rangle \langle j | j' \rangle \langle j' | M' \rangle \langle M' | \Omega_0 \rangle \end{aligned}$$

Up to a relative phase, the interacting eigenstates $|M\rangle$ are invariant under time evolution. Therefore, overlap matrix elements are discussed with respect to these states.

Dephasing. Now a dephasing argument is applied, reading off that only terms with vanishing phase factors contribute to the long-time average. This constrains $\epsilon_{M'} = \epsilon_M$. As non-degeneracy of energy levels has been demanded, it implies that all contributions vanish except those for coinciding quantum numbers $M' = M$.

$$\overline{\langle \Omega_0 | e^{-iHt} \mathcal{O} e^{iHt} | \Omega_0 \rangle} = \sum_{Mj} O_j |\langle M | \Omega_0 \rangle|^2 |\langle j | M \rangle|^2 \quad (7.8)$$

The first set of matrix elements $\{\langle M | \Omega_0 \rangle\}_M$ describes a decomposition of the initial state in terms of Hamiltonian eigenstates. This is a statement about the particular initial conditions of the quench problem. Since I discuss a quench from the noninteracting Hamiltonian this is a decomposition of the noninteracting ground state in terms of interacting eigenstates.

The second set of matrix elements $\{\langle j | M \rangle\}_{M,j}$ encapsulates the overlap between the eigenbasis of the observable and the eigenbasis of the Hamiltonian. Since (7.3) holds one can work in the common eigenbasis of the observable and the noninteracting Hamiltonian. Then the overlap between the eigenbasis of the interacting and of the noninteracting Hamiltonian is discussed.

Perturbative evaluation of overlap matrix elements. In both cases the matrix elements can be evaluated by applying perturbation theory to the Hamiltonian $H = H_0 + H_{\text{int}}$, treating H_{int} as a small perturbation. Making this explicit to leading order reads

$$|\langle m | M \rangle|^2 \stackrel{\text{PT}}{=} \begin{cases} 1 & \text{for } M = m \\ \left| \frac{\langle m | H_{\text{int}} | M \rangle}{(\epsilon_M^0 - \epsilon_m^0)} \right|^2 & \text{for } M \neq m \end{cases}$$

As (7.2) implies $O_0 = 0$ the direct overlap between the interacting and the noninteracting ground state does not contribute to the sums in both (7.7) and (7.8); hence they are at least second order in g . We compare the right hand side of both equations for any fixed value of j . In the nonequilibrium case, second order contributions require a resonance condition for the involved quantum numbers, $M = j$ or $M = 0$.

$$|\langle M | \Omega_0 \rangle|^2 \times |\langle j | M \rangle|^2 \stackrel{\text{PT}}{=} \begin{cases} |\langle J | \Omega_0 \rangle|^2 \times 1 & \text{for } M = j =: J \\ 1 \times |\langle j | \Omega \rangle|^2 & \text{for } M = 0 \end{cases}$$

Because of the symmetry $|\langle J | \Omega_0 \rangle|^2 = |\langle j | \Omega \rangle|^2$ in leading order perturbation theory, both contribute equally $|\langle j | \Omega \rangle|^2$ to the sum over M . Then in second order perturbation theory holds

$$\overline{\langle \Omega_0 | e^{-iHt} \mathcal{O} e^{iHt} | \Omega_0 \rangle} = 2 \sum_j \mathcal{O}_j |\langle j | \Omega \rangle|^2 = 2 \langle \Omega | \mathcal{O} | \Omega \rangle$$

and the theorem is proven.

Discussion of the first proof. The first proof highlights the important rôle of dephasing arguments as well as the particular nature of the observable which is expressed by the demand (7.3). Only the existence of a common eigenbasis allows for the application of perturbation theory for the Hamiltonian to study overlap matrix elements of the eigenstates of the observable with eigenstates of the total Hamiltonian. This observation emphasizes that a mismatch between nonequilibrium and equilibrium expectation values can be also expected if H_0 is not a quadratic Hamiltonian. Then, however, suitable observables have to be found which may be different from the occupation.

7.3.2 Second proof of the theorem by applying unitary perturbation theory

The second proof of the theorem is constructed in analogy to unitary perturbation theory and aims at a clearer understanding of this approach and its particular merits. Hence I follow the scheme presented in Fig. 5.2 and sketch the same steps of a calculation based on unitary perturbation theory which will re-appear in the discussion of the quenched Fermi liquid.

Definition of a unitary transformation. Here a *single* unitary transformation $\mathcal{U}_s^\dagger = e^{\eta_s}$ is defined by its anti-hermitian generator $\eta_s = -\eta_s^\dagger$, demanding that its application to the Hamiltonian disposes the interaction part of the Hamiltonian to first order of g . Expanding its unitary action onto the Hamiltonian

$$\tilde{H} = e^{\eta_s} H e^{-\eta_s} = H_0 + \underbrace{H_{\text{int}} + [\eta_s, H_0]}_{\mathcal{O}(g)} + [\eta_s, H_{\text{int}}] + \frac{1}{2} [\eta_s, [\eta_s, H_0 + H_{\text{int}}]] + \mathcal{O}(g^3) \quad (7.9)$$

hence allows to read off an implicit definition of η_s by

$$[\eta_s, H_0] = -H_{\text{int}}$$

which justifies the assumption $\eta_s \sim \mathcal{O}(g)$ in (7.9). Then the transformed Hamiltonian equals the free Hamiltonian up to second order corrections.

Computation of the interacting ground state expectation value. In the following I exploit a formal coincidence which holds for all systems with a nondegenerate single ground state: For any such Hamiltonian, the diagonal representation of the interacting ground state in terms of the diagonal degrees of freedom can be formally identified with the ground state of the noninteracting Hamiltonian; thus they can be related by $\mathcal{U}_s^\dagger |\Omega\rangle = |\Omega_0\rangle$ or, to leading order, by $|\Omega\rangle = (1 - \eta_s) |\Omega_0\rangle + \mathcal{O}(g^2)$. As every Hamiltonian can be diagonalized, this does not pose any further restrictions. Hence with (7.2)

$$\langle \Omega | \mathcal{O} | \Omega \rangle = \langle \Omega_0 | \mathcal{U}_s^\dagger \mathcal{O} \mathcal{U}_s | \Omega_0 \rangle = - \langle \Omega_0 | \eta_s \mathcal{O} \eta_s | \Omega_0 \rangle + \mathcal{O}(g^3) \quad (7.10)$$

The simple diagonal representation of the interacting ground state motivates the application of operator-based transformation schemes like the flow equation method in equilibrium since correlation effects are, formally, fully transferred from the description of an interacting ground state to the particular form of transformed observables. Thus one can avoid to discuss the full complexity of the interacting ground state and restrict to those correlation effects which become actually relevant for a particular observable. The transformation $\mathcal{U}_s^\dagger \mathcal{O} \mathcal{U}_s$ can be performed in the most convenient way.

Real-time dynamics of the observable after the quench. For the evaluation of the nonequilibrium expectation value $\bar{\mathcal{O}}$ I start with the sequential application of three unitary transformations. Firstly, at time $t = 0$ the observable is represented approximately in the energy-diagonal eigenbasis of the Hamiltonian.

$$\tilde{\mathcal{O}}(0) = \mathcal{O}(0) + [\eta_s, \mathcal{O}(0)] + \frac{1}{2} [\eta_s, [\eta_s, \mathcal{O}(0)]] + \mathcal{O}(g^3) \quad (7.11)$$

Now we apply unitary time evolution to the transformed observable with respect to $\tilde{H} = H_0 + \mathcal{O}(g^2)$. This is time-dependent perturbation theory to first order.

$$\tilde{\mathcal{O}}(t) = e^{-iH_0 t} \tilde{\mathcal{O}}(0) e^{iH_0 t} \quad (7.12)$$

Then one inserts (7.11) into (7.12) and attributes the time dependence to the generator $\eta_s \rightarrow \eta_s(t) = e^{-iH_0 t} \eta_s(0) e^{iH_0 t}$. This is possible because of (7.3) and ensures that (7.2) holds for all times. Finally, the backward transformation $\eta_B = -\eta_s(0)$ is applied.

$$\begin{aligned} \mathcal{O}(t) &= \tilde{\mathcal{O}}(t) - [\eta_s(0), \tilde{\mathcal{O}}(t)] + \frac{1}{2} [\eta_s(0), [\eta_s(0), \tilde{\mathcal{O}}(t)]] + \mathcal{O}(g^3) \\ &= \mathcal{O}(0) + [\eta_s(t), \mathcal{O}] + \frac{1}{2} [\eta_s(t), [\eta_s(t), \mathcal{O}]] - [\eta_s(0), \mathcal{O}] \\ &\quad - [\eta_s(0), [\eta_s(t), \mathcal{O}]] + \frac{1}{2} [\eta_s(0), [\eta_s(t), \mathcal{O}]] + \mathcal{O}(g^3) \end{aligned} \quad (7.13)$$

One evaluates the expectation value of $\mathcal{O}(t)$ in the initial state $|\Omega_0\rangle$. Due to (7.2) many contributions vanish.

$$\langle \Omega_0 | \mathcal{O}(t) | \Omega_0 \rangle = \left\langle 2 \left(-\frac{1}{2} \right) \eta_s(t) \mathcal{O} \eta_s(t) + \eta_s(0) \mathcal{O} \eta_s(t) + \eta_s(t) \mathcal{O} \eta_s(0) - 2 \left(\frac{1}{2} \right) \eta_s(0) \mathcal{O} \eta_s(0) \right\rangle_{\Omega_0} \quad (7.14)$$

Dephasing. Inserting unity $\mathbb{1} = \sum_m |m\rangle \langle m|$ in terms of eigenstates of the noninteracting Hamiltonian H_0 shows that the second and the third term in (7.14) dephase and do not contribute to the long time average:

$$\begin{aligned} \langle \Omega_0 | \eta_s(0) \mathcal{O} \eta_s(t) | \Omega_0 \rangle &= \sum_m \langle \Omega_0 | \eta_s(0) \mathcal{O} | m \rangle \langle m | e^{-iH_0 t} \eta_s(0) e^{iH_0 t} | \Omega_0 \rangle \\ &= \sum_m O_m e^{i(\epsilon_m - \epsilon_0)t} \langle \Omega_0 | \eta_s(0) | m \rangle \langle m | \eta_s(0) | \Omega_0 \rangle \end{aligned} \quad (7.15)$$

For $m = 0$ equation (7.2) implies $\mathcal{O}_0 = 0$. As I have assumed a nondegenerate Hamiltonian H_0 one obtains

$$\overline{\langle \Omega_0 | \eta_s(0) \mathcal{O} \eta_s(t) | \Omega_0 \rangle} = \overline{\langle \Omega_0 | \eta_s(t) \mathcal{O} \eta_s(0) | \Omega_0 \rangle} = 0$$

On the other hand, making use of the commutation of H_0 and \mathcal{O} (7.3)

$$\langle \Omega_0 | e^{-iH_0 t} \eta_s e^{iH_0 t} \mathcal{O} e^{-iH_0 t} \eta_s e^{iH_0 t} | \Omega_0 \rangle = \langle \Omega_0 | \eta_s(0) \mathcal{O} \eta_s(0) | \Omega_0 \rangle$$

Consequently, one arrives at $\overline{\mathcal{O}} = -2 \langle \Omega_0 | \eta_s(0) \mathcal{O} \eta_s(0) | \Omega_0 \rangle$. With (7.10) the theorem is proven.

Discussion of the second proof. The second proof explains the factor of two as the accumulation of equal second order corrections both from the forward and from the backward transformation. The drop-out of transient or oscillatory behavior in (7.14) due to time averaging is more explicit. This depicts the major merit of the transformation scheme: Fundamental correlation-induced effects – as it is, for example, the difference between the interacting and the noninteracting ground state – enter a perturbative study of time evolution performed in an energy-diagonal representation already as time-independent offsets. That their influence is stronger in nonequilibrium than in equilibrium can be seen directly.

7.4 Corollary to the Theorem regarding the kinetic energy of quenched systems

In many systems the noninteracting part H_0 of an interacting Hamiltonian H represents the kinetic energy for which the following relation holds¹:

$$\overline{E^{\text{NEQ, KIN}}} = 2E^{\text{EQU, KIN}}$$

.

Proof: Define $E^{\text{NEQ, KIN}}(t) := \langle \Omega_0 | H_0(t) | \Omega_0 \rangle$ and apply the theorem for $\mathcal{O} = H_0$.

The above theorem explains the factor 2 in the ratio between nonequilibrium and equilibrium expectation values as a rather general observation in systems with discrete energy spectra. In the following I will show how this factor 2 appears for an interaction quench in a Fermi liquid with continuous spectrum and what rôle it plays for the nonequilibrium dynamics.

¹Note that the increase in the kinetic energy beyond its value for the interacting ground state, however, does not necessarily indicate its thermal distribution. Only the later would describe heating effects.

Chapter 8

Flow equations

The cornerstone for the application of unitary perturbation theory to a quantum model is the construction of a sufficient approximation of the diagonalizing transformation. For the one-particle quenched oscillator it was possible to simply write down a single unitary transformation suited for this purpose and to show that a perturbative approach leads to consistent results. Yet the diagonalization of many-particle systems is, in general, more intricate. In some cases, exact diagonalization using e.g. Bethe ansatz or bosonization techniques is feasible. For other systems, the *flow equation method* provides a generic frame for an approximate treatment.

Conceptually, it has been inspired by Jacobi's method for the simple numerical solution of coupled linear equations [238], which became an established and widely available tool for the numerical diagonalization of matrices in the 20th century. Therefore, approaches comparable with the flow equation technique appeared first in numerical mathematics [239–241] where they are known as similarity transformations. In 1993 Glazek and Wilson [242, 243] applied it to condensed matter problems, calling it *Similarity renormalization scheme*. Independently, Wegner studied *Flow equations for Hamiltonians* [244]. As he is one of my scientific ancestors, I will follow his way of formulating the method.

In the meantime, the flow equation technique has been applied to a great variety of many-body systems both in equilibrium and nonequilibrium. An extensive list of model systems and problems which have been tackled by the flow equation method can be found in [245] and a comprehensive textbook review is available [246]. Quite recently, it has been successfully applied to nonequilibrium problems [233, 235, 247, 248].

8.1 General introduction

The flow equation method rests on the grounds of many-body quantum theory. A band model of one-particle states is described by the kinetic part of the Hamiltonian which is diagonal in a momentum representation. The large (infinite) number of degrees of freedom forms a continuous band of one-particle energies ϵ_k . Thus in the thermodynamic limit of large particle number ϵ_k can be treated as a continuous parameter. Interactions impose couplings between states at different energies and enter the Hamiltonian by H_{int} . They can be understood as two-, few- and many-particle scattering processes which depict joint in- and out- scattering from and into one-particle states; they are represented by interaction matrix elements and characterized by the corresponding difference in one-particle energies

$\Delta\epsilon = \sum_{i=\text{out}} \epsilon_i - \sum_{j=\text{in}} \epsilon_j$. If for a process $\Delta\epsilon = 0$ holds the corresponding matrix element is called *energy diagonal*.

8.1.1 Renormalization group ideas.

Although for systems at low temperature only low-energy properties are observed, high energy interaction terms influence the low energy behavior and cannot be neglected. For instance, in condensed matter problems on a regular lattice only lattice momenta within a Brillouin zone are relevant. The explicit calculation of further modes is usually not needed and schemes have been developed to include their influence on low energy observations by the joint modification of low-energy coupling constants and the elimination of high energy modes. This can be done continuously for a small shell of highest energy modes, typically by integrating those out in a path integral or by a similar coarse-graining transformation. By this procedure automatically different energy scales are separated and treated one after the other. The continuous modification of the low energy parameters can be depicted as a flow in the parameter space of all Hamiltonians with similar structure. All Hamiltonians represented by parameters on the trajectory of the flow describe the same low energy physics. This is, in essence, the *renormalization group approach*, which became a standard method for the treatment of many-body systems and has been widely reviewed [249].

8.1.2 Philosophy of the flow equations.

Although it is influenced by renormalization group ideas the flow equation method follows a different philosophy: While RG methods intend to reduce the complexity of a given Hamiltonian by constructing an effective Hamiltonian in a restricted low-energy sector of the original Hilbert space which still describes the same low energy physics, the flow equation method does not downsize the effective Hamiltonian at all. No modes are eliminated and, in principal, no restriction to low energy behavior takes place. Instead, a continuous sequence of infinitesimal unitary transformations is applied to redistribute the influence of interactions in a controlled way onto the form of the considered observables. The flow equation transformation is set up in such a way that its exact implementation would lead to a Hamiltonian which is precisely diagonal in *energy* space. This implies that all interparticle correlations induced by energy nondiagonal interaction processes, i.e. processes for which $\Delta\epsilon \neq 0$, are not longer described by the Hamiltonian but by a composite form of formerly simple observables. Energy scale separation holds with respect to the transfer energy $\Delta\epsilon$ in that sense that by the action of the infinitesimal unitary transformations those interactions connecting states with largest energy distance $\Delta\epsilon$ are erased first. Simultaneously, the value of the other Hamiltonian parameters are renormalized. With the ongoing of the continuous transformation their change can be described as a flow; it is parametrized by a scalar, nonnegative and monotonously growing *flow parameter* $B \in [0, \infty[$ which can be related to an energy scale $\Lambda_B = 1/\sqrt{B}$. $B = 0$ describes the initial setup of the problem, $B \rightarrow \infty$ corresponds to the "most diagonal" representation which is achievable by the flow equation method. Contrary to an renormalization group scheme the Hamiltonian flow itself is a rather meaningless object; it only specifies to what extend a particular setup of the method actually reaches Hamiltonian diagonalization and serves, in this sense, as a feature to control the method. Yet together with the flow of related parameters in the observables it provides valuable insight into the energetic structure of the model.

8.1.3 Limited diagonalization of the flow equation method.

However, the flow equation transformation does not fully diagonalize the Hamiltonian with respect to the many-particle Hilbert space. This is a disadvantage caused by technicalities of the method. It implies that correlations imposed by energy diagonal processes are always described by a many-body energy-diagonal Hamiltonian $\tilde{H} = \tilde{H}_0 + \tilde{H}_{\text{int}}$. In the context of unitary perturbation theory this requires a perturbative treatment of the time evolution generated by \tilde{H}_{int} and diminishes the particular use of the transformation scheme. Therefore, a flow equation implementation of the diagonalizing transformation leads to a remaining non-trivial time evolution; its perturbative treatment may produce secular terms. Their relevance and effects on the dynamics of a particular observable have to be individually discussed for every observable.

This problem is most relevant for one-dimensional systems where a linear dispersion relation is applicable. Then energy and momentum are equivalent; diagonalizing a Hamiltonian up to energy diagonal terms then does not diagonalize in the momentum sector of the Hilbert space and, consequently, does not provide a sufficient diagonalization. A naïve extension of the method and the observations presented here for a Fermi liquid to a one-dimensional system is therefore not possible.

8.2 Definition of the infinitesimal transformations

8.2.1 Setup of a differential flow equation for observables

Infinitesimal unitary transformations $\mathcal{U}(B_0 + dB, B_0)$ which map a system at one value of the flow parameter $B = B_0$ onto a differentially close other value $B = B_0 + dB$ can be generated by a generator $\eta(B_0)$ which is an element of the corresponding Lie algebra. Hence it is linked to an *infinitesimal* transformation via $\mathcal{U}(B_0 + dB, B_0) = \exp[\eta(B_0)dB]$.

In general, the generator does not commute with itself at different points of the flow, i.e. $[\eta(B), \eta(B')] \neq 0$ for $B \neq B'$. This requires to consider B -ordering (denoted by the ordering operator \mathcal{T}_B) when a finite unitary transformation has to be constructed from infinitesimal steps, in full analogy to time ordering in a perturbative approach to quantum time evolution.

$$U(B, B_0) = \mathcal{T}_B e^{\int_{B_0}^B dB' \eta(B')} \quad (8.1)$$

Because of the difficulties involved with B -ordering this explicit form of the transformation will never be used. Instead, the differential action of the unitary transformation applied to a particular observable \mathcal{O} can be, to leading order in a Baker-Campbell-Hausdorff-expansion, expressed as a differential equation

$$\mathcal{O}(B_0 + dB) = \mathcal{U}^\dagger(B_0 + dB, B_0) \mathcal{O}(B_0) \mathcal{U}(B_0 + dB, B_0) = \mathcal{O}(B_0) + dB[\eta(B_0), \mathcal{O}(B_0)] + \mathcal{O}(dB^2)$$

In the infinitesimal limit $dB \rightarrow 0$ this leads to the operator *flow equation for an observable*

$$\frac{d\mathcal{O}(B)}{dB} = [\eta(B), \mathcal{O}(B)] \quad (8.2)$$

This holds for all observables, including the Hamiltonian itself. The later, however, has a distinguished rôle as it sets the decisive constraints for the diagonalization transformation. However, since only the initial Hamiltonian and, to a lesser degree, the final, approximately

energy-diagonal Hamiltonian are fixed boundary conditions there is a large degree of freedom how the continuous sequence of infinitesimal unitary transformations is actually constructed. This allows for the implementation of other desirable features like energy scale separation or a flexible adaption of the method to particularities of a discussed observable. Energy scale separation, for instance, implies that during the diagonalization process deeply inelastic scattering processes (i.e. $|\Delta\epsilon| \gg 0$) are suppressed already at small values of the flow parameter. Successively, those with lower energy differences are treated while elastic scattering processes ('energy-diagonal ones') remain unchanged. This links the flow equation method to the renormalization group and allows to study the renormalization flow of the Hamiltonian parameters.

8.2.2 Canonical generator.

The definition of the generator of each infinitesimal unitary transformation for any real value of the flow parameter between zero and infinity defines the full unitary transformation. Wegner [244] showed that energy scale separation can be achieved by the *canonical generator* which represents a differential form of equation (6.4).

$$\eta(B) = [H_0(B), H_{\text{int}}(B)] \quad (8.3)$$

It is obviously anti-hermitian since both the noninteracting Hamiltonian H_0 and the full Hamiltonian H are hermitian.

8.2.3 Intrinsic flexibility and fine-tuning of the method.

This definition, however, still does not exhaust the full flexibility of the method. Now the decisive conceptual point lies in the split-up of the Hamiltonian into a noninteracting $H_0(B)$ ¹ which denote and an interacting part $H_{\text{int}}(B)$ at *any* point of the flow. For values of B different from the starting point $B = 0$ this is to a certain degree arbitrary and there is no plausible argument to justify a particular choice *a priori*. Instead, one encounters a major feature of the flow equation technique, namely the strong interdependence between initial definitions, truncations of intermediate expressions and final results for the Hamiltonian and other observables. This allows to systematically fine-tune the method for many particular questions with respect to the particular energetic structure of the Hamiltonian and the nature of the discussed observable. I think that much of the success of the flow equation method is owed to this intrinsic flexibility. It may be reminiscent of a self-consistent or iterative procedure which is effective both in a full numerical implementation of the method and in analytical approximations. For instance, it is very typical to use the explicit behavior of a n^{th} order result of a flowing coupling constant as a parametrization for the computation of its $(n+1)^{\text{th}}$ order correction.

8.3 Representations of observables and normal ordering.

A suitable approximate representation of observables connects the differential action of an infinitesimal unitary transformation as defined by the flow equation (8.2) to the actual properties of the generated flow. Therefore, it is gained from an iterative behavior, starting with

¹The notation $H_0(B)$ might be misleading. It does *not* refer to the evolution of the observable $\mathcal{H}_0(B)$ (which describes the kinetic energy) under the flow. See the following section for details.

an initial ansatz, studying the flow of its components and the generation of higher order terms due to the commutator in (8.2) and re-defining the initial ansatz according to the observations made. This allows to identify the most relevant implications of a diagonalizing transformation onto the observables.

8.3.1 Representations of flowing observables

In order to provide a frame for such a representation, a difference between physical observables and operators linked to a physical statement made in the initial basis representation on the one hand and a formal operator basis on the other hand must be made. The first class includes, for instance, the number operator \mathcal{N}_k (an observable), the Hamiltonian \mathcal{H} (read as an observable for the total energy) or the creation operator of a physical electron in the momentum mode k , \mathcal{C}_k^\dagger (no observable). In this thesis these physically meaningful objects are denoted by calligraphic letters. Although their physical meaning persists throughout the different unitary representations, *their representation* depends on the flow parameter and—in the context of unitary perturbation theory—on time; this is indicated by making a B - or time dependence explicit, e.g. $\mathcal{C}_k^\dagger(B; t)$.

On the other hand, a formal operator basis is introduced and denoted by formal operators which do not explicitly flow. They are denoted by Latin letters and represent one-, two- and many-particle operators in the language of second quantization $T_r \in \{c_i^\dagger, c_j, c_i^\dagger c_j, \dots\}$. For zero flow and zero time both representations match, i.e. $\mathcal{C}_k(B=0, t=0) = c_k$. Beyond that point, scalar flowing coupling constants $g(B; t)$ absorb the unitary and the time dynamics of the discussed physically meaningful object. Their flow is discussed by the flow equation method.

$$\mathcal{O}(B; t) = \sum_{r \in N_0} g_r(B; t) :T_r: \quad (8.4)$$

Note that the B -dependent representation may be very different from the initial representation of a simple observable. While, typically, all but one of the flowing coupling constants g_r vanish at $B=0$, higher order terms acquire nonzero weight under the flow. In most practical cases, this cannot be dealt with exactly but requires truncations. These truncations can be made systematically by perturbative arguments, discussing the dependence of the flowing coupling constants on an expansion parameter.

8.3.2 Normal ordering and truncations

The representation of an observable according to (8.4) suggests an interpretation as a split-up into one-, two- and many-particle contributions. Normal ordering the operators T_r with respect to a particular state $|\Psi_N\rangle$ allows for a clear separation of these aspects. This can be easily seen:

Wegner formular for normal ordering of operator products. Following Wegner [250], normal ordering of higher products $A(a)B(b)$ of elementary fermionic operators $a_l, b_l \in \{c_l^\dagger, c_l\}$ can be recursively defined; one only assumes that Wick's theorem holds, the ground state correlators read $G_{kl} = \langle a_k a_l \rangle$ and the anticommutator relates to it via $\{a_k, a_l\} = G_{kl} + G_{lk}$.

$$:A(a)::B(b): = :e^{\sum G_{kl} \frac{\partial^2}{\partial a_k \partial b_l}} A(a)B(b): \Big|_{b=a} \quad (8.5)$$

The operators c_k and the derivatives $\partial/\partial a_k$ are both Grassmannian, producing a minus sign under interchange. In particular, $\partial a_k/\partial a_l = \delta_l^k - a_k \partial/\partial a_l$.

Explicit example for common fermions. For fermions, only two correlators do not vanish: $n_k = \langle c_k^\dagger c_k \rangle$ and $n_k^- = 1 - n_k = \langle c_k c_k^\dagger \rangle$. Expanding the exponential produces all contractions according to Wick's theorem for known individual normal ordering of $:A(a):$ and $:B(b):$. Making this explicit shows that due to normal ordering all lower rank contractions present in higher order operator products (e.g. by 'coincidences of indices' between creation and annihilation operators) are effectively removed; for instance,

$$\begin{aligned} :c_1^\dagger c_1 c_2^\dagger c_2: &= c_1^\dagger c_1 c_2^\dagger c_2 - :c_1^\dagger c_1: \delta_2^{2'} n_2 - :c_2^\dagger c_2: \delta_1^{1'} n_1 + :c_2^\dagger c_1: \delta_2^{1'} n_2 \\ &\quad - :c_1^\dagger c_2: \delta_1^{2'} (1 - n_1) - \delta_2^{1'} \delta_1^{2'} n_2 (1 - n_1) + \delta_1^{1'} \delta_2^{2'} n_1 n_2 \end{aligned}$$

Obviously, normal ordering extracts lower rank contractions from the 'bare' two-particle term such that only four-point correlations are retained in the normal ordered lhs. This illustrates that with respect to the particular state $|\Psi_N\rangle$ (8.4) describes a hierarchy of strictly separated one-, two- and many-body features.

Normal ordering and truncation. Although normal ordering only redistributes the effects of certain lower rank contractions, it becomes decisive in combination with truncations of higher many-body terms in (8.4). There only the truncation of normal-ordered terms can be justified since 'bare' higher many-body contain a hidden contribution to lower many-body processes. This feedback is made explicit by normal ordering and can be properly included into a flow equation analysis. It is the source of couplings between the differential flow equations for the coupling constants which I will set up shortly; hence normal ordering is vital for the flow equation method.

Normal ordering with respect to which state? Naturally, the question arises with respect to what state $|\Psi_N\rangle$ normal ordering should be imposed. Since this is part of an approximation scheme the best justification for whatever choice has been made is *a posteriori*. For the analysis of a Fermi liquid which is presented here a pronounced perturbative point of view is taken. For every step of the flow it is again grounded on the interplay of eigenmodes defined by the noninteracting part of the Hamiltonian $H_0(B)$, a perturbative shift of their occupation under the influence of $H_{\text{int}}(B)$ and a (negligible) renormalization of the mode frequencies $\epsilon_k(B)$. Since this view should be consistently reflected in the arrangement of any perturbation series expansion, normal ordering with respect to the current ground state of $H_0(B)$ is both technical simple and plausible. It ensures that all aspects of perturbation theory are related to a single common reference state $|\Psi_N(B)\rangle = |\Omega_0(B)\rangle$. Under the flow, this implies a constant re-adjustment of the normal ordering procedure. However, it can be easily implemented since the ground state of a noninteracting Hamiltonian always corresponds to a filled Fermi sea in suitable degrees of freedom. Hence the correlator remains invariant $n_k(B) = \langle \Omega_0(B) | c_k^\dagger c_k | \Omega_0(B) \rangle = n_k(B=0) = n_k$.

It may be pointed out that the successful application of the flow equation method to a nonequilibrium Fermi liquid can be traced back to the joint simplicity of $H_0(B) = H_0(B=0)$ and $n_k(B) = n_k(B=0)$.

8.4 Continuous sequence of infinitesimal transformations

Inserting (8.4) into (8.2) allows to separate the flow equation for the observable into a set of coupled differential equations for the flowing coupling constants. This requires that the representation (8.4) already includes all terms which are generated by the commutator $[\eta(B), \mathcal{O}(B)]$. In practice, however, one constructs this representation by starting with the initial form of the observable and adding all those terms to an ansatz (8.4) which are influential in the final result. Again, this may require an iterative procedure to achieve consistency on a certain fixed order of perturbation theory.

Part II

Quench of a Fermi liquid

Chapter 9

The flow equation transformation for the Hubbard Hamiltonian

In the following chapter the flow equation method is applied to the Hubbard Hamiltonian. The later is adapted appropriately, firstly by promoting the parameters in the Hamiltonian to 'flowing', B - and momentum dependent variables and, secondly, by imposing normal ordering with respect to the flowing ground state $|\Psi_N(B)\rangle = |\Omega_0(B)\rangle$ of $H_0(B)$. Thus one particle properties hidden in two-particle scattering terms are effectively reallocated to the kinetic energy and a clear separation of one- and two-particle features in the Hamiltonian is achieved. Translation invariance ensures that there is no potential scattering term like $P_{k'k}c_{k'\sigma}^\dagger c_{k\sigma}$; hence the one-particle term is already energy diagonal. In the following only times after the quench ($t > 0$) are considered.

$$\mathcal{H}(t > 0; B) = \sum_{k \in \mathcal{K}, \sigma \in \{\uparrow, \downarrow\}} \epsilon_k(B) :c_{k\sigma}^\dagger c_{k\sigma}: + \sum_{1'12'2 \in \mathcal{K}} U_{1'2'12}(B) :c_{1'\uparrow}^\dagger c_{1\uparrow} c_{2'\downarrow}^\dagger c_{2\downarrow}: \delta_{1'+2'}^{1'+2'} \quad (9.1)$$

9.1 Construction of the canonical generator

The construction of the canonical generator demands for a split-up of the Hamiltonian into a noninteracting and an interacting part. In a first place it may be taken in the obvious way, assuming that it holds for all values of B . This is, certainly, a plausible approximation at the beginning of the flow, i.e. for small values of the flow parameter. Its validity throughout the flow, however, must be justified *a posteriori* by studying the renormalization flow of the Hamiltonian.

9.1.1 Implicit definition of the canonical generator

Inserting the kinetic and the interaction part of (9.1) into (8.3) makes the canonical generator more explicit. With $\Delta\epsilon_{1'12'2}(B) = \epsilon_{1'}(B) - \epsilon_1(B) + \epsilon_{2'}(B) - \epsilon_2(B)$ it reads

$$\eta(B) = \sum_{1'12'2} U_{1'12'2}(B) \Delta\epsilon_{1'12'2}(B) :c_{1'\uparrow}^\dagger c_{1\uparrow} c_{2'\downarrow}^\dagger c_{2\downarrow}: \delta_{1'+2'}^{1'+2'} \quad (9.2)$$

This is still an implicit definition of the generator since the functional form of the flowing interaction strength is not known explicitly. Hence an iterative approach to the correct and

consistent definition of the generator is necessary. It starts with a first parametrization of the flowing coupling constants in (9.2). In a second step the examination of the renormalization flow of the Hamiltonian leads to an improved parametrization.

9.1.2 Leading order renormalization flow of the Hamiltonian

Parametrizing the canonical generator by the initial values $\epsilon_k(B) \stackrel{\text{I}}{=} \epsilon_k(B=0)$ and $U_{1'12'2}(B) \stackrel{\text{I}}{=} U_{1'12'2}(B=0) = U$ defines the generator as a first order object in U . Then, to leading order, the flow equation for the Hamiltonian

$$\frac{d\mathcal{H}(B)}{dB} = [\eta(B), \mathcal{H}(B)] \quad (9.3)$$

only describes a renormalization flow of the interaction. The eigenenergies are renormalized only in second order of U .

$$\frac{dU_{1'12'2}}{dB} \stackrel{\mathcal{O}(U)}{=} -U(\Delta\epsilon_{1'12'2})^2 \quad (9.4)$$

Its solution

$$U_{1'12'2}(B) = U e^{-(\Delta\epsilon_{1'12'2})^2 B} \quad (9.5)$$

exhibits an exponential suppression with growing flow parameter and growing transfer energy $\Delta\epsilon$. The exponential decay of off-diagonal matrix elements is a very generic and characteristic trait of the flow equation method; it allows to relate the flow parameter to an energy scale $\Lambda_E \sim B^{-1/2}$ and can be compared to an intrinsically emergent cut-off function which becomes effective for energy differences larger than that scale.

Beyond the cut-off behavior there is no significant first order renormalization flow of the Hamiltonian. Since second order effects like the renormalizations of the eigenenergies or second order corrections to the flowing interaction will not influence the final results it is safe to discard all aspects of the Hamiltonian flow. This is a particular simplification which only arises for the Hubbard model and does not hold in many other model systems.

9.1.3 Leading order parametrization of the canonical generator

With this parametrization the first-order implementation of the canonical generator can be made explicit:

$$\eta^{(1)}(B) = U \sum_{1'12'2 \in \mathbf{K}} \Delta\epsilon_{1'12'2} e^{-(\Delta\epsilon_{1'12'2})^2 B} \delta_{k_1+k_2}^{k_{1'}+k_{2'}} :c_{1'\uparrow}^\dagger c_{1\uparrow} c_{2'\downarrow}^\dagger c_{2\downarrow}: \quad (9.6)$$

For the purpose of this work this defines a sufficient approximation to the diagonalizing transformation.

9.2 Transformation of the creation operator

In the following the evolution of particular quantities is discussed, namely of the total kinetic energy, the total interaction energy and the momentum distribution function. They are expectation values with respect to the initial state $|\Omega_0\rangle$ of time-dependent observables given in the Heisenberg picture. Hence all of them carry at least a trivial time dependence with respect to the Hamiltonian. The interaction part of the Hamiltonian is, moreover, even

explicitly time dependent. The corresponding observables are $\mathcal{H}_0(t)$, $\mathcal{H}_{\text{int}}(t)$ and the number operator of a fermionic quantum gas

$$\mathcal{N}_k(t) = \begin{cases} \mathcal{C}_k^\dagger(t)\mathcal{C}_k(t) & : k > k_F \\ 1 - \mathcal{C}_k^\dagger(t)\mathcal{C}_k(t) & : k \leq k_F \end{cases} \quad (9.7)$$

All of them can be composed from the creation operator $\mathcal{C}_{k\uparrow}^\dagger(B; t)$ for which the flow equation transformation is established explicitly.

9.2.1 Constructing an ansatz for the creation operator

The initial condition of this operator $\mathcal{C}_{k\uparrow}^\dagger(B=0; t=0) = c_{k\uparrow}$ describes the creation of a single electron in a momentum mode k of the original basis representation of the problem. From it the leading contributions to a general representation for different values of the flow parameter can be constructed. This generation of higher order terms follows directly from applying the commutator on the right hand side of

$$\frac{d\mathcal{C}_{k\uparrow}^\dagger(B)}{dB} = [\eta(B), \mathcal{C}_{k\uparrow}^\dagger(B)] \quad (9.8)$$

It shows that $\mathcal{C}_{k\uparrow}^\dagger$ acquires a composite multiparticle structure under the flow which mirrors the dressing of an original electron by electron-hole excitations due to interaction effects. After a first iteration, the ansatz

$$\mathcal{C}_{k\uparrow}^\dagger(B) = h_{k\uparrow}(B) c_{k\uparrow}^\dagger \quad (9.9a)$$

$$+ \sum_{1'2'1} M_{1'2'1\uparrow\downarrow\downarrow}(B) \delta_{1'+2'}^{k+1} :c_{1'\uparrow}^\dagger c_{2'\downarrow}^\dagger c_{1\downarrow}: \quad (9.9a)$$

$$+ \sum_{1'2'1} M_{1'2'1\uparrow\uparrow\uparrow}(B) \delta_{1'+2'}^{k'+1} :c_{1'\uparrow}^\dagger c_{2'\uparrow}^\dagger c_{1\uparrow}: \quad (9.9b)$$

can be established. All terms obey momentum and spin conservation. The first term includes the continued features of the original fermionic particle, i.e. the coherent overlap of $\mathcal{C}_{k\uparrow}^\dagger(B)$ with $\mathcal{C}_{k\uparrow}^\dagger(B=0)$. Its flowing coupling constant $h_{k\uparrow}(B)$ relates to the quasiparticle residue via $h_{k_F}(B) = \sqrt{Z(B)}$. The two other terms are the leading representatives of an infinite hierarchy of incoherent many-particle (dressing) processes. Since the Pauli principle fosters dressing by particles with opposite spin, the second term will dominate over the third. This can be read off from the set of differential flow equations for the flowing coupling constants $h(B)$ and $M(B)$ and allows to neglect the later.

9.2.2 Flow equations for the creation operator

Inserting this ansatz into (9.8) leads to the differential flow equations for the flowing parameters $h(B)$ and $M(B)$. A consistent normal ordering of all newly generated terms is essential and causal for the emergence of characteristic fermionic phase space factors like

$$Q_{122'} = n_1 n_2 (1 - n_{2'}) + (1 - n_1)(1 - n_2) n_{2'} \stackrel{\text{Def}}{=} Q_{122'}^{(1)} + Q_{122'}^{(2)}$$

. The definitions of $Q_{122'}^{(1)}$ and $Q_{122'}^{(2)}$ refer to the first and second summand in $Q_{122'}^{(1)}$. All three phase space factors are symmetric under the interchange of the first two indices¹.

$$\frac{\partial h_{k\uparrow}(B)}{\partial B} = U \sum_{12'2} \Delta\epsilon_{k12'2} e^{-B(\Delta\epsilon_{k12'2})^2} Q_{122'} M_{122'\uparrow\downarrow}(B) \quad (9.10)$$

$$\frac{\partial M_{5'6'5\uparrow\uparrow\uparrow}(B)}{\partial B} = -U \sum_{2'2} [n(2') - n(2)] \Delta\epsilon_{2'25'5} e^{-B(\Delta\epsilon_{2'25'5})^2} M_{6'22'\uparrow\downarrow}(B) \quad (9.11)$$

$$\begin{aligned} \frac{\partial M_{5'6'5\uparrow\downarrow\downarrow}(B)}{\partial B} &= U \sum_1 h_{1\uparrow}(B) \Delta\epsilon_{5'56'1} e^{-B(\Delta\epsilon_{5'56'1})^2} \quad (9.12) \\ &+ U \sum_{12'} [n(1) - n(2')] M_{16'2'\uparrow\downarrow\downarrow}(B) \Delta\epsilon_{2'15'5} e^{-B(\Delta\epsilon_{2'15'5})^2} \\ &+ U \sum_{12} [1 + n(2) - n(1)] M_{125\uparrow\downarrow\downarrow}(B) \Delta\epsilon_{5'16'2} e^{-B(\Delta\epsilon_{5'16'2})^2} \\ &+ U \sum_{1'1} [M_{15'1'\uparrow\uparrow\uparrow} - M_{5'11'\uparrow\uparrow\uparrow}] [n(1') - n(1)] \Delta\epsilon_{1'16'5} e^{-B(\Delta\epsilon_{1'16'5})^2} \end{aligned}$$

A perturbative expansion in U of the flowing parameters $h(B)$ and $M(B)$ allows to reduce the complexity of the differential equations but depends on their initial conditions. Since the differential equations are linear, a solution for general initial conditions can be achieved as a linear superposition of solutions for independent initial configurations. Two cases can be discussed:

- (A) *Fully coherent initialization* of one fermion in the momentum mode k :
 $h_{i\uparrow}(B_0) = \delta_i^k$ and $M(B_0) = 0$ for all possible indices
- (B) *Fully incoherent initialization* in the dressing state $p'q'p \uparrow\downarrow\downarrow$: $h_i(B_0) = 0$, $M_{1'2'1\uparrow\downarrow\downarrow}(B_0) = \delta_{1'}^{p'} \delta_{2'}^{q'} \delta_1^p$ and $M_{\uparrow\uparrow\uparrow}(B_0) = 0$ for all possible indices²

Case A: Perturbative analysis at the onset of the flow

I discuss iteratively the action of the differential flow equations at the onset of the flow. In a first step, the flowing parameters h and M on the right hand side of the differential equations can be parametrized by their initial conditions (A). Hence only the first term at the rhs of (9.12) remains influential and is, due to its pre-factor, of order U . Consequently, $M_{\uparrow\downarrow\downarrow}(B > 0)$ is generated in first order of U . Re-inserted into (9.10) it accounts for a second order correction to the flowing parameter $h(B)$. This describes the leading changes to the quasiparticle residue. Re-inserted into (9.11) and (9.12) it unfolds second order effects on flowing parameters of the M type. Since those do not influence second order results on the momentum distribution function (which will be shown later), this calculation can be, fortunately, dropped. Moreover, the initial conditions (A) are the natural ones to study the behavior of physical fermions. As they do not generate $M_{\uparrow\uparrow\uparrow}$ in relevant order, the ansatz for $\mathcal{C}_{k\uparrow}^\dagger$ can be restricted to (9.9a).

¹Compared to previous definitions [251] the two symmetric indices in $Q_{122'}$ are denoted first and the "exceptional" index is denoted last. Hence it holds $Q_{122'} = Q_{212'}$.

²To avoid confusion it is stressed that in the full context of the problem, this initial condition comes with a pre-factor proportional to U . Perturbative arguments always include it.

This is a consequence of the Pauli principle which disadvantages dressing of a fermion with excitations in the same spin state. Simplified flow equations read

$$\frac{\partial h_{k\uparrow}(B)}{\partial B} = U \sum_{12'2} \Delta\epsilon_{k12'2} e^{-B(\Delta\epsilon_{k12'2})^2} Q_{122'} M_{122'\uparrow\downarrow\downarrow} \quad (9.13a)$$

$$\frac{\partial M_{5'6'5\uparrow\downarrow\downarrow}(B)}{\partial B} = U \sum_1 h_{1\uparrow} \Delta\epsilon_{5'56'1} e^{-B(\Delta\epsilon_{5'56'1})^2} \quad (9.13b)$$

I stress that this analysis is based on an approximate parametrization of the flowing parameters. It requires that their magnitude under the flow is still sufficiently described by the magnitude of their initial conditions. The following study will show that for the initial conditions of a physical electron at the Fermi energy this remains the case throughout the flow and that, then, non-perturbative effects do not arise.

Approximate analytical solution of the flow equations

I integrate the simplified flow equations (9.13) with respect to the flow parameter B . Similar to the above analysis I iteratively develop the flowing parameters from their initial conditions (A). I apply the same parametrization $h_{1\uparrow} = \delta_1^k$ and integrate (9.13b) from $B_0 = 0$ to $B_f = B$.

$$M_{5'6'5\uparrow\downarrow\downarrow}^{(A),FT}(B) = U \frac{1 - e^{-B(\Delta\epsilon_{5'56'k})^2}}{\Delta\epsilon_{5'56'k}} \quad (9.14)$$

This serves as an improved parametrization in (9.13a) and allows to write down a formal second order correction of $h_{k\uparrow}$.

$$h_{k\uparrow}^{(A)}(B) = 1 - U^2 \int_{-\infty}^{\infty} \rho dE \frac{(1 - e^{-B(\epsilon_k - E)^2})^2}{2(\epsilon_k - E)^2} I_k(E) \quad (9.15)$$

with a phase space factor

$$I_k(E) := \sum_{1'2'1} Q_{1'2'1} \delta(E - \epsilon_{1'} - \epsilon_{2'} + \epsilon_1) \delta_{1+k}^{1'+2'} \quad (9.16)$$

Since the one-particle energies are restricted to a band with bandwidth $2D$ nonzero values for $I_k(E)$ can only be expected within an energy window $E \in [-3D, 3D]$. Hence the energy integral in (9.15) can be restricted to this limited support.

Evaluation of the phase space factor

For a further understanding of the flow of $h_{k\uparrow}^{(A)}$ my focus is on the energy dependence of the phase space factor $I_k(E)$. Momentum conservation allows to eliminate the momentum index $1 = 1' + 2' - k$; I keep it as a dependent shorthand notation. I evaluate $I_k(E)$ in energy space assuming a constant density of states ρ

$$I_k(E) = \rho^2 \int_{-\infty}^{\infty} d\epsilon_{1'} \int_{-\infty}^{\infty} d\epsilon_{2'} Q(\epsilon_{1'}, \epsilon_{2'}, \epsilon_1) \delta(E - \epsilon_{1'} - \epsilon_{2'} + \epsilon_1) \quad (9.17)$$

and observe that, at zero temperature, the phase space factor $Q(\epsilon_{1'}, \epsilon_{2'}, \epsilon_2)$ vanishes for all but two configurations of its energy arguments [246]: In both cases the limits of the energy

Case	Energies			Phase space factors			Constraint by delta function
	$\epsilon_{1'}$	$\epsilon_{2'}$	ϵ_1	$Q^{(1)}$	$Q^{(2)}$	Q	$E = \epsilon_{1'} - \epsilon_1 + \epsilon_{2'}$
(a)	$> \epsilon_F$	$> \epsilon_F$	$< \epsilon_F$	0	1	1	$E = + \epsilon_{1'} + \epsilon_{2'} + \epsilon_1 > 0$
(b)	$< \epsilon_F$	$< \epsilon_F$	$> \epsilon_F$	1	0	1	$E = - \epsilon_{1'} - \epsilon_{2'} - \epsilon_1 < 0$
	otherwise			0	0	0	not relevant

Table 9.1: Discussion of phase space factors at zero temperature

integrations in (9.17) can be restricted by an approximate evaluation of the delta function. Its argument can be rewritten by considering the signs of the one-particle energies ϵ_i which is done in the last column of the above table. From there one reads off that, since E is a sum of either solely positive or solely negative summands, E forms an upper or lower bound on *both* energy integrations individually. Then both cases (a) and (b) lead to the same approximate expression for the phase space factor

$$I_k(E) = \rho^2 \int_{\epsilon_F}^E d\epsilon_{1'} d\epsilon_{2'} = \rho^2 (E - \epsilon_F)^2 \quad (9.18)$$

I finally remark that the phase space factor $Q(\epsilon_{1'}, \epsilon_{2'}, \epsilon_1)$ mirrors the particle-hole symmetry of the Hubbard model. It implies that all odd powers of a perturbative expansion vanish [171]. I will see in (10.3) that $Q(\epsilon_{1'}, \epsilon_{2'}, \epsilon_1)$ is, in particular, responsible for the suppression of secular terms.

Analysis of the later flow of $h_{k\uparrow}(B)$

The approximation (9.18) allows to interpret the physical relevance of the formal result (9.15): At the Fermi surface, i.e. for $k = k_F$, and at zero temperature its quadratic divergence is cancelled exactly by the phase space factor. This implies that the corrections to $h_{k_F\uparrow}^{(A)}$ remain small in second order of U throughout the flow. Hence the parametrization $h_{k_F\uparrow}^{(A)} = 1$ used above is justified even beyond the onset of the flow and the approximate analytical solution gives a correct description of the changes to the quasiparticle residue for all values of B .

Away from the Fermi surface, however, there is no such cancellation by a phase space factor. Now the energy denominator indicates nonperturbative effects. Expanding the exponential in (9.15) shows that the numerator smoothes the peaked energy structure on a B -dependent scale such that a pole only emerges in the limit of infinite B . Nonetheless, the contribution of an environment around $\epsilon_{k \neq k_F}$ to the energy integral in (9.15) grows under the flow until it infers a nonperturbative correction to $h_{k \neq k_F\uparrow}^{(A)}$. This implies a full decay of a particle into incoherent excitations. The corresponding scales can be extracted from a first order expansion in B^3 . Since this is only justified for $B(\epsilon_k - E)^2 < 1$ I continuously restrict the environment $[\epsilon_k - 1/\sqrt{B}, \epsilon_k + 1/\sqrt{B}]$ around the later pole. This is only meaningful for not too small values of B such that $1/\sqrt{B} < D$ or $B > 1/D^2$. This sets a lower limit to the flow parameter whenever aspects of the flow are discussed. With $e_k = E - \epsilon_k$ and (9.18), the correction term

³A similar analysis based on scaling out the B -dependence from the energy integral leads to the same scales but requires a discussion of logarithmic and power-law divergences.

in (9.15) reads

$$\begin{aligned} \Delta h_{k \neq k_F \uparrow}^{(A)}(B) &\approx -U^2 B^2 \frac{\rho^3}{2} \int_{-1/\sqrt{B}}^{1/\sqrt{B}} de_k (e_k + \epsilon_k - \epsilon_F)^2 e_k^2 \\ &\approx -U^2 \rho^3 \left[\frac{2}{5} \frac{1}{\sqrt{B}} + \frac{2}{3} \sqrt{B} (\epsilon_k - \epsilon_F)^2 \right] = -\frac{U^2}{D^2} \left[\frac{2}{5} \frac{1}{D} \frac{1}{\sqrt{B}} + \frac{2}{3} \frac{\sqrt{B}}{D} (\epsilon_k - \epsilon_F)^2 \right] \end{aligned} \quad (9.19)$$

Since $1/\sqrt{B} < D$ the first summand within the brackets is always smaller than $2/5$ and vanishes for large values of B . Then the second term exhibits the decay scale

$$B^* = \frac{1}{U^4 \rho^6 (\epsilon_k - \epsilon_F)^4} \quad \text{or} \quad E^* = U^2 \rho^3 (\epsilon_k - \epsilon_F)^2 \quad (9.20)$$

The quadratic energy dependence of E^* resembles the characteristic finite lifetime of Landau quasiparticles away from the Fermi surface $\tau \sim (\epsilon_k - \epsilon_F)^{-2}$. Here it illustrates the complete decay of a physical fermion. This implies that on a scale set by B^* the straightforward parametrization of $h_{1\uparrow} = \delta_1^k$ (see above) becomes unjustified and the analytical solution (9.15) breaks down. Instead, a better solution of the differential flow equations would show a complete transfer of the spectral weight from the one-particle to many-particle representations.

This allows to discuss the reliability of the solution: For particles in a perturbatively small environment around the Fermi energy, i.e. $\epsilon_k - \epsilon_{k_F} \approx U$, the energy scale $E^* \sim \mathcal{O}(U^4)$ is beyond the resolution of a second order calculation. Hence the particle decay cannot be observed on all accessible times. Therefore the extension of the approximate solution (9.14, 9.15) to an environment around the Fermi energy of radius U leads to a consistent second order result. Equilibrium calculations have shown that the broadening of the momentum distribution due to interaction effects is concentrated in this region [187, 252].

Outside of this environment, particles decay completely into incoherent multiparticle excitations. This implies that, strictly speaking, the validity of (9.14) breaks down. Nonetheless, it shows that under the flow the spectral width $\Gamma_M(B)$ of newly arising incoherent M -terms continuously decreases. This indicates that at the decay scale spectral weight is transferred from coherent particles (with a sharp spectral distribution) primarily to excitations with $\Gamma_M \sim E^*$. Since even far away from the Fermi energy this is perturbatively small in U^2 , the effects of this small widening will not influence the shape of the momentum distribution function. Therefore the solution (9.14, 9.15) allows for a calculation of the momentum distribution function on all energies.

Composition of the number operator

Since the transformation for the creation operator of an electron around the Fermi energy has been established in second order perturbation theory, the number operator $\mathcal{N}_k = \mathcal{C}_k^\dagger \mathcal{C}_k$ can be easily composed from the ansatz (9.9a). The momentum distribution is given by its expectation value with respect to a filled Fermi sea of fermions $|FS\rangle$. Their interpretation is different in equilibrium and in nonequilibrium, suitable quasiparticles or physical electrons, respectively. Normal ordering can always be considered as with respect to a filled Fermi sea of the appropriate particles; possible corrections caused by a reinterpretation of the correlator n_k are beyond the accuracy of a second order calculation. This implies that only quadratic

terms in $h(B)$ and $M(B)$ contribute:

$$\begin{aligned} N_k(B, t) &= \langle FS | \mathcal{N}_k(B, t) | FS \rangle \\ &= |h_k(B, t)|^2 n_k + \sum_{1'2'1} n_{1'} n_{2'} (1 - n_1) |M_{1'2'1\uparrow\downarrow}^k(B, t)|^2 \delta_{1+k}^{1'+2'} \end{aligned} \quad (9.21)$$

A possible time dependence has already been included for later reference.

9.2.3 Equilibrium momentum distribution

Similarly to the approach in [253] I observe that the flow equation transformation resembles in many aspects a unitary implementation of Landau's theory of a Fermi liquid. Although a strict identification of the diagonal degrees of freedom obtained from the flow equation approach with Landau quasiparticles is not possible, they motivate an analogous picture of flow equation quasiparticles; like their Landau counterparts they are stable only at the Fermi energy and subject to a residual quasiparticle interaction which is carried by the nonvanishing two-particle component of the energy-diagonal Hamiltonian. Nonetheless, these quasiparticles absorb most of the interaction effects into their definition such that the quasiparticle representation of the interacting ground state is, in good approximation, the filled Fermi sea.

Hence the momentum distribution in equilibrium can be calculated in a similar way as the equilibrium occupation of the squeezed oscillator (6.12) using (9.21), (9.14) and (9.15).

$$\begin{aligned} N_k^{EQU} &= \langle \Omega | \mathcal{C}_k^\dagger(B=0) \mathcal{C}_k(B=0) | \Omega \rangle = \langle \Omega_0 | \mathcal{C}_k^\dagger(B \rightarrow \infty) \mathcal{C}_k(B \rightarrow \infty) | \Omega_0 \rangle = \\ &= -U^2 \int_{-\infty}^{\infty} dE \frac{J_k(E; n)}{(E - \epsilon_k)^2} \end{aligned} \quad (9.22)$$

where the phase space factor

$$J_k(E; n) = \sum_{1'2'1} \delta_{1+k}^{1'+2'} \delta(\epsilon_{1'} + \epsilon_{2'} - \epsilon_1 - E) [n_k n_1 (1 - n_{1'}) (1 - n_{2'}) - (1 - n_k) (1 - n_2) n_{1'} n_{2'}] \quad (9.23)$$

resembles the quasiparticle collision integral of a quantum Boltzmann equation [254]. I will compare (9.22) with the time dependent momentum distribution after an interaction quench.

Chapter 10

Unitary perturbation theory for the quenched Fermi liquid

In the previous chapter the flow equation transformation for the Hubbard Hamiltonian has been established and the momentum distribution function in equilibrium has been calculated. In the following the scheme of unitary perturbation theory is applied to the quenched Fermi liquid. It delivers directly the time dependent 'creation' operator in the initial representation $\mathcal{C}_{k\uparrow}^\dagger(B=0, t)$ which already depicts the time-resolved transition from pure fermions to composite degrees of freedom (quasiparticles), i.e. the buildup of many-particle correlations. The physical observable, however, is the momentum distribution function in nonequilibrium.

10.1 Time dependent fermion operator $\mathcal{C}_{k\uparrow}^\dagger(B=0, t)$

To make use of analogous notation, the time evolved operator $\mathcal{C}_{k\uparrow}^\dagger(B, t)$ may be represented by the same operator ansatz as $\mathcal{C}_{k\uparrow}^\dagger(B, t=0)$ (9.9a) but with modified coupling constants. Each of the three main steps of the unitary transformation scheme, namely the forward transformation, the time evolution and the backward transformation (c.f. Fig. 5.2) are unitary transformations and, in particular, linear operations. Hence, on each step their impact can be constructed in analogy to the action of the forward transformation, mapping the simple initial conditions (A) and (B) in (9.2.2) onto new coefficients $h_I^{UT}(B, t)$ and $M_I^{UT}(B, t)$ where $UT \in \{FT, T, BT\}$ denotes the the forward transformation (FT; see 9.2.2), the backward transformation (BT; see 10.1.2) and the time evolution (T; see 10.1.1) and $I \in \{A, B\}$ the initial condition. Finally, all these contributions are linearly superimposed and effective time-dependent parameters $h(0, t)$ and $M(0, t)$ are constructed. Then the evolution of the fermion operator can be given as

$$\mathcal{C}_{k\uparrow}^\dagger(B=0, t) = h_{k\uparrow}(0, t) c_{k\uparrow}^\dagger + \sum_{1'2'1} M_{1'2'1\uparrow\downarrow}(0, t) \delta_{1'+2'}^{k+1} :c_{1'\uparrow}^\dagger c_{2'\downarrow}^\dagger c_{1\downarrow}: \quad (10.1)$$

Fig. 10.1 illustrates some of the used notation. Although the fermion operator is no physical observable, it is a useful object to make the buildup of particle correlations and dressing more explicit.

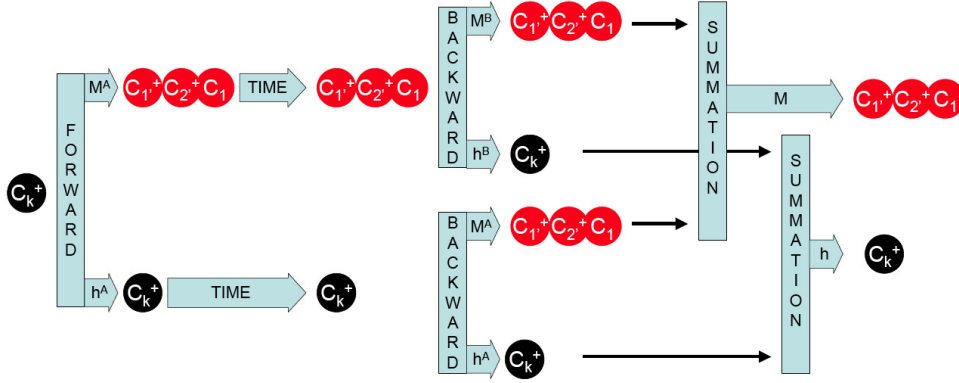


Figure 10.1: The above figure shows the decay of a fermionic particle C_k in nonequilibrium with time. This decay can be formally attributed to a forward and backward transformation. Additional particle decay due to an energy-diagonal residual interaction are not depicted here.

10.1.1 Time evolution

The construction of the parameters $h(0, t)$ and $M(0, t)$ directly includes the forward transformation which was implemented in the past chapter. In a second step, the time evolution of the creation operator in its energy-diagonal representation $C_{k\uparrow}(B \rightarrow \infty)$ is performed with respect to the energy-diagonal Hamiltonian. Its leading part, the noninteracting Hamiltonian, generates a time evolution according to $\mathcal{U}(t, t_0 = 0) = e^{iH_0 t}$ which can be treated exactly. Corrections arise due to the energy-diagonal interacting part of the Hamiltonian and cause the appearance of secular terms. It will be shown in section (10.3) that they can be neglected in a second order calculation. Hence the action of \mathcal{U} onto the ansatz (9.9a)

$$\begin{aligned} C_{k\uparrow}^\dagger(B, t) &= h_{k\uparrow}^{(A),FT}(B) \mathcal{U}^\dagger(t, 0) c_{k\uparrow}^\dagger \mathcal{U}(t, 0) \\ &+ \sum_{1'2'1\uparrow\downarrow} M_{1'2'1\uparrow\downarrow}^{(A),FT}(B) \delta_{1'+2'}^{k+1} \mathcal{U}^\dagger(t, 0) :c_{1'\uparrow}^\dagger c_{2'\downarrow}^\dagger c_{1\downarrow}: \mathcal{U}(t, 0) \end{aligned} \quad (10.2)$$

is for $B \rightarrow \infty$ fully described by additional phase shifts accompanying the parameters $h^{(A),FT}$ and $M^{(A),FT}$.

$$h_{k\uparrow}(B \rightarrow \infty, t) = e^{i\epsilon_k t} h_{k'\uparrow}^{(A),FT}(B \rightarrow \infty) \quad (10.3a)$$

$$M_{1'2'1\uparrow\downarrow}(B \rightarrow \infty, t) = e^{i(\epsilon_{1'} + \epsilon_{2'} - \epsilon_1)t} M_{1'2'1\uparrow\downarrow}^{(A),FT}(B \rightarrow \infty) \quad (10.3b)$$

10.1.2 Inverse transformation

The final step depicted in Fig. 5.2 is the backward mapping of the time-evolved observables into the original representation of physical fermions. It is implemented by the inverse sequence of differential unitary transformations and simply achieved by interchanging the limits of the B -integration in the forward transformation or, intuitively, by 'running the transformation backwards' [235]. This holds because the order of its infinitesimal constituents remains unchanged and the non-commutativity of the generator at different points of the flow $[\eta(B), \eta(B')] \neq 0$ does not become relevant. Yet the decay of a physical fermion under

the forward transformation has generated nonvanishing incoherent contributions in order U ; therefore different initial conditions for the backward transformation of $\mathcal{C}_{k\uparrow}(B=\infty, t > 0)$ apply. According to (9.2.2) a linear combination of the solutions for (A) and (B) leads to a full solution at arbitrary initial conditions. Case (A) can directly be taken from (9.2.2) with $M^{(A),BT} = -M^{(A),FT}$ and invariant $h^{(A)}$. The discussion of case (B) is simplified by noting that the pre-factor of its nonvanishing initial condition is proportional to U because of the generation of this term under the forward transformation. I will consider this additional power of U in a perturbative analysis of the relevant contributions but solve the differential equations for the unweighted initial conditions of case (B).

Case B: Perturbative analysis and approximate solution

At the onset of the backward flow, i.e. for large values of the flow parameter ($B_0 = \infty$), I insert the weighted initial conditions of case (B) as a constant parametrization into the right hand side of the flow equations (9.10-9.12). With $M_{\uparrow\downarrow} \sim \mathcal{O}(U)$, $h_{k\uparrow}(B)$ is generated by (9.10) to second order in U ; hence, within a second order calculation, the parametrization $h_{k\uparrow} = 0$ holds throughout the backward transformation. Consequently, corrections to $M_{\uparrow\downarrow}$ are second order in U , as well is the generation of $M_{\uparrow\uparrow}$. Looking out at (10.5b) and back to (9.21) shows that a second order result of the momentum distribution only requires the knowledge of M to first order. This is *a priori* known by the weighted initial condition. Integrating (9.10) gives

$$h_{k\uparrow}^{(B),BT}(B) = U Q_{p'q'p} \frac{e^{-B(\Delta\epsilon_{p'pq'k})^2}}{\Delta\epsilon_{p'pq'k}} \quad (10.4a)$$

$$M_{1'2'1\uparrow\downarrow}^{(B),BT}(B) = \delta_{1'}^{p'} \delta_{2'}^{q'} \delta_1^p \quad (10.4b)$$

10.1.3 Composite transformation

I finish the computation of the time dependent creation operator by composing the forward transformation (FT), the approximate time evolution and the backward transformation (BT) and represent the joint result in terms of time dependent parameters $h_{k\uparrow}(B=0, t)$ and $M_{\uparrow\downarrow}(B=0, t)$. Fig. 10.1 gives a pictorial representation of these expressions.

$$h_{k\uparrow}(B=0, t) = h_{k\uparrow}^{(A),BT} e^{i\epsilon_k t} h_{k\uparrow}^{(A),FT} + \sum_{p'q'p} h_{k\uparrow}^{(B),BT} e^{i(\epsilon_{p'} + \epsilon_{q'} - \epsilon_p)t} M_{p'q'p\uparrow\downarrow}^{(A),FT} \quad (10.5a)$$

$$M_{1'2'1\uparrow\downarrow}^k(B=0, t) = M_{1'2'1\uparrow\downarrow}^{(A),BT} e^{i\epsilon_k t} h_{k\uparrow}^{(A),FT} + \sum_{p'q'p} M_{p'q'p\uparrow\downarrow}^{(B),BT} e^{i(\epsilon_{p'} + \epsilon_{q'} - \epsilon_p)t} M_{p'q'p\uparrow\downarrow}^{(A),FT} \quad (10.5b)$$

Inserting the results (9.14, 9.15, 10.3 and 10.4) into (10.5) makes the time evolution of the operator $\mathcal{C}_{k\uparrow}^\dagger(B=0, t)$ (cf. 10.1) explicit. As h is required in second order but M only to first order this reads explicitly

$$h_{k\uparrow}(B=0, t) = e^{i\epsilon_k t} \left[1 - U^2 \int \rho dE \frac{I_k(E)}{(\epsilon_k - E)^2} \right] + U^2 \int \rho dE e^{iEt} \frac{I_k(E)}{(\epsilon_k - E)^2} \quad (10.6a)$$

$$M_{1'2'1\uparrow\downarrow}^k(B=0, t) = \frac{U}{\epsilon_{1'} + \epsilon_{2'} - \epsilon_1 - \epsilon_k} \left[-e^{i\epsilon_k t} + e^{i(\epsilon_{1'} + \epsilon_{2'} - \epsilon_1)t} \right] \quad (10.6b)$$

10.2 Nonequilibrium momentum distribution

From the time-dependent fermion operator the nonequilibrium time-dependent momentum distribution function for the initial state $|\Omega_0\rangle$ can be constructed in analogy to the equilibrium case (9.21).

$$N_k^{\text{NEQ}}(t) := \langle \Omega_0 | \mathcal{N}_k(B=0, t) | \Omega_0 \rangle = n_k - 4U^2 \int_{-3D}^{3D} dE \frac{\sin^2((E - \epsilon_k)t/2)}{(E - \epsilon_k)^2} J_k(E; n) \quad (10.7)$$

For convenience, the correlation-induced time-dependent correction to the momentum distribution is defined as

$$\Delta N_k^{\text{NEQ}}(t) = N_k^{\text{NEQ}}(t) - n_k = -4U^2 \int_{-3D}^{\infty} dE \frac{\sin^2\left(\frac{(\epsilon_k - E)t}{2}\right)}{(\epsilon_k - E)^2} J_k(E; n) \quad (10.8)$$

and the long-time limit of its time average is performed.

10.2.1 Comparison with a golden rule argument and long-time limit

This result invites for a comparison with the 'derivation' of Fermis golden rule in section (5.3.1): The modulus of the transition matrix element $|\langle n | H_{\text{int}} | i \rangle|$ seems to translate into the constant U , the time-dependent energy kernel has a similar $[\sin(t\Delta E)/\Delta E]^2$ structure. However, a phase space factor $J_k(E; n)$ characteristic for fermionic many-particle systems appears. It describes the analogue to the selection rules which a constant matrix element cannot provide; these turn out to be extremely restrictive and dramatically modify the behavior at the Fermi surface.

Since $J_{k_F}(E; n) \sim \rho^3(E - \epsilon_F)^2$ the phase space factor compensates for the energy denominator in (10.8). Then the energy kernel does no longer represent a regularization of the Dirac delta distribution. Instead, a plain sinusoidal time dependence remains. The long-time limit is no longer given by a delta function but, effectively, by the time average $\lim_{t \rightarrow \infty} \langle \sin^2(\alpha t) \rangle_t = 1/2$. For the correction to the momentum distribution around the Fermi surface, this means

$$\overline{\Delta N_{k \approx k_F}^{\text{NEQ}}} := \lim_{t \rightarrow \infty} \langle \Delta N_{k \approx k_F}^{\text{NEQ}}(t) \rangle_t = -2U^2 \int_{-3D}^{3D} dE \frac{J_{k \approx k_F}(E; n)}{(\epsilon_{k \approx k_F} - E)^2} \stackrel{(9.22)}{=} \mathbf{2} \Delta N_{k \approx k_F}^{\text{EQU}} \quad (10.9)$$

10.2.2 Plot of the time dependent momentum distribution function

To illustrate the initial dynamics of the momentum distribution it is helpful to plot equation (10.8) as a function of energy ϵ_k for different points in time. Unfortunately, the internal momentum summations present in the phase space factor $J_k(E; n)$ may cause severe restrictions to a numerical evaluation. Moreover, any explicit evaluation requires the specification of a particular lattice geometry. Since the aim of this work is not to draw attention to particularities of certain implementations of the Hubbard model in unconventional lattices but to conclude on the generic behavior of a Fermi liquid by studying the Hubbard model the simplest lattice geometry may be chosen.

For computational convenience a hypersquare lattice in the limit of infinite dimensions is considered here. It is generally assumed as well as confirmed *a posteriori* that in this limit the generic features of a Fermi liquid are retained. However, a dramatic simplification results

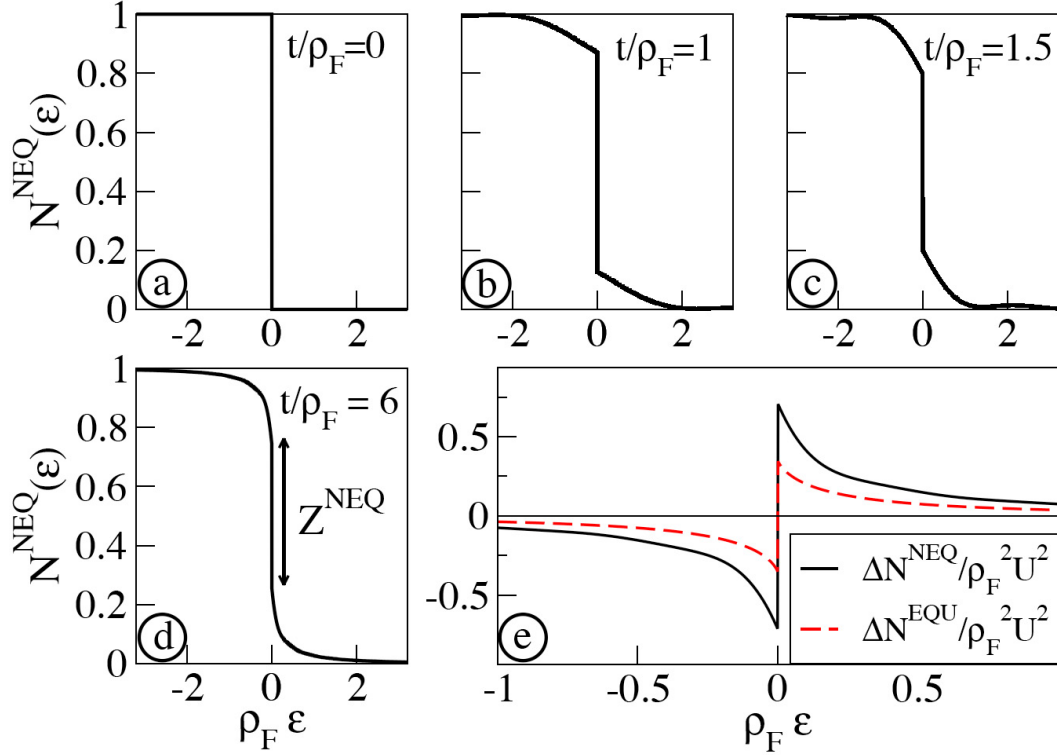


Figure 10.2: (a)-(d): Time evolution of $N^{\text{NEQ}}(\epsilon)$ plotted around the Fermi energy for $\rho_F U = 0.6$. A fast reduction of the discontinuity and $1/t$ -oscillations can be observed. The arrow in (d) indicates the size of the quasiparticle residue in the quasi-steady regime. In (e) the universal curves for $\Delta N_k = N_k - n_k$ are given for both equilibrium and for the nonequilibrium quasi-steady state in the weak-coupling limit.

from the fact that in infinite dimensions momentum sums can be evaluated as energy integrals over a Gaussian density of states given by (3.6). For lower dimensions than infinity this can be understood in the spirit of a dynamical mean-field approximation.

For three time steps explicit results are depicted in Fig. 10.2.

10.2.3 Findings for the 2nd order nonequilibrium momentum distribution

The relation (10.9) contains the main observations of this thesis. Its physical origins and implications will be discussed in detail in chapter (11). Here only statements are made to give an overview of the relevant features.

- Since equation (10.8) is a second order perturbative result, it depicts the time evolution reliable on a time scale set by $t_{PT} \sim 1/U^2$. This includes the initial buildup of correlations. Plotting the time dependent momentum distribution for various times in Fig. 10.2 shows that for small values of U within this time frame both a buildup phase and a later (quasi-)steady regime can be observed. Since a nontrivial evolution of the momentum distribution seems to cease already for times smaller than t_{PT} this motivates the discussion of a formal long-time limit of this second order result.

- Comparing the modifications of the nonequilibrium momentum distribution function in this formal long-time limit with the corresponding equilibrium result exhibits a decisive *factor of two* in (??). Since the calculation is valid only around the Fermi surface, the main conclusion is that the quasiparticle residue Z is characterized by a similar mismatch: In a second order perturbative calculation, its reduction due to correlation effects is doubled in nonequilibrium compared to the equilibrium result $1 - Z^{\text{NEQ}} = 2(1 - Z^{\text{EQ}})$. Nonetheless, a nonvanishing quasiparticle residue indicates a picture of Landau quasiparticles. A thorough discussion of these consequences can be found in chapter (11).
- Equation (10.8) defines the momentum distribution function in the initial representation, i.e. for *physical particles*. However, it allows to conclude on the related momentum distribution in a quasiparticle picture.
- Obviously, the phase space factor $J_{k \approx k_F}(E; n)$ depends on the correlator $n_k = \langle \Omega_0 | c_k^\dagger c_k | \Omega_0 \rangle$. This is a tricky point. On the one hand, this dependence originates largely from a consistent application of the normal ordering prescription. According to its definition in section (8.3.2) the correlator is frozen at its initial value. This seems to be plausible for the flow equation transformation at zero time. On the other hand, however, a physical interpretation of the phase space factor as the restriction of scattering processes due to the Pauli principle suggests to replace the fixed correlator by the *time evolved* momentum distribution. This would describe the opening of phase space because of correlation effects. Then the relations (10.7) and (10.9) are considered as self-consistent equations for a determination of N_k and ΔN_k , respectively.

10.3 Vanishing influence of leading secular terms

The main motivation for the application of unitary perturbation theory lies in the avoidance of secular terms. Such terms may arise from a simultaneous expansion in both the interaction and time and limit the trustworthiness of any result on rather short time scales. Unfortunately, the flow equation transformation only diagonalizes the Hamiltonian in energy space. This produces an energy diagonal two-particle interaction term in the final Hamiltonian $H(B \rightarrow \infty)$. In section (10.1.1) time evolution was discussed with respect to the noninteracting Hamiltonian only. This equals a zeroth order approximation in U to the diagonal Hamiltonian $e^{iH(B \rightarrow \infty)t} \approx e^{iH_0 t}$. In higher orders, however, secular terms are generated. Here I will show that these secular terms do not affect the second order momentum distribution.

10.3.1 Factorization of the noninteracting and the energy-diagonal interacting dynamics

Up to second order the decomposition of the time evolution operator in the energy-diagonal representation, i.e. for $B \rightarrow \infty$,

$$\begin{aligned} \mathcal{U}_{H(\infty)}^\dagger(t, t_0 = 0) &= e^{iH(\infty)t} = e^{iH_0(\infty)t} e^{iH_{\text{int}}(\infty)t} e^{t^2[H_0(\infty), H_{\text{int}}(\infty)]/2} = e^{iH_0(\infty)t} e^{iH_{\text{int}}(\infty)t} \\ &= \mathcal{U}_{H_{\text{int}}(\infty)}^\dagger(t, t_0 = 0) \mathcal{U}_{H_0(\infty)}^\dagger(t, t_0 = 0) \end{aligned} \quad (10.10)$$

is exact because in the energy-diagonal representation the generator vanishes due to its energy prefactor in (9.2) and $0 = \eta(B \rightarrow \infty) = [H_0(\infty), H_{\text{int}}(\infty)]$. The energy-diagonal interaction

Hamiltonian can be easily constructed from the Hubbard interaction by restricting to diagonal energies since the energy-diagonal interaction is not renormalized under the flow (cf. 9.5).

$$H_{\text{int}}(B \rightarrow \infty) = U \sum_{1'12'2} :c_{1'\uparrow}^\dagger c_{1\uparrow} c_{2'\downarrow}^\dagger c_{2\downarrow} : \delta(\epsilon_{1'} + \epsilon_{2'} - \epsilon_1 - \epsilon_2) \delta_{1'+2'}^{1'+2'} \quad (10.11)$$

10.3.2 Discussion of individual secular terms in the energy-diagonal representation

In the following I show by explicit calculation that up to second order in U the additional time evolution by $\mathcal{U}_{H_{\text{int}}}^\dagger$ imposed on the 'creation' operator $\mathcal{C}_{k\uparrow}^\dagger(B, t)$, which is in the diagonal basis represented by the ansatz (9.9a), does not influence the momentum distribution.

The further analysis is simplified by the observation that these correction terms (which, of course, solely root in the time evolution of the creation operator) can be *formally* written as time-dependent corrections to the forward transformation. This allows to straightforwardly evaluate their contribution to the full time evolution of the momentum distribution function by inserting corrections into (10.5) and (9.21):

Ansatz for diagonal time evolution Corrections to the time evolution of $\mathcal{C}_{k\uparrow}^\dagger(B \rightarrow \infty, t)$ are considered by the following ansatz

$$\begin{aligned} \mathcal{U}_{H_{\text{int}}}^\dagger \mathcal{C}_{k\uparrow}^\dagger(\infty, t) \mathcal{U}_{H_{\text{int}}} &= h_{k\uparrow}^{(A),FT}(\infty) e^{i\epsilon_k t} \mathcal{U}_{H_{\text{int}}}^\dagger c_{k\uparrow}^\dagger \mathcal{U}_{H_{\text{int}}} + \\ &\sum_{1'2'1} M_{1'2'1\uparrow\downarrow}^{(A),FT}(\infty) e^{i(\epsilon_{1'} + \epsilon_{2'} - \epsilon_1)t} \delta_{1'+2'}^{k+1} \mathcal{U}_{H_{\text{int}}}^\dagger :c_{1'\uparrow}^\dagger c_{2'\downarrow}^\dagger c_{1\downarrow} : \mathcal{U}_{H_{\text{int}}} \end{aligned} \quad (10.12)$$

Using the commutators given in the appendix (A) the leading order correction to the time evolution is obtained from a Baker-Hausdorff expansion

$$\begin{aligned} \mathcal{U}_{H_{\text{int}}}^\dagger \mathcal{C}_{k\uparrow}^\dagger(\infty, t) \mathcal{U}_{H_{\text{int}}} &= \mathcal{C}_{k\uparrow}^\dagger(\infty, t) + it[H_{\text{int}}(\infty), \mathcal{C}_{k\uparrow}^\dagger(\infty, t)] \\ &- \frac{t^2}{2}[H_{\text{int}}(\infty), [H_{\text{int}}(\infty), \mathcal{C}_{k\uparrow}^\dagger(\infty, t)]] + \mathcal{O}(t^3) \end{aligned} \quad (10.13)$$

Linear secular terms. Firstly, the terms linear in time are discussed:

$$\mathcal{U}_{H_{\text{int}}}^\dagger c_{k\uparrow}^\dagger \mathcal{U}_{H_{\text{int}}} - c_{k\uparrow}^\dagger = itU \sum_{1'12'2} \delta_1^k :c_{1'\uparrow}^\dagger c_{2'\downarrow}^\dagger c_{2\downarrow} : \delta(\epsilon_{1'} + \epsilon_{2'} - \epsilon_1 - \epsilon_2) \delta_{1'+2'}^{1'+2'} + \mathcal{O}(U^2) \quad (10.14a)$$

$$\begin{aligned} \mathcal{U}_{H_{\text{int}}}^\dagger :c_{5'\uparrow}^\dagger c_{6'\downarrow}^\dagger c_{5\downarrow} : \mathcal{U}_{H_{\text{int}}} - :c_{5'\uparrow}^\dagger c_{6'\downarrow}^\dagger c_{5\downarrow} : &= itU \sum_{1'12'2} \delta(\epsilon_{1'} + \epsilon_{2'} - \epsilon_1 - \epsilon_2) \delta_{1'+2'}^{1'+2'} \\ &\left\{ :c_{1'\uparrow}^\dagger c_{5'\uparrow}^\dagger c_{1\uparrow} : (n_2 - n_5) \delta_2^{6'} \delta_5^{2'} \right. \end{aligned} \quad (10.14b)$$

$$+ :c_{1'\uparrow}^\dagger c_{2'\downarrow}^\dagger c_{5\downarrow} : (1 - n_1 - n_2) \delta_1^{5'} \delta_2^{6'} \quad (10.14c)$$

$$+ :c_{1'\uparrow}^\dagger c_{6'\downarrow}^\dagger c_{2\downarrow} : (n_1 - n_5) \delta_5^{2'} \delta_1^{5'} \quad (10.14d)$$

$$+ c_{1'\uparrow}^\dagger Q_{122'} \delta_1^{5'} \delta_2^{6'} \left. \right\} \quad (10.14e)$$

Again, power counting in U reveals the relevance of the discussed terms for a second order time evolution of the momentum distribution. Since $h_{k\uparrow}^{(A),FT}(\infty) \sim \mathcal{O}(1)$ the secular term

(10.14a) could be relevant for a second order calculation. Inserted into (10.12) it can be written as

$$\sum_{1'2'1} \left[it U h_{k\uparrow}^{(A),FT}(\infty) \delta_{1'+2'}^{k+1} \delta(\epsilon_{1'} + \epsilon_{2'} - \epsilon_1 - \epsilon_k) \right] e^{i(\epsilon_{1'} + \epsilon_{2'} - \epsilon_1)t} :c_{1'\uparrow}^\dagger c_{2'\downarrow}^\dagger c_{1\downarrow}: \quad (10.15)$$

When comparing with the expression for the time evolution generated by the noninteracting Hamiltonian in (10.1.1) it becomes clear that this secular term can be formally written as a time dependent correction to the forward transformation

$$\Delta M_{1'2'1}^{FT} = it U h_{k\uparrow}^{(A),FT} \delta(\epsilon_{1'} + \epsilon_{2'} - \epsilon_1 - \epsilon_k) \delta_{1'+2'}^{1+k} \quad (10.16)$$

This simplifies the further analysis. Power counting also applies to the other terms. Since the incoherent terms are generated by the forward transformation in order U , these secular terms are effectively of order tU^2 . To obtain a second order result for the momentum distribution it is sufficient to calculate all final constants $M(B=0;t)$ to first order only. Hence these secular terms will not modify the final $M(B=0;t)$ constants. However, the final one-particle constant $h(B=0;t)$ has to be calculated to second order. Reviewing the perturbative analysis for the initial condition (B) in (10.1.2) makes clear that the terms (10.14b-10.14d) could only contribute to h in third order and can be neglected. However, the direct feedback onto the single creation operator (10.14e) may lead to a relevant contribution; it can, again, be written as a time-dependent correction to the forward transformation.

$$\begin{aligned} \Delta h_{k\uparrow}^{FT} &= it U \sum_{p'q'p} M_{p'q'p}^{(A),FT} Q_{p'q'p} \delta_{p'+q'}^{p+k} \delta(\epsilon_{p'} + \epsilon_{q'} - \epsilon_p - \epsilon_k) \\ &\stackrel{(9.14)}{=} it U^2 \int dE \frac{I_k(E)}{E - \epsilon_k} \delta(E - \epsilon_k) \stackrel{(9.18)}{=} 0 \end{aligned} \quad (10.17)$$

(10.17) vanishes at the Fermi surface because of the phase space evaluation presented in (9.2.2).

Influence of linear secular terms on the fermionic creation operator. Since (10.18a) vanishes in the same way as (10.17) the only linear secular term which contributes to the creation operator is given by (10.18b)

$$\begin{aligned} \Delta h_{k\uparrow}^{\text{LST}}(B=0,t) &= \sum_{p'q'p} h_{k\uparrow}^{(B),BT} e^{i(\epsilon_{p'} + \epsilon_{q'} - \epsilon_p)t} \Delta M_{p'q'p\uparrow\downarrow}^{(A),FT} = 0 \quad (10.18a) \\ \Delta M_{1'2'1\uparrow\downarrow}^{k;\text{LST}}(B=0,t) &= \sum_{p'q'p} M_{p'q'p\uparrow\downarrow}^{(B),BT} e^{i(\epsilon_{p'} + \epsilon_{q'} - \epsilon_p)t} \Delta M_{p'q'p\uparrow\downarrow}^{(A),FT} \\ &= it e^{i(\epsilon_{1'} + \epsilon_{2'} - \epsilon_1)t} U h_{k\uparrow}^{(A),FT} \delta(\epsilon_{1'} + \epsilon_{2'} - \epsilon_1 - \epsilon_k) \delta_{1'+2'}^{1+k} \quad (10.18b) \end{aligned}$$

For the time evolved 'creation' operator $\mathcal{C}_{k\uparrow}^\dagger(B=0,t)$ this is a nonvanishing linear secular term, i.e. proportional to Ut . It is strongly restricted by energy diagonality but cannot be excluded *a priori*.

Vanishing influence of linear secular terms in one-particle objects. Although the linear secular term (10.18b) does not vanish directly its second order correction to the one

particle expectation value $\langle \mathcal{C}_k^\dagger(t) \mathcal{C}_k(t') \rangle$ is zero. This is because the phase space factor that results from the contraction of higher order terms $n_1 n_{2'} (1 - n_1)$ (cf. 9.21) can be evaluated in analogy to (10.17). Together with energy diagonality which is contributed by the secular term (10.18b) it leads to a vanishing of the considered expression. For example,

$$\begin{aligned}
\Delta \langle \mathcal{C}_k^\dagger(t) \mathcal{C}_k(t') \rangle^{\mathcal{O}(U^2)\text{LST}} &= \sum_{1'2'1} n_1 n_{2'} (1 - n_1) \left[\Delta M_{1'2'1\uparrow\downarrow}^k(t) \Delta M_{1'2'1\uparrow\downarrow}^{k*}(t') + \right. \\
&\quad \left. + \left(\Delta M_{1'2'1\uparrow\downarrow}^k(t) M_{1'2'1\uparrow\downarrow}^{k*}(t') + \Delta M_{1'2'1\uparrow\downarrow}^{k*}(t') M_{1'2'1\uparrow\downarrow}^k(t) \right) \right] \\
&\approx \int \rho dE \frac{\delta(E - \epsilon_k)}{E - \epsilon_k} \sum_{1'2'1} n_1 n_{2'} (1 - n_1) \delta(\epsilon_{1'} + \epsilon_{2'} - \epsilon_1 - E) \delta_{1'+2'}^{1+k} \\
&\approx \int \rho dE \frac{\delta(E - \epsilon_k)}{E - \epsilon_k} (E - \epsilon_F)^2 = 0
\end{aligned} \tag{10.19}$$

This sketchy but correct argument shows that energy diagonal linear secular terms do not effect the momentum distribution function or one-particle correlation functions at the Fermi energy. It is remarked that for the momentum distribution function, i.e. for $\mathcal{N}_k(t) = \mathcal{C}_k^\dagger(t) \mathcal{C}_k(t)$ this correction vanishes because of symmetry even away from the Fermi surface.

Quadratic secular terms. Quadratic secular terms arise from the second order of the Baker-Hausdorff expansion in (10.13) and are proportional to t^2 . Fortunately, there is no quadratic secular term contributing to the momentum distribution. The only one conceivable could result from the following sequence of transformations which generically enfolds a second order feedback onto the coherent contribution $c_k^\dagger(B=0; t)$ by

$$c_{k\uparrow}^\dagger(B=0; t=0) \xrightarrow[\mathcal{O}(1)]{\text{FT}} c_{k\uparrow}^\dagger(B=\infty; t=0) \xrightarrow[\mathcal{O}(Ut)]{H_{\text{int}}} :c_{1'\uparrow}^\dagger c_{2'\downarrow}^\dagger c_{1\downarrow} : \xrightarrow[\mathcal{O}(Ut)]{H_{\text{int}}} c_{k\uparrow}^\dagger(B=\infty; t) \xrightarrow[\mathcal{O}(1)]{\text{BT}} c_k^\dagger(B=0; t)$$

The corresponding correction can be constructed from (10.17) and (10.16)

$$\begin{aligned}
&\sum_{5'6'5} \left[itU h_{k\uparrow}^{(A),FT}(\infty) \delta_{5'+6'}^{k+5} \delta(\epsilon_{5'} + \epsilon_{6'} - \epsilon_5 - \epsilon_k) \right] e^{i\epsilon_k t} \times \\
&\quad \times \left[itU \sum_{1'12'2} \delta(\epsilon_{1'} + \epsilon_{2'} - \epsilon_1 - \epsilon_2) \delta_{1'+2'}^{1'+2'} Q_{122'} \delta_1^{5'} \delta_2^{6'} \right] = \\
&= -U^2 t^2 e^{i\epsilon_k t} h_{k\uparrow}^{(A),FT}(\infty) \sum_{12'2} \delta(\epsilon_1 + \epsilon_2 - \epsilon_5 - \epsilon_k) \delta(\epsilon_{1'} + \epsilon_{2'} - \epsilon_1 - \epsilon_2) Q_{122'} \left. \begin{array}{l} 1'=1+2-2' \\ 5=1+2-k \end{array} \right.
\end{aligned}$$

and vanishes like (10.17).

$$\Delta h_k^{U^2} \sim U^2 t^2 I_k(\epsilon_k) = 0 \tag{10.20}$$

Here I observe the suppression of secular terms due to the interplay of time evolution with respect to an energy diagonal Hamiltonian and fermionic phase space factors. It occurs, in most cases, already on the level of the transformation of the creation operator. This illustrates the advantages of the chosen transformation scheme. One secular term, however, only vanishes because of the particular structure of the transformed number operator.

I conclude that the time evaluation with respect to the noninteracting Hamiltonian H_0 in (10.1.1) is justified and that the second order long-time limit (10.9) is not modified by secular corrections.

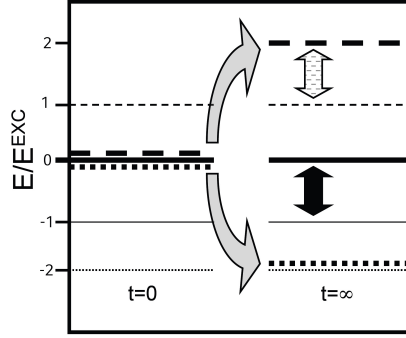


Figure 10.3: Sketch of the total energy (full line), kinetic energy (broken line) and interaction energy (dotted line) for the equilibrium (thin lines) and nonequilibrium (thick lines) case in second order perturbation theory. Nonequilibrium energies are compared at the quenching time and in the limit of infinite time. The bowed arrows indicate the corresponding energy relaxation, the straight arrows the gain in kinetic energy (broken filling) which equals the total excitation energy over the equilibrium ground state (full filling).

10.4 Nonequilibrium energy relaxation

The discussion of the momentum distribution function will be complemented by an analysis of energetic aspects of the dynamics. Since both the full Hamiltonian H and the noninteracting one H_0 are hermitian, so is the interacting part H_{int} . In a Heisenberg picture, they represent the time dependent observables for the total energy, the kinetic energy and the interaction energy, respectively. Contrary to the resolution of single momentum modes by the momentum distribution these observables are mode-averaged quantities only.

Although the total energy of a closed system is conserved, its partition onto kinetic energy and interaction energy after the quench is time dependent.

$$E^{\text{NEQ,INT}}(t) := U \langle \Omega_0 | \mathcal{H}_{\text{int}}(t) | \Omega_0 \rangle \quad (10.21)$$

$$E^{\text{NEQ,KIN}}(t) := U \langle \Omega_0 | \mathcal{H}_0(t) | \Omega_0 \rangle = \int_{-\infty}^{\infty} d\epsilon_k \epsilon_k N_k(t) \quad (10.22)$$

The energy zero point is defined by the Fermi energy of the noninteracting Fermi gas $\epsilon_F = \langle \Omega_0 | H_0 | \Omega_0 \rangle \equiv 0$. It agrees with the kinetic energy $E^{\text{NEQ,KIN}}(t = 0_+) = 0$ shortly after the quench because the state of the system is not changed by the quench directly and the time evolution of H_0 with respect to H has not been effective. Moreover, as H_{int} is normal ordered with respect to $|\Omega_0\rangle$, also the interaction energy shortly after the quench vanishes $E^{\text{NEQ,INT}}(t = 0_+) = 0$. This implies that the total energy before and after the quench remains identically zero $E^{\text{NEQ}} = \langle \Omega_0 | H | \Omega_0 \rangle := 0$. However, since the ground state of the interacting normal-ordered Hamiltonian is *lower* than that of the Fermi gas, the system is initialized in an excited state.

10.4.1 Equilibrium energies

Therefore, the first interest and the point of reference of all later energy considerations is the total energy of the equilibrium ground state of the interacting system. It can be calculated

in perturbation theory with respect to the noninteracting Hamiltonian H_0 . For convenience its eigenstates $|m\rangle$ ($m \in N_0$ with $|\Omega_0\rangle = |0\rangle$) are assumed nondegenerate.

$$E^{\text{EQU}} := \langle \Omega | H | \Omega \rangle \stackrel{P.T.}{=} \underbrace{\langle 0 | H_0 | 0 \rangle + \langle 0 | H_{\text{int}} | 0 \rangle}_{E^{\text{NEQ}=0}} + \underbrace{\sum_{m \neq 0} \frac{|\langle 0 | H_{\text{int}} | m \rangle|^2}{\epsilon_0 - \epsilon_m}}_{\approx -E^{\text{EXC}}} + \mathcal{O}(U^3) \quad (10.23)$$

This allows to read off the excitation energy of the quenched quantum system above the interacting ground state $E^{\text{EXC}} := E^{\text{NEQ}} - E^{\text{EQU}} = U^2 \rho_F \alpha \geq 0$. It is positive, second order in U and its precise value depends – due to the summation over all quantum numbers m – on the lattice structure. I hide such details in a numerical prefactor α .

Further equilibrium energies can be calculated from the Feynman-Hellman theorem [255]. As the norm of the interacting ground state is invariant (*), it holds

$$\frac{\partial E^{\text{EQU}}(U)}{\partial U} \stackrel{(*)}{=} \langle \Omega(U) | \frac{\partial H(U)}{\partial U} | \Omega(U) \rangle \stackrel{(10.23)}{=} -\frac{2}{U} E^{\text{EXC}} \stackrel{H}{=} \langle \Omega(U) | \frac{H_{\text{int}}}{U} | \Omega(U) \rangle = \frac{E^{\text{EQU,INT}}}{U} \quad (10.24)$$

From (10.23) one knows

$$E^{\text{EQU,INT}} = -2E^{\text{EXC}}$$

and with (10.24) it follows from $E^{\text{EQU}} = E^{\text{EQU,KIN}} + E^{\text{EQU,INT}}$ that

$$E^{\text{EQU,KIN}} = E^{\text{EXC}}$$

.

10.4.2 Nonequilibrium energies

Next I calculate the nonequilibrium energies in the long-time limit of the second order calculation. As the Fermi energy is set to zero,

$$\overline{E^{\text{NEQ,KIN}}} = \int d\epsilon_k \epsilon_k \overline{\Delta N_k^{\text{NEQ}}} \stackrel{(10.9)}{=} 2E^{\text{EQU,KIN}} = 2E^{\text{EXC}} \quad (10.25)$$

and $\overline{E^{\text{NEQ,INT}}} = -2E^{\text{EXC}}$. All energies are sketched in Fig. 10.3. Hence a second order calculation shows that the excitation energy of the quench is fully converted into additional kinetic energy such that $\overline{E^{\text{NEQ,KIN}}} = E^{\text{EQU,KIN}} + E^{\text{EXC}}$ while $\overline{E^{\text{NEQ,INT}}} = E^{\text{EQU,INT}}$. This is a remarkable observation.

Chapter 11

Discussion of the dynamics of a quenched Fermi liquid

The results for the energies and the momentum distribution found in the previous chapter are the foundation of the following analysis of the dynamics of a weakly quenched Fermi liquid. They are observations gained from the study of particular observables. One may object that they cannot catch all aspects of the full quantum dynamics of the Hubbard model and a full treatment of the density operator would be more elusive. This objection is true but fortunately unjustified since important physics can already be deduced from the behavior of these simple observables. The focus on the momentum distribution mirrors the approach taken in Landau's Fermi liquid theory and the results confirm *a posteriori* that this parallelism is appropriate. Moreover, despite all limitations this approach is capable of unfolding the multi-step dynamics of the Hubbard model which can be explained by reference to fundamental properties of many-particle fermionic systems.

11.1 Short-time quasiparticle buildup and nonequilibrium transient state

The first time regime is the one covered by the above second order perturbative calculation. It extends on a time scale set by $0 < t \lesssim \rho_F^{-1} U^{-2}$. There the evolution of the time dependent momentum distribution for physical fermions exhibits the build-up of multi-particle correlations as well as the formation of a quasiparticle description in nonequilibrium. The validity of second order perturbative results can be extended by the observation that corrections are not relevant until a much longer time-scale is reached.

11.1.1 Buildup of a correlated many-particle state

The most pronounced feature of this regime is the shrinking of the Fermi surface discontinuity of the momentum distribution to a finite, nonzero value. A numerical evaluation of the initial behavior of the momentum distribution (Fig. 10.2 a-d) mirrors the fast reduction of the quasiparticle residue from one to $Z^{\text{NEQ}} < 1$. Although the sharp Fermi surface is broken up by an interaction induced shift of occupation from states below the Fermi surface to states above, the remaining discontinuity indicates the existence of elementary excitations. Moreover, no heating effects (which would broaden the distribution at the Fermi energy such that the

discontinuity would be completely lost) can be read off from the momentum distribution. Thus the later resembles the distribution of a zero temperature gas of correlated fermions. This suggests that a Fermi liquid picture builds up from the excited initial state; then quasiparticles are well-defined quantities around the Fermi surface. $1/t$ -oscillations accompany this process.

11.1.2 Nonequilibrium transient state

After the buildup phase has been accomplished, one observes a quasi-steady transient behavior of the momentum distribution. This indicates that the dynamics of the corresponding quantum state is dramatically slowed down within an intermediate time regime.

Time scale of the transient state

The related time scale $t_T \sim \rho_F U^{-2}$ is linked to the order in perturbation theory on which the features of the transient dynamics can be observed. Its signatures are extracted from a second order calculation which can be, for times beyond the buildup phase, discussed in a (formal) long time limit. For the Hubbard model this long time limit only describes a transient behavior and *not* the physical long-time limit of the full dynamics. Since there are no immediate changes to the state of the system for times $t \gtrsim \rho_F^{-1} U^{-2}$ the nonequilibrium Fermi liquid-like state represents an intermediate quasi-steady regime of the dynamics; for small values of the interaction U the transient regime can be long lasting.

Corrections to the second order result only appear in fourth order of the interaction because the Hubbard model is particle-hole symmetric [171]. They set an upper bound for the temporal extension of the transient regime. On even larger times their influence on the further dynamics will lead to a different regime which can be related to thermalization.

Characteristics of the intermediate regime: Mismatch of the quasiparticle residue

In the intermediate time regime the momentum distribution shows the signatures of a zero temperature Fermi liquid (Fig. 10.2 d). Obviously, such a transient state cannot be the ground state of a Fermi liquid description since the excitation energy, which has been inserted by the quench, is conserved; it prevents a relaxation towards a zero temperature Fermi liquid ground state.

Deviations from the zero temperature ground state are also visible in the momentum distribution but do not relate to any signatures of higher temperature. Instead, the most distinguished feature of the transient state is the "mismatch" of its quasiparticle residue: Since the correlation-induced reduction of the residue from the value one (for a noninteracting Fermi gas) to the value for the interacting Fermi liquid is twice as strong in nonequilibrium than in equilibrium (10.9), the mismatch incorporates and specifies the nonequilibrium character of the transient state. This behavior is rooted in the combined influence of interaction and nonequilibrium and therefore of particular physical interest.

Momentum distribution of particles and quasiparticles

For a further understanding it is helpful to change the point of view from the momentum distribution of physical fermions (PF) to one of quasiparticles (QP). They agree with each

other on the main features. However, since interaction effects are absorbed into the definition of the quasiparticles, the quasiparticle distribution exhibits less pronounced correlation-induced signatures. In equilibrium they vanish completely and a zero temperature quasiparticle distribution always equals a filled Fermi sea with a Fermi surface discontinuity of size one $N_k^{\text{EQU;QP}} = \Theta(\epsilon_F - \epsilon_k)$.

In the nonequilibrium transient state, this absorption of interaction effects into the definition of interacting degrees of freedom is not sufficient. Due to the increased correlation-dependent reduction of the quasiparticle residue by a factor of two a mapping of the nonequilibrium momentum distribution for physical fermions into a quasiparticle representation will generate a distribution with a reduced Fermi surface discontinuity. In second order perturbation theory $N_k^{\text{NEQ;QP}} = N_k^{\text{EQU,PF}}$. The reduced discontinuity of the quasiparticle distribution now describes the deviation from equilibrium. It is retained throughout the transient regime.

Energy relaxation and prethermalization

As observed from the momentum distribution, the full relaxation of momenta has been postponed to a later stage of the dynamics. This, however, is not the case for the total kinetic energy which is an integrated quantity; hence, the behavior of single momentum modes is averaged out. The second order calculation shows a complete transfer of the *excitation energy* from interaction energy to kinetic energy [*cf.* Fig. 10.3]. However, since the momentum distribution still exhibits zero-temperature features, this cannot be related to heating. The simultaneous relaxation of average energies and non-relaxation of other, mode-specific expectation values shows a universal far-from-equilibrium phenomenon which is known as *prethermalization*.

Split-up of two temperatures. Prethermalization can be expressed in terms of a split-up of the notion of temperature: While systems in thermal equilibrium are characterized by a universal temperature which is the same for all observables, in nonequilibrium an analogous universal temperature does not exist. Instead, different temperatures may apply for different observables. In the transient state, two temperatures are separated. One is related to the kinetic energy and already refers to the final temperature of the relaxation process. However, as the momentum distribution has not relaxed so far it relates to a second temperature, which is zero.

Prethermalization in quantum field theories. Prethermalization has been first described in nonequilibrium quantum field theories modeling, for instance, the early universe. For a low-energy, chiral quark-meson model which was subjected to a sudden perturbation Berges observed it studying the time evolution of quantum fields [256]. He found a multi-step dynamics for the momentum mode occupations which is independent of the precise details of the applied couplings. Rapid initial changes of the momentum distribution are followed by oscillations which are damped on a short time scale t_{damp} . Afterwards, a quasi-stationary still far-from-equilibrium state formed which showed no memories of the initial state any more. In this time regime a constant ratio of pressure over energy density holds although the momentum modes have not arrived at their final values. Therefore on a short time scale related to the inverse of the mass scale m prethermalization is observed. It is not related to scattering processes but caused by the dephasing of oscillating contributions to an integral taken over momentum modes with a continuous frequency spectrum. Scattering processes,

however, have been identified as the reason for later thermalization and become important on the much larger equilibration time scale which follows the long transient regime.

11.2 Long-time behavior – Thermalization

The mentioned fourth order corrections to the flow equations calculation describe the characteristic dynamics of a third time regime on a scale $t \sim \rho_F^{-3} U^{-4}$. They originate from two sources: firstly from a more accurate implementation of the diagonalizing transformation. These are corrections to the quasiparticle picture. Since Fermi liquid theory is exact only strictly at the Fermi energy, they are expected in any microscopic foundation of Fermi liquid theory. In this work they may, moreover, indicate a possible higher order difference between two quasiparticle pictures, namely of the Landau quasiparticles on the one hand and the energy-diagonal degrees of freedom of the flow equation approach on the other. Secondly, the energy diagonal interaction Hamiltonian generates an additional time evolution which is based on the influence of energy diagonal (i.e. elastic) scattering processes. Therefore fourth order secular terms can be expected. The full calculation of these corrections is beyond the scope of this work. Here only an effective treatment can be given which leaves many questions open for a further analysis.

11.2.1 Self-consistent treatment of the momentum distribution

However, the existence of an additional dynamics can be already seen from a simple motivation: One can read (10.7) as an implicit equation for the momentum distribution. Then substituting $n_i = N_i^{\text{NEQ}}$ in the phase space factor $J_k(E; n)$ leads to

$$N_k^{\text{NEQ}}(t) = n_k - 4U^2 \int_{-3D}^{3D} dE \frac{\sin^2((E - \epsilon_k)t/2)}{(E - \epsilon_k)^2} J_k(E; n = N^{\text{NEQ}}) \quad (\rightarrow 10.7)$$

This self-consistent treatment induces an additional dynamics of the momentum distribution. Since the initial buildup of correlations has redistributed momentum mode occupations such that $N_i^{\text{NEQ}} \neq n_i$, the evaluation of the phase space factor for zero temperature as it was done in section (9.2.2) is not exact any more. Hence, the denominator in (10.7) is not exactly cancelled at the Fermi energy any more. These corrections, however, become relevant only for higher orders of the perturbative expansion which correspond to longer time scales. Since then the short-time regime has already ended the time dependent kernel in (10.7) can be treated analogously to the derivation of Fermi's golden rule in section (5.3.1), i.e. in a long time limit for which $\lim_{t \rightarrow \infty} \frac{\sin^2((E - \epsilon_k)t/2)}{(E - \epsilon_k)^2} = \frac{\pi}{2} t \delta(E - \epsilon_k)$. There it motivates a differential equation for the momentum distribution which is driven by a nonvanishing scattering integral for elastic two-particle scattering processes.

$$\frac{dN_k^{\text{NEQ}}(t)}{dt} \approx \lim_{\langle t \gg 1 \rangle} \frac{N_k^{\text{NEQ}}(t) - n_k}{t} = -2\pi t U^2 J_k(E = \epsilon_k; n = N^{\text{NEQ}}) \quad (11.1)$$

This suggests a quantum Boltzmann description of the residual dynamics. However, one should not naïvely solve (11.1) since it represents only one among many fourth order correction terms. It is only presented to indicate the direction of the following argument.

11.2.2 Quantum Boltzmann equation

As it has been explained in the introduction a quantum Boltzmann description aims at the residual dynamics of quasiparticles. This fits well to the scenario of the quenched Fermi liquid: Since a quasiparticle picture has been established by a second order calculation, corrections in fourth order can be treated as such an residual interaction.

Quasiparticle picture for later times

However, one has to ensure that the quasiparticle picture is pertained also for (much) later times. This is a delicate prerequisite of any quantum Boltzmann approach but can be justified in a small neighborhood around the Fermi energy. There scattering processes between quasiparticles are suppressed by phase space arguments. Therefore the lifetime of quasiparticles is extended on a time scale $\tau_k = (\epsilon_k - \epsilon_F)^{-2}$. Sufficiently close to the Fermi energy this scale becomes large. If quasiparticle stability is required, say, on a time related to fourth order perturbation theory in U , this can be safely assumed for an environment of $|\epsilon_k - \epsilon_F| < \rho U^2$ around the Fermi energy. Making statements only within this energy window, no decay processes of quasiparticles need to be considered.

Application of the quantum Boltzmann equation

Instead of calculating the other fourth order correction terms to the dynamics of the momentum distribution for physical fermions which would complement the self-consistency treatment in (11.1) I perform all further analysis in a quasiparticle representation. This equals approximately working in the diagonal basis of the flow equations approach. According to the remark made above the quasiparticle picture can be used to describe the subsequent dynamics of low energy excitations around the Fermi energy even beyond the time regime of the quasi-steady state. This is done by studying the time evolution of the momentum distribution which is initialized in the quasi-steady, transient state. Its quasiparticle momentum distribution can be made explicit by the approximation $\overline{N}_k^{\text{NEQ,QP}} = N_k^{\text{EQU,PF}}$ which serves as an initial condition. The effective kinetic equation which describes the residual interaction between Landau quasiparticles is the quantum Boltzmann equation [254]. For a translationally invariant system it can be written as

$$\frac{\partial N_k^{\text{QP}}(t)}{\partial t} = -\rho_F U^2 J_k(E = \epsilon_k, N^{\text{QP}}(t)) . \quad (11.2)$$

The characteristic features of the dynamics induced by the quantum Boltzmann equation can be read off its right hand side which is commonly referred to as the collision integral [167].

Thermalization of the momentum distribution

Since inserting $N_k^{\text{QP:NEQ}}$ into $J_k(E = \epsilon_k, n)$ allows nonzero phase space for scattering processes in the vicinity of the Fermi surface, linearizing the phase space factor in the collision integral shows that the initial quasiparticle distribution function starts to evolve on the time scale $t \propto \rho_F^{-3} U^{-4}$. This implies that the quasi-steady fermionic distribution function depicted in Fig. 10.2d) starts to decay on the same time scale. The further dynamics of the quasiparticle momentum distribution function follows, again, from the collision integral. Since $J_k(E = \epsilon_k, n)$ vanishes for Fermi-Dirac distributions ($n = n^{\text{FD}}$) these are the stable fixed points of (11.2) for a fixed total kinetic energy. Since around the Fermi surface the quasiparticle picture

is retained on a long time scale the prediction of thermalization of the momentum distribution can be concluded from the overall quantum dynamics of a Boltzmann equation on a lattice. For nonequilibrium initial conditions with energies far below the Fermi energy it describes a flow towards a thermal distribution which is its only attractive fixed point or, mathematically speaking, its unique solution [147].

However, the fourth order corrections which motivate a quantum Boltzmann treatment on a long time scale are present at *all* times. Hence they cause an obliteration of the Fermi surface discontinuity already at the onset of the dynamics. For short times after the quench, the momentum distribution still shows a steep descent; therefore its widening can be safely neglected. Yet the assumption of a persistent quasiparticle picture for all later times may be questioned. This is a general shortcoming of a quantum Boltzmann approach and is usually accepted.

Final temperature

Moreover, the collision integral conserves the kinetic energy such that the evolution towards a fixed point is constrained to an energy hypersurface in phase space. As the quantum Boltzmann dynamics continues until it reaches a stable fixed point, thermalization of the momentum distribution can be expected. This implies that the excitation energy, which has relaxed into an excess of kinetic energy already at an earlier stage, is redistributed among the momentum modes until a thermal distribution is achieved. The corresponding temperature T_{th} of the thermal momentum distribution follows directly from fitting its Sommerfeld expansion [8] to the excitation energy. Equally, one relates the total kinetic energy to the temperature via the specific heat C_V of a Fermi liquid which depends linearly on temperature (cf. table 2.2.6). This reads

$$\overline{E^{\text{NEQ,KIN}}} = 2E^{\text{EXC}} = 2\rho_F\alpha U^2 = C_V T_{\text{th}} \quad \Rightarrow \quad T_{\text{th}} = \sqrt{\frac{6\rho_F\alpha}{m^*k_F k_B^2}} U \quad (11.3)$$

Quantum Boltzmann equation and the flow equation approach

In the following I will point out that a quantum Boltzmann description of a dynamics caused by a residual interactions is a most natural extension of a flow equation implementation of unitary perturbation theory. The matching point of both approaches are energy diagonal, i.e. elastic scattering processes described by the interaction term in the Hamiltonian. On the one hand, they remain untouched by a flow equation transformation such that an energy diagonal interaction Hamiltonian generates a nontrivial time evolution. On the other hand, only elastic *two-quasiparticle* scattering processes contribute to the scattering integral of the quantum Boltzmann equation which is responsible for the further dynamics of the momentum distribution. Since the flow equation transformation implements approximately Landau's quasiparticle mapping, connecting interacting physical fermions to diagonal degrees of freedom which are described by the same quantum numbers as a gas of noninteracting fermions, the nontrivial energy diagonal time evolution in the final representation of a flow equation treatment and the quasiparticle scattering contribution to the evolution of the momentum distribution can be approximately identified. Hence a quantum Boltzmann approach appears as the most adequate extension of a real-time analysis based on the flow equation technique. It stands in a historic line with prior treatments of residual interactions (c.f. 1.4.5).

11.3 Physical origin of the observed dynamics

In the past section I have presented the separation of two time scales of the Hubbard dynamics. While interaction effects lead to a rapid establishment of a quasiparticle picture, the equilibration of the momentum distribution, i.e. heating, is deferred to a much later time.

11.3.1 Delayed relaxation caused by Pauli principle and translation invariance

This delayed relaxation is a consequence of two fundamental properties: Firstly, the *Pauli principle* imposes characteristic phase space restrictions on a multiparticle fermionic system. These are responsible for the generic appearance of particle-like low energy excitation physics in a Fermi liquid and justify a meaningful analogy between the behaviour of the squeezed one-particle oscillator and the many-body Hubbard model. Secondly, *translational invariance* implies the conservation of lattice momenta. Hence there is no other way of momentum relaxation than by momentum transfer in two-particle (or higher) scattering processes. In combination, these two properties form a restrictive bottleneck for the relaxation dynamics. Since the Pauli blocking of scattering is less effective in the regimes of higher temperatures or larger excitation energies this is a zero temperature effect which is only visible for small quenches of the interaction, i.e. for small energy intake.

11.3.2 Generalization to large class of interactions

The particular form of the interaction is less important. For the above calculations I have assumed the applicability of perturbation theory in the interaction strength. Since only second order and fourth order terms describe the evolution of the momentum distribution, there is no difference between attractive and repulsive interactions; moreover, a generalization to nonlocal interactions is easily possible by introducing momentum dependent matrix elements. The main observation of a characteristic mismatch between the –interaction dependent– zero temperature correlated equilibrium ground state of the momentum distribution and a similarly shaped distribution in the intermediate regime of the nonequilibrium case persists. Hence I expect similar nonequilibrium behaviour for a large class of weakly interacting and perturbatively approachable model systems independent of the exact nature and the particular form of the interaction. This reflects the rather generic applicability of Fermi liquid theory to not too strongly interacting systems in equilibrium.

11.4 Comparison of the Hubbard dynamics

The observations made in this thesis for the Hubbard model in more than one dimension agree well with related results for the fermionic and bosonic Hubbard model in one dimension. An overview is provided by Fig. 11.4.

11.4.1 Hubbard model in one dimension

An analogous analysis of the real-time dynamics following a quench in the forward scattering has been performed for the Hubbard model in one dimension by Cazalilla [93]. In one dimension the Hubbard model is integrable and can be solved exactly by bosonization and a final

	Fermionic Hubbard model	Bose-Hubbard model
One dimension	<div style="text-align: center; border: 1px solid black; padding: 2px;">integrable</div> <p>Solved by Miguel A. Cazalilla for switched-on forward scattering using bosonization techniques</p> <p>Exponents of correlation functions mismatch their equilibrium value</p>	<div style="text-align: center; border: 1px solid black; padding: 2px;">nonintegrable</div> <p>Mapped to a Heisenberg model by T. Barthel et al. and studied for nonequilibrium initial states</p> <p>Transient state relates to exact solution of Heisenberg model</p>
Larger dimensions	<div style="text-align: center; border: 1px solid black; padding: 2px;">nonintegrable</div> <p>Discussed in this thesis in the limit of weak interaction strength</p> <p>Transient Fermi-liquid like state and thermalization due to residual interaction between quasiparticles</p>	<div style="text-align: center; border: 1px solid black; padding: 2px;">nonintegrable</div> <p style="text-align: center;">Unexplored</p>

Figure 11.1: State of the art of an analytic real-time analysis for the Hubbard model, dating April 2009. The one dimensional cases are discussed and briefly compared in section 11.4.1 for fermions and section 11.4.2 for bosons. Numerical works based on a time dependent density matrix renormalization group (t-DMRG) approach are also available for the one-dimensional Bose-Hubbard model [257], for spinless fermions [258] and local relaxation in superlattices [131]. While an initial buildup of correlations can be easily observed, long-time predictions are constrained by limited numerical resources. Therefore, these results are not fully conclusive. Most recently, calculations based on dynamical mean-field theory, which becomes exact in the limit of infinite dimensions, have been presented [259] and are discussed in section 11.5.

Bogoliubov transformation within the bosonic degrees of freedom. Since in the later step the treatment of the different bosonic momentum modes decouples the Bogoliubov transformation equals the diagonalization of the quenched one-particle oscillator (cf. 6.3) for every pair of modes $(k, -k)$. Although the weakly interacting phase of the one-dimensional Hubbard model is a Luttinger liquid instead of a Fermi liquid in higher dimensions, very similar observations have been made.

First of all, an analogous mismatch between equilibrium and the nonequilibrium expectation values has been found in the exponents of power-law decaying correlation functions. This mismatch is the same as observed for the quenched oscillator in (6.17). Hence, in nonequilibrium a different decay of correlations holds than in equilibrium. Contrary to the observations in the higher dimensional case, this result for the one-dimensional Hubbard model is exact. Therefore there is no residual interaction between the degrees of freedom which could induce a further dynamics. Seen from the perspective of the higher dimensional case, the integrable dynamics of the one-dimensional Hubbard model is trapped in the transient state of the higher dimensional one. The 'transient' state already represents the physical long-time limit such that there is no second time-scale in the relaxation dynamics. Hence there is no thermalization in the one-dimensional case but it is observed in higher dimensions. This behavior illustrates the particular rôle of one dimension where, due to a linear dispersion relation for fermions around the Fermi surface, translational invariance both imposes momentum conservation and, in consequence, energy diagonality.

Fermionic Hubbard model with long range hopping. The lacking of a second time scale in the relaxation dynamics has equally been observed by M. Kollar and M. Eckstein [260] in the one-dimensional fermionic Hubbard model with long range hopping. There the non-local hopping matrix elements $t_{m,j}$ decay proportionally to the inverse distance. Since the model is integrable [261], relaxation to a thermal state is not expected *a priori*. However, relaxation to steady states has been found studying the double occupation $d(t)$. These states coincide with the predictions of a generalized Gibbs ensemble based on correctly chosen integrals of motion.

11.4.2 Bose-Hubbard model in one dimension

Motivated by experiments in optical superlattices, a similar approach to the dynamics of the one-dimensional Bose-Hubbard model with an alternating one-particle potential has been presented by Barthel et al. [223]. They map the Bose-Hubbard model at half filling by means of a Schrieffer-Wolff transformation approximately to the ferromagnetic or antiferromagnetic Heisenberg model (depending on the initial state). The later model is an effective model for the low energy dynamics and is integrable by Bethe ansatz methods. However, Barthel et al. solve it in a mean-field approximation. This two-step solution is in analogy to Cazalilla's treatment of the one-dimensional fermionic Hubbard model: an integrable model is reached by means of bosonization or the Schrieffer-Wolff transformation, respectively. Then it is diagonalized either by a Bogoliubov transformation (see above) or, similarly, by a mean-field treatment of Jordan-Wigner transformed spin operators in the case of the Heisenberg model. However, contrary to the fermionic Hubbard model this is not exact for the Bose-Hubbard model and a residual interaction is retained. This residual interaction resembles the residual is partly caused by an approximate implementation of the Schrieffer-Wolff transformation. However, partly it also roots in the projective nature of this transformation which reduces

the Hilbert space of the Hubbard model in the limit of strong two-particle interaction to the more restricted (effective) Hilbert space of the Heisenberg spin model. Hence, the Heisenberg Hamiltonian generated by the Schrieffer-Wolff transformation is not exact and corresponds to the truncated energy-diagonal Hamiltonian obtained after the flow equation transformation in this thesis. Then the time evolution of particular observables is studied with respect to the approximately diagonalized Heisenberg Hamiltonian. Afterwards the backward transformation of the time-evolved observables is implemented by the inverse Schrieffer-Wolff transformation and the dynamics of nonequilibrium initial states is studied.

The dynamics of the integrable Heisenberg model is caused by dephasing of an initial state and corresponds well to numerical calculations for the Bose-Hubbard model at short times. The buildup of a stationary state in the Heisenberg model indicates a quasisteady state of the Bose-Hubbard model. For the later thermalization can be expected due to residual interactions. Since in Barthel's work their strength can be tuned the temporal extension of the quasi-steady state and, which is the same, the time delay of thermalization can be varied. Here, the 'stabilization' of a quasi-steady regime caused by a closeness of the nonintegrable Hamiltonian to an integrable one can be quantified.

11.5 Numerical confirmation of the results

Recently, the results for the quenched Fermi liquid which were presented and explained in this thesis have been numerically confirmed by M. Eckstein, M. Kollar, and P. Werner [259]. Using a nonequilibrium extension of dynamical mean field theory (DMFT) and assuming a semicircle density of states they studied the evolution of the Fermi surface discontinuity of the momentum distribution (i.e. the quasiparticle residue) and the double occupation after various interaction quenches both within the Fermi liquid phase and beyond. A plot from their recent preprint is reprinted in Fig. 11.2 and shows, for selected values of the final interaction strength, the time dependence of the Fermi surface discontinuity (which they denote by Δn in discrepancy to my notation where Δn represents the reduction of the quasiparticle residue due to correlation effects). In the case of a weak quench ($U = 0.5$) they observe the transient state on all numerically accessible times. This state is characterized by a quasi-constant nonequilibrium value of the quasiparticle residue which complies exactly with the calculations presented above. From the calculation of this thesis the onset of the final relaxation to equilibrium is expected (assuming, however, a constant density of states) on a much later time $t_{\text{th}} = \rho_F^3/U^4$.¹

For quenches to stronger interactions $U > 1$ the perturbative approach to a time-scale separation of prethermalization ($t \gtrsim \rho_F^{-1}U^{-2}$) and thermalization ($t \propto \rho_F^{-3}U^{-4}$) does not hold any more. Nonetheless, a transient state still appears during a shorter intermediate time regime. This allows to observe a later further reduction of the quasiparticle residue which indicates the second stage of the dynamics, namely the onset of thermalization. For intermediate values of the interaction quench ($1 \leq U \leq 1.5$) the quasiparticle residue in the transient state is still very close to the perturbatively predicted value. For larger values of the interaction the reduction of the Fermi edge discontinuity is increased. This corresponds to the findings for

¹A hand-waving argument which transgresses the regime of strict validity of the perturbation calculation and neglects particularities of the density of states suggests that thermalization should become observable on a time scale sixteen times later than in the case of $U = 1$. Taking $t_{\text{th}}(U = 0.5) \approx 3$ from Fig. 11.2 this would result in $t_{\text{th}}(U = 0.5) \approx 50V^{-1}$ where V^{-1} is the time unit used by Eckstein, Kollar and Werner. This illustrates the difficulty of finding long-term behavior in numerical approaches.

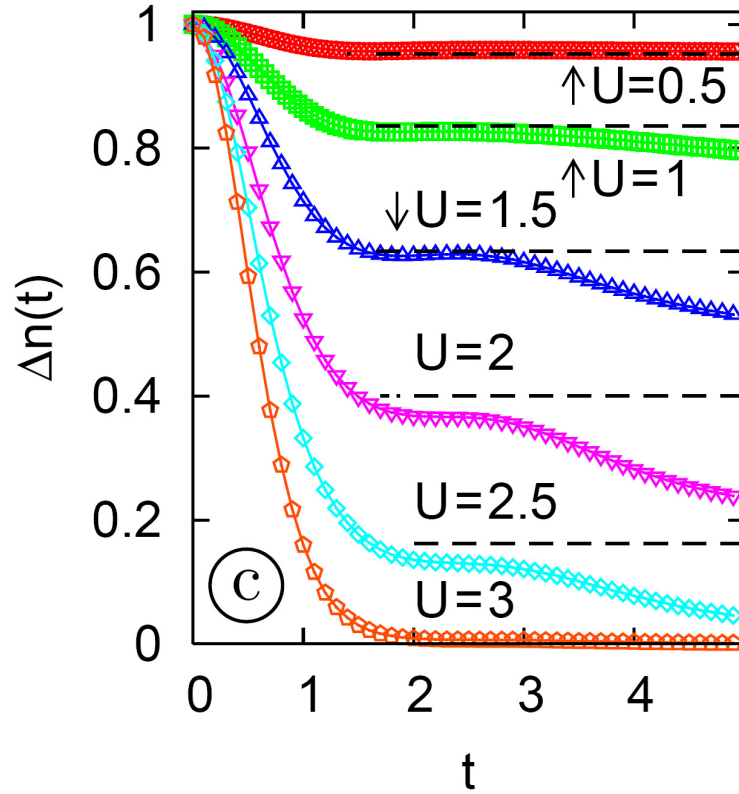


Figure 11.2: The Fermi surface discontinuity $\Delta n(t)$ of the momentum distribution is plotted with respect to time for different values of the interaction U . Horizontally dashed lines correspond to its value in the intermediate transient state as calculated in this thesis. For small quenches ($U = 0.5$, red line) the prethermalized regime extends beyond the longest calculated time such that the delayed onset of thermalization cannot be observed. The separation of two dynamical time scales and a well-defined regime of prethermalization is visible for values of $1 \leq U \leq 2.5$. For larger interaction strength no prethermalization is observed any more. Reprinted from [259] with kind permission by M. Kollar.

the exactly solved quenched oscillator where, similarly, the mismatch between the equilibrium and nonequilibrium expectation value of the occupation is increased with growing interaction g (cf. Fig. 6.1). Finally, for $U \gtrsim 3$ no signatures of prethermalization have been found.

Chapter 12

Conjectures on the generic nature of the mismatch for *many*-particle systems

The analytical description of prethermalization in a Fermi liquid and its numerical confirmation raise the question on the generic nature of a delayed relaxation to equilibrium. For one-particle systems, the generality of the mismatch of nonequilibrium and equilibrium expectation values has been proved in chapter 7. In the following chapter very recent similar findings in many-particle systems are quoted. They support the formulation of a conjecture on the generic nature of the mismatch between equilibrium and nonequilibrium expectation values for particular observables in quenched many-particle quantum systems.

12.1 Similar observations in other many-particle systems

In the meantime, a similar real-time analysis following a quantum quench has been performed for other many-body systems. For comparable quench scenarios which start from a noninteracting configuration and quench within a weakly interacting regime the characteristic mismatch of long-time averaged nonequilibrium and equilibrium expectation values has equally been observed in other model systems and observables; corresponding perturbative calculations reproduce a ratio given by the characteristic factor of two. This supports the conjecture that the mismatch of equilibrium and nonequilibrium expectation values is a rather generic observation even when many-body systems are considered.

12.1.1 Spin relaxation in the ferromagnetic Kondo model

A recent preprint by A. Hackl et al. [262] reports about a quantum quench for a Kondo impurity in the ferromagnetic regime: There the coupling of the impurity spin with a band of metal electrons J is switched on suddenly at zero time, assuming an initial polarization of the impurity spin ($S_z = 1/2$). Then a real-time analysis of the subsequent spin dynamics is performed, studying the nonequilibrium expectation value of the impurity magnetization $\langle S_z \rangle$. For comparison, this calculation has been obtained twice: analytically, using the flow equations technique, but also with exact numerical (time dependent NRG) methods [262]. The respective results agree very well on all considered time scales. Comparing, up to leading

order in the coupling J , the long-time limit of the nonequilibrium result $\langle S_z(t \rightarrow \infty) \rangle$ with the equilibrium value the above-mentioned characteristic mismatch of expectation values by a factor of two is observed.

12.1.2 Interaction quench in the sine-Gordon model

The sine-Gordon model is an integrable 1+1 dimensional field-theory with a nontrivial phase diagram and many relations to other model systems [263]. Therefore it turned into a paradigmatic description of low-dimensional systems and their phase transitions, for instance the Mott transition for one-dimensional bosons (see, e.g. [183, 264, 265]). Its Hamiltonian, expressed in terms of a bosonic field operator $\Phi(x)$ and its conjugate momentum operator $\Pi(x)$, for which canonical commutation relations¹ hold, reads

$$H = \frac{1}{2} \int dx \Pi^2(x) + (\partial_x \Phi)^2 + g(t) \cos(\beta \Phi(x)) \quad (12.1)$$

where $g(t)$ is typically taken as a constant. β^2 and g span the equilibrium phase diagram of the model. There is a Kosterlitz-Thouless type phase transition line $g_{KT}(\beta^2)$ which occurs, in the limit of vanishing interaction, at $\beta_0^2 = 8\pi = g_{KT}^{-1}(0_+)$. Beyond that line ($\beta^2 \gg \beta_0^2$) a renormalization group approach shows a flow towards the weak-coupling limit. In this regime a quantum quench was performed and the successive dynamics of the momentum distribution was studied, in analogy to the treatment of the Fermi liquid, by J. Sabio and S. Kehrein [266]². According to the expectations for an integrable system they found no relaxation of the momentum distribution to a thermal state; instead, undamped oscillations were seen. Nonetheless, the characteristic mismatch of the equilibrium and a long-time averaged nonequilibrium expectation value with a perturbatively calculated ratio $m = 2$ (cp. definition in equation 6.17) could be confirmed in this model, too. This observation is reminiscent of the integrable Hubbard model (cf. 11.4.2) where integrability prevents a further relaxation, too. Moreover, they report that a flow equation treatment is essential to obtain the above-mentioned result for the nonequilibrium momentum distribution. This is different from my findings for a Fermi liquid for which, as I will show in chapter 14, Keldysh perturbation theory already provides a sufficient description.

12.2 Synopsis of the discussed findings

A synopsis of the mentioned findings suggests that the mismatch of equilibrium and nonequilibrium expectation values in quench scenarios represents more than a freak of nature in certain exotic quantum models. A strong point is made by the proof of a general theorem for the one-body case (7.6). However, the proof cannot be naïvely extended to general many-body systems. This is because the continuous energy spectra of many-body quantum systems in the

¹Canonical commutation relations read: $[\Phi(x), \Pi(y)] = i\hbar\delta(x - y)$, all unrelated commutator relations vanish

²Alternatively, a quench in the sine-Gordon field theory resembles a boundary field theory with an initial condition. An exact solution for the boundary sine-Gordon problem with a spatial boundary is available [267] and has been applied to study quantum impurity problems (cf. citations in [268]). Since in the boundary sine-Gordon model space and time coordinates appear in a symmetric way this provides a solution for the initial state boundary, too. This approach has been used to study the spectrum of collective excitations by means of a quantum quench [91].

thermodynamic limit prevent, similar to the case of energy degeneracy, the straightforward application of the dephasing argument used in equation (7.8) or (7.15)³.

For the following considerations I assume that the prerequisites of the theorem (7.6) are met. Then there is indication that the statement of the theorem holds beyond the limits set by the given proof. Some aspects motivate that reasoning:

12.2.1 Conclusion on the behavior of integrable model systems

Integrable models are constrained by additional constants of motion such that thermalization cannot be expected. According to the Bohigas, Giannoni and Schmidt conjecture [101] and its later confirmations by other authors integrability influences the spectral properties of a quantum model. In particular there is no 'energy level repulsion' in corresponding random matrix ensembles, i.e. small energy differences between neighboring eigenenergies of the total Hamiltonian are not suppressed as it is the case for nonintegrable systems. This spectral property of the Hamiltonian may delay or even restrict the complete dephasing of a typical⁴ initial state. Note that dephasing is, on the one hand, essential to observe a nontrivial initial dynamics leading to a characteristic mismatch of equilibrium and nonequilibrium expectation values; on the other hand, it is the only relaxation mechanism in an eigenstate representation of a closed quantum system. Therefore the characteristic mismatch of nonequilibrium and equilibrium expectation values should appear in the discussion of many integrable models. Such an expectation is in agreement with the above-mentioned findings in integrable models as discussed exemplary for the Hubbard model in one dimension [93] in section 11.4.1. Moreover, since relaxation processes beyond eigenstate dephasing are not available, the mismatch of equilibrium and nonequilibrium expectation values is retained for all times.

12.2.2 Conclusions on the behavior of nonintegrable model systems

A different view is taken on nonintegrable models, for which thermalization is commonly expected, at least on a long time scale. In consequence, characteristic nonequilibrium expectation values are expected to appear only as transient behavior on intermediate time scales. The example of the quenched Fermi liquid shows that there the characteristic nonequilibrium regime results from initial dephasing. Then the separation of time scales allows the observation of a transient state before other relaxation processes become important. This behavior follows from phase space restrictions which constrain the system in an early stage of the dynamics but are softened under the ongoing dynamics. This suggests the conclusion that the observation of a mismatch of equilibrium and nonequilibrium expectation values in nonintegrable systems requires the existence of almost-conserved constraints on further relaxation processes, e.g. by scattering. Such constraints can, for instance, originate from a particular closeness of the nonintegrable model Hamiltonian to an integrable one; then these almost conserved constraints may show up as "faked" integrals of motion [256] in leading order perturbation theory. Almost conserved constraints, however, are most efficient to restrict the evolution of a system if its energy is not too large. This limits the observation of a prethermalized regime presumably to weak interaction quenches, as observed in [259].

³Note that for vanishing energy difference $\epsilon_n - \epsilon_m \rightarrow 0$ in the exponential argument of relative phase factors $\exp(i(\epsilon_n - \epsilon_m)t)$ dephasing would –at the best– occur on a diverging time scale.

⁴Here I use the notion *typical* for a state which can be represented by a linear combination of Hamiltonian eigenstates with *small* coefficients, following roughly the idea of microcanonical typicality in a high-dimensional Hilbert space (cp. [125]).

12.3 Conjectures on the generic nature of the mismatch of equilibrium and nonequilibrium expectation values in many-body quantum systems

Therefore a summary of these findings and discussions suggests the formulation of the following two conjectures:

Conjecture 1:

Let me assume the prerequisites of chapter 7.1 for the observable and for the definition of the applied interaction quench which is, however, performed for a *many-body* quantum system. Then I expect the observation of a mismatch of the equilibrium expectation value of such an observable and its large-time average expectation value with respect to the time-evolved initial state if additional exact or approximate restrictions on the dynamics exists which prevent or delay the onset of relaxation processes other than initial dephasing.

Conjecture 2:

If the scenario of Conjecture 1 holds a leading order perturbative calculation of the mismatch results in a ratio of the nonequilibrium and the equilibrium expectation value which approaches, in the limit of weak perturbation, the value $m = 2$.

12.4 Call for debate

These conjectures suggest that exhibiting the characteristic mismatch of equilibrium and nonequilibrium expectation values is a generic behavior which, therefore, should be visible in many model systems. The requirement of additional constraints in quenching scenarios is not exotic and has already been used to tailor (exotic) metastable states in quantum many-particle systems. For instance, in the fermionic Hubbard model, implemented in optical lattices, energy conservation provides a bottleneck for the relaxation of doubly occupied sites after a quench of the trapping potential; this allows to observe their Bose-Einstein condensation and superfluidity [97].

A natural next step would be to test these conjectures for a prototypical interacting quantum field theory, for instance Φ^4 theory. As prethermalization was originally observed in 1+1 dimensional and 3+1 dimensional quantum field theories [256] there is reasonable grounds for the expectation that related findings can be made in other quantum field theories. Perhaps it can even be proven that the conjectures describe the generic behavior of a quantum field theory subjected to a quantum quench.

Finally, more research is encouraged to proof, specify, adjust, extend, restrict or falsify these conjectures and to relate them to a larger picture of the nonequilibrium dynamics of correlated many-body quantum systems. The author of these lines would be happy to engage in further discussions and to read about progress made in this field.

Part III
Outlook

Chapter 13

Nonequilibrium physics of a system with a Fermi-liquid instability

The findings presented in this thesis can be relevant for studies focussing on the nonequilibrium physics of models with a Fermi liquid instability (FLI). Consider a quench from a noninteracting Fermi gas into a phase which exhibits such an instability. In the subsequent dynamics on a buildup time $t_{\text{FLI-B}}$ one expects both the buildup of the Fermi liquid instability and characteristic nonequilibrium physics related to it. Since non-perturbative weak interaction instabilities are typically linked to exponentially small energy scales, $t_{\text{FLI-B}}$ will be large such that characteristic features of the instability are not observable for short times after the quench. In this regime, a perturbative calculation for the nonequilibrium Fermi liquid applies approximately even in the presence of a nonperturbative instability. Quenching into a FLI-phase then requires us to compare the timescales of the dynamics of the nonequilibrium Fermi liquid with that of the instability.

If the FLI-phase is nonperturbative and distinguished by a gap in the energy spectrum, as it is, for example, the superconducting phase of a Hubbard model with an attractive interaction, an excitation beyond the energy gap is essential to observe any characteristic nonequilibrium behavior. This excitation can be induced by a sudden interaction quench. As it has been shown the inserted energy causes heating effects which may wipe out all signatures of the FLI. However, the delayed onset of heating in a Fermi liquid can open a time window for the observation of the nonequilibrium dynamics even in the FLI regime.

A popular example for such behavior is the BCS instability. Recently the study of its nonequilibrium dynamics following a sudden quench in the BCS interaction has attracted a lot of attention; depending on the precise conditions of the quench, for instance oscillatory behavior in the order parameter $\Delta_{\text{BCS}}(t)$ has been found [81, 269, 270]. These studies only focus on the behavior of the (nonlocal) BCS Hamiltonian which is an effective low energy description of a superfluid. Since its dynamics is integrable a complete topological classification of the behavior of all excited states could be given [81] and no heating is observed. The actual experimental realization in optical lattices, however, only allows for a quench of the local two-particle Hubbard interaction. Aside from the emergence of an effective BCS interaction, the persistent influence of ordinary Fermi liquid behavior can be expected in such systems. Then a quench simultaneously initializes the nonequilibrium dynamics of the instability and heating effects. For a sudden quench heating dominates in agreement with [270] (since $T_{\text{eff}} \gg \Delta_{\text{BCS}} = \exp(-1/|\rho U|)$) and makes the nonequilibrium BCS dynamics

unobservable.

This is a first motivation for a more detailed analysis of the crossover between instantaneous and adiabatic switching. Starting from the question of visibility of nonequilibrium BCS behavior the aim of such an investigation would be to find a parameter regime for which the ramp-up times are short enough to excite the superfluid (the "nonadiabatic requirement") but long enough either to avoid overheating beyond the critical temperature of superfluidity at all or to allow, at least, for a window where heating effects are deferred on a sufficiently long time scale. A first analysis has been performed on the grounds of a golden rule argument for the BCS case [270]. However, the applicability of a golden rule approach is not obvious. Therefore, a more detailed analysis is required and will be outlined in the following.

Chapter 14

Keldysh approach to time dependent switching processes

The analysis of BCS systems in nonequilibrium is a first motivation for a more detailed analysis of the crossover between instantaneous and adiabatic switching. Starting from the question of visibility of nonequilibrium BCS behavior the aim of such an investigation would be to find a parameter regime for which the ramp-up times are short enough to excite the superfluid (the "nonadiabatic requirement") but long enough either to avoid overheating beyond the critical temperature of superfluidity at all or to allow, at least, for a window where heating effects are deferred on a sufficiently long time scale. A first analysis has been performed on the grounds of a golden rule argument for the BCS case [270]. However, the applicability of the golden rule is not obvious. Therefore, a more detailed analysis is desirable and will be outlined here.

14.1 Different requirements in the case of slow switching

In the case of non-instantaneous switching a nontrivial time dependence of the interaction $U(t)$ has to be considered. Firstly, this implies that the eigenbasis of the full Hamiltonian becomes time dependent and that the time evolution of eigenvectors becomes more complicated than just accumulating time dependent relative phase factors. Hence a straightforward diagonalization of the Hamiltonian and a naïve application of unitary perturbation theory is not obviously advantageous any more.

Therefore a first approach to the study of non-instantaneous switching processes is taken in the original representation of the now time-dependent Hamiltonian and a diagonalization of the Hamiltonian is not applied. Instead, perturbation theory is implemented directly following the Keldysh technique [231]. Although the systematic reduction of secular terms provided by a flow equation based implementation of unitary perturbation theory is not achieved in Keldysh perturbation theory, this approach can be more easily generalized to nontrivial switching procedures. Therefore the following calculation of the time evolution of the momentum distribution after the interaction has been continuously ramped up allows to

- (i) identify the relevance of secular terms for the time evolution of the momentum distribution function under the Hubbard Hamiltonian in second order (e.g. in 14.4.2)
- (ii) study the cross-over from instantaneous to adiabatic switching if a certain functional dependence on a crossover parameter (e.g. the slope of a linear ramp) is assumed

14.2 Second order nonequilibrium (Keldysh) perturbation theory for the Hubbard model

In the following I apply the Keldysh formalism to the Hubbard model. Firstly, the link between the momentum distribution and the Keldysh Greens function will be stated and Feynman rules will be formulated for the Hubbard interaction. Then the problem will be simplified by showing that only a single diagram contributes to a second order expansion. Finally this diagram is evaluated.

14.2.1 Momentum distribution function from Keldysh component Greens function

In the following a diagrammatic expansion for the Larkin-Ovchinnikov representation of the Keldysh Greens function $\mathbf{G}(x, t, \sigma_z, x', t', \sigma'_z)$ is used. This gives direct access to the Keldysh component Greens function G^K which represents the momentum distribution

$$N^{\text{NEQ}}(x, t) = -i \sum_{\sigma_z} G^K(x, t, \sigma_z, x, t, \sigma_z) \quad (14.1)$$





Hence a perturbative analysis of the Keldysh component Greens function G^K is sufficient. It can be implemented by mapping the Feynman rules found for the contour-ordered Greens function onto Keldysh space, which results in modified prescriptions: Firstly, propagators and vertices are 2×2 - dimensional objects in Keldysh space. Internal integration over contour times τ is mapped onto a contraction of internal Keldysh indices and integration over physical time t .

14.2.2 Nonequilibrium Feynman rules for Hubbard interaction

For the study of the two-particle fermion-fermion interaction Feynman rules can be constructed from a Fermi-Bose interaction model. This corresponds to the fundamental view of the Coulomb interaction between two charged fermions as an exchange interaction with the photon as the exchange boson.

For the on-site and instantaneous two-particle interaction in the Hubbard model this exchange is trivial. However, this approach has the advantage to avoid the explicit construction of the two-particle Keldysh vertex (which is a tensor of rank four) and it illustrates the difference of two aspects: A possibly time dependent Hubbard interaction represents nonetheless an instantaneous microscopic interaction which is not retarded in a perturbative sense but described by a trivially time dependent propagator. Yet the external time dependent variation of the interaction strength promotes the vertices to time dependent functions.

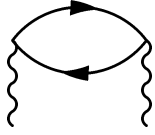
Here I will present the Feynman rules in the Larkin-Ovchinnikov representation, again following [231]. Unfortunately, in this representation the absorption vertex γ and the emission vertex $\tilde{\gamma}$ for the intermediate boson are not identical and have to be listed separately.

Fermionic propagator:		$\mathbf{G}_{\kappa\kappa'}(x, t, \sigma_z, x', t', \sigma'_z)$
Boson propagator: (on-site, instantaneous int.)		$\mathbf{D}_{\kappa\kappa'}(x, t, \sigma_z, x', t', \sigma'_z) = \delta(t - t')\delta(x - x')\delta_{\kappa}^{\kappa'}\delta_{\sigma_z}^{\sigma'_z}$
Bosonic absorption vertex:		$\gamma_{\kappa'\kappa''}^{\kappa}(t) = \begin{pmatrix} \gamma_{\kappa'\kappa''}^1 \\ \gamma_{\kappa'\kappa''}^2 \end{pmatrix} = \frac{\sqrt{U(t)}}{\sqrt{2}} \begin{pmatrix} \delta_{\kappa'\kappa''} \\ \tau_{\kappa'\kappa''}^{(1)} \end{pmatrix}$
Bosonic emission vertex:		$\tilde{\gamma}_{\kappa'\kappa''}^{\kappa}(t) = \begin{pmatrix} \tilde{\gamma}_{\kappa'\kappa''}^1 \\ \tilde{\gamma}_{\kappa'\kappa''}^2 \end{pmatrix} = \frac{\sqrt{U(t)}}{\sqrt{2}} \begin{pmatrix} \tau_{\kappa'\kappa''}^{(1)} \\ \delta_{\kappa'\kappa''} \end{pmatrix}$

The definition of the vertices includes an external time dependence of the interaction $U(t)$. Note that they are 3-tensors in Keldysh space.

Polarization operator

An example for the particular application of Feynman rules in Keldysh space and for later reference is the polarization ("bubble") operator $\mathbf{\Pi}$.



In the polarization operator both bosonic legs are truncated; in a diagrammatic pictorial representation they only serve as an illustration of the vertices. One vertex represents an absorption of an boson, the other an emission. Therefore both vertices differ according to the Feynman rules stated above.

For convenience, I introduce the shorthand notation $i = \{x_i, t_i, \sigma_i^z\}$ where i is an integer number. To avoid confusion, this shorthand notation does not extend to Keldysh indices which are generically denoted by Greek letters or by their explicit values (1 or 2).

$$\mathbf{\Pi}_{\kappa_3\kappa_2}(3, 2) = \sum_{\eta_4\eta_5\nu_4\nu_5} \tilde{\gamma}_{\eta_5\nu_5}^{\kappa_3}(t_3)\mathbf{G}_{\eta_5\eta_4}(3, 2)\mathbf{G}_{\nu_5\nu_4}(2, 3)\gamma_{\eta_4\nu_4}^{\kappa_2}(t_2) \quad (14.2)$$

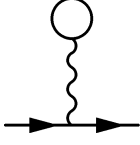
Performing the contractions of the Keldysh indices allows to represent the polarization operator as a 2×2 matrix. With (5.21) the components of the Keldysh Greens function correspond to ordinary Greens functions.

$$\mathbf{\Pi}(3, 2) = \frac{\sqrt{U(t_3)U(t_2)}}{2} \left(\begin{array}{c|c} G^R(3, 2)G^K(2, 3) & G^A(3, 2)G^R(2, 3) + G^R(3, 2)G^A(2, 3) \\ +G^K(3, 2)G^A(2, 3) & +G^K(3, 2)G^K(2, 3) \\ \hline 0 & G^A(3, 2)G^K(2, 3) + G^K(3, 2)G^R(2, 3) \end{array} \right) \quad (14.3)$$

This defines naturally the components $\Pi^R = \Pi_{11}$, $\Pi^K = \Pi_{12}$ and $\Pi^A = \Pi_{22}$. In a real-time formalism no internal integrations are performed in the polarization operator. Hence it only serves as a suitable shorthand notation for combinations of Greens functions.

14.2.3 Discussion of vanishing diagrams

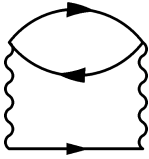
For the Hubbard model at half filling particle-hole symmetry is *imposed* for each individual spin species separately. Applying this transformation maps an attractive two-particle interaction onto a repulsive one and vice versa. Since the dynamics must be invariant under the transformation it is required that for the Greens function holds $G(U) = G(-U)$. Hence only even powers can appear in a perturbative expansion in U .



The bare Hartree diagram is cancelled by a symmetric definition of the Hubbard interaction in (3.3) and the renormalized Hartree contributions vanish to all orders because of particle-hole symmetry [171]. Fock diagrams do not contribute because the Hubbard interaction acts only between fermions of different spin.

14.2.4 The 'setting sun' diagram

There is only a single diagrammatic contribution to a second order perturbative expansion of the contour-ordered Greens function. It has been affectionately linked to both the 'setting sun' and the 'London underground'.



Although the Hubbard interaction is effective only between different spin species the degeneracy of the spin dependent Greens functions allows to suppress spin variables. The 'setting sun' diagram for the fermion propagator has no symmetry factor. Therefore the prefactor of the exponential expansion in (5.18) is not cancelled and has to be explicitly considered $1/n = 1/2$.

Hence the only relevant second order diagram to the Keldysh matrix Greens function can be written using the polarization operator

$$\mathbf{G}_{\kappa_1 \kappa_{1'}}^{(2)}(1, 1') = \frac{1}{2} \int dx_2 dx_3 dx_4 dx_5 \int dt_2 dt_3 dt_4 dt_5 \sum_{\kappa_2 \kappa_3 \kappa_4 \kappa_5 \eta_2 \eta_3 \nu_2 \nu_3} \mathbf{G}_{\kappa_1 \eta_3}(1, 3) \gamma_{\eta_3 \nu_3}^{\kappa_3}(t_3) \\ \times \mathbf{D}_{\kappa_3 \kappa_5}(3, 5) \mathbf{\Pi}_{\kappa_5 \kappa_4}(5, 4) \mathbf{D}_{\kappa_4 \kappa_2}(4, 2) \mathbf{G}_{\nu_3 \nu_2}(3, 2) \tilde{\gamma}_{\nu_2 \eta_2}^{\kappa_2}(t_2) \mathbf{G}_{\eta_2 \kappa_1}(2, 1') \quad (14.4)$$

The trivial internal integrations related to the bosonic propagator are eliminated.

$$\mathbf{G}_{\kappa_1 \kappa_{1'}}^{(2)}(1, 1') = \frac{1}{2} \int dx_2 dx_3 \int dt_2 dt_3 \sum_{\kappa_2 \kappa_3 \eta_2 \eta_3 \nu_2 \nu_3} \mathbf{G}_{\kappa_1 \eta_3}(1, 3) \gamma_{\eta_3 \nu_3}^{\kappa_3}(t_3) \\ \times \mathbf{\Pi}_{\kappa_3 \kappa_2}(3, 2) \mathbf{G}_{\nu_3 \nu_2}(3, 2) \tilde{\gamma}_{\nu_2 \eta_2}^{\kappa_2}(t_2) \mathbf{G}_{\eta_2 \kappa_1}(2, 1') \quad (14.5)$$

Performing all further contractions over Keldysh indices leads to

$$\mathbf{G}_{\kappa_1 \kappa_{1'}}^{(2)}(1, 1') = \frac{1}{2} \int dx_2 dx_3 \int dt_2 dt_3 \frac{\sqrt{U(t_3)U(t_2)}}{2} \\ \left\{ G_{\kappa_1 1}(1, 3) G^R(3, 2) \mathbf{\Pi}^R(3, 2) G_{2 \kappa_1}(2, 1') + \right. \quad (14.6a)$$

$$G_{\kappa_1 1}(1, 3) G^K(3, 2) \mathbf{\Pi}^R(3, 2) G_{1 \kappa_1}(2, 1') + \quad (14.6b)$$

$$G_{\kappa_1 2}(1, 3) G^A(3, 2) \mathbf{\Pi}^R(3, 2) G_{1 \kappa_1}(2, 1') + \quad (14.6c)$$

$$G_{\kappa_1 1}(1, 3) G^A(3, 2) \mathbf{\Pi}^A(3, 2) G_{2 \kappa_1}(2, 1') + \quad (14.6d)$$

$$G_{\kappa_1 2}(1, 3) G^R(3, 2) \mathbf{\Pi}^A(3, 2) G_{1 \kappa_1}(2, 1') + \quad (14.6e)$$

$$G_{\kappa_1 2}(1, 3) G^K(3, 2) \mathbf{\Pi}^A(3, 2) G_{2 \kappa_1}(2, 1') + \quad (14.6f)$$

$$G_{\kappa_1 1}(1, 3) G^R(3, 2) \mathbf{\Pi}^K(3, 2) G_{1 \kappa_1}(2, 1') + \quad (14.6g)$$

$$G_{\kappa_1 1}(1, 3) G^K(3, 2) \mathbf{\Pi}^K(3, 2) G_{2 \kappa_1}(2, 1') + \quad (14.6h)$$

$$G_{\kappa_1 2}(1, 3) G^A(3, 2) \mathbf{\Pi}^K(3, 2) G_{2 \kappa_1}(2, 1') \left. \right\} \quad (14.6i)$$

On the right hand side G denotes the respective Greens function of the noninteracting system. However, to avoid overnotation an appropriate superscript is suppressed.

From this the second order corrections to all components of the Keldysh matrix Greens function can be extracted by specifying the remaining indices κ_1 and κ'_1 . Here this is done only for the Keldysh component G^K which includes the information on the momentum distribution function.

14.3 Explicit calculation of the second order correction to the Keldysh component

In the following the second order correction to the Keldysh component Greens function is evaluated. With equation (14.1) this will allow to obtain a perturbative result for the momentum distribution.

14.3.1 Noninteracting Greens functions and polarization operator

This starts from an explicit representation of the building blocks of a Keldysh calculation, namely the noninteracting Greens functions and, for convenience, the first order polarization operator. Both can be expressed as a superposition of plain waves.

$$G^R(x_1, t_1, x_2, t_2) = -i\Theta(t_1 - t_2) \sum_k e^{ik(x_1 - x_2)} e^{-i\epsilon_k(t_1 - t_2)} \quad (14.7)$$

$$G^A(x_1, t_1, x_2, t_2) = i\Theta(t_2 - t_1) \sum_k e^{ik(x_1 - x_2)} e^{-i\epsilon_k(t_1 - t_2)} \quad (14.8)$$

$$G^K(x_1, t_1, x_2, t_2) = -i \sum_k (1 - 2n_k) e^{ik(x_1 - x_2)} e^{-i\epsilon_k(t_1 - t_2)} \quad (14.9)$$

Then the first order result for the polarization operator reads explicitly

$$\begin{aligned} \Pi(3, 2) = \frac{\sqrt{U(t_3)U(t_2)}}{2} \sum_{pp'} \left(\begin{array}{cc} \Theta(t_3 - t_2)(n_{p'} - n_p) & n_{p'} + n_p - 2n_{p'}n_p \\ 0 & -\Theta(t_2 - t_3)(n_{p'} - n_p) \end{array} \right) \times \\ \times e^{i(x_3 - x_2)(p - p')} e^{-i(t_3 - t_2)(\epsilon_p - \epsilon_{p'})} \quad (14.10) \end{aligned}$$

Note that for all noninteracting Greens functions and all components of the polarization operator the same exponential dependencies on space and time occur. Moreover, under the momentum sums there is a factorization of phase space factors and time dependence. This allows for a separate discussion of both aspects.

14.3.2 Keldysh component Greens function

For an explicit calculation of the Keldysh component I set $\kappa_1 = 1$ and $\kappa'_1 = 2$ in (14.6). Inserting (14.7-14.10) into (14.6) shows that due to mismatching time restrictions imposed by the involved Θ -functions terms (14.6c) and (14.6e) vanish. Hence only seven terms are

retained:

$$\mathbf{G}_{\kappa_1 \kappa_{1'}}^{(2)}(1, 1') = \frac{1}{2} \int dx_2 dx_3 \int dt_2 dt_3 \frac{\sqrt{U(t_3)U(t_2)}}{2} \left\{ \begin{aligned} & G^R(1, 3)G^R(3, 2)\Pi^R(3, 2)G^A(2, 1') + G^R(1, 3)G^A(3, 2)\Pi^A(3, 2)G^A(2, 1') + & (14.11.1+3) \\ & G^R(1, 3)G^K(3, 2)\Pi^R(3, 2)G^K(2, 1') + G^K(1, 3)G^K(3, 2)\Pi^A(3, 2)G^A(2, 1') + & (14.11.2+4) \\ & G^R(1, 3)G^R(3, 2)\Pi^K(3, 2)G^K(2, 1') + G^K(1, 3)G^A(3, 2)\Pi^K(3, 2)G^A(2, 1') & (14.11.5+7) \\ & G^R(1, 3)G^K(3, 2)\Pi^K(3, 2)G^A(2, 1') \end{aligned} \right\} \quad (14.11.6)$$

For the evaluation of these terms it is helpful to note that

- All terms share the same five momentum summations and spatial dependence. Integrating out the internal positions leads to two momentum constraints which can be written as $\delta(q_3 - q_1)\delta(p' - p - q_2 + q_1)$. While the first reduces the sum of five momentum indices to four, the second imposes momentum conservation in two-particle scattering events.
- For all summands in (14.11) it holds that their time dependence only differs because of different theta functions ($\Theta(t - t')$) present in the noninteracting Greens functions and the components of $\mathbf{\Pi}$. The oscillating time dependent phases always read $e^{it_2\Delta\epsilon}e^{-it_3\Delta\epsilon}$ with $\Delta\epsilon = \epsilon_p - \epsilon_{p'} + \epsilon_{q_2} - \epsilon_{q_1}$. Each summand is characterized by a product of a time kernel $\mathfrak{I}_i(t_1, t_{1'}, \Delta\epsilon, U)$ and a phase space factor $\mathfrak{P}_i(n_{p'}, n_p, n_{q_1}, n_{q_2})$. It is helpful to evaluate both kernels independently for each summand.

Then the Keldysh component Greens function can be written as

$$\mathbf{G}^{K(2)}(1, 1') = \frac{i}{4} \sum_{p' p q_1 q_2} e^{iq_1(x_1 - x_{1'})} e^{-i\epsilon_{q_1}(t_1 - t_{1'})} \times \sum_{i=1\dots 7} \mathfrak{I}_i(t_1, t_{1'}, \Delta\epsilon, U) \mathfrak{P}_i(n_{p'}, n_p, n_{q_1}, n_{q_2}) \delta(p' - p - q_2 + q_1) \quad (14.12)$$

Extraction of the phase space factors

From the definitions one reads easily off

$$\mathfrak{P}_1(n_{p'}, n_p, n_{q_1}, n_{q_2}) = \mathfrak{P}_3(n_{p'}, n_p, n_{q_1}, n_{q_2}) = -(n_{p'} - n_p) \quad (14.13)$$

$$\mathfrak{P}_2(n_{p'}, n_p, n_{q_1}, n_{q_2}) = \mathfrak{P}_4(n_{p'}, n_p, n_{q_1}, n_{q_2}) = (1 - 2n_{q_1})(1 - 2n_{q_2})(n_{p'} - n_p) \quad (14.14)$$

$$\mathfrak{P}_5(n_{p'}, n_p, n_{q_1}, n_{q_2}) = \mathfrak{P}_7(n_{p'}, n_p, n_{q_1}, n_{q_2}) = (1 - 2n_{q_1})[n_{p'} + n_p - 2n_{p'}n_p] \quad (14.15)$$

$$\mathfrak{P}_6(n_{p'}, n_p, n_{q_1}, n_{q_2}) = -(1 - 2n_{q_2})[n_{p'} + n_p - 2n_{p'}n_p] \quad (14.16)$$

For equal phase space factors the corresponding time kernels can be added. In the following examples it will be observed that $\mathfrak{I}_1 + \mathfrak{I}_3 = \mathfrak{I}_2 + \mathfrak{I}_4 = \mathfrak{I}_5 + \mathfrak{I}_7 = \mathfrak{I}_6$. Then all phase space factors can be summed and generate a total phase space factor which describes correctly the phase space restrictions of two-particle scattering processes for fermions.

$$\mathfrak{P} = \mathfrak{P}_1 + \mathfrak{P}_2 + \mathfrak{P}_5 + \mathfrak{P}_6 = -4[n_{q_1}n_{p'}(1 - n_p)(1 - n_{q_2}) - (1 - n_{q_1})(1 - n_{p'})n_p n_{q_2}] \quad (14.17)$$

14.3.3 Linear ramp up of a time dependent interaction

In the following I calculate the time kernels $\mathfrak{F}_i(t_1, t_{1'}, \Delta\epsilon, U)$ for a linearly switched on Hubbard interaction. The *switch-on time* or *ramp-up time* is denoted by T and the functional dependence reads

$$U(t) = U \begin{cases} 0 & t \leq 0 \\ t/T & 0 < t < T \\ 1 & t > T \end{cases}$$

In the following it is assumed that the dynamics is only discussed for times $t_1, t_{1'} > T$, i.e. after the full interaction strength has been reached. Then integrating out the internal times leads to

$$\frac{\mathfrak{F}_1 + \mathfrak{F}_3}{U^2} = \frac{\mathfrak{F}_2 + \mathfrak{F}_4}{U^2} = \frac{\mathfrak{F}_5 + \mathfrak{F}_7}{U^2} = \frac{1}{T^2} \frac{2(1 - \cos(\Delta\epsilon T))}{(\Delta\epsilon)^4} \quad (14.18)$$

$$+ \frac{1}{T} \frac{i}{(\Delta\epsilon)^3} \left[e^{i\Delta\epsilon(T-t_1)} - e^{-i\Delta\epsilon(T-t_{1'})} + e^{i\Delta\epsilon t_{1'}} - e^{i\Delta\epsilon t_1} \right]$$

$$+ \left[\frac{1}{(\Delta\epsilon)^2} + i \frac{t_{1'} - t_1}{\Delta\epsilon} \right]$$

$$\frac{\mathfrak{F}_6}{U^2} = \frac{1}{T^2} \frac{2(1 - \cos(\Delta\epsilon T))}{(\Delta\epsilon)^4} \quad (14.19)$$

$$+ \frac{1}{T} \frac{i}{(\Delta\epsilon)^3} \left[e^{i\Delta\epsilon(T-t_1)} - e^{-i\Delta\epsilon(T-t_{1'})} + e^{i\Delta\epsilon t_{1'}} - e^{-i\Delta\epsilon t_1} \right]$$

$$+ \frac{1}{(\Delta\epsilon)^2} e^{i\Delta\epsilon(t_{1'} - t_1)}$$

Obviously, this calculation has produced a secular term in (14.18) which is proportional to a time difference. This term is not important for the further analysis.

14.4 Evaluation of the momentum distribution

The evaluation of the momentum distribution is simplified by the later observation that secular terms are not important. Due to its definition only equal times $t_{1'} = t_1 = t$ contribute such that all secular terms proportional to an arbitrary power of the time difference $t_{1'} - t_1 = 0$ vanish.

$$N^{\text{NEQ}}(x, t) = -i \sum_{\sigma_z} G^K(x, t, \sigma_z, x, t, \sigma_z) \quad (\rightarrow 14.1)$$

14.4.1 Result for a linear ramping of the interaction

Fortunately, in the case of ramping up the interaction linearly in time all secular terms which appeared in the Keldysh component Greens function are with respect to the time difference $t_{1'} - t_1$ and vanish for the momentum distribution. This is a particular result which roots in the special simplicity of the number operator. Therefore, all time kernels $\mathfrak{F} = \mathfrak{F}_i$ with

$i = 1 \dots 7$ are equal.

$$\begin{aligned}
\Delta N^{\text{NEQ}}(x, t, T) &= -i \sum_{\sigma_z} G^{K(2)}(x, t, \sigma_z, x, t, \sigma_z) \\
&= -U^2 \sum_{q_1} e^{iq_1(x_1 - x_{1'})} \sum_{q_2 p' p} \delta(p' - p - q_2 + q_1) \\
&\quad \times [n_{q_1} n_{p'} (1 - n_p) (1 - n_{q_2}) - (1 - n_{q_1}) (1 - n_{p'}) n_p n_{q_2}] \\
&\quad \times \left\{ \frac{1}{T^2} \frac{2(1 - \cos(\Delta\epsilon T))}{(\Delta\epsilon)^4} + \frac{1}{(\Delta\epsilon)^2} - \right. \\
&\quad \left. - \frac{1}{T} \frac{2}{(\Delta\epsilon)^3} [\sin(\Delta\epsilon T) \cos(\Delta\epsilon t) + \sin(\Delta\epsilon t) (1 - \cos(\Delta\epsilon T))] \right\}
\end{aligned} \tag{14.20}$$

Then the momentum $q_1 \equiv k$ can be identified as the external momentum index of a momentum space representation (which can be simply read off from the Fourier sum). Expanding the right hand side with $\int dE \delta(\epsilon_p - \epsilon_{p'} + \epsilon_{q_2} - E)$ and following the lines of (9.22) the phase space integrations can be absorbed in a phase space factor which couples into a time dependent kernel via a single energy E only.

$$\begin{aligned}
\Delta N_k^{\text{NEQ}}(t, T) &= -U^2 \int dE J_k(E; n) \left\{ \frac{1}{T^2} \frac{2(1 - \cos((E - \epsilon_k)T))}{(E - \epsilon_k)^4} + \frac{1}{(E - \epsilon_k)^2} - \right. \\
&\quad \left. - \frac{2 \sin((E - \epsilon_k)T) \cos((E - \epsilon_k)t) + \sin((E - \epsilon_k)t) (1 - \cos((E - \epsilon_k)T))}{T (E - \epsilon_k)^3} \right\}
\end{aligned} \tag{14.21}$$

14.4.2 No secular terms

Note that secular terms do not arise in the result (14.21). This is an interesting observation which justifies the application of Keldysh perturbation theory for studying the time evolution of the momentum distribution in second order of U which is ramped-up linearly. It is a consequence of the combined simplicity of the number operator, the instantaneous nature of the Hubbard interaction and of the linear ramping procedure.

14.4.3 Limiting cases for the linear ramping

For the correction to the momentum distribution two limiting cases can be easily discussed.

Adiabatic limit

The adiabatic limit is given by an arbitrary slow linear increase of the interaction strength and corresponds to $T \rightarrow \infty$. As only the T -independent term $(E - \epsilon_k)^{-2}$ contributes the equilibrium result (9.22) is reproduced.

$$\lim_{T \rightarrow \infty} \Delta N_k^{\text{NEQ}}(t, T) = -U^2 \int dE J_k(E; n) \frac{1}{(E - \epsilon_k)^2} \tag{14.22}$$

This is a truly stationary state.

Quench limit

The limit of a sudden switch-on of the interaction is obtained for $T \rightarrow 0$. Replacing $1 - \cos((E - \epsilon_k)T) = 2 \sin^2((E - \epsilon_k)T/2)$ the correction to the momentum distribution shows a time dependence.

$$\lim_{T \rightarrow 0} \Delta N_k^{\text{NEQ}}(t, T) = -U^2 \int dE J_k(E; n) \frac{2(1 - \cos((E - \epsilon_k)t))}{(E - \epsilon_k)^2} \quad (14.23)$$

Again, this second order result agrees with the flow equation calculation (10.8). Consequently, all features have already been discussed before. It exhibits a nontrivial temporal evolution which describes the initial buildup of correlations as well as the decisive factor of two in the long-time limit (cf section 10.2).

14.4.4 Comparison of the Keldysh and the flow equation approach to the nonequilibrium momentum distribution function

The formal coincidence of the results obtained for the momentum distribution in a flow equation treatment (10.8) and using Keldysh perturbation theory (14.23) is obvious. This invites for some remarks:

- Firstly, it can be attributed to the particular simplicity of the number operator that the full power of unitary perturbation theory, namely a systematic reduction of the number and the relevance of secular terms in a time dependent perturbative approach, is not required for the study of the momentum distribution function in the Hubbard model. This can be seen best in the Keldysh approach to linear ramping: The time dependence of the secular terms in (14.18) and (14.19) is with respect to relative time, and the definition of the momentum distribution (14.1) picks out equal-time contributions to the Keldysh component Greens function only.
- Secondly, it is noted that the flow equation method and Keldysh perturbation theory are complementary techniques with different advantages for the study of time-dependent problems in correlated many-body systems: The flow equation treatment provides a sophisticated renormalization group approach to an interacting many-body system. It allows to identify the particularly simple renormalization flow of the interaction strength in the Hubbard Hamiltonian, which flows, in leading order, monotonously to the weak coupling limit as shown in section 9.1.2. Moreover, the flow equation analysis of the creation operator provides a direct approach to the intrinsic energetic structure of the correlated many-particle system. It allows to follow the transformation of the initial degrees of freedom, i.e. physical fermions, into new objects which are dressed with particle-hole like excitations. Simultaneously, it exhibits the singular behavior of fermions around the Fermi surface where this decay of the original particle is delayed or even prohibited. This redraws Landau's picture of quasiparticles which are stable degrees of freedom at the Fermi energy and ensures that this picture extends to the case of a Fermi liquid which has been initialized by a quench in a nonequilibrium state. Hence the flow equation renormalization treatment of the quenched Hubbard model provides the justification for viewing the transient, prethermalized state of the dynamics in the light of a Fermi liquid description. Moreover, it provides a tool to examine the limitations of this approach and restricts the careful observer to statements around the Fermi energy since only there the performed approximate solution of the flow equation can claim validity.

- The merits of Keldysh perturbation theory are different. Like any perturbative approach it assumes that the noninteracting degrees of freedom provide a good frame of reference for the description of variations caused by a weak perturbation. In this sense it assumes or naturally builds on results which can be only gained from a renormalization flow treatment. Effects like the decay of quasiparticles would be, typically, visible only in higher orders of the calculation. Hence it is plausible that a Keldysh approach should follow, and not precede, a flow equation approach. As the flow equation treatment of an interaction quench has established a quasiparticle picture and as an interaction quench represents the strongest deviation from equilibrium among all switch-on procedures, the crossover to adiabatic switching can now be safely discussed using simpler perturbative approaches like Keldysh perturbation theory. Nonetheless the caveat remains in place that all statements obtained from low order calculations are well-grounded only in a neighborhood around the Fermi energy. Fortunately, this is the most interesting energy regime of a Fermi system. For the case of linear ramping up the interaction, the particular simplicity of the internal Keldysh time integrations has been shown explicitly. The resulting expression (14.21) will allow for a more detailed analysis of the crossover behavior and the crossover scale in the switching dynamics. This will, however, be published elsewhere.

14.4.5 Kinetic energy

Here I only continue with writing down the kinetic energy which can be calculated, *cum grano salis*, by one additional integration. For arbitrary switching processes (T) and arbitrary times (t) it is given by

$$\begin{aligned}
 E_{\text{kin}}(t, T) &= \int \rho d\epsilon_k \epsilon_k \Delta N_k^{\text{NEQ}}(t, T) \\
 &= -U^2 \rho \int d\epsilon_k \epsilon_k \int dE J_k(E; n) \left\{ \frac{1}{T^2} \frac{2(1 - \cos((E - \epsilon_k)T))}{(E - \epsilon_k)^4} + \frac{1}{(E - \epsilon_k)^2} - \right. \\
 &\quad \left. - \frac{2 \sin((E - \epsilon_k)T) \cos((E - \epsilon_k)t) + \sin((E - \epsilon_k)t)(1 - \cos((E - \epsilon_k)T))}{(E - \epsilon_k)^3} \right\}
 \end{aligned} \tag{14.24}$$

This allows, in principle, to follow the buildup of the prethermalized state. Thermalization, however, cannot be seen from this 'mode-averaged' quantity.

Since $0 < E_{\text{kin}}(t, T)$ and $E_{\text{kin}}(t = 0, T) = 0$ one expects for all nontrivial switching-on procedures the kinetic energy to be a growing function at least during an initial phase of the dynamics. The same holds for the temperature $T_{\text{KE}}(t, T)$ which is related to the kinetic energy. It follows for a Fermi liquid from $T_{\text{KE}}(t, T) = E_{\text{kin}}(t, T)/C_V(T_{\text{KE}}(t, T))$ where $C_V(T_{\text{KE}}(t, T))$ is the specific heat of a Fermi liquid. The later depends linearly on the temperature.

14.4.6 Addressing nonequilibrium BCS behavior

Plotting the kinetic temperature $T_{\text{KE}}(t, T)$ as a function of t and T allows to answer the question whether nonequilibrium BCS physics can be straightforwardly observed in ramp-up experiments. The minimal requirement that heating does not exceed the critical temperature of superconductivity T_c , i.e. $T_{\text{KE}}(t, T) < T_c$, is accompanied by the demand that the ramp-up procedure must be fast enough to excite nonequilibrium behavior. This can be expressed by $T < 1/\Delta_{\text{BCS}}$ where Δ is the BCS order parameter. Moreover, in order to detect nonequilibrium behavior which is, for instance, characterized by oscillations of the order parameter on a frequency scale set by Δ_{BCS} , the onset of heating must be deferred to a time $t \gg 1/\Delta_{\text{BCS}}$.

Nonequilibrium BCS behavior already during prethermalization. If such a regime exists and is sufficiently large, nonequilibrium physics can be easily observed by ramp-up experiments, independent of the behavior of a nonequilibrium Fermi liquid. Then already the slow build-up of the prethermalized state allows for a window where heating has not yet destroyed the BCS dynamics. Since in such a 'mode averaged' argument no difference is made between the prethermalized state and the final long-term behavior a golden rule approach as presented in [270] should give an equivalent prediction.

Nonequilibrium BCS behavior observed in the prethermalized state. However, the results presented in this thesis state that for a sudden quench the initial buildup of correlations is fast and prethermalization is obtained rapidly. Yet in the subsequent transient state there is no universal temperature of the system. While the total kinetic energy has already relaxed and gives rise to the temperature $T_{\text{KE}}(t \rightarrow \infty, T)$, the momentum distribution has not smeared out and resembles a zero temperature Fermi liquid. Therefore, even if the temperature $T_{\text{KE}}(t \rightarrow \infty, T)$ exceeds the critical temperature of the BCS system, it might not destruct the observation of BCS nonequilibrium dynamics in the same way as in equilibrium. This motivates the definition of a second temperature $T_{\text{MD}}(t, T)$ based on the shape of the **m**omentum **d**istribution function. For a sudden quench it is zero throughout the prethermalized transient state and grows as the distribution function thermalizes at a later time scale. This temperature can be obtained by fitting the actual momentum distribution to a Fermi-Dirac distribution in a *small environment* around the Fermi energy. The energy difference from the Fermi energy must be much smaller than the energy scale of the temperature related to the kinetic energy, $k_B T_{\text{KE}}$, where k_B is the Boltzmann factor. Otherwise one would only badly fit to a Fermi-Dirac distribution with temperature T_{KE} . This is because due to the Pauli principle, all temperature and correlation effects of a many-body fermionic system are rather well-localized around the Fermi energy.

In the beginning of the relaxation of the transient state this second temperature measures the effect of real scattering processes since only those can change momentum mode occupations on longer time scales. Therefore the increase of this temperature beyond T_c indicates the breakdown of any BCS dynamics. This, however, can be delayed to a later time. To avoid over-emphasis it is noted that, since temperature is not a universal property in nonequilibrium, such comparisons are to be handled carefully. Instead, a full quantum solution of the nonequilibrium BCS problem as it is actually implemented in optical lattices, i.e. including all related heating effects, is a desirable goal for further research.

Chapter 15

Further prospects

The discussion of the nonequilibrium behavior of a Fermi liquid has opened a variety of further questions and possible extensions which require further numerical and analytical study. In the following chapter I will point out to some prospects for future research.

15.1 Further analysis of the quenched Fermi liquid

Some further questions about the behavior of the quenched Fermi liquid suggest themselves and barely deserve mentioning. For completeness, they are nevertheless listed here.

15.1.1 Higher correlation functions and other observables

First of all, the dynamics of higher correlation functions in the quench scenario could shed additional light on the relaxation dynamics. Since the momentum distribution is a particular simple object, the problem of secular terms was practically absent. In the flow equation approach these terms could be solved by an individual analysis of their contributions to the momentum distribution. However, it has been shown above that for the transformation of the creation operator one secular term does not vanish. This makes a consistent and reliable calculation of higher order correlation functions more difficult. Similarly, the interest in other observables which are not one- but two- or many-particle objects could exhibit further steps in the relaxation dynamics. The naïve intuition of the author motivates the speculation that a full hierarchy of transient states which become observable in even more complicated observables may arise. Such observations, however, would imply calculations in higher orders of the interaction.

15.1.2 Calculation to higher orders for the momentum distribution

Calculations to higher orders in the interaction, however, would also allow for additional observations within the already discussed observables: First of all the relaxation of the momentum distribution could be followed in detail on larger time scales. This would give insight how the effective quantum Boltzmann dynamics emerges as an approximation of the full quantum solution. Note that the full dynamics described by the quantum Boltzmann equation has not been calculated in this thesis. Instead, only its long-time behavior has been concluded from a fixed point argument. Thus the relaxation dynamics in the scattering regime has not been

studied in detail. As the quantum Boltzmann equation is a highly nonlinear differential equation possible further intermediate steps cannot be excluded *a priori* even for the momentum distribution.

Decay of quasiparticles Secondly, a calculation to higher orders could expose the dynamical character of the quasiparticles. In Landau's Fermi liquid theory quasiparticles are unstable away from the Fermi surface. In a flow equation treatment, an analogous instability could be seen in higher orders. Then the parametrization of the flowing coupling constant which relates to the quasiparticle residue, $h_k(B) \approx h_k(B=0)$ in (9.2.2), is not sufficient any more. Instead, a full decay of the quasiparticle under the flow can be expected. This implies that the weight of the original physical fermion described by $C_k^\dagger(B=0)$ is fully transferred to many-body excitations. With increasing accuracy of the flow equation treatment, i.e. with increasing order in the interaction strength, the representation of the creation operator has to be extended; incoherent dressing with two-, three- or many- particle-hole excitations has to be added stepwise to the truncated ansatz (9.9a) and more and more weight will be shifted to the multiparticle terms. The loss of a nonvanishing overlap of the physical fermion and the diagonal degrees of freedom would imply the breakdown of the quasiparticle picture. Although there is evidence for such behavior already for fourth order corrections, this will not alter the observations made for short times. How it may effect the applicability of the quantum Boltzmann equation on a long time scale (until the flow reaches its fixed point) is a challenging question of mathematical physics.

15.2 Quenches in and between other parameter regimes of the Hubbard model

Another natural extension of the analysis for the quenched Fermi liquid would be to do a similar analysis for other phases of Hubbard model. Quenches within the Mott insulator are expected to show a very different relaxation behavior since the mobility of lattice fermions is strongly restricted in this phase. As the Mott phase is characterized by strong interactions, a perturbative expansion in powers of the interaction strength is not possible. Alternative approaches are provided, for instance, by nonequilibrium DMFT. Moreover, a flow equation treatment of perturbations around the atomic limit (i.e. $U \rightarrow \infty$) is currently investigated. Most interesting, however, would be an analytical treatment of quenches between the Fermi-liquid phase and the Mott insulator phase of the Hubbard model. Then the relaxation of an initial state which differs fundamentally from the equilibrium state of the later phase could be studied. Yet for a flow equation approach, which needs to define a split-up of a Hamiltonian into a noninteracting and an interacting part, the study of the dynamical crossover from the Fermi-liquid to the Mott insulator remains a very difficult challenge.

15.3 Nonadiabatic switching processes and fully time dependent Hamiltonian

A similarly close extension of a quench problem is to model the switching process more realistically since in all experimental setups a certain non-zero ramp-up time cannot be avoided. Then a nontrivial time dependence of the interaction $U(t)$ has to be considered. Firstly, this

implies that a straightforward diagonalization of the Hamiltonian does not provide a solution of the switching problem any more since the eigenbasis of the full Hamiltonian becomes time dependent. Hence the time evolution of eigenvectors becomes more complicated than just accumulating time dependent relative phase factors. This questions the usefulness and applicability of unitary perturbation theory. While Keldysh perturbation theory can extract the behavior of the momentum distribution function under a linear ramp-up of the interaction (cf. chapter 14) the advantage of unitary perturbation theory, namely a controlled general restriction of secular terms, is lost. An extension of a flow equation implementation of unitary perturbation theory to nontrivial time dependence is currently investigated; one possible approach is to include the continuous change of the Hamiltonian eigenbasis into a redefinition of the –then time dependent– canonical generator [271]. This would allow to systematically improve time dependent perturbation theory for many-body problems.

15.4 Measuring non-adiabaticity in systems with a continuous energy spectrum

A first possible application of the mismatch of expectation values in equilibrium and nonequilibrium described in this thesis lies in the definition of a criterion for adiabatic vs. sudden switching of interactions in the case of systems with a continuous energy spectrum.

In discrete systems the minimal energy level distance of non-degenerate energy levels $(\Delta\epsilon)_{\min}$ sets a natural time scale $t_0 = 1/(\Delta\epsilon)_{\min}$ which separates fast from slow external constraints on the Hamiltonian. This can be easily seen in the light of Landau-Zener physics where excitations from the ground state are only excited if the transition velocity exceeds a threshold which is related to the energy difference between the ground state and the first excited state. However, taking the thermodynamic limit leaves, generically, a system without any gap in the energy spectrum. Hence excitations with virtually zero energy are possible and the assumption of an adiabatic procedure seems to require that all changes applied to parameters of the Hamiltonian occur on a very large, theoretically even diverging time scale.

An alternative way to differ quantitatively adiabatic from nonadiabatic scenarios can be obtained by relating adiabatic and nonadiabatic expectation values of suitable observables. Since this relation is in general different from one but bounded and can be calculated approximately in perturbation theory it could provide a useful measure. Instead of an intrinsic energy scale of the model a level of significance for a deviation of an expectation value from its equilibrium result would characterize the continuous crossover from adiabatic to sudden switching. This seems to be an appropriate approach although it requires more computational effort.

15.5 Extension to the nonequilibrium Bose-Hubbard model in more than one dimensions

Since ultracold bosonic gases can be generated experimentally much easier than ultracold fermions and many such experiments have been established around the world, zero temperature many-particle effects are best studied in bosonic systems. Therefore it would be interesting to fill the open gap in Fig. 11.4 and translate the flow equation calculation for the quenched Fermi liquid to the quench of a noninteracting Bose gas. Currently numerical approaches based on DMFT are developed to study the nonequilibrium behavior of bosonic

models. Complementing these works with observations based on the flow equation technique could contribute to elucidate possible time-scale separations there. Obviously, the expected physics is quite different: Instead of fermionic phase space restrictions due to the Pauli principle the bosonic case is characterized by the Bose-Einstein condensation (BEC), i.e. a macroscopic occupation of the ground state of the system. There is ample literature about excitations of the BEC by external forces which lead to vortex formation (see, for instance, quotations in [209] and [272]). However, quenching the Bose-Hubbard Hamiltonian may exhibit novel nonequilibrium physics. It will be characterized by a redistribution of occupation within the excited states; however, by a sudden quench even a macroscopic occupation of an excited state might be achievable. The creation of such a state has been suggested already 12 years ago by Yukalov et al. [273]. They proposed that under resonant pumping processes a Bose-Einstein condensate can be moved to an excited state and quasistationary ground state occupations can be expected. Subsequently, the properties of such non ground states of BECs were studied using the Gross-Pitaevskii equation which provides a mean-field approach to a BEC and is well-established in equilibrium. Its stationary solutions of higher energy are known as nonlinear coherent modes of a BEC; topological modes describing vortices are only one example. Prerequisites for their resonant excitation have been outlined and their temporal dynamics has been studied in detail for various initial conditions and two scale oscillations of interference patterns and interference currents have been found [274]. Some findings have been linked to dynamical critical phenomena and the dynamics of such non ground state Bose-Einstein condensates has been investigated on the grounds of the Gross-Pitaevskii equation. Dynamical transitions between mode-locked and mode-unlocked regimes have been reported [275] and an order parameter has been suggested [276]. Finally, a non ground state BEC (orbital band BEC) has been recently prepared experimentally [277]. The flow equation method would allow to perturbatively study the full quantum dynamics of the nonequilibrium relaxation behavior that follows a quantum quench of a Bose-Einstein condensate. This would allow to compare to what extent mean-field predictions based on the Gross-Pitaevskii equations are reliable beyond the ground state. Although only a limited number of initial states can be addressed by this approach, there is the hope that, again, different time scales in the relaxation of the condensate could be specified.

Chapter 16

Conclusions

In this thesis I have contributed to the question how nonequilibrium initial conditions and correlations jointly influence the dynamics of quantum many-particle systems. This problem was addressed by a real-time analysis of the quantum dynamics of suitable model systems which have been subjected to a quantum quench, i.e. to a sudden switching-on of an additional interaction term in the Hamiltonian. This implies that for all times after the quench the full quantum evolution of all observables is generated by a time-independent Hamiltonian. In consequence, its eigenbasis constitutes the preferred frame of reference for all investigations and diagonalization techniques have been applied. Since throughout this thesis most observations are grounded on perturbative arguments the general assumption is that the strength of the switched-on interaction is not too strong.

The main findings of this thesis are concluded from a formal but rather general observation made for the scenario of a quantum quench: the discovery of a characteristic mismatch of two quantum mechanical expectation values of particular observables. The first expectation value is evaluated in the initial state of the nonequilibrium problem (which is the ground state of the noninteracting part of the Hamiltonian) and then time-averaged with respect to long times; the second one is evaluated in the (static) equilibrium ground state of the full Hamiltonian.

Throughout this work I have illustrated the origin and the character of this mismatch in different systems, starting with the pedagogical example of the one-particle squeezed oscillator. There an exact solution can be compared with a perturbative calculation to second order in the interaction. Both approaches describe the mismatch of the nonequilibrium and equilibrium expectation values of the occupation but provide different numerical values for their ratio m . This indicates that already a perturbative calculation captures essential nonequilibrium physics. In a perturbative treatment of the squeezed oscillator to leading order, the ratio of these nonequilibrium and equilibrium expectation values acquires a universal value of $m = 2$.

For one-particle systems the existence and the perturbative value of this mismatch can be proven on the grounds of second order perturbation theory. For pedagogical reasons the proof has been formulated in two versions. It illustrates the main requirement, namely the vanishing of the commutator of the considered observable and the noninteracting part of the Hamiltonian. This is the reason why perturbation theory in Hamiltonian eigenstates is sufficient to describe the observed mismatch. Moreover, the proof rests on a dephasing argument. This requires to restrict to systems which are nondegenerate in energy. Moreover, this feature of the proof prevents its straightforward generalization to many-body systems.

Although the characteristic mismatch has already appeared in previous calculations for integrable many-particle quantum systems [93], its has not been recognized as a widespread structure and its relevance for the nonequilibrium dynamics of nonintegrable (and, in particular, almost integrable) systems could not be learned from these models. However, seen in the light of my own results for the quenched Fermi liquid and considering related results of others I have conjectured on a corresponding (but not fully equivalent) statement for many-particle systems. Contrary to the theorem for the one-particle case this conjecture requires the existence of additional constraints on the dynamics of the many-body system.

This requirement is met in the case of a quenched Fermi liquid. The real-time analysis of its dynamics constitutes the main part of this thesis. For this purpose the Fermi liquid is studied in a microscopic model, namely the Hubbard model at zero temperature and in more than one dimension. In order to avoid complications by possible phase transitions, only weak interaction quenches within the Fermi liquid regime of this model are discussed. The diagonalization of the Hubbard Hamiltonian is achieved by means of the flow equation method following Wegner. It represents a renormalization technique of its own kind which requires the simultaneous diagonalization of the Hamiltonian and the transformation of all observables into the (approximate) eigenbasis of the Hamiltonian. Contrary to the common numerical solution of the differential flow equations, in this thesis an approximate analytical solution has been used which reproduces perturbation theory up to second order in the interaction.

To leading order, the renormalization flow of Hamiltonian parameters, i.e. of the interaction (which flows monotonously to weak coupling) and of the one-particle energies (no flow) turns out to be unimportant. Yet the transformation of the creation operator exhibits a continuous change from a description based on noninteracting particles to a many-particle representation; there the original particle appears to be dressed by correlation-induced electron-hole pairs which is characteristic for an interacting many-fermion system. Its careful analysis shows that this change is not complete around the Fermi surface; instead, an overlap is retained between the noninteracting fermions and the degrees of freedom of a diagonal representation. This overlap represents a quasiparticle residue and therefore Landau's quasiparticle picture can be extended to a Fermi liquid for the considered nonequilibrium initial condition. The establishment of a quasiparticle description is essential for the further analysis of the evolution of the quenched Fermi liquid since it allows to discuss a residual dynamics of quasiparticles. This is done by a quantum Boltzmann equation which is the kinetic equation for the quasiparticle momentum distribution; it describes its evolution from a nonequilibrium distribution towards a Fermi-Dirac distribution at an appropriate effective temperature.

However, the Boltzmann equation is not applied directly to the initial state. Instead, the first phase of the dynamics is analyzed by a perturbative implementation of the full quantum mechanical time evolution. Since it is second order in the interaction, it gives reliable results on a corresponding time scale proportional to the inverse of the squared interaction strength. Initially, one finds a rapid build-up of a correlated many-particle description due to dephasing. Afterwards, the evolution of the momentum distribution almost freezes in a transient state which can be long-lasting for weak interactions. This transient state exhibits prethermalization of the total kinetic energy, i.e. the total kinetic energy has already relaxed to its final value. This, however, does not imply heating of the momentum distribution: due to the persistence of a Fermi surface discontinuity the later still resembles a zero temperature Fermi liquid throughout the transient regime. Such a disagreement of temperatures derived from expectation values of different observables is known to be a characteristic trait of many systems in nonequilibrium. Simultaneously, one observes the characteristic mismatch of nonequilib-

rium and equilibrium expectation values in the transient state. This is most prominently seen in the correlation-induced reduction of the quasiparticle residue. For the perturbative solution of the flow equations the value of their ratio is, again, $m = 2$.

Phase space restrictions due to the Pauli principle together with the translational invariance of the Hubbard model have been identified as the origin of this delayed equilibration of the momentum distribution. They form a bottleneck to the further relaxation by scattering events and are responsible for the clear separation of a second time scale from the one related to initial dephasing. Thus a window is opened for the observation of the prethermalized transient state.

The second time scale can be deduced from forth order corrections to the second order result which mirror the structure of the scattering integral of a quantum Boltzmann equation. Equally, one can map the momentum distribution in the prethermalized state to a quasiparticle representation and use it as an 'initial' condition for the later Boltzmann dynamics. From a linearization of the scattering integral one equally reads off that this second stage of the dynamics occurs on a time scale proportional to the inverse forth power of the interaction. If one assumes that a quasiparticle picture can be retained until the Boltzmann dynamics has been accomplished (which holds trivially only in an arbitrarily close environment around the Fermi surface) thermalization of the quenched Fermi liquid can be predicted.

These findings for the dynamics of a quenched Fermi liquid agree well with previously known experimental results on the relaxation behavior of electron gases in semiconductors or metals. Yet to the knowledge of the author it has not been before this work that a contiguous analytical calculation of the dynamics of the momentum distribution function on the grounds of its quantum mechanical time evolution has been given from the initial dephasing, throughout the quasi-stationary regime of a prethermalized state until the onset of thermalization.

In a final outlook the calculation of the momentum distribution has been repeated using Keldysh perturbation theory. On the one hand, this has exposed the particular simplicity of the momentum distribution function in the Hubbard model for which even a direct second order perturbative (Keldysh) calculation of its quantum mechanical time evolution would not suffer from the otherwise widespread problem of secular terms¹.

On the other hand, Keldysh perturbation theory simplifies the analysis of the crossover from instantaneous to adiabatic switching processes. Since nonvanishing ramp-up times are unavoidable in many experiments, a proper derivation of the crossover scale is desirable. For instance, recent proposals suggest to study the nonequilibrium dynamics of BCS systems in ultracold atomic gases. This leads to the question if and how a sufficiently strong excitation can be reached without heating up the system beyond the critical temperature of a BCS system. The calculations and findings presented in this thesis may contribute to answer this question more rigorously. Moreover they may stimulate the creative mind to think about other sensitive nonequilibrium many-particle phenomena which can be excited by a quantum quench and may become observable (only) within the time window spanned by the prethermalized transient state of a Fermi liquid.

¹Nonetheless, a trustworthy analysis of the extension of Landau's quasiparticle picture to nonequilibrium initial conditions (which are not captured by minimizing an energy functional) requires more insight than that provided by the second order Keldysh perturbation approach presented here.

Part IV
Appendix

Appendix A

Brief dictionary of definitions, formulae and commutators

In the following appendix a little dictionary of helpful relations is given which are useful when performing flow equation calculations. First of all, common textbook relations are reprinted and definitions are repeated. Then some commutators of arbitrary operators are presented.

List of definitions

Energy difference

$$\Delta\epsilon_{1'12'2}(B) = \epsilon_{1'}(B) - \epsilon_1(B) + \epsilon_{2'}(B) - \epsilon_2(B)$$

Fermionic phase space factors

$$\begin{aligned} Q_{122'} &= n_1 n_2 (1 - n_{2'}) + (1 - n_1)(1 - n_2) n_{2'} \\ Q_{122'}^{(1)} &= n_1 n_2 (1 - n_{2'}) \\ Q_{122'}^{(2)} &= (1 - n_1)(1 - n_2) n_{2'} \end{aligned}$$

All three definitions of phase space factors are symmetric under the interchange of the first two indices (see 9.2.2). For the Fermi liquid, the momentum dependence is summed up, leading to the integrated phase space factor $I_k(E)$ which can be evaluated easily for zero temperature ($T = 0$)

$$I_k(E) := \sum_{1'2'1} Q_{1'2'1} \delta(E - \epsilon_{1'} - \epsilon_{2'} + \epsilon_1) \delta_{1+k}^{1'+2'} \stackrel{T=0}{=} \rho^2(E - \epsilon_F)^2$$

A variant of this is the phase space factor of the scattering integral in a quantum Boltzmann equation

$$J_k(E; n) = \sum_{1'2'1} \delta_{1+k}^{1'+2'} \delta(\epsilon_{1'} + \epsilon_{2'} - \epsilon_1 - E) [n_k n_1 (1 - n_{1'}) (1 - n_{2'}) - (1 - n_k)(1 - n_2) n_{1'} n_{2'}]$$

Formulae

Baker-Hausdorff-relation:

For operators A and B holds that

$$e^A B e^{-A} = B + [A, B] + \frac{1}{2} [A, [A, B]] + \dots = \sum_{n=0}^{\infty} \frac{1}{n!} [A, [A, [A, \dots B]]] \quad (\text{A.1})$$

Note that if the right hand side becomes cyclic (i.e. $[A, B] = cB$) it can be explicitly summed up, leading to an exponential.

General relations between commutators of operators

Let A, B, C, D, E, F, G, H be arbitrary operators, i.e. elements of a common operator space. Then the following relations for the commutator ($[\cdot, \cdot]$) and anti-commutator ($\{\cdot, \cdot\}$) hold:

Decomposition of commutators into commutators

$$\begin{aligned} [AB, C] &= A[B, C] + [A, C]B \\ [AB, CD] &= AC[B, D] + A[B, C]D + C[A, D]B + [A, C]DB \end{aligned}$$

Decomposition of commutators into anticommutators

$$\begin{aligned} [AB, C] &= A\{B, C\} - \{A, C\}B \\ [AB, CD] &= -AC\{B, D\} + A\{B, C\}D - C\{A, D\}B + \{A, C\}DB \\ [ABCD, EF] &= ABEC\{D, F\} - ABE\{C, F\}D + \\ &\quad ABC\{D, E\}F - AB\{C, E\}DF + \\ &\quad EA\{B, F\}CD - E\{A, F\}BCD + \\ &\quad A\{B, E\}FCD - \{A, E\}BFCD \end{aligned}$$

$$\begin{aligned} [ABCD, EFGH] &= ABEFC\{D, G\}H - ABEFG\{C, H\}D + \\ &\quad ABEF\{C, G\}HD - ABEFCG\{D, H\} + \\ &\quad ABC\{D, E\}FGH - ABE\{C, F\}DGH + \\ &\quad AB\{C, E\}FDGH - ABCE\{D, F\}GH + \\ &\quad EFA\{B, G\}HCD - EFG\{A, H\}BCD + \\ &\quad EF\{A, G\}HBCD - EFAG\{B, H\}CD + \\ &\quad A\{B, E\}FGHCD - E\{A, F\}BGHCD + \\ &\quad \{A, E\}FBGHCD - AE\{B, F\}GHCD \end{aligned}$$

List of Figures

1.1	Energy level diagram for the quench scenario	10
4.1	Sketch of time scales in suddenly perturbed many-electron systems	46
4.2	Collapse and revival of quenched ultracold bosons on an optical lattice Experimental observations made by M. Greiner [214]	50
5.1	Canonical perturbation theory for the weakly anharmonic oscillator	61
5.2	Scheme of the transformations applied in unitary perturbation theory	63
6.1	Ratio between the interaction-induced variations of the equilibrium and nonequilibrium expectation values for the squeezed oscillator	72
10.1	Decay of a fermionic particle \mathcal{C}_k in nonequilibrium with time.	98
10.2	Time evolution of the momentum distribution after a quench of a Fermi liquid	101
10.3	Energy relations for the quenched Fermi liquid	106
11.1	Available nonequilibrium solutions for different types of the Hubbard model .	116
11.2	Numerical confirmation of prethermalization Results provided by M. Kollar [259]	119

List of Tables

2.1	Properties of a Fermi liquid	35
9.1	Discussion of phase space factors at zero temperature	94

Deutsche Zusammenfassung

Die Untersuchung des Zusammenspiels von wechselwirkungsinduzierten Korrelationen und Nichtgleichgewichts-Anfangsbedingungen in Vielteilchensystemen ist Gegenstand aktueller Forschung. Neue experimentelle Techniken ermöglichen die hochpräzise Manipulation von Systemparametern, wodurch deren Nichtgleichgewichtsverhalten zugänglich wird. Beispiele sind u.a. Transportmessungen in Halbleiter-Heterostrukturen, Pump-probe-Experimente, in denen die zeitliche Relaxation angeregter Moleküle oder Festkörper verfolgt wird, oder Versuche an ultrakalten Atomgasen in optischen Gittern. In all diesen Fällen können die Nichtgleichgewichtseigenschaften einer Fermiflüssigkeit relevant für eine korrekte Beschreibung sein. Ein erster Zugang zu diesen ist der wesentliche Inhalt dieser Dissertation.

Am Anfang dieser Arbeit steht ein Überblick über wichtige Nichtgleichgewichtsphänomene und beispielhafte Experimente sowie die Formulierung zentraler Fragen und Konzepte neben einer kurze Einführung u.a. in Landau's Fermiflüssigkeitstheorie, das Hubbard-Modell sowie die Flussgleichungsrenormierungsmethode nach Wegner.

Die zentrale Beobachtung dieser Dissertation, eine charakteristische Verschiedenheit von quantenmechanischen Erwartungswerten im Gleichgewicht und im Nichtgleichgewicht, wird zuerst am Beispiel des gequetschten Oszillators verdeutlicht. Dabei zeigt ein Vergleich der exakten Lösung mit einer störungstheoretischen, dass diese Verschiedenheit physikalischer Natur und in Störungstheorie beobachtbar ist. Anschliessend werden diese Beobachtungen auf eine größere Klasse von Einteilchenmodellen verallgemeinert.

Daraufhin wird das Nichtgleichgewichtsverhalten einer Fermiflüssigkeit, eines Vielteilchen-Quantensystems, untersucht, indem man einem freien Fermigas der Temperatur $T = 0$ instantan eine Zweiteilchenwechselwirkung aufschaltet und dessen Relaxation verfolgt. Als mikroskopisches Modell dazu dient das Hubbardmodell in mehr als einer Dimension. Eine unitäre Flussgleichungstransformation diagonalisiert dessen Hamiltonoperator näherungsweise und bildet alle Observablen auf neue Operatoren in der Diagonalebasis ab. Dort können deren Heisenberg-Bewegungsgleichungen leicht gelöst werden. Die Diskussion der zeitabhängigen Impulsverteilungsfunktion und der kinetischen Energie enthüllt einen dreistufigen Relaxationsprozess: Dephasierungsprozesse bedingen einen schnellen Korrelationsaufbau, führen zur Etablierung eines Quasiteilchenbildes und münden ein in einen quasistationären Zwischenzustand. Letzterer zeigt Präthermalisierung in der kinetischen Energie, die bereits zu ihrem Endwert relaxiert ist. Gleiches gilt jedoch nicht für die Impulsverteilungsfunktion. Letztere ähnelt nach wie vor der einer Fermiflüssigkeit bei $T = 0$, das Quasiteilchenresiduum zeigt die beschriebene charakteristische Verschiedenheit seines Wertes im Nichtgleichgewicht vom korrespondierenden Wert im Gleichgewicht. Die Ursache dieser verzögerten Relaxation der Impulsverteilungsfunktion liegt in der Translationsinvarianz des Hubbardmodells und dem Pauli-Prinzip für Fermionen, die gemeinsam den Phasenraum für Quasiteilchenstreuung beschränken. Aufgrund der Nichtgleichgewichtsnatur des Zwischenzustandes gilt diese Beschränkung jedoch nicht exakt und erlaubt eine weitere Relaxation, die jedoch erst auf einer längeren Zeitskala wirksam wird. Diese verzögerte Thermalisierung wird mittels einer Quanten-Boltzmann-Gleichung beschrieben, aus welcher auch die zugehörige Zeitskala folgt.

Diese Ergebnisse und ähnliche Beobachtungen in anderen Arbeiten rechtfertigen eine Vermutung über das generische Verhalten von Vielteilchen-Quantensystemen nach plötzlichen Anschaltvorgängen, die Beschreibung des Übergangs von instantanen zu adiabatischen Schaltvorgängen wird in einem Ausblick auf Grundlage einer Keldysh - Störungsrechnung skizziert.

Acknowledgements

At the end of this thesis it is my great pleasure to acknowledge manifold support by many people and various institutions.

- I acknowledge the financial assistance from public funds of the Free State of Bavaria, the Federal Republic of Germany and, to a lesser extend, from moneys previously made available to the European Union. They were provided partly indirectly via a scholarship of the Studienstiftung des Deutschen Volkes, partly by employment under third-party grants of the Deutsche Forschungsgemeinschaft under the schemes SFB 484 in the University of Augsburg, SFB 631 and SFB TR 12 in the Ludwig-Maximilians-University Munich (LMU), and partly by employment as regular scientific staff at the LMU.
- I acknowledge additional travel exhibitions by the Arnold-Sommerfeld-Center for Theoretical Physics (ASC) and the Center for Nanosciences (CeNS) in the University of Munich, the Nanosystems Initiative Munich (NIM) funded by the Excellence Initiative of the Federal Government of Germany, and the European Science Foundation under the scheme INSTANS. I acknowledge access to activities provided by the Internationales Doktorandenkolleg NanoBioTechnology (IDK-NBT). Moreover, I acknowledge the generous and repeated hospitality of the Max-Planck-Institute for the Physics of Complex Systems in Dresden and of the Carl-Friedrich-von-Siemens Stiftung, Munich.
- I am deeply indebted to my PhD advisor Prof. Dr. Stefan Kehrein. His experience, professional advice and teaching laid the foundations of this work, his continued interest in my progress provided me with an abundant source of motivation, his tremendous efforts, endless patience, his trust as well as his humor were my permanent encouragement. I am very grateful for his willingness to share many aspects of his scientific life on a common way of teaching and learning. Dir, lieber Stefan, für Deine stete Hilfe und die Aufmerksamkeit eines stets wohlwollenden Doktorvaters ein herzliches 'Vergelt's Gott!'
- I acknowledge many valuable discussions with Florian Marquardt, Clemens Neuenhahn, Markus Kollar, Martin Eckstein, Thomas Barthel, and many others.
- I am thankful for the company and assistance by my current and former office mates Peter Fritsch, Hamed Saberi, Ferdinand Helmer, and Georg Heinrich, for the computer support provided by Ralph Simmler and his team, for the services of the secretaries Sylvia Kaiser and Stéphane Schoonover, the caring presence of Theresa Hecht, and for the good company of all members of the Chair for Theoretical Condensed Matter.
- I am deeply grateful for all the love, support and encouragement which I have received from my parents throughout the years, and I am thankful for the guidance and orientation provided by Hanspeter Beißer, P. Herrmann Breulmann and P. Dominik Terstriep.

Bibliography

- [1] M. Ivanchenko, O. Kanakov, V. Shalfeev and S. Flach. *Discrete breathers in transient processes and thermal equilibrium*. Physica D **198**, 120–135 (2004).
- [2] M. Cross and P. Hohenberg. *Pattern formation outside of equilibrium*. Rev. Mod. Phys. **65**, 851 (1993).
- [3] S. Lepri, R. Livi and A. Politi. *Thermal conduction in classical low-dimensional lattices*. Physics Reports **377**, 1 (2003).
- [4] K. Saito, S. Takesue and S. Miyashita. *Thermal conduction in a quantum system*. Phys. Rev. E **54**, 2404 (1996).
- [5] C. Giardinà and J. Kurchan. *The Fourier law in a momentum-conserving chain*. J. Stat. Mech. P05009 (2005).
- [6] J. C. Dyre. *The glass transition and elastic models of glass-forming*. Rev. Mod. Phys. **78**, 953 (2006).
- [7] L. Boltzmann. *Vorlesungen über Gastheorie I/II*. Ambrosius Barth, Leipzig (1896).
- [8] N. W. Ashcroft and N. D. Mermin. *Solid State Physics*. Thomson Learning (1976).
- [9] B. Derrida. *An exactly soluble non-equilibrium system: The asymmetric simple exclusion process*. Phys. Rep. **301**, 65 (1998).
- [10] Z. Rieder, J. L. Lebowitz and E. Lieb. *Properties of a harmonic crystal in a stationary nonequilibrium state*. J. Math. Phys. **8**, 1073 (1967).
- [11] M. Michel. *Nonequilibrium Aspects of Quantum Thermodynamics*. PhD thesis, Universität Stuttgart (2006).
- [12] J. M. Luttinger. *Theory of Thermal Transport Coefficients*. Phys. Rev. **135(6A)**, A1505 (1964).
- [13] H. Nyquist. *Thermal Agitation of Electric Charge in Conductors*. Phys. Rev. **32**, 110 (1928).
- [14] H. B. Callen and T. A. Welton. *Irreversibility and Generalized Noise*. Phys. Rev. **83**, 34 (1951).
- [15] J. Jäckle. *Einführung in die Transporttheorie*. Vieweg (1978).

- [16] P. W. Anderson. *Concepts in Solids: Lectures on the Theory of Solids*. Addison-Wesley (1992).
- [17] A. V. Ponomarev, J. Madronero, A. R. Kolovsky and A. Buchleitner. *Atomic Current across an Optical Lattice*. Phys. Rev. Lett. **96**, 050404 (2006).
- [18] K. Binder and A. P. Young. *Spin glasses: Experimental facts, theoretical concepts, and open questions*. Phys. Rev. Mod. **58**, 801 (1986).
- [19] M. Mezard and G. Parisi. *Statistical Physics of Structural Glasses*. cond-mat/0002128 (2000).
- [20] J. Kurchan. *In and out of equilibrium*. Nature (London) **433**, 222 (2005).
- [21] A. Weiss, V. Hill and T. G. Abel. *The First Stars. Proceedings of the MPA/ESO Workshop Held at Garching, Germany, 4-6 August 1999 (ESO Astrophysics Symposia)*. Springer (2000).
- [22] V. Eisler and I. Peschel. *Evolution of entanglement after a local quench*. J. Stat. Mech. P06005 (2007).
- [23] P. Nozières and C. T. de Dominicis. *Singularities in the X-Ray Absorption and Emission of Metals. III. One-Body Theory Exact Solution*. Phys. Rev. **178**, 1097 (1969).
- [24] G. D. Mahan. *Excitons in Metals: Infinite Hole Mass*. Phys. Rev. **163**, 612 (1967).
- [25] B. Roulet, J. Gavoret and P. Nozières. *Singularities in the X-Ray Absorption and Emission of Metals. I. First-Order Parquet Calculation*. Phys. Rev. **178**, 1072 (1969).
- [26] P. Nozières, J. Gavoret and B. Roulet. *Singularities in the X-Ray Absorption and Emission of Metals. II. Self-Consistent Treatment of Divergences*. Phys. Rev. **178**, 1084 (1969).
- [27] K. Ohtaka and Y. Tanabe. *Theory of the soft-x-ray edge problem in simple metals: historical survey and recent developments*. Rev. Mod. Phys **62**, 929 (1990).
- [28] P. W. Anderson. *Infrared Catastrophe in Fermi Gases with Local Scattering Potentials*. Phys. Rev. Lett. **18**, 1049 (1967).
- [29] G. D. Mahan. *Many-Particle Physics*. Plenum Press, New York (1990).
- [30] K. D. Schotte and U. Schotte. *Tomonaga's Model and the Threshold Singularity of X-Ray Spectra of Metals*. Phys. Rev. **182**, 479 (1969).
- [31] M. Combescot and B. Roulet. *Absorption-edge singularities for two coupled nonequilibrium Fermi seas*. Phys. Rev. B **61**, 7609 (2000).
- [32] B. Muzykantskii, N. d Ambrumenil and B. Braunecker. *Fermi - Edge Singularity in a Nonequilibrium System*. Phys. Rev. Lett. **91**, 266602 (2003).
- [33] B. Braunecker. *On Solutions of the nonequilibrium x-ray edge problem*. Phys. Rev. B **68**, 153104 (2003).

- [34] M. Hentschel, D. Ullmo and H. U. Baranger. *Fermi-Edge Singularities in the Mesoscopic X-Ray Edge Problem*. Phys. Rev. Lett. **93**, 176807 (2004).
- [35] H. Frahm, C. v. Zobeltitz, N. Maire and R. J. Haug. *Fermi-edge singularities in transport through quantum dots*. Phys. Rev. B **74**, 035329 (2006).
- [36] M. Hentschel, G. Roeder and D. Ullmo. *Many - body effects in the mesoscopic x-ray edge problem*. Prog. Theor. Phys. Suppl. **166**, 143 (2007).
- [37] E. Barouch, B. M. McCoy and M. Dresden. *Statistical Mechanics of the XY Model. I*. Phys. Rev. A **2**, 1075 (1970).
- [38] L. F. Cugliandolo. *Quantum Aging in Mean-Field Models*. Phys. Rev. Lett. **80**, 4979 (1998).
- [39] G. M. Schütz and S. Trimper. *Relaxation and aging in quantum spin systems*. Europhys. Lett. **47**, 164 (1999).
- [40] F. Igloi and H. Rieger. *Long-Range Correlations in the Nonequilibrium Quantum Relaxation of a Spin Chain*. Phys. Rev. Lett. **85**, 3233 (2000).
- [41] L. Amico and A. Osterloh. *Out of equilibrium correlation functions of quantum anisotropic XY model: one-particle excitations*. J. Phys. **37**, 291 (2004).
- [42] K. Sengupta, S. Powell and S. Sachdev. *Quench dynamics across quantum critical points*. Phys. Rev. A **69**, 053616 (2004).
- [43] P. Calabrese and J. Cardy. *Evolution of entanglement entropy in one-dimensional systems*. J. Stat. Mech. 04010 (2005).
- [44] A. Das, K. Sengupta, D. Sen and B. K. Chakrabarti. *Infinite-range Ising ferromagnet in a time-dependent transverse magnetic field: Quench and ac dynamics near the quantum critical point*. Phys. Rev. B **74**, 144423 (2006).
- [45] P. Barmettler, M. Punk, V. Gritsev, E. Demler and E. Altman. *Relaxation of antiferromagnetic order in spin-1/2 chains following a quantum quench*. Phys. Rev. Lett. **102**, 130603 (2009).
- [46] W. Zurek, U. Dorner and P. Zoller. *Dynamics of a Quantum Phase Transition*. Phys. Rev. Lett. **95**, 105701 (2005).
- [47] J. Dziarmaga. *Dynamics of a Quantum Phase Transition: Exact Solution of the Quantum Ising Model*. Phys. Rev. Lett. **95**, 245701 (2005).
- [48] R. W. Cherg and L. S. Levitov. *Entropy and Correlation Functions of a Driven Quantum Spin Chain*. Phys. Rev. A **73**, 043614 (2006).
- [49] P. Calabrese and J. Cardy. *Quantum quenches in extended systems*. J. Stat. Mech. 06008 (2007).
- [50] C. Bäuerle, Y. M. Bunkov, S. N. Fisher, H. Godfrin and G. R. Pickett. *Laboratory simulation of cosmic string formation in the early Universe using superfluid ^3He* . Nature (London) **382**, 332 (1995).

- [51] V. M. H. Ruutu, V. B. Eltsov, A. J. Gill, T. W. B. Kibble, M. Krusius, Y. G. Makhlin, B. Placais, G. E. Volovik and W. Xu. *Vortex formation in neutron-irradiated superfluid ^3He as an analogue of cosmical defect formation*. Nature(London) **382**, 334 (1995).
- [52] M. E. Dodd, P. C. Hendry, N. S. Lawson, P. V. E. McClintock and C. D. H. Williams. *Nonappearance of Vortices in Fast Mechanical Expansions of Liquid ^4He through the Lambda Transition*. Phys. Rev. Lett. **81**, 3703 (1998).
- [53] P. C. Hendry, N. S. Lawson, R. A. M. Lee, P. V. E. McClintock and C. D. H. Williams. *Generation of defects in superfluid ^4He as an analogue of the formation of cosmic strings*. Nature(London) **368**, 315 (1998).
- [54] I. Chang, R. Durrer, N. Turok and B. Yurke. *Cosmology in the Laboratory: Defect Dynamics in Liquid Crystals*. Science **251**, 1336 (1991).
- [55] M. J. Bowick, L. Chandar, E. A. Schiff and A. M. Srivastava. *The Cosmological Kibble Mechanism in the Laboratory: String Formation in Liquid Crystals*. Science **263**, 943 (1994).
- [56] J. Dziarmaga, A. Smerzi, W. H. Zurek and A. R. Bishop. *Dynamics of Quantum Phase Transition in an Array of Josephson Junctions*. Phys. Rev. Lett. **88**, 167001 (2002).
- [57] A. Maniv, E. Polturak and G. Koren. *Observation of Magnetic Flux Generated Spontaneously During a Rapid Quench of Superconducting Films*. Phys. Rev. Lett. **91**, 197001 (2003).
- [58] J. R. Anglin and W. H. Zurek. *Vortices in the Wake of Rapid Bose-Einstein Condensation*. Phys. Rev. Lett. **83**, 1707 (1998).
- [59] C. N. Weiler, T. W. Neely, D. R. Scherer, A. S. Bradley, M. J. Davis and B. P. Anderson. *Spontaneous vortices in the formation of Bose-Einstein condensates*. Nature (London) **455**, 948 (2008).
- [60] T. W. B. Kibble. *Topology of cosmic domains and strings*. J. Phys. A: Math. Gen. **9**, 1387 (1976).
- [61] W. H. Zurek. *Cosmological experiments in superfluid helium?*. Nature (London) **317**, 505 (1985).
- [62] L. D. Landau and E. M. Lifschitz. *Lehrbuch der theoretischen Physik*. Harri Deutsch (1997).
- [63] W. H. Zurek. *Cosmological experiments in condensed matter systems*. Phys. Rep. **276**, 5177 (1996).
- [64] L. Landau. *Zur Theorie der Energieübertragung. II*. D. Phys. Z. **2**, 46 (1932).
- [65] C. Zener. *Non-Adiabatic Crossing of Energy Levels*. Proc. R. Soc. A **137**, 696 (1932).
- [66] E. C. G. Stückelberg. *Theorie der unelastischen Stösse zwischen Atomen*. Helv. Phys. Acta **5**, 369 (1932).

- [67] W. Lichten. *Quantum Mechanics of Double Perturbation: Application of the Zeeman Effect of Metastable Hydrogen Molecules*. Phys. Rev. A **3**, 594 (1970).
- [68] J. R. Rubbmark, M. M. Kash, M. G. Littman and D. Kleppner. *Dynamical effects at avoided level crossings: A study of the Landau-Zener effect using Rydberg atoms*. Phys. Rev. A **23**, 3107 (1981).
- [69] Y. Abe and J. Y. Park. *Evidence for nuclear Landau-Zener effect: New resonance mechanism in heavy/ion reactions*. Phys. Rev. C **28**, 2316 (1983).
- [70] H. Nakamura. *Theoretical Studies of Chemical Dynamics: Overview of Some Fundamental Mechanisms*. Annu. Rev. Phys. Chem. **48**, 299 (1997).
- [71] E. E. Nikitin. *Nonadiabatic Transitions: What We Learned from Old Masters and How Much We Owe Them*. Annu. Rev. Phys. Chem. **50**, 1 (1999).
- [72] Y. Kayanuma and S. Fukuchi. *On the probability of non-adiabatic transitions in multiple level crossings*. J. Phys. B: At. Mol. Phys. **18**, 4089 (1985).
- [73] S. Brundobler and V. Elser. *S-matrix for generalized Landau-Zener problem*. I. Phys. A: Math. Gen. **26**, 1211 (1993).
- [74] W. Wernsdorfer and R. Sessoli. *Quantum Phase Interference and Parity Effects in Magnetic Molecular Clusters*. Science **284**, 133 (1999).
- [75] J. Keeling and V. Gurarie. *Collapse and Revivals of the Photon Field in a Landau-Zener Process*. Phys. Rev. Lett. **101**, 033001 (2008).
- [76] A. Altland, V. Gurarie, T. Kriecherbauer and A. Polkovnikov. *Non-adiabaticity and large fluctuations in a many particle Landau Zener problem*. Phys. Rev. A **79**, 042703 (2008).
- [77] B. Damski. *The Simplest Quantum Model Supporting the Kibble-Zurek Mechanism of Topological Defect Production: Landau-Zener Transitions from a New Perspective*. Phys. Rev. Lett. **95**, 035701 (2005).
- [78] R. A. Barankov, L. S. Levitov and B. Y. Spivak. *Collective Rabi Oscillations and Solitons in a Time-Dependent BCS Pairing Problem*. Phys. Rev. Lett **93**, 160401 (2004).
- [79] E. A. Yuzbashyan, B. L. Altshuler, V. B. Kuznetsov and V. Z. Enolskii. *Nonequilibrium cooper pairing in the nonadiabatic regime*. Phys. Rev. B **72**, 220503 (2005).
- [80] E. A. Yuzbashyan and M. Dzero. *Dynamical Vanishing of the Order Parameter in a Fermionic Condensate*. Phys. Rev. Lett. **96**, 230404 (2006).
- [81] E. A. Yuzbashyan, O. Tsyplatyev and B. L. Altshuler. *Relaxation and Persistent Oscillation of the Order Parameter in Fermionic Condensates*. Phys. Rev. Lett. **96**, 097005 (2006).
- [82] G. L. Warner and A. J. Leggett. *Quench dynamics of a superfluid Fermi gas*. Phys. Rev. B **71**, 134514 (2005).

- [83] J. Bardeen, L. N. Cooper and J. R. Schrieffer. *Microscopic Theory of Superconductivity*. Phys. Rev. **106**, 162 (1957).
- [84] A. V. Andreev, V. Gurarie and L. Radzihovsky. *Nonequilibrium Dynamics and Thermodynamics of a Degenerate Fermi Gas Across a Feshbach Resonance*. Phys. Rev. Lett. **93**, 130402 (2004).
- [85] M. H. Szymanska, B. D. Simons and K. Burnett. *Dynamics of the BCS-BEC Crossover in a Degenerate Fermi Gas*. Phys. Rev. Lett. **94**, 170402 (2005).
- [86] A. Faribault. *Quantum quenches from integrability: the fermionic pairing model*. J. Stat. Mech. P03018 (2009).
- [87] D. M. Gangardt and M. Pustilnik. *Correlations in an expanding gas of hard-core bosons*. Phys. Rev. A **77**, 041604 (2007).
- [88] M. Rigol, A. Muramatsu and M. Olshanii. *Hard-core bosons on optical superlattices: Dynamics and relaxation in the superfluid and insulating regimes*. Phys. Rev. A **74**, 053616 (2006).
- [89] M. Rigol, V. Dunjko, V. Yurovsky and M. Olshanii. *Relaxation in a Completely Integrable Many-Body System: An ab Initio Study of the Dynamics of the Highly Excited States of 1D Lattice Hard-Core Bosons*. Phys. Rev. Lett. **98**, 050405 (2007).
- [90] C. Kollath, A. Läuchli and E. Altmann. *Quench dynamics and non equilibrium phase diagram of the Bose-Hubbard model*. Phys. Rev. Lett. **98**, 180601 (2007).
- [91] V. Gritsev, E. Demler, M. Lukin and A. Polkovnikov. *Spectroscopy of Collective Excitations in Interacting Low-Dimensional Many-Body Systems Using Quench Dynamics*. Phys. Rev. Lett. **99**, 200404 (2007).
- [92] A. Iucci and M. A. Cazalilla. *Quantum quench dynamics of some exactly solvable models in one dimension*. arXiv:0903.1205 (2009).
- [93] M. A. Cazalilla. *Effect of Suddenly Turning on Interactions in the Luttinger Model*. Phys. Rev. Lett. **97**, 156403 (2006).
- [94] E. Perfetto. *Time-dependent evolution of two coupled Luttinger liquids*. Phys. Rev. B **74**, 205123 (2006).
- [95] S. R. Manmana, S. Wessel, R. M. Noack and A. Muramatsu. *Strongly Correlated Fermions after a Quantum Quench*. Phys. Rev. Lett. **98**, 210405 (2007).
- [96] M. Eckstein and M. Kollar. *Non-thermal steady states after an interaction quench in the Falicov-Kimball model*. Phys. Rev. Lett. **100**, 120404 (2008).
- [97] A. Rosch, D. Rasch, B. Binz and M. Vojta. *Metastable Superfluidity of Repulsive Fermionic Atoms in Optical Lattices*. Phys. Rev. Lett. **101**, 265301 (2008).
- [98] G. Gallavotti. *Quasi-integrable mechanical systems*. Les Houches Summer School (informal lecture notes) (1984).

-
- [99] T. Gramespacher and S. Weigert. *Small denominators, frequency operators, and Lie transforms for nearly integrable quantum spin systems*. Phys. Rev. A **53**, 2971 (1996).
- [100] X. Gong-ou, Y. Ya-tian and X. Yong-zhong. *Dynamical symmetry, integrability of quantum systems, and general character of quantum regular motion*. Phys. Rev. A **61**, 042104 (2000).
- [101] O. Bohigas, M. J. Giannoni and C. Schmit. *Characterization of Chaotic Quantum Spectra and Universality of Level Fluctuation Laws*. Phys. Rev. Lett. **52**, 1 (1984).
- [102] S. Müller, S. Heusler, P. Braun, F. Haake and A. Altland. *Semiclassical Foundation of Universality in Quantum Chaos*. Phys. Rev. Lett. **93**, 014103 (2004).
- [103] S. Müller, S. Heusler, P. Braun, F. Haake and A. Altland. *Periodic-orbit theory of universality in quantum chaos*. Phys. Rev. B **72**, 046207 (2005).
- [104] G. Roux. *On quenches in non-integrable quantum many-body systems: the one-dimensional Bose-Hubbard model revisited*. Phys. Rev. A **79**, 021608 (2009).
- [105] H. Bethe. *Zur Theorie der Metalle*. Z. Phys. **71**, 205 (1931).
- [106] E. H. Lieb and F. Y. Wu. *Absence of Mott Transition in an Exact Solution of the Short-Range, One-Band Model in One Dimension*. Phys. Rev. Lett. **20**, 1445 (1968).
- [107] N. Andrei. *Diagonalization of the Kondo Hamiltonian*. Phys. Rev. Lett. **45**, 379 (1980).
- [108] P. B. Wiegmann. *Exact solution of the s-d exchange model (Kondo problem)*. J. Phys. C **14**, 1463 (1981).
- [109] J. Dukelsky, S. Pittel and G. Sierra. *Exactly solvable Richardson-Gaudin models for many-body quantum systems*. Rev. Mod. Phys. **76**, 643 (2004).
- [110] A. R. Kolovsky and A. Buchleitner. *Quantum chaos in the Bose-Hubbard model*. Europhys. Lett. **68**, 632 (2004).
- [111] G. Gallavotti. *Ergodicity, Ensembles, Irreversibility in Boltzmann and Beyond*. J. Stat. Phys. **78**, 1571 (1995).
- [112] E. Fermi, J. Pasta and S. Ulam. *Collected Papers of Enrico Fermi: 266. Studies of Non Linear Problems, Document LA-1940 (May 1955)*. The University of Chicago Press (1965).
- [113] J. Ford. *The Fermi-Pasta-Ulam problem: Paradox turns discovery*. Phys. Rep. **213**, 271–310 (1992).
- [114] G. Gallavotti, editor. *The Fermi-Pasta-Ulam Problem – A Status Report*. Springer (2007).
- [115] *International workshop on Anderson Localization in Nonlinear and Many-Body Systems, held March 16 - 20, 2009 at the Max-Planck-Institute for the Physics of Complex Systems, Dresden, Germany*.

- [116] Fucito et al. *Approach to equilibrium in a chain of nonlinear oscillators*. J. de Physique **43**, 707 (1982).
- [117] G. Parisi. *Statistical Field Theory*. Perseus Books (1988).
- [118] L. Berchiolla, A. Giorgilli and S. Paleari. *Exponentially long times to equipartition in the thermodynamic limit*. Phys. Lett. A **321**, 167 (2004).
- [119] G. Parisi. *On the approach to equilibrium of a Hamiltonian chain of anharmonic oscillators*. Europhys. Lett. **40**, 357 (1997).
- [120] D. Bambusi and A. Ponno. *On Metastability in FPU*. Commun. Math. Phys. **264**, 539 (2006).
- [121] V. I. Arnold. *Instability of dynamical systems with several degrees of freedom*. Sov. Math. Dokl. **6**, 581 (1964).
- [122] L. Markus and K. Meyer. *Generic Hamiltonian Dynamical Systems Are Neither Integrable Nor Ergodic*. Mem. Amer. Math. Soc. **144** (1974).
- [123] H. Tasaki. *From Quantum Dynamics to the Canonical Distribution: General Picture and a Rigorous Example*. Phys. Rev. Lett. **80**, 1373 (1997).
- [124] J. Gemmer, M. Michel and G. Mahler. *Quantum Thermodynamics*. Springer (2004).
- [125] S. Goldstein, J. L. Lebowitz, R. Tumulka and N. Zanghi. *Canonical Typicality*. Phys. Rev. Lett. **96**, 050403 (2006).
- [126] S. Popescu, A. J. Short and A. Winter. *Entanglement and the foundations of statistical mechanics*. Nature Physics **2**, 754 (2006).
- [127] N. Linden, S. Popescu, A. J. Short and A. Winter. *Quantum mechanical evolution towards thermal equilibrium*. Preprint, arXiv:0812.2385 (2008).
- [128] P. Borowski, J. Gemmer and G. Mahler. *Relaxation into equilibrium under pure Schrödinger dynamics*. Eur. Phys. J. B **35**, 255 (2003).
- [129] T. Barthel and U. Schollwöck. *Dephasing and the steady state in quantum many-particle systems*. Phys. Rev. Lett **100**, 100601 (2008).
- [130] M. Cramer, C. Dawson, J. Eisert and T. Osborne. *Exact Relaxation in a Class of Nonequilibrium Quantum Lattice Systems*. Phys. Rev. Lett. **100**, 030602 (2008).
- [131] M. Cramer, A. Flesch, I. P. McCulloch, U. Schollwöck and J. Eisert. *Exploring Local Quantum Many-Body Relaxation by Atoms in Optical Superlattices*. Phys. Rev. Lett. **101**, 063001 (2008).
- [132] H. Schmidt and G. Mahler. *Control of local relaxation behavior in closed bipartite quantum systems*. Phys. Rev. E **72**, 016117 (2005).
- [133] H. Schmidt and G. Mahler. *Nonthermal equilibrium states of closed bipartite systems*. Phys. Rev. E **75**, 061111 (2007).

-
- [134] S. Goldstein, J. L. Lebowitz, R. Tumulka and N. Zanghi. *On the Distribution of the Wave Function for Systems in Thermal Equilibrium*. J. Stat. Phys. **125**, 1197 (2006).
- [135] E. Schrödinger. *Energieaustausch nach der Wellenmechanik*. Ann. Phys. (Berlin) [digital] **388**, 956 (1927).
- [136] J. Deutsch. *Quantum statistical mechanics in a closed system*. Phys. Rev. A **43**, 2046 (1991).
- [137] M. Srednicki. *Chaos and quantum thermalization*. Phys. Rev. E **50**, 888 (1994).
- [138] M. Rigol, V. Dunjko and M. Olshanii. *Thermalization and its mechanism for generic isolated quantum systems*. Nature (London) **452**, 854 (2008).
- [139] M. V. Berry. *Regular and irregular semiclassical wavefunctions*. J. Phys. A **10**, 2083 (1977).
- [140] L. Erdős, M. Salmhofer and H.-T. Yau. *On the Quantum Boltzmann Equation*. J. of Stat. Phys. **116**, 367–380 (2004).
- [141] E. T. Jaynes. *Information Theory and Statistical Mechanics*. Phys. Rev. **106**, 620 (1957).
- [142] D. C. Brody, D. W. Hook and L. P. Hughston. *Unitarity, ergodicity and quantum thermodynamics*. J. Phys. A: Math. Theor. **40**, F503 (2007).
- [143] L. Boltzmann. *Weitere Studien über das Wärmegleichgewicht unter Gasmolekülen*. In *Wissenschaftliche Abhandlungen*, volume I, 316–402. F. Hasenöhrl (1872).
- [144] C. Cercignani. *The Boltzmann Equation and Its Applications*. Springer (1988).
- [145] J. L. Lebowitz and E. W. M. (Eds.). *Nonequilibrium Phenomena I, The Boltzmann equation*. North Holland Publishing Company (1983).
- [146] C. Cercignani, W. Greenberg and P. F. Zweifel. *Global Solutions of the Boltzmann Equation on a Lattice*. J. Stat. Phys. **20**, 449 (1979).
- [147] H. Spohn. *Boltzmann Equation on a Lattice: Existence and Uniqueness of Solutions*. J. Stat. Phys. **20**, 463 (1979).
- [148] E. Cohen and W. T. (Eds.). *The Boltzmann Equation - Theory and Applications*. Springer-Verlag (1973).
- [149] R. Peierls. *Quantum theory of solids*. Oxford University Press (1955).
- [150] G. Gallavotti. *Statistical Mechanics - A Short Treatise*. Springer (1999).
- [151] H. Lorentz. *Le mouvement des électrons dans les métaux..* Arch. Néerl. **10**, 336371 (1905).
- [152] R. Kubo. *The Boltzmann equation in solid state physics*. Acta Physica Austriaca **Suppl. X**, 301–340 (1973).

-
- [153] A. Sommerfeld. *Zur Elektronentheorie der Metalle*. Die Naturwissenschaften **15/41**, 63 (1927).
- [154] G. Roati, E. de Mirandes, F. Ferlaino, H. Ott, G. Modugno and M. Inguscio. *Atom Interferometry with Trapped Fermi Gases*. Phys. Rev. Lett. **92**, 230402 (2004).
- [155] F. Bloch. *Über die Quantenmechanik der Elektronen in Kristallgittern*. Zeitschrift für Physik A **52.7-8**, 555 (1928).
- [156] L. Landau. Soviet. Phys. JETP **3**, 920 (1957).
- [157] L. Landau. Soviet. Phys. JETP **5**, 101 (1957).
- [158] L. Landau. Soviet. Phys. JETP **8**, 70 (1958).
- [159] I. M. Khalatnikov. *Kinetic equations for elementary excitations in quantum systems*. Acta Physica Austriaca **Supp. X**, 563 (1973).
- [160] G. Baym. *Landau fermi liquid theory*. Wiley-VCH (2004).
- [161] D. Pines and P. Nozières. *The Theory of Quantum Liquids (Vol. I)*. W. A. Benjamin, Inc. (1966).
- [162] P. W. Anderson. *Basic Notions of Condensed Matter Physics*. Westview Press (1997).
- [163] J. Harris. *Adiabatic-connection approach to Kohn-Sham theory*. Phys. Rev. A **29**, 1648 (1984).
- [164] F. Anfuso and A. Rosch. *String order and adiabatic continuity of Haldane chains and band insulators*. Phys. Rev. B **75**, 144420 (2007).
- [165] A. Rosch. *Breakdown of Luttinger's theorem in two-orbital Mott insulators*. Eur. Phys. J. B **59**, 495 (2007).
- [166] J. M. Luttinger. *Fermi Surface and Some Simple Equilibrium Properties of a System of Interacting Fermions*. PR **119**, 1153 (1960).
- [167] A. Abrikosov, L. Gorkov and I. Dzyaloshinski. *Methods of Quantum Field Theory in Statistical Physics*. Dover Publications (1963).
- [168] J. W. Negele and H. Orland. *Quantum Many Particle Systems*. Addison-Wesley (1988).
- [169] A. L. Fetter and J. D. Walecka. *Quantum Theory of Many-Particle Systems*. McGraw-Hill Book Company (1971).
- [170] J. M. Luttinger and J. C. Ward. *Ground-State Energy of a Many-Fermion System. II*. Phys. Rev. **118**, 1417 (1960).
- [171] F. Gebhard, E. Jeckelmann, S. Mahler, S. Nishimoto and R. Noack. *Forth-order perturbation theory for the half-filled Hubbard model in infinite dimensions*. Eur. Phys. J. B **36**, 491–509 (2003).
- [172] J. Hubbard. *Electron correlations in narrow energy bands..* Proc. R. Soc. London, Ser. A **276**, 238 (1963).

- [173] D. Vollhardt. *Investigation of correlated electron systems using the limit of high dimensions*. In V. Emery, editor, *Correlated Electron Systems*, 57. World Scientific, Singapore (1993).
- [174] H. Tasaki. *The Hubbard model – an introduction and selected rigorous results*. J. Phys.: Condens. Matter **10**, 4353 (1998).
- [175] H. Tasaki. *From Nagaoka’s ferromagnetism to flat-band ferromagnetism and beyond – An introduction to ferromagnetism in the Hubbard model*. Prog. **99**, 489 (1998).
- [176] B. S. Shastry. *Mott transition in the Hubbard model*. Modern Physics Letters B **6**, 1427 (1992).
- [177] M. Imada, A. Fujimori and Y. Tokura. *Metal-insulator transitions*. Phys. Rev. Mod. **70**, 1039 (1998).
- [178] A. Georges, G. Kotliar, W. Krauth and M. J. Rozenberg. *Dynamical mean-field theory of strongly correlated fermion systems and the limit of infinite dimensions*. Phys. Rev. Mod. **68**, 13 (1996).
- [179] G. Kotliar and D. Vollhardt. *Strongly Correlated Materials: Insights From Dynamical Mean-Field Theory*. Physics Today **3/2004**, 53 (2004).
- [180] A. Montorsi, editor. *The Hubbard Model (Reprint Volume)*. World Scientific (1992).
- [181] D. Baeriswyl, D. K. Campbell, J. M. Carmelo and F. Guinea. *The Hubbard Model - Its Physics and Mathematical Physics*. Plenum Press (1995).
- [182] F. Mancini. *The Mott-Hubbard transition and the paramagnetic insulating state in the two-dimensional Hubbard model*. Europhys. Lett. **50**, 229 (2000).
- [183] T. Giamarchi. *Quantum Physics in One Dimension*. Oxford Science Publications (2004).
- [184] P. W. Anderson. *The Resonating Valence Bond State in La_2CuO_4 and Superconductivity*. Science **235**, 1196 (1987).
- [185] E. Müller-Hartmann. *The Hubbard model at high dimensions: some exact results and weak coupling theory*. Z. Phys. B **76**, 211–217 (1989).
- [186] D. V. W. Metzner. *Correlated Lattice Fermions in $d = \infty$ Dimensions*. Phys. Rev. Lett. **62**, 324 (1989).
- [187] A. Georges and W. Krauth. *Physical properties of the half-filled Hubbard model in infinite dimensions*. Phys. Rev. B **48**, 7167–7182 (1993).
- [188] G.-S. Tian. *Particle-hole transformations and sum rules for the Hubbard model*. Physics Letters A **228**, 383– (1997).
- [189] F. Rossi and T. Kuhn. *Theory of ultrafast phenomena in photoexcited semiconductors*. Rev. Mod. Phys. **74**, 895 (2002).
- [190] K. Morawetz (Ed.). *Nonequilibrium Physics at Short Time Scales*. Springer (2004).

- [191] R. Huber et al. *How many-particle interactions develop after ultrafast excitation of an electron-hole plasma*. Nature (London) **414**, 286 (2001).
- [192] M. Betz et al. *Ultrafast Formation of Quasiparticles in Semiconductors: How Bare Charges Get Dressed*. In K. Morawetz, editor, *Nonequilibrium Physics at Short Time Scales*, 232. Springer (2004).
- [193] F. Krausz and M. Ivanov. *Attosecond Physics*. Rev. Mod. Phys. **81**, 163 (2009).
- [194] A. L. Cavalieri et al. *Attosecond spectroscopy in condensed matter*. Nature (London) **449**, 1029 (2007).
- [195] K. Morawetz, P. Lipavski and M. Schreiber. *Femtosecond formation of collective modes due to mean-field fluctuations*. Phys. Rev. B **72**, 233203 (2005).
- [196] H. Petek and S. Ogawa. *Femtosecond time-resolved two-photon photoemission studies of electron dynamics*. Prog. Surf. Sci. **56**, 239 (1998).
- [197] N.-H. Kwong and M. Bonitz. *Real-Time Kadanoff-Baym Approach to Plasma Oscillations in a Correlated Electron Gas*. Phys. Rev. Lett. **84**, 1768 (2000).
- [198] W.-D. Schöne and W. Ekardt. *Time-dependent screening of a positive charge distribution in metals: Excitons on an ultrashort time scale*. Phys. Rev. B **62**, 13464 (2000).
- [199] T. Brabec and F. Krausz. *Intense few-cycle laser fields: Frontiers of nonlinear optics*. Rev. Mod. Phys. **72**, 545 (2000).
- [200] See, for instance, the webpage of the Junior Research Group Attosecond Dynamics at the Max-Planck-Institute for Quantum Optics, Garching, Germany, in its version dating 22/03/09..
- [201] L. Bányai, Q. T. Vu, B. Mieck and H. Haug. *Ultrafast Quantum Kinetics of Time-Dependent RPA-Screened Coulomb Scattering*. Phys. Rev. Lett. **81**, 882 (1998).
- [202] D. Kremp, D. Semkat and M. Bonitz. *Short-Time Kinetics and Initial Correlations in Quantum Kinetic Theory*. J. Phys.: Conference Series **11**, 1 (2005).
- [203] M. Anderson, J. Ensher, M. Matthews, C. Wieman and E. Cornell. *Observation of Bose-Einstein Condensation in a Dilute Atomic Vapor*. Science **269**, 198 (1995).
- [204] K. B. Davis, M. O. Mewes, M. R. Andrews, N. J. van Druten, D. S. Durfee, D. M. Kurn and W. Ketterle. *Bose-Einstein Condensation in a Gas of Sodium Atoms*. Phys. Rev. Lett. **75**, 3969 (1995).
- [205] W. Ketterle. *private communication*. (Spring 2008). The hospitality of the Siemens foundation, München, is kindly acknowledged.
- [206] B. P. Anderson and M. A. Kasevich. *Macroscopic Quantum Interference from Atomic Tunnel Arrays*. Science **282**, 1686 (1998).
- [207] P. Jessen and I. Deutsch. *Optical Lattices*. Adv. At. Mol. Opt. Phys. **37**, 95 (1996).
- [208] R. P. Feynman. *Simulating physics with computers*. Int. J. Theor. Phys. **21**, 467 (1982).

- [209] I. Bloch, J. Dalibard and W. Zwerger. *Many-Body Physics with Ultracold Gases*. Rev. Mod. Phys. **80**, 885 (2008).
- [210] A. Leggett. *Quantum Liquids: Bose Condensation and Cooper Pairing in Condensed-Matter Systems*. Oxford University Press (2007).
- [211] M. Greiner, O. Mandel, T. Esslinger, T. Hänsch and I. Bloch. *Quantum phase transition from a superfluid to a Mott insulator in a gas of ultracold atoms*. Nature **415**, 39–44 (2002).
- [212] M. Greiner, O. Mandel, T. Hänsch and I. Bloch. *Collapse and revival of the matter wave field of a Bose-Einstein condensate*. Nature **419**, 51–54 (2002).
- [213] M. O. Scully and M. S. Zubairy. *Quantum Optics*. Cambridge University Press (1997).
- [214] M. Greiner. *Ultracold quantum gases in three-dimensional optical lattice potentials*. PhD thesis, LMU Muenchen (2003).
- [215] W. Zwerger. *Mott-Hubbard transition of cold atoms in optical lattices*. J. Opt. B: Quantum Semiclass. Opt. **5**, S9 (2003).
- [216] T. Kinoshita, T. Wenger and D. Weiss. *A quantum Newton's cradle*. Nature **440**, 4693 (2006).
- [217] B. Paredes, A. Widera, V. Murg, O. Mandel, S. Fölling, I. Cirac, G. V. Shlyapnikov, T. W. Hänsch and I. Bloch. *Tonks-Girardeau gas of ultracold atoms in an optical lattice*. Nature (London) **429**, 277 (2004).
- [218] G. R. et al. *Anderson localization of a non-interacting Bose-Einstein condensate*. Nature (London) **453**, 895 (2008).
- [219] S. Foelling et al. *Direct Observation of Second Order Atom Tunnelling*. Nature (London) **448**, 1029 (2007).
- [220] S. Trotzky et al. *Time-resolved Observation and Control of Superexchange Interactions with Ultracold Atoms in Optical Lattices*. Science **319**, 295 (2008).
- [221] L.-M. Dua, E. Demler and M. D. Lukin. *Controlling Spin Exchange Interactions of Ultracold Atoms in Optical Lattices*. Phys. Rev. Lett. **91**, 090402 (2003).
- [222] P. Barmettler, A. M. Rey, E. Demler, M. D. Lukin, I. Bloch and V. Gritsev. *Quantum many-body dynamics of coupled double-well superlattices*. Phys. Rev. A **78**, 012330 (2008).
- [223] T. Barthel, C. Kasztelan, I. P. McCulloch and U. Schollwöck. *Magnetism, coherent many-particle dynamics, and relaxation with ultracold bosons in optical superlattices*. cond/mat **0809.5141** (2008).
- [224] W. Hofstetter, J. I. Cirac, P. Zoller, E. Demler and M. D. Lukin. *High-Temperature Superfluidity of Fermionic Atoms in Optical Lattices*. Phys. Rev. Lett. **89**, 220407 (2002).

- [225] M. Köhl, H. Moritz, T. Stöferle, K. Günther and T. Esslinger. *Fermionic atoms in a 3D optical lattice: Observing Fermi-surfaces, dynamics and interactions*. Phys. Rev. Lett. **94**, 080403 (2004).
- [226] T. Rom, T. Best, D. van Oosten, U. Schneider, S. Fölling, B. Paredes and I. Bloch. *Free fermion antibunching in a degenerate atomic Fermi gas released from an optical lattice*. Nature (London) **444**, 733 (2006).
- [227] J. Chin, D. Miller, Y. Liu, C. Stan, W. Setiawan, C. Sanner, K. Xu and W. Ketterle. *Evidence for superfluidity of ultracold fermions in an optical lattice*. Nature (London) **443**, 961 (2006).
- [228] N. Strohmaier, Y. Takasu, K. Günther, R. Jördens, M. Köhl, H. Moritz and T. Esslinger. *Interaction-Controlled Transport of an Ultracold Fermi Gas*. Phys. Rev. Lett. **99**, 220601 (2007).
- [229] R. Jördens, N. Strohmaier, K. Günter, H. Moritz and T. Esslinger. *A Mott insulator of fermionic atoms in an optical lattice*. Nature (London) **455**, 204 (2008).
- [230] J. J. Sakurai. *Modern Quantum Mechanics*. Addison-Wesley (1994).
- [231] J. Rammer. *Quantum Field Theory of Non-equilibrium States*. Cambridge University Press (2007).
- [232] M. Gell-Mann and F. Low. *Bound States in Quantum Field Theory*. Phys. Rev. **84**, 350 (1951).
- [233] A. Hackl and S. Kehrein. *A unitary perturbation theory approach to real-time evolution problems*. J. Phys.: Condens. Matter **21**, 015601 (2008).
- [234] H. Goldstein, C. Poole and J. Safko. *Classical Mechanics*. Addison-Wesley (2002).
- [235] A. Hackl and S. Kehrein. *Real Time Evolution in Quantum Many-Body Systems with Unitary Perturbation Theory*. Phys. Rev. B **78**, 092303 (2007).
- [236] K. Goda et al. *A quantum-enhanced prototype gravitational-wave detector*. Nature Physics **4**, 472 (2008).
- [237] C. F. Lo. *Squeezing by tuning the oscillator frequency*. J. Phys. A: Math. Gen. **23**, 1155 (1990).
- [238] C. Jacobi. *Über ein leichtes Verfahren die in der Theorie der Säcularstörungen vorkommenden Gleichungen numerisch aufzulösen*. Journal für die reine und angewandte Mathematik **30**, 7 (1846).
- [239] M. T. Chu. *A continuous Jacobi-like approach to the simultaneous reduction of real matrices*. Linear Alg. Appl. **147**, 75 (1991).
- [240] R. Brockett. *Dynamical systems that sort lists, diagonalize matrices, and solve linear programming problems*. Linear Algebra Appl. **146**, 79 (1991).
- [241] M. T. Chu. *A List of Matrix Flows with Applications*. Fields Institute Communications **3**, 87 (1994).

- [242] S. D. Glazek and K. G. Wilson. *Renormalization of Hamiltonians*. Phys. Rev. B **48**, 5863 (1993).
- [243] S. D. Glazek and K. G. Wilson. *Perturbative renormalization group for Hamiltonians*. Phys. Rev. D **49**, 4214 (1994).
- [244] F. Wegner. *Flow Equations for Hamiltonians*. Ann. Physik (Leipzig) **3**, 77 (1994).
- [245] F. Wegner. *Flow equations and normal ordering: a survey*. J. Phys. A **39**, 8221 (2006).
- [246] S. Kehrein. *The Flow Equation Approach to Many-Particle Systems*. Springer (2006).
- [247] S. Kehrein. *Scaling and Decoherence in the Nonequilibrium Kondo Model*. Phys. Rev. Lett. **95**, 056602 (2005).
- [248] M. Moeckel and S. Kehrein. *Interaction Quench in the Hubbard Model*. Phys. Rev. Lett. **100**, 175702 (2008).
- [249] P. W. Anderson. *Basic Notions of Condensed Matter Physics*. Addison-Wesley (1984).
- [250] F. J. Wegner. *Expectation Values, Wick's Theorem and Normal Ordering*. unpublished (2000).
- [251] M. J. Moeckel. *Application of the flow equation method to the out-of-equilibrium Anderson impurity model*. Diploma thesis, LMU Muenchen (2005).
- [252] P. Fulde. *Electron Correlations in Molecules and Solids*. Springer (1993).
- [253] C. P. Heidbrink and G. S. Uhrig. *Landau's Quasiparticle Mapping: Fermi Liquid Approach and Luttinger Liquid Behavior*. Phys. Rev. Lett. **88**, 146401 (2002).
- [254] J. Rammer and H. Smith. *Quantum field-theoretical methods in transport theory of metals*. Rev. Mod. Phys. **58** (2), 323 (1986).
- [255] C. Cohen-Tannoudji, B. Diu and F. Laloë. *Quantenmechanik*. Walter de Gruyter (1999).
- [256] J. Berges. *Introduction to nonequilibrium quantum field theory*. AIP Conf. Proc. **739**, 3–62 (2005).
- [257] C. Kollath and A. Läuchli. *Spreading of correlations and entanglement after a quench in the one-dimensional Bose-Hubbard model*. J. Stat. Mech. P05018 (2008).
- [258] S. R. Manmana, S. Wessel, R. M. Noack and A. Muramatsu. *Time evolution of correlations in strongly interacting fermions after a quantum quench*. Preprint arXiv: 0812.0561 (2008).
- [259] M. Eckstein, M. Kollar and P. Werner. *Dynamical phase transition in correlated fermionic lattice systems*. arXiv:0904.0976 (2009).
- [260] M. Kollar and M. Eckstein. *Relaxation of a one-dimensional Mott insulator after an interaction quench*. Phys. Rev. A **78**, 013626 (2008).

- [261] F. Gebhard and A. E. Ruckenstein. *Results for a Hubbard Chain with Long-Range Hopping*. Phys. Rev. Lett. **68**, 244 (1992).
- [262] A. Hackl, D. Rosen, S. Kehrein and W. Hofstetter. *Nonequilibrium Spin Dynamics in the Ferromagnetic Kondo Model*. Phys. Rev. Lett. (accepted for publication) arXiv:0903.1079 (2009).
- [263] J. Sólyom. *The Fermi gas model of one-dimensional conductors*. Adv. i. Phys. **28**, 201 (1979).
- [264] S. Kehrein. *Flow equation approach to the Sine-Gordon model*. Nuc. Phys. B **592**, 512 (2001).
- [265] V. Gritsev, A. Polkovnikov and E. Demler. *Linear response theory for a pair of coupled one-dimensional condensates of interacting atoms*. Phys. Rev. B **75**, 174511 (2007).
- [266] J. Sabio and S. Kehrein. To be published (2009).
- [267] S. Ghoshal and A. Zamolodchikov. *Boundary State and Boundary S Matrix in Two-Dimensional Integrable Field Theory*. Int. J. Mod. Phys. **A 9**, 3841 (1994).
- [268] H. Saleur, S. Skorik and N. Warner. *The boundary sine-Gordon theory: classical and semi-classical analysis*. Nucl. Phys. B **441**, 421 (1995).
- [269] R. A. Barankov and L. S. Levitov. *Synchronization in the BCS Pairing Dynamics as a Critical Phenomenon*. Phys. Rev. Lett. **96**, 230403 (2006).
- [270] R. A. Barankov and L. S. Levitov. *Dynamical selection in developing fermionic pairing*. Phys. Rev. A **73**, 033614 (2006).
- [271] S. Kehrein. *private communication* (2008).
- [272] K.-P. Marzlin and W. Zhang. *Quantized circular motion of a trapped Bose-Einstein condensate: Coherent rotation and vortices*. Phys. Rev. A **57**, 4761 (1998).
- [273] V. I. Yukalov, E. P. Yukalova and V. S. Bagnato. *Non-ground-state Bose-Einstein condensates of trapped atoms*. Phys. Rev. A **56**, 4845 (1997).
- [274] V. I. Yukalov, E. P. Yukalova, and V. S. Bagnato. *Nonlinear coherent modes of trapped Bose-Einstein condensates*. Phys. Rev. A **66**, 043602 (2002).
- [275] V. Yukalov and E. Yukalova. *Dynamics of Nonground-State Bose-Einstein Condensates*. J. of Low Temp. Phys. **138**, 657 (2005).
- [276] E. R. F. Ramos, L. Sanz, V. I. Yukalov and V. S. Bagnato. *Order parameter for the dynamical phase transition in Bose-Einstein condensates with topological modes*. Phys. Rev. A **76**, 033608 (2007).
- [277] T. Müller, S. Fölling, A. Widera and I. Bloch. *State Preparation and Dynamics of Ultracold Atoms in Higher Lattice Orbitals*. Phys. Rev. Lett. **99**, 200405 (2007).

List of Previous Publications

- (1) M. Moeckel and S. Kehrein.
Interaction Quench in the Hubbard Model.
Physical Review Letters **100**, 175702 (2008)
Preprint arXiv:0802.3202

- (2) M. Moeckel and S. Kehrein.
Real-time evolution for weak interaction quenches in quantum systems.
Accepted for publication in Annals of Physics (N. Y.)
<http://dx.doi.org/10.1016/j.aop.2009.03.009> (2009)
Preprint arXiv:0903.1561

ISBN 978-3-00-028464-9